

# **Predicting the Crystal Morphology Grown from Aqueous Solution**

## **DISSERTATION**

zur Erlangung der akademischen Grades

Doktor-Ingenieur (Dr.-Ing.)

eingereicht am

Zentrum für Ingenieurwissenschaften

der Martin-Luther-Universität Halle-Wittenberg

als organisatorische Grundeinheit für Forschung und Lehre im Range einer Fakultät

(§75 Abs. 1 HSG LSA, §19 Abs. 1 Grundordnung)

von

Dipl. Wirt.-Ing. Christiane Schmidt

geb. am 19.07.1983 in Lutherstadt Eisleben

Geschäftsführender Direktor des Zentrums für Ingenieurwissenschaften:

Prof. Dr.-Ing. habil. Dr. h.c. J. Ulrich

Gutachter:

Prof. Dr.-Ing. habil. Dr. h.c. J. Ulrich

Prof. Dr.-Ing. habil. G. Schulte

Termin der Verteidigung:

26.03.2012

Halle, den 27.03.2012



### **Eidesstattliche Erklärung**

Ich versichere hiermit, dass ich die vorliegende Arbeit selbstständig verfasst und keine anderen als die angegebenen Hilfsmittel verwendet wurden. Die aus fremden Quellen direkt oder indirekt übernommenen Stellen sind als solche kenntlich gemacht und werden in der Arbeit aufgeführt.

Die Arbeit hat in gleicher oder ähnlicher Form noch keiner Prüfungsbehörde vorgelegen.

Halle (Saale), 27.03.2012

Christiane Schmidt





**Danksagung**

Ich richte meinen besonderen Dank an meinen Doktorvater, Prof. Dr.-Ing. Dr. h.c. Ulrich. Vielen Dank für das mir entgegengebrachte Vertrauen, für Diskussionen und die motivierenden Worte.

Meiner Familie danke ich von ganzem Herzen für die Unterstützung, den Beistand, die vielen Gespräche und für das Zuhören. Danke.

Halle (Saale) im März 2012

Christiane Schmidt



**Content**

<b>1. Introduction .....</b>	<b>1</b>
<b>2. State of the Art.....</b>	<b>3</b>
2.1 Computational Methods.....	3
2.2 Morphology Prediction.....	3
2.3 Pure Morphology .....	3
2.4 Presence of Additives .....	5
2.5 Presence of Solvents .....	7
2.6 Summary.....	8
2.7 Aim of Work.....	9
<b>3. Methods and Materials .....</b>	<b>11</b>
3.1 Methods .....	11
3.1.1 Computational .....	11
3.1.2 Experimental.....	15
3.2 Materials .....	16
3.2.1 Solvent.....	16
3.2.2 Benzoic Acid .....	17
3.2.3 Succinic Acid.....	18
3.2.4 Ascorbic Acid .....	19
3.2.5 Caprolactam.....	19
<b>4. Results .....</b>	<b>21</b>
4.1 Water.....	21
4.1.1 Molecular Optimization.....	21
4.1.2 Water in Morphology Predictions .....	23
4.2 Benzoic Acid.....	23
4.2.1 Surface Docking Method.....	24
4.2.2 Layer Docking Method.....	28
4.3 Succinic Acid.....	31
4.3.1 Surface Docking Method.....	31
4.3.2 Layer Docking Method.....	33



---

4.4	Ascorbic Acid .....	36
4.4.1	Surface Docking Method .....	37
4.4.2	Layer Docking Method .....	39
4.5	Caprolactam .....	40
4.5.1	Surface Docking Method .....	40
4.5.2	Layer Docking Method .....	43
<b>5.</b>	<b>Discussion .....</b>	<b>46</b>
5.1	Water .....	46
5.1.1	Molecular Optimization .....	46
5.2	Surface Docking Method .....	46
5.2.1	Water Models .....	46
5.2.2	Constraints .....	47
5.2.3	Thermostats .....	49
5.3	Layer Docking Method .....	49
5.3.1	Liquid Side .....	49
5.3.2	Liquid and Solid Side .....	51
<b>6.</b>	<b>Conclusion .....</b>	<b>53</b>
<b>7.</b>	<b>Summary .....</b>	<b>55</b>
<b>8.</b>	<b>Zusammenfassung .....</b>	<b>56</b>
<b>9.</b>	<b>List of Symbols and Abbreviation .....</b>	<b>58</b>
<b>10.</b>	<b>Literature .....</b>	<b>59</b>
<b>11.</b>	<b>Appendix A .....</b>	<b>66</b>
<b>12.</b>	<b>Appendix B (Userguide) .....</b>	<b>68</b>
	<b>Curriculum Vitae .....</b>	<b>69</b>
	<b>List of Publications .....</b>	<b>70</b>



## 1. Introduction

The morphology of crystals grown from the fluid phase is in the focus of the present work. In view on industrial crystallization processes it is aimed to grow crystals of a specific morphology. In order to achieve the controlled change of the morphology additives are used. Since, the production of an undesired morphology can disturb the operating conditions of further process steps as filtration or sieving and even impact the product quality the probability of an unexpected morphology change is to be lowered. Avoiding the production of an undesired crystal morphology is achieved via a screening. Currently, the majority of screening is performed in laboratory experiments which are conducted for the feed substances which are involved in the crystallization, such as possible solvents, solute and morphology modifying agents (additives and impurities). The number of chemical substances which are involved in the crystallization processes makes these experiments timeconsuming and expensive.

The investigations of the past decades generated an enormous gain of knowledge in terms of crystal growth. Coupled with the technological developments in computerscience it is now possible to simulate crystal growth processes in molecular level simulations. Herein, numerous approaches for the prediction of crystal morphology which is grown under certain conditions are introduced. Employing computational methods for the prediction of the crystal morphology aims to skip laboratory scale experiments in order to save time and accelerate the development and even the marketing of new products. Thus, the mayor aim of the present work is to develop a reliable method for the prediction of crystal morphology. Regarding the industrial application the goal is to lower expenses for experiments and make products more competative on the international market.

Despite of all advantages the available computational methods lack from the consideration of the presence of a liquid phase in crystallization and the specific levels of concentration, respectively (see chapter State of the Art). In the work at hand it is aimed to fill this gap. Thus, the modeling of the concentration of the solute and the solvent molecules in the solution is performed (see chapter Materials and Methods). The presented modeling methodology considers the solid as well as the liquid side of the crystallization process for the morphology prediction.

In application of the solvent water in the introduced method was the premise of this work, as it is indispensable in solution crystallization regarding the pharmaceutical and the food industry. The number of available investigations on pure water is painstaking (seen in

Materials and Methods) but, nonetheless, it is rarely investigated in morphology prediction. The application of available water models in morphology prediction is presented in this work (see chapters Results and Discussion).

Using the herein presented computational method it is possible to achieve reliable morphology predictions if considering the appropriate solvent at the desired concentration and when carefully selecting the simulation conditions (see chapters Results and Discussion). The number of possible simulation conditions may have strong impact on the generated results. Thus, a clear user manual for both methods, the surface docking and the layer docking method, is given in the appendix.



## **2. State of the Art**

### **2.1 Computational Methods**

Molecular modeling is related to the availability of different methods of computation. The general classification is found with Foresman and Frisch [For96]. Therein, the electronic structure methods (such as ab initio, semi-empirical and density functional theory DFT) and the molecular mechanics are listed as tools in computational chemistry. The electronic structure methods employ the laws of quantum mechanics, thus, related properties of a molecule (e.g. energy) are derived by solving the Schrödinger equation. The accuracy as well as the computational cost of those methods is very high. Based on the laws of classical physics, molecular mechanics methods provide a good alternative.

Molecular mechanics calculations are characterized by a force field, consisting of potential energy equations, a series of atom types and parameter sets. Those methods enable the user to handle systems of thousands of atoms within an acceptable time. The main drawback is, however, that due to the limitation in the parameters of the force field the amount of molecules which can be modeled are limited. A general application of a force field for all systems of interest is therefore not possible. For more details see e.g. Myerson [Mye99], Foresman and Frisch [For96] or Leach [Lea01]. Due to the work of e.g. Hartman and Bennema [Har80], Docherty and Roberts [Cly91], F.J.J. Leussen [Asm09] modern software packages allow an easy handling and applications of those methods for a broad range of users.

### **2.2 Morphology Prediction**

The methods developed for the computation of crystal morphologies allow the consideration of only the pure substance as well as the presence of various external factors. The following chapter gives an overview on such methods and approaches, as well as an introduction to various approaches for the prediction of the pure morphology. The following chapters introduce different molecular dynamics methods to take into account the presence of additives and solvents for a subsequent morphology prediction. The Appendix A supplies with a general listing of herein introduced modeling methods.

### **2.3 Pure Morphology**

The prediction of the pure crystal morphology is implemented as a routine method to most available software packages as MaterialsStudios [Acc05].

The pure morphology is obtained by using the laws of Bravais, Friedel, Donnay and Harker (BFDH) [Bra66, Fri07, Don38]. Bravais [Bra66] stated that the morphological importance (MI) of a face is proportional to the interplanar spacing  $d_{hkl}$ . The morphologically most important faces grow the slowest:

$$R_G \propto \frac{1}{d_{hkl}} \quad 2-1$$

In 1907 Friedel [Fri07] gave experimental proof to this law and Donnay and Harker [Don38] implemented further improvements. The BDFH theory is based on a purely geometry consideration and does not take any chemical interactions into account. Thus, it is a weak approach to estimate the pure morphology, but supplies with a first habit approach.

Another method to determine the pure crystal morphology is to employ the Periodic Bond Chain Theory (PBC) [Har55]. It states the presence of strong chemical bonds within the crystal. It is stated that the attachment energy  $E_{hkl}^{att}$  (AE), as energy released free upon the attachment of one growth unit to the crystal surface, is growth rate controlling. Faces of high attachment energy grow relatively faster than faces with lower attachment energies:

$$E_{hkl}^{att} \propto MI \quad 2-2$$

The attachment energy of a crystal face is depending on the strong periodic chains of molecules parallel to the corresponding face. The vector sum of such a chain is a periodic bond chain (PBC). Three types of PBCs are defined according to the category of the face. A flat face (f-face) is parallel to at minimum two crossing PBCs, a stepped face (s-face) is parallel to one PBC and a kinked face (k-face) has no parallel PBCs. The corresponding attachment energies are  $E_{Kinked}^{att} > E_{Stepped}^{att} > E_{Flat}^{att}$ . Thus, flat faces grow the slowest and dominate the habit. Neither the PBC nor the attachment energy theory considers external factors (supersaturation, temperature etc.). Moreover, the attachment energy is no measurable parameter which is a further drawback. Extended methods are necessary to explicitly consider the external effects.

The attachment energy is related to a measureable value since the energy of crystallization is the sum of the attachment energy and the energy released free when a new growth slice is formed:

$$E^{cr} = E_{hkl}^{att} + E_{hkl}^{sl} \quad 2-3$$

The Attachment Energy Theory [Har80] states that the growth rate of a crystal face is direct proportional to the attachment energy of the corresponding face. The model takes chemical interactions within the crystal into account. The drawback of these approaches is that no influence of foreign molecules and external effects such as supersaturation or temperature level is considered.

## 2.4 Presence of Additives

Industrial crystallization processes rarely involve pure materials but are rather used as purification process to achieve purified material and are often conducted from melt or solution. The presence of any other molecules but the crystalline material (substrate) frequently leads to significant changes in the crystalline morphology (see [Bun91, Dav76, Dav82, Wir87]). Components denoted as additives or impurities predominantly occur in small amounts, whereas a solvent is represented by a large number of molecules in a mixed system. Here the modeling procedure conducted for morphology prediction in the presence of additives is described. For a better comprehension the connection between the introduced methods is given in Figure 2-1.

The focus of the investigations of the group around Lahav, Leiserowitz started around 1980 is on the tailor-made additives [Add82] which disrupt or block crystal growth depending on the molecular structure. Berkovich-Yellin 1982 [Ber82] suggested the presence of a polar axis within the crystal and therefore a selective incorporation of tailor made additives at specific faces. Due to the nature of the additive a significant change of the AE and, hence, the morphology is induced. The corresponding publication of 1985 [Ber85] suggests a simple approach for morphology prediction in presence of additives. Therein, the additive molecule is build into the unit cell to replace each of the host molecules stepwise. The structure of the polar surfaces is analyzed and the mappings of the corresponding electrostatic potentials are employed to determine the solvent effect. The method supplies accurate results and considers the solvent and the additive effect, respectively. Nonetheless it is lacking the implementation of the concentration of solute, solvent and potential additives and their enrichment in the boundary layer around a crystal in the solution.

Bennema *et al.* [Ben92] introduce a modeling concept for the prediction of crystal morphology grown in the presence of additives which is based on the knowledge of the

internal crystal structure. The method employs the theory of the roughening temperature [Jac58]. Preliminary investigations on the solid liquid interface revealed an intensive structuring of molecules in the interfacial fluid phase and none in the bulk fluid phase [Liu92].

By means of the approach presented by Liu and Bennema [Liu96a, Liu96b] the habit controlling factors and the relative growth rate are related via the crystal growth mechanism. The PBC theory as well as the interfacial structure analysis forms the basis of the approach.

Investigations of Docherty *et al.* [Cly94a, Cly94b] aimed to model the effect of tailor made additives. Disruptive and blocking additives disturb the local symmetry of the crystal. In terms of the presented approach the molecules in the central crystal unit cell are stepwise replaced by an additive molecule, the surrounding unit cells consist of host molecules (build-in). The obtained slice and attachment energies in presence of the additive are averaged. The attachment energy in presence of additives and without additives is then compared. A second method is assuming the additive incorporation of an outer growth slice, thus, not in the central unit cell. Here, the obtained slice energies in presence of the additive are averaged and the incorporation energy is calculated. The results are presented for disruptive tailor made additives [Cly94a]. The presence of blocking tailor made additives is modeled via the vacancy approach [Cly94b].

Myerson and Jang [Mye95] developed an approach to reveal additives as possible growth inhibitors according to the binding energy difference. The method is based on the implementation of an additive molecule onto a crystal surface. Subsequently by means of the binding energy is obtained as interaction energy between additive and surface. The larger absolute value of the binding energy the stronger the interaction between the molecule and the corresponding face.

Despite the high accuracy of some methods when modeling the effect of additives on crystals there is a drawback which is the large amount of manual steps and time-consuming analysis required for a proper prediction. Furthermore, some of the aforementioned methods are very complex and difficult to handle for untrained users. Nonetheless, the presented investigations and findings provide with a good base for the development of approaches for morphology prediction. Simple approaches such as the Build-In [Nie95, Mat96, Sch04] and the Surface Docking [Lu04a, b] are deduced from the fundamental findings of these preliminary achievements. These methods are approaching the attachment energy via the building-in of additives [Nie95, Mat96, Mat99, Nie96,

Nie97a, Nie97b], use the PBC and build in coupled [Sch04] or docking those molecules on the surface [Lu04a]. All of those methods estimate the attachment energy in the presence of additives based on the binding energy differences between additive and solute molecule on the crystalline surface. Additionally, the latter the method (surface docking) is successfully applied for the presence of various solvents [Sch11a, Sch11b].

However, these methods and approaches are neglecting the concentration and the enrichment of crystalline material in the boundary layer on the crystal surface.

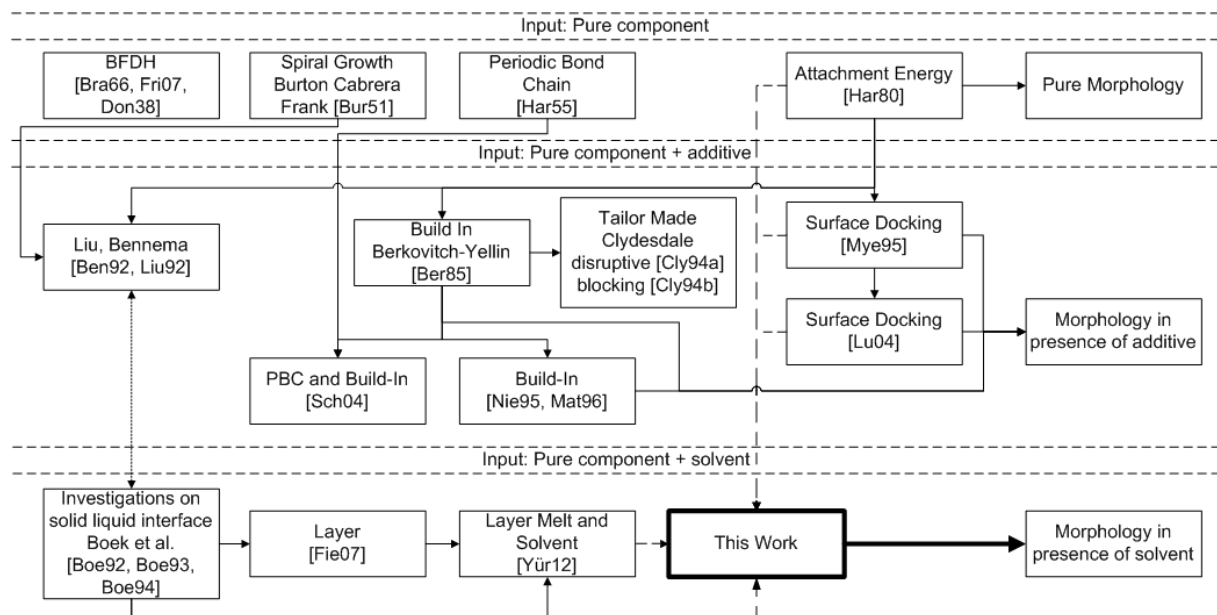
## 2.5 Presence of Solvents

Numerous investigations aimed to model the effect of solvents on the crystal morphology. A selection of those which are commonly referred to is presented in the following chapter. Additionally, it can be traced by means of the scheme given in Figure 2-1.

Boek *et al.* [Boe92, Boe93, Boe94] conducted molecular dynamics investigations on the solid-liquid interface for the pure solvent [Boe92] and the corresponding investigations on the clustering of water in the solution are presented [Boe93]. Subsequently a saturated solution consisting of solute and solvent molecules is modelled in molecules dynamics for the solid-liquid investigations [Boe94]. A detailed study is presented and provides plenty of information for a simple application in MD, since clear instructions are given in the corresponding publications. Nonetheless, the investigations do not focus on morphology prediction and estimation of the face growth rates.

The approach of Winn and Docherty [Win98] aims to predict the morphology of solution grown crystals based on the properties of pure components. The crystal structure, the internal energy of the solid and the surface free energy of the solvent is required to employ the method. It considers the 2D nucleation, the Birth and Spread Model (see e.g. Ohara and Reid [Oha73]), Spiral Growth according to Burton *et al.* [Bur51] and the occurrence of surface roughening. The provided concept aims to predict the morphology of crystals in the presence of solvents without an intensive molecular dynamics simulation of the liquid phase. Solely a computational procedure for the calculation of the attachment energy for the pure crystal is carried out, while subsequent steps proceed manually as described by Winn and Docherty [Win98]. Further works (e.g. Winn and Docherty [Win00, Win02]) improved the predicted results for the presence of polar solvents. The drawback of intensive computation on the liquid side is eliminated and the method proceeds fast.

The drawback of the aforementioned approaches for modeling the additive effect is the missing implementation of a concentration at the liquid side. The method which is presented by Fiebig [Fie07a] is a first step to overcome the issue and include the additive concentration. The presence of high amounts of various molecular species (in melt and solution) is studied in further intensive MD studies conducted by Ulrich and co-workers (see [Yür08, Yür10, Yür12, Sch11a-e]). The investigations considered the solid-liquid interface in the crystal growth process. Therein, based on the method of Boek et al. [Boe92, Boe93, Boe94] a modeling of the effect of a liquid boundary layer to the crystal morphology is conducted. Yürüdü introduced a first assumption for the calculation of the diffusion coefficients for crystal surfaces in presence of a liquid growth environment.



*Figure 2-1 Tracing of modeling approaches and methods according to [Sch11e].*

## 2.6 Summary

Regarding the presented state of the art molecular modeling achieved the possibility of a general industrial application is close. The prediction methods which are presented can provide with satisfactory results in morphology predictions of crystals for a number of compounds. In limits the presence of various additives and solvents can be modeled.

The attachment energy calculation of the pure crystal morphology is reliable for pure compounds. The modified morphology caused by the presence of additives or solvents is computed for molecules which are built into the unit cell (e.g. [Nie95]) and for the presence of one additive molecule on the crystal surface [Lu04a]. Additives in different concentrations in a melt are successfully modeled for morphology predictions [Fie07b]

but the liquid side modeling in the presence of solvents in a specific concentration [Boe92, Boe93, Boe94, Yür10] is not yet reflected in the morphology prediction.

The listing of these methods is none exhaustive, nonetheless, the literature survey revealed the lacking implementation of the concentration in the liquid side for the morphology prediction. The gap which imaged in Figure 2-1 shall be filled by the findings of the present work.

## **2.7 Aim of Work**

Technical crystallization processes in pharmaceutical and chemical industry (see for example Sanofi Aventis [Mag11], BASF [Rie11]) often involve additives and solvents in various concentrations. Some of these substances are known to have a habit modifying effect on the crystalline substance. An uncontrolled change of the crystal morphology in the production process can cause problems or even a non wanted product. Thus, it is aimed to know the potential morphological changes in the stage of the design of a crystallization process.

Different computational methods for the morphology prediction in presence of additives and solvents are developed in the recent past. The reinforced interest in the use of predictive methods in the industrial crystallization (e.g. Degussa [Hen09]) is due to the desire to reduce expenses in the production cycles by avoiding lab experiments and technical break downs as it may be caused by plugged filtration processes.

These empirical methods of computation are far developed, but not yet covering the whole range of industrial desire, since ignoring the liquid surrounding of the solid crystals and as a consequence lacking in the implementation of the supersaturation and the additive or solvent enrichment in the boundary layer.

Water enjoys high attention in industrial processes since it is not harmful if used as solvent. Hitherto, it is a specific issue in molecular modeling as up to date the focus is on the modeling of purely organics (organic crystalline substances and organic solvents), but not on inorganics as water. Furthermore, the numerous anomalies of water complicate further investigations. Moreover a number of water models were developed to illustrate and model as many properties and anomalies as possible. Thus, the selection of an appropriate water model for the morphology prediction is complicated.

This work aims to introduce a concept for the implementation of the concentration of the involved substances. The concentration and the enrichment of solute molecules in the boundary layer around a crystal should be employed in the morphology prediction. The

progress which could be achieved by the use of such a new method is demonstrated for various crystalline substances in the combination with the solvent water, what is not possible up to date.



### **3. Methods and Materials**

The investigations which are reflected in the following passages are conducted according to the schemes presented in the chapter 3.1 Methods. The general methodology in the modeling which is conducted for the subsequently presented investigations is outlined in the chapter 3.1.1 Computational. The preliminary laboratory experiments are performed as described in the chapter 3.1.2 Experimental. The focus is on the substances which are presented in the chapter 3.2 Materials.

#### **3.1 Methods**

The chapter Methods guides the reader through the employed methods in laboratory and computer experiments. The holistic and detailed reflection of methods which is developed in terms of molecular level experiments is presented as a userguide in the appendix.

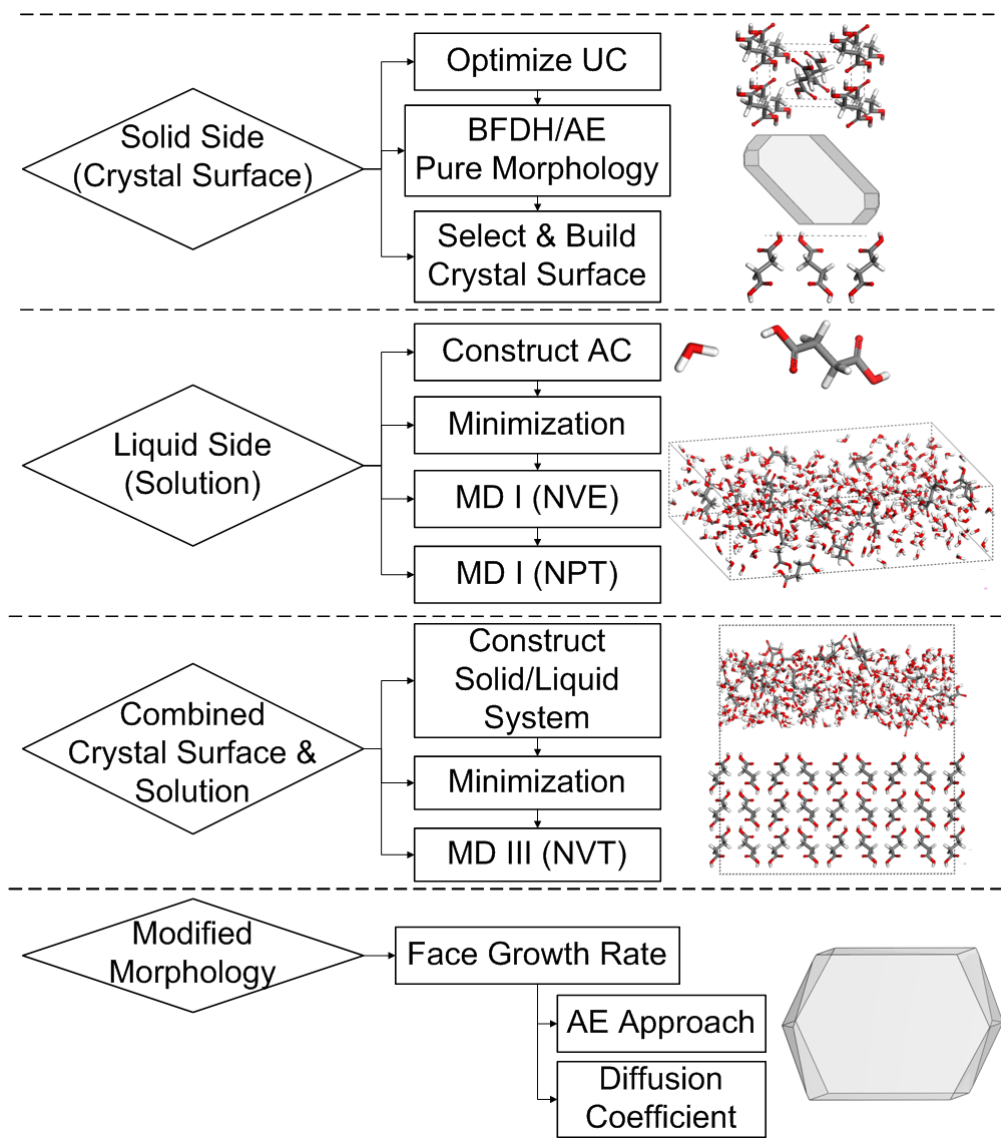
##### **3.1.1 Computational**

All molecular dynamics and morphology predictions are performed using the program MaterialsStudio 4.0 (Accelrys Inc., USA) [Acc05] with the Polymer Consistent Force Field (PCFF) [Map88]. The general procedure of modeling the modified crystal morphology with the software MaterialsStudio is developed on the basis of former works. Initial investigations on the Surface Docking theory are conducted by Lu [Lu04b]. The therein introduced methods of surface selection and construction are employed for this work. The findings of Fiebig [Fie97a] and Yürüdü [Yür10] are fundamental for the development of a method for the liquid side consideration. The herein presented approach comprises the attachment of an amorphous layer to the surface. The successful application of the new modeling procedure of this work is introduced in literature (Schmidt et al. e.g. [Sch11a, Sch11b]).

The schematic representation of the developed modeling approach which is used in MaterialsStudios 4.0 is illustrated in Figure 3-1. All details on the implementation of the subsequently presented method into this commercial software are found in the appendix. Therein a clear path with illustrations is given to enable the user to reproduce the introduced method. A rough outline of the procedure is given hereafter.

From the illustration the stepwise performance of the modeling is seen. The procedure begins on by modeling the crystalline surface as solid side. The second task is modeling the solution as the liquid side. The “production run” is a the simulation on the combined

solid and liquid system. Once these steps are conducted the morphology in presence of the liquid growth environment is obtained. The detailed modeling proceeds as follows.



*Figure 3-1 Scheme of the modeling procedure of the Layer Docking Approach.*

For the solid side consideration, the pure crystal morphology is calculated using the attachment energy method [Har80] and those faces which are morphologically important (MI) are determined. The eight most important of these faces are selected for the subsequent steps. The surfaces are cleaved from the crystal and surface boxes are built (see Appendix chapter “The Solid Side (Crystal Surface)”).

The liquid side modeling requires the construction of amorphous cells. Three sets of amorphous cells are constructed at different molecular compositions. In the first set of simulations the amorphous cells consist of solvent and solute molecules, respectively. The concentration of solute and solvent molecules is based on the experimental solubility data.

The second and third sets of simulations are carried out on amorphous systems of either solute molecules or solvent molecules. For the latter case the total of molecules is identical to the amount which is used in the mixed cell. The dimensions of the cell are predetermined by the lattice parameters of the crystal surface at which it is later attached. Therefore, eight faces of the highest morphological importance are selected and supplied with the required lattice parameters for the amorphous cell. The cells are constructed with a density which is in accordance to the experimental data for the corresponding system (see Table 3-2).

The next task is the optimization of the amorphous cell. All amorphous cells are minimized at 5,000 up to 20,000 iteration steps. The subsequent equilibration on the cell comprises 100 ps NVE (N-constant number of particles, V-constant volume, E-constant energy) and 5 ps Parrinello-Rahman [Par80, Par81] NpT (N-constant number of particles, p-constant pressure, T-constant temperature) runs. The corresponding paragraph in the appendix is entitled “The Liquid Side (Solution)”.

For the modeling of the combined solid and liquid system each of the equilibrated cells is attached to the associated surface. In this context the amorphous cell is named “*amorphous layer*”. As a constraint the atoms belonging to the surface are fixed in their Cartesian position. NVT (N-constant number of particles, V-constant volume, T-constant temperature) calculations on this setup are conducted for 100 ps at a time step of 1 fs. The NVT simulations are performed with either the Nosé [Nos84] or the Velocity Scale [Woo75] algorithms of temperature control (called “thermostats”), respectively.

The result of this “production run” is a trajectory file from which the lowest energy conformation of the system is found. The minimum energy conformation of the system is minimized for further 10,000 iterations. The obtained potential energy of the structure – containing both, crystal surface and amorphous layer is denoted as  $E_{total}$ .

Subsequently the energies of the separated structures of the surface and the amorphous layer are calculated and denoted as  $E_{surface}$  and  $E_{amorph}$ . The corresponding energy of the amorphous layer of pure solute molecules is denoted as  $E_{solute}$ . The corresponding appendix chapter is entitled “Combined Surface and Solution”.

In preparation of the morphology prediction as the remaining task the modified attachment energy is calculated. Lu and Ulrich [Lu04a] established the calculation of the modified attachment energy  $E_{att,hkl}^{mod}$  of the solid-additive system as:

$$E_{att,hkl}^{mod} = E_{att,hkl} - \frac{E_{att,hkl} \cdot \Delta b_{hkl}}{E_{b,hkl}^{solute}} \quad 3-1$$

The implementation of the liquid layer requires a new consideration for  $\Delta b_{hkl}$ . The new binding energy difference is  $\Delta b_{hkl}^{amorph}$  with:

$$\Delta b_{hkl} = \Delta b_{hkl}^{amorph} = E_{b,hkl}^{amorph} - E_{b,hkl}^{solute} \quad 3-2$$

where

$$E_{b,hkl}^{amorph} = E_{total} - (E_{surface} + E_{amorph}) \quad 3-3$$

and

$$E_{b,hkl}^{solute} = E_{total} - (E_{surface} + E_{solute}) \quad 3-4$$

The modified habit is generated based on the relation stated by Hartman and Bennema [Har80]:

$$R_{G,hkl} \sim |E_{att,hkl}^{mod}| \quad 3-5$$

The tool ‘‘Morphology’’, which is embedded in the software MaterialsStudio 4.0, is employed for the prediction of the morphology in presence of solvents (see Appendix ‘‘The Modified Morphology’’).

As an additional feature, the data obtained from the production run (NVT dynamics) allows the calculation of the diffusion coefficient [Boe92, Yür10]. The module ‘‘Discover’’ of software package MaterialsStudio 4.0 enables to calculate the mean squared displacement (MSD). Transferring the units to the SI-system provides with the simulated diffusion coefficient according to the following equation

$$D_{hkl} = \frac{B_{hkl}}{6} \cdot 10 \quad 3-6$$

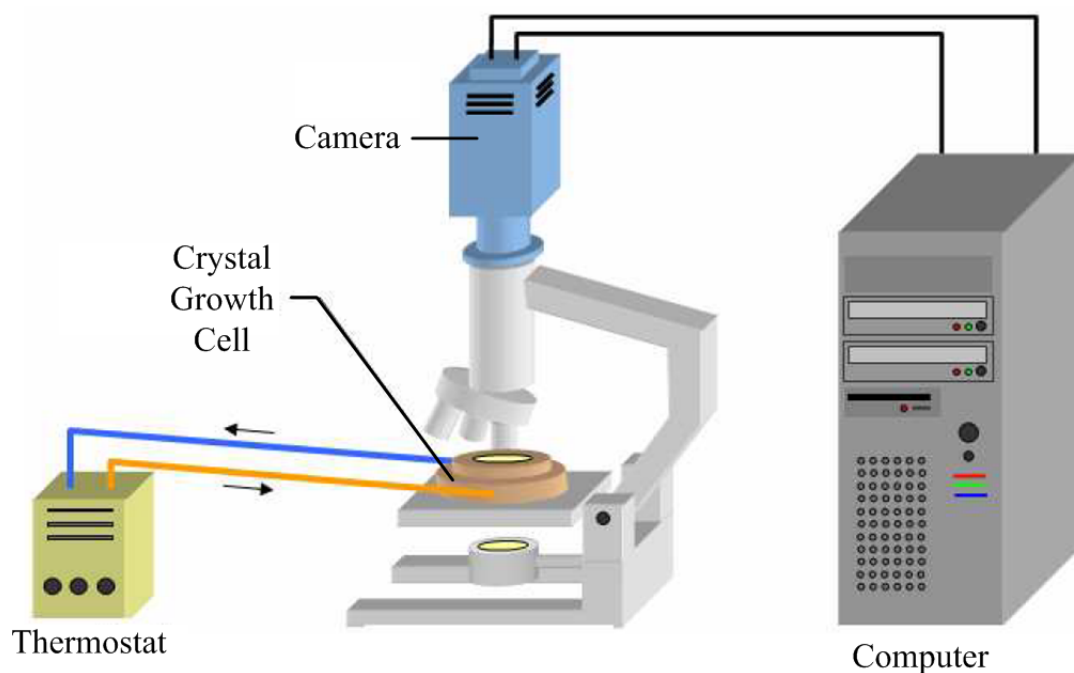
The reference value is the empirical diffusion coefficient which is calculated by means of the equation of Wilke and Chang [Wil55]:

$$D_{1,2} = 7.4 \cdot 10^{-8} \cdot \frac{(\varphi \cdot M_2)^{0.5} \cdot T}{\eta_2 \cdot (V_1)^{0.6}} \quad 3-7$$

Further information is found in the appendix where a detailed reflection of the modeling methodology and the requirements of such a modeling is provided.

### 3.1.2 Experimental

In experiments the crystals are grown from an aqueous solution. The process is observed in a double walled, temperature controlled crystal growth cell. The device is fitted with glass windows, at the bottom and the covering cap, to facilitate the observation of the crystal growth process by microscope and enable the continuous data processing via a computer (Figure 3-2). The saturated solution of solute and solvent is filled into the cell. The crystal growth is induced by seeding with crystals of the solute material and subsequent under cooling. The experiments are conducted at a temperature range of 290-310 K. The cooling rates of 0.5 to 2 K/h are employed for slow and fast induction of crystallization. The variation of the cooling rates aims to obtain crystals which are not modified by driving force. The computed morphologies are compared and validated with the experimentally found crystals.



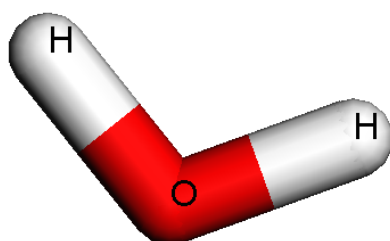
*Figure 3-2 Experimental setup of the crystal growth cell.*

## 3.2 Materials

The investigations are performed using different organic crystalline compounds with the focus on the solvent water. The present chapter gives an overview on the substances.

### 3.2.1 Solvent

The modeling is conducted using the solvent water. The schematic representation of the molecule is illustrated in Figure 3-3.



*Figure 3-3 Sketch of a water molecule.*

The investigations which are introduced in the chapter State of the Art presented selected approaches to determine crystal morphologies prior to the crystallization. It is shown that the crystal habit in presence of additives and even some solvents can be modeled. The developed models are successfully applied to a number of organic crystals, solvents [Nie97a] and additives [Sch04, Sch05].

Unfortunately, transferring these models to the non-organic solvent water still needs further investigation. Since water models were developed for special purposes, their variety seems to be unlimited. Regarding the selection of 46 water models given by Guillot in 2002 [Gui02] this fact becomes evident. The presented models are complex in their atomistic aspects as they are comprising a different total of atoms. As an example the 3-site water model contains three atoms (two hydrogens and one oxygen), the 4-site model comprises an additional hydrogen as dummy atom (three hydrogens and one oxygen, a total of 4 atoms) and the 5-site water contains two dummy atoms (a total of five atoms). In addition to this the strong variations in geometry and electrostatic properties (see Table 3-1 for a selection) are large and have contributed to the complicated application of water in the modeling methods.

Arbitrarily selecting only one of these water models for the morphology prediction would limit the holistic reflection of all relevant properties. Hence, ab initio methods are employed to the water molecules presented in Table 3-1 and a molecule with average

properties of the literature models is found. The obtained optimized water and the aforementioned selection of 3- to 5-site water models are implemented in the modeling approach according to Lu and Ulrich [Lu04a].

The effect of the initial water monomer geometry and the charges to the morphology prediction, are studied by using flexible water molecules. The impact of the initial charges on the morphology is studied by applying geometry constraints to the water molecules (rigid water). The molecule with average properties of the literature models which is found in the preliminary study is used in all of the subsequent molecular mechanics aiming for the morphology prediction of crystals in the presence of water.

*Table 3-1 Geometric and electrostatic properties of the reference water molecules.*

Model	SPC/E [Ber81]	TIP3P [Jor83]	TIP4P/E [Jor83]	TIP5P/E [Mah01]
r(OH) [Å]	1	0.9572	0.9572	0.9572
$\alpha$ (HOH) [deg]	109.28	104.52	104,52	104.52
q(H) [e]	0.41	0.417	0.52422	0.241

The crystalline substances listed in the subsequent chapter are employed as model substances. The modeling and experimental investigations are carried out for the crystalline benzoic acid, succinic acid, ascorbic acid, caprolactam and sucrose. The unit cells for these substances are obtained from the Cambridge Crystallographic Structure Database (CCSD) [Csd09]. Throughout all computer and laboratory experiments water is used as solvent.

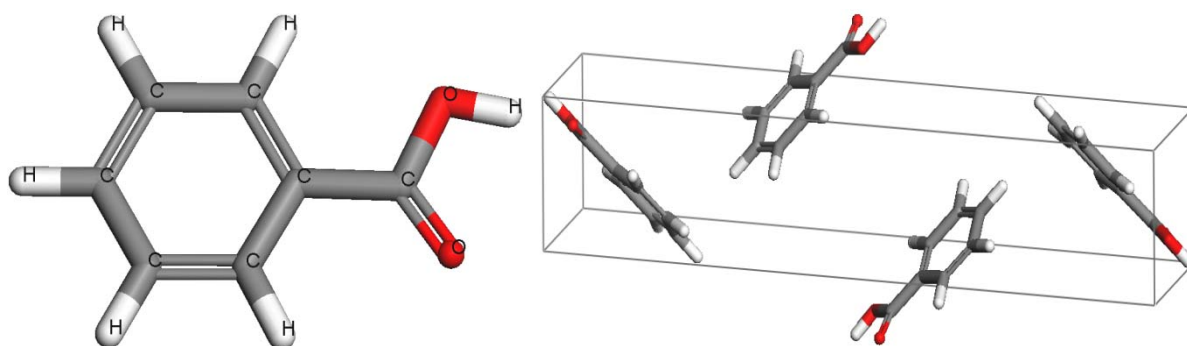
The solvent ethanol is used to extend the application of the introduced method to multi-component solutions. Since the substance is well studied, a less exhaustive preliminary investigation is required for the solvent ethanol. The ethanol molecule is optimized based on the force field methods since the parameter sets are optimized for organic substances as ethanol. The charge equilibration is obtained using the algorithm “QEq\_charged1.1” [Rap91] which is implemented in the software MaterialsStudio 4.0 [Acc05].

### 3.2.2 Benzoic Acid

The model compound benzoic acid is commonly used as food preservative in food industries, and as plasticizer in the chemical industries. In the conducted modeling

crystalline benzoic acid is used with the solvent water.

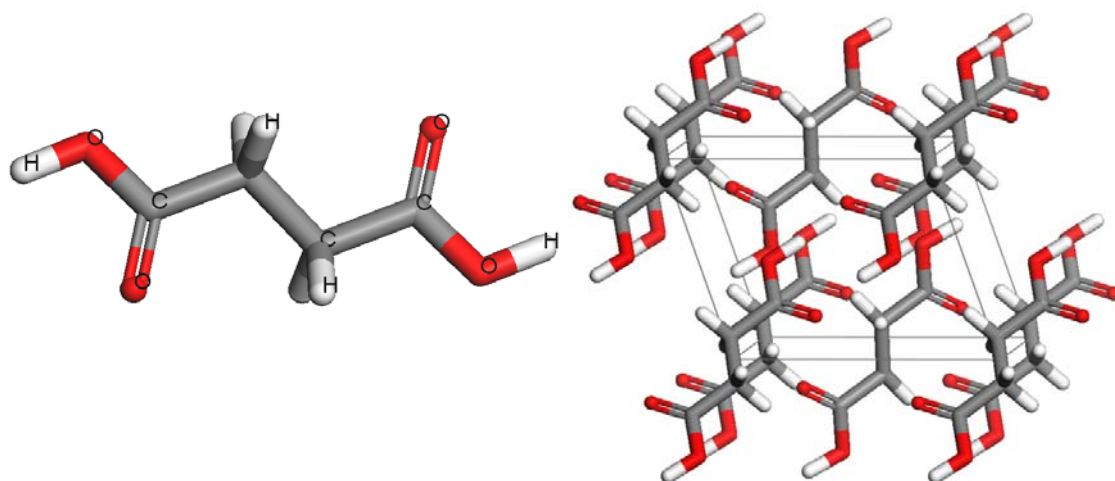
The molecular structure of the benzoic acid unit cell is determined by Feld et al. [Fel81]. The characteristics of the monoclinic unit cell as well as some thermodynamic properties are given in Table 3-2. A visualization of the unit cell and the benzoic acid molecule is depicted in Figure 3-4. In this case study benzoic acid is used as model substance with water, as well as ethanol as solvents. Via hydrogen bonding the molecules form dimers in the solution as well as in the crystal lattice.



*Figure 3-4 Benzoic Acid molecule (left) and unit cell (right).*

### 3.2.3 Succinic Acid

In this case study succinic acid is used as model substance with water and ethanol as solvents. The molecular structure of the succinic acid unit cell as presented in Figure 3-5 is determined by Leviel et al. [Lev81]. The lattice parameters of the monoclinic unit cell and selected thermodynamic properties are given in Table 3-2. According to the literature the succinic acid molecules are relatively planar and within the crystal form linear chains via hydrogen bonds.

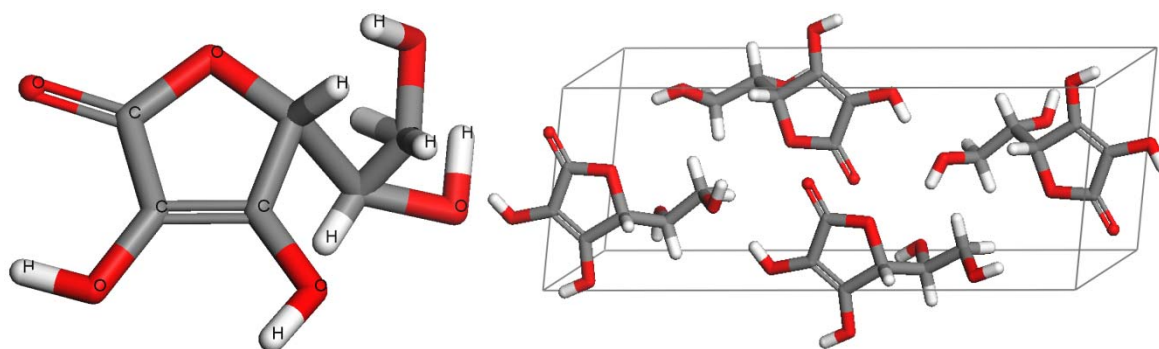


*Figure 3-5 Succinic acid molecule (left) and unit cell (right).*



### 3.2.4 Ascorbic Acid

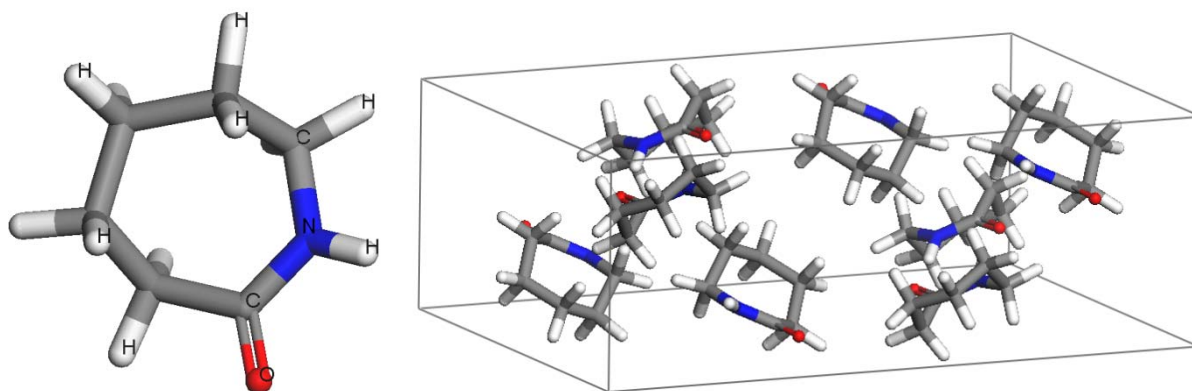
The modeling methods are applied to crystalline ascorbic acid and the solvent water. The molecular structure of the ascorbic acid unit cell is obtained from the Cambridge Crystallographic Database (CCDC) found with the deposition number: CCDC 725333 [Csd09]. The corresponding visualization of the molecule and the unit cell is presented in Figure 3-6. The characteristics of the monoclinic unit cell are and selected thermodynamic data are given in Table 3-2. It is seen from the simulations that the ascorbic acid molecules are not planar and are spatially twisted by various torsions. Within the crystal the molecules form a strong network of intermolecular bonds.



*Figure 3-6 Ascorbic acid molecule (left) and unit cell (right).*

### 3.2.5 Caprolactam

The modeling methods are applied to crystalline caprolactam and the solvent water. The molecular structure of the caprolactam unit cell is determined by Winkler et al. [Win75]. The characteristics of the monoclinic unit cell are given in Table 3-2 and the corresponding visualization is depicted in Figure 3-7.



*Figure 3-7 Caprolactam molecule (left) and unit cell (right).*

Table 3-2 Structural and thermodynamic properties of crystalline substances.

Caprolactam	Ascorbic Acid	Succinic Acid	Benzoic Acid	Space Group	Dimensions	Molecules	Molar Weight	Density (300 K)	T <sub>Melting</sub>	T <sub>Boiling</sub>	Solubility in Water (300 °C)
C2/C	P2 <sub>1</sub>	P2 <sub>1</sub> /C	P2 <sub>1</sub> /C		$a=19.28 \text{ \AA}$ $b=7.78 \text{ \AA}$ $c=9.57 \text{ \AA}$ $\beta=112,39^\circ$	8	113.16 g/mol [Ges12]	1.126 g/cm <sup>3</sup> [Ges12]	343 K [Ges12]	543 K [Ges12]	5,500 g/L [experimental]
					$a=6.396 \text{ \AA}$ $b=6.242 \text{ \AA}$ $c=17.099 \text{ \AA}$ $\beta=99.33^\circ$	4	176.13 g/mol [Ges12]	1.65 g/cm <sup>3</sup> [Ges12]	463 K (decomposition) [Ges12]	Descomposes when heated [Ges12]	333 g/L [Ges12]
					$a=5.519 \text{ \AA}$ $b=8.862 \text{ \AA}$ $c=5.101 \text{ \AA}$ $\beta=91,59^\circ$	10	118.09 g/mol [Ges12]	1.56 g/cm <sup>3</sup> [Ges12]	457 K [Ges12]	508 K [GES12]	58 g/L [experimental]
					$a=5.500 \text{ \AA}$ $b=5.128 \text{ \AA}$ $c=21.950 \text{ \AA}$ $\beta=97,37^\circ$	4	122.12 g/mol [Ges12]	1.27 g/cm <sup>3</sup> [Ges12]	395 K [Ges12]	523 K [Ges12]	2.9 g/L [Ges12]

## 4. Results

### 4.1 Water

The data presented in the following chapters are generated by the use of water as solvent. Consequently, the necessity of a careful study of the properties of water is given. The selected water models which are obtained from literature (as presented in the previous chapter 3.2.1 Solvent) are optimized by use of ab initio methods. The result is a water molecule with average properties. The data presented in this chapter are crucial for all subsequently performed steps since the optimized water molecule is implemented in the following morphology predictions of crystals in the presence of water.

The effect of the initial water monomer geometry and the charges to the morphology prediction, is studied by using flexible water molecules. The effect of the initial charges on the morphology is investigated by applying geometry constraints to the water molecules (rigid water). In a limited extend the implementation of clustering is performed.

#### 4.1.1 Molecular Optimization

The characteristic properties of the water molecule after the use of semi-empirical, ab initio (Hartee-Fock) and density functional optimization methods are given in the Table 4-1. The results of the optimized water molecules indicate significant differences for each of the applied calculation methods.

The resulting bond lengths obtained by the use of the semi-empirical method exhibit an average of 0.95 Å at fluctuations of 0.01 Å. The INDO optimization method computed a conspicuous value for the r(OH) bond. Furthermore, the use of the INDO method causes the disappearance of intramolecular bonds between the oxygen and the hydrogen atoms. The result is not the desired type of a water molecules and is excluded from further considerations. The semi-empirically determined hydrogen charges q(H) presented in Table 4-1 are lower than the charges of reference water molecules (Table 3-1). The MINDO3 method as an exception generates higher charges on the hydrogens.

The ab initio calculations are performed using the Hartee-Fock method with different basis sets. The results presented in Table 4-1 are listed according to the order of the basis set size (smallest to largest). The computed bond lengths decrease with increasing basis set. Overall a convergence of r(OH) to 0.94 Å is seen, as a consequence the obtained bond lengths are shorter than the reference values (Table 3-1). The obtained charges are close to the references of SPC and TIP3P water. The higher the chosen basis set, the closer is the

convergence of  $q(\text{H})$  to the 0.41 e. The application of the 6-311G+ (2d,p) basis set causes a significant change of the resulting hydrogen charges of 0.283. Similar charges are exposed in the results of the DFT optimizations which are carried out with the same basis set.

The results of the Density Functional Theory (DFT) calculations at different basis sets are given in Table 4-1. The optimized bond lengths are in the range 0.97 Å which corresponds to the average between the SPC and TIPxP bond lengths. Similar to the Hartee-Fock calculations, the bond lengths decreased with increasing basis set. Slight changes are caused in the molecular arrangement, hence, in the bond lengths, if the diffuse functions (indicated by the “+” in the name of the basis set) and multiple polarization functions (2p,d) are added to the basis set 6-311G.

*Table 4-1 Calculated bond lengths  $r(\text{OH})$  and charges  $q(\text{H})$  of the water molecule.*

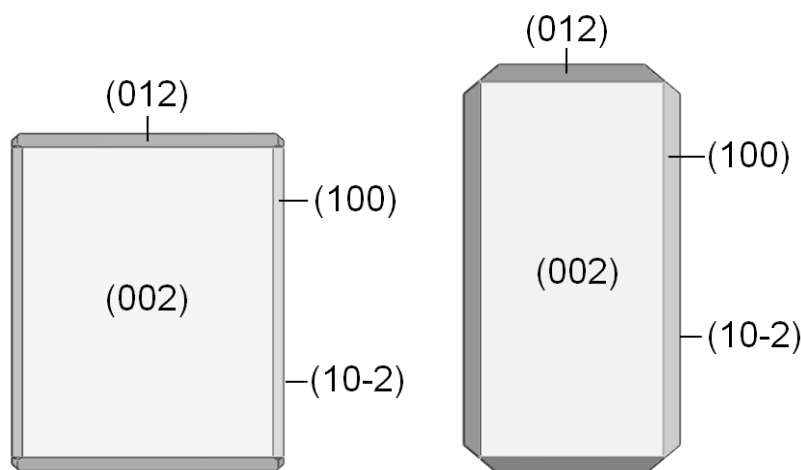
Method	$r(\text{OH})$ [Å]	$q(\text{H})$
semi-empirical		
AM1	0.9613	0.1914
PM3	0.9509	0.1793
PM3MM	0.9509	0.1793
MNDO	0.9432	0.1628
MINDO/3	0.9488	0.2526
INDO	1.0336	0.1561
CNDO	0.9572	0.1330
Hartee-Fock (HF)		
STO3G	0.9894	0.1653
3-21G	0.9667	0.3664
6-31G	0.9496	0.4056
6-311G	0.9454	0.4082
6311G+ 2d, p	0.9423	0.2830
Density Functional Theory (DFT)		
B3LYP; 6-31G	0.9759	0.3590
B3LYP; 6-311G+ 2p d	0.9631	0.2720
B3PW91; 6-31G	0.9730	0.3710
B3PW91; 6-311G+ 2p d	0.9611	0.2740

### 4.1.2 Water in Morphology Predictions

In the following chapter the effect of the employed water molecule on the crystal morphology is exemplarily presented for the model substance benzoic acid. The morphology prediction is conducted using the water molecule as obtained from the DFT optimization using the B3PW91 (basis set) 6-31G. In the following chapters, the optimized water molecule will be denoted as DFT. Additionally, the presented 3- to 5-site reference water models are employed in the morphology prediction using the surface docking method which is introduced by Lu and Ulrich [Lu04a]. The aim is to obtain the comparison of the performance of the models for the application in the morphology prediction.

## 4.2 Benzoic Acid

The pure morphology of benzoic acid crystals is presented in Figure 4-1. The computation of the morphologies is obtained for the BFDH and the subsequent attachment energy calculation by means of a computational routine which is implemented in the commercial software, based on vapour or melt crystalliation (no solvent).



*Figure 4-1 Pure morphology of a benzoic acid crystal: BFDH (left) and Attachment Energy (right).*

The prediction of the morphologies in presence of the additive or solvent is conducted on the basis of molecular dynamics simulations. The aim is to investigate on the interactions of solvent or additive molecules with the molecules of the surface, the solid crystalline phase. Thus, it is crucial to be familiar with the molecular structure of the considered crystal surfaces. The following paragraph gives such analysis for the benzoic acid crystal.

### Structure of the Crystal Surface

Benzoic acid is a polar molecule which is consisting of a nonpolar phenyl ring and a polar moiety, the carboxylic group. This group has a positive site - the carbonyl - and the negative site - the hydroxyl moiety. The molecules within a crystal are oriented along a polar axis [Mer01]. One end of the axis exposes the carboxylic group and the other end the phenyl ring.

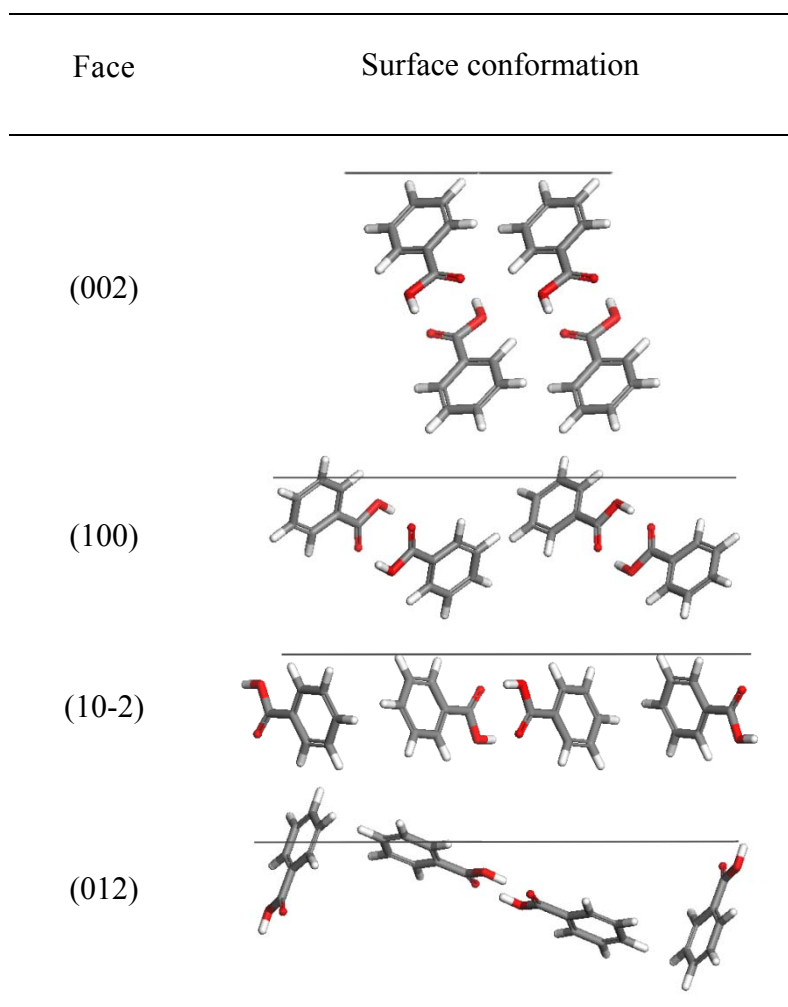
The benzoic acid crystal has polar faces which are covered by polar moieties. Polar solvents - as water - prefer to interact with polar faces [Ber85]. In the following section presents the classification in the polarity of the morphological important faces of the benzoic acid crystal according to the method of Hengstermann [Hen09].

The attachment energy calculation provides with the most important visible faces which are (002), (100), (10-2) and (012), respectively. The molecular arrangements of these faces are presented in Table 4-2. The mapping of face (002) illustrates a plane face which is covered by hydrophobic phenyl rings. Thus, the face is classified as nonpolar. The wavy face (100) and the plane face (10-2) are covered by dimers of benzoic acid. These faces are semi-polar. Despite the moieties are accessible for the interaction with the water molecules, all the carboxylic groups are engaged in dimerbonding. Additionally, the hydrophobic phenyl rings on the faces inhibit the interaction of water with the carboxyl moieties. The face (012) is characterized by a wavy structure and the surface is covered by non-bonded benzoic acid monomers. The polar moieties are oriented perpendicular to the surface. Polar molecules as water can interact with this surface and can lower the growth rate [Hol99]. Hence, the face is classified as polar.

#### **4.2.1 Surface Docking Method**

In the following chapter outlines the effect of the selected water model on the crystal morphology of benzoic acid when using the surface docking method. The morphology prediction is conducted using the water molecule as obtained from the DFT optimization using the B3PW91 (basis set) 6-31G. Additionally, the presented 3- to 5-site reference water models (Table 3-1) are employed with the modeling approach. For this purpose the morphology prediction is carried out based on the surface docking method as introduced by Lu and Ulrich [Lu04a]. The conducted modeling comprises molecular dynamics calculations and a subsequent minimization for the crystal faces. The details on the modeling procedure is found with the appendix (chapter "The Surface Docking Method").

*Table 4-2 Surface conformations of a benzoic acid crystal.*



*Impact of Water on the Morphology Prediction*

The morphologies of pure benzoic acid crystals and modified crystals in the presence of various water molecules are illustrated in Table 4-3. The focus is on the pure morphology. It is seen from the corresponding illustration of the crystal that the nonpolar face (002) is the most important face. An interaction of the polar molecule water with this nonpolar face can be excluded and, as a consequence, the absolute growth rate will not be lowered. In contrast to this the semipolar and polar faces (100), (10-2) and (012) expose an increasing degree of the polarity. Thus, the water molecule will strongly interact with these faces and the growth rate will be affected. Polar faces grow slower in the presence of water and, thereby, they remain important (visible) on the crystal habit. In contrast, the nonpolar faces grow relatively fast until they do completely lose their visibility (morphological importance). As a consequence, the morphology of the benzoic acid crystals will be modified, if crystallized from an aqueous solution.

The prediction of the morphology of benzoic acid crystals in presence of water is performed according to the surface docking method. The procedure is based on molecular dynamics where the position of the water molecules can change. A modification of the initial molecular geometry in MD is only possible, if the flexible body assumption is applied. Herein, the atoms bonded in a molecule can move freely to any Cartesian position independently from each other. The atoms of the rigid molecule restricted in their ability to move in the molecular dynamics simulation, since a rigid molecule is constrained to fixed OH-bond lengths and HOH-angles. Nonetheless, the whole molecule can change its Cartesian position. The results presented in the Table 4-3 confirm the impact of the constraints on the interaction of the water molecule with the surface and, hence, the morphology prediction.

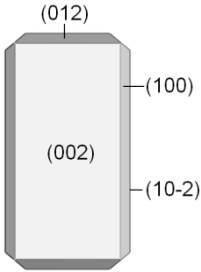
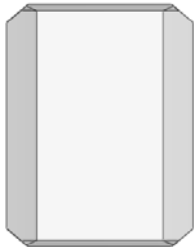







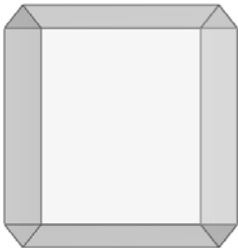

The presented morphologies indicate which molecules interact with the crystal and modify the habit. Particularly with regard to the geometry constraint, the morphological changes depict the effect of the initial geometry and the charges, respectively. This allows a conclusion of the effect of the initial water model on the modified morphology.

The test showed that all water models are able to simulate the water effect on a non-polar face. Significant differences are observed on the semi-polar and polar surfaces. Here, the SPC, as well as 4- and 5-site water models showed a weak performance in terms of surface interaction. The SPC water model predicted too high modified attachment energies the polar surfaces. The 3-site water models DFT and TIP3P did not exhibit weak points in terms of surface interaction. Similar morphologies are computed by both models. Conspicuous morphologies are obtained depending on the geometry constraint. As a consequence, the constraint can effect the predicted morphology.

The findings derived from modeling are related to the experimental results. As a consequence for the morphology prediction it is sufficient to employ the DFT water model as a flexible molecule (without any constraint) in the modelings. The benefit of choosing the flexible DFT water is seen with the surface docking method as well as in the modeling conducted for the liquid phases.



*Table 4-3 Predicted morphologies of benzoic acid crystals in the presence of water [Sch11a].*

Pure Morphology (Attachment Energy)		
		
Watermodel	Constraint	
	flexible	rigid
DFT		
SPC		
TIP3P		
TIP4P		
TIP5P		

### 4.2.2 Layer Docking Method

The results of the Layer Docking method are presented starting with the results for the liquid side modeling and modeling for the combined liquid and solid side. Finally the result of the morphology prediction is illustrated.

#### *The liquid side*

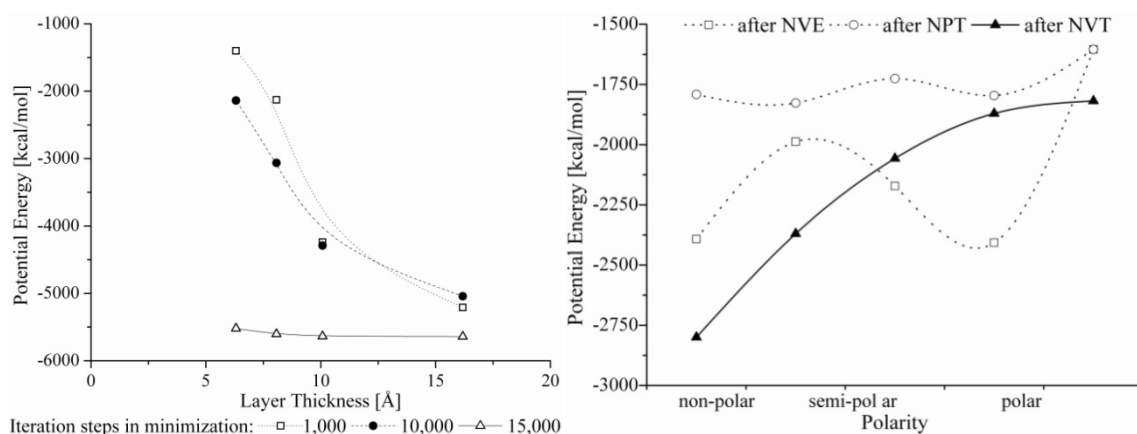
The amorphous cells are optimized at different steps as described in the previous chapter. The plot presented in Figure 4-2 left depicts the impact of the intensity of the minimization of the amorphous system. An inverse proportionality of the thickness of the solution layer to the optimization steps required for an energy minimization is observed (Figure 4-2 left). Despite every AC has the same molecular composition more iteration steps are necessary for thin layers. Performing 15,000 iteration steps ensures to achieve the adjustment of energy for various layer thicknesses. The smallest dimension of the lattice of the solution layer should not be lower than 5 Å. Increase of the parameter will significantly lower the amount of minimization steps required for optimization as seen from Figure 4-2 (left). Furthermore, minimizing the system at a higher intensity (e.g. 15,000 iterations) a significant lower potential energy is obtained in the following steps of the modeling procedure (e.g. after the MD [Sch11d]).

The graph in Figure 4-2 right depicts the potential energies of the amorphous cell (liquid system) in various stages of the MD simulations. The simulations with the NVE and NPT ensemble are conducted without any surface contact of the solid and liquid phase. The results of the NVT simulations reflect the impact of the polarity in the simulations. In case of surface contact an increasing polarity affects the potential energy of the liquid side.

The optimization of the solution layer as the liquid side is the initial step of the presented procedure. Differently sized systems require modified conditions in the optimization procedure. The number of atoms in the system as well as the lattice dimensions may affect the time consumption in the optimization.

#### *The liquid and the solid side*

The MD simulations on the layered system of solution and crystal surface comprised 100 ps of NVT dynamics simulation (NVT ensemble) followed by a minimization. The corresponding diffusion coefficients are presented in Figure 4-3.



*Figure 4-2 Left: Potential energy according to the iterations steps in minimization for various layer thicknesses. Right: Potential energy in different stages of the simulation, depending on the polarity of the surface [Sch11d]. (Lines are plotted for a better visualization of the trend, but do not represent a steady graph.)*

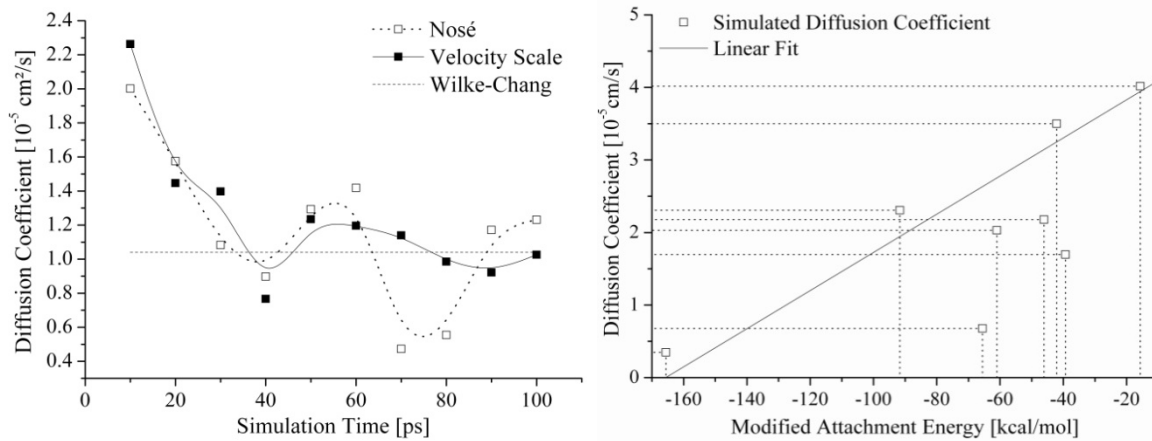
### Thermostats

The computation time required to approach the empirical diffusion coefficient can be reduced depending on the method of temperature control used in the NVT dynamics [Sch11d]. In this context the computation time is lower when employing the Velocity Scale method [Woo75] of temperature control at NVT runs (Figure 4-3 left). The use of the Nosé temperature control [Nos84] is not accomplishing the estimation of the diffusion coefficient in agreement with coefficient according Wilke-Chang [Wil55]. Augmenting the duration of the MD simulations can overcome this drawback, but is time consuming.

### Diffusion coefficient

The diffusion coefficient is obtained from the NVT simulations on the layered system of the solid and the liquid phase. Plotting the diffusion coefficient over the modified attachment energy is indicating a linear trend (Figure 4-3 right). The strong initial decrease of the diffusion coefficient (Figure 4-3 left) in early simulation time is due to equilibration after the (manual, forced) combination of the crystal surface and the solution layer.

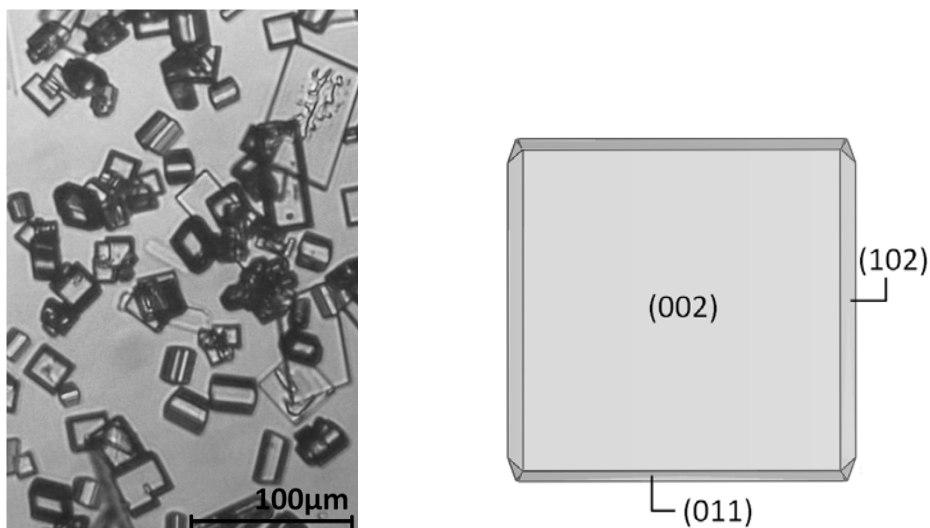
The diffusion coefficient and the attachment energy are related to the growth rate of a crystal face. The direct proportionality is a proof for the correctness of the estimated diffusion coefficient. Consequently the use of the determined diffusion coefficients for the morphology prediction is justified.



*Figure 4-3 Left: Diffusion coefficients on a crystal surface estimated within a 100 ps NVT simulation. The Velocity Scale and the Nosé algorithms are employed for temperature control. Right: Diffusion coefficient vs. Attachment energy of the corresponding face.*

#### Morphology prediction

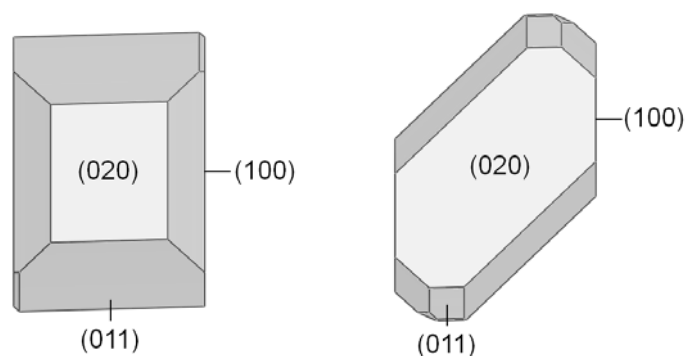
The experimental morphologies of benzoic acid crystals obtained by cooling crystallization are depicted in Figure 4-4 (left). The morphology which is computed by means of the diffusion coefficient is seen in Figure 4-4 (right). The morphology predicted with the new modeling approach is in good agreement with the experimentally found crystals. Hence, modeling the diffusion coefficient is an appropriate method to estimate the morphology in presence of solvents and hence, the face growth rate.



*Figure 4-4 Left: Experimental morphologies of benzoic acid crystals grown from aqueous solution. Right: Morphology of a benzoic acid crystal predicted by means of the diffusion coefficient.*

### 4.3 Succinic Acid

The pure morphology of a succinic acid crystal is computed based on the method of Bravais, Friedel, Donnay and Harker and a subsequent use of the attachment energy method. The resulting morphologies of the pure crystal are illustrated in Figure 4-5.



*Figure 4-5 Pure morphology of a succinic acid crystal: BFDH (left) and Attachment Energy (right).*

The molecular conformation of selected surfaces is presented in Table 4-4. In the visualizations an obvious distinguishing between polar and semi polar is seen. The face (020) consists of non-polar (hydrophobic) molecular arrangements as well as polar regions. The faces (011) and (100) exhibit a clearly polar structure consisting of carboxyl moieties directed perpendicular to the surface. Thus, a different interaction with a polar solvent molecule is expected.

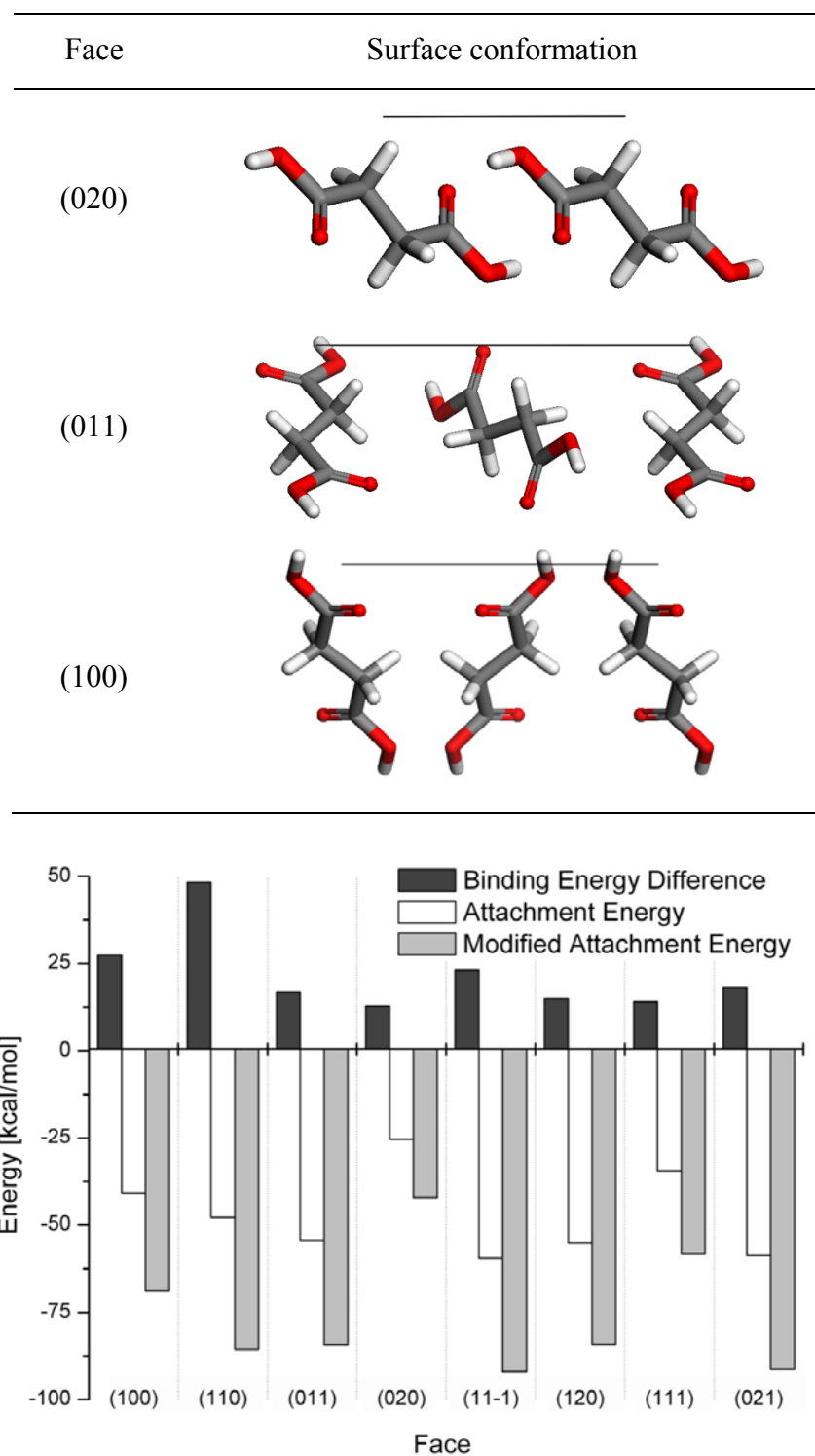
#### 4.3.1 Surface Docking Method

The computed energies in presence of the DFT-water model are presented in the chart of Figure 4-6. The absolute modified attachment energy for the face (020) is the lowest. Thus, the face which is covering the largest share of the pure and the modified crystal is the face (020). Furthermore, it is seen from the bar chart that the binding energy difference for this face is the lowest. The preferential interaction of water molecules with specific faces is indicated by a high binding energy. Consequently, the thereby affected faces exhibit higher absolute attachment energies and cover a lower share of the crystal surface.

The pure as well as the modified morphologies are presented in Table 4-5. Slight morphological modifications are observed depending on the thermostat algorithm which is employed for the temperature control in MD. This is seen in case of employing flexible

water models. In contrast the morphological changes which are induced by the geometry and the charges of water model (rigid) are low. Looking at the morphologies which are generated in the presence of rigid water shows no significant differences.

*Table 4-4 Molecular structure of selected surfaces of a succinic acid crystal.*



*Figure 4-6 Binding energy differences, attachment energy of the pure morphology and modified attachment energy of the succinic acid crystal.*

### 4.3.2 Layer Docking Method

The computation which is conducted in terms of the layer docking method comprised different steps. Firstly, the amorphous cell is generated, followed by the aforementioned optimization procedure and the subsequent combination of the optimized amorphous cell (liquid phase) and the crystal surface (solid phase).

#### The liquid side

The amorphous cell is optimized stepwise. The potential energies computed for the single steps are plotted in the Figure 4-7. The presentation comprises three different compositions of the cell: pure succinic acid molecules, pure water molecules and a solution containing a mixture of succinic acid and water molecules. The initial energies for all of the mentioned compositions are clearly optimized after the NPT.

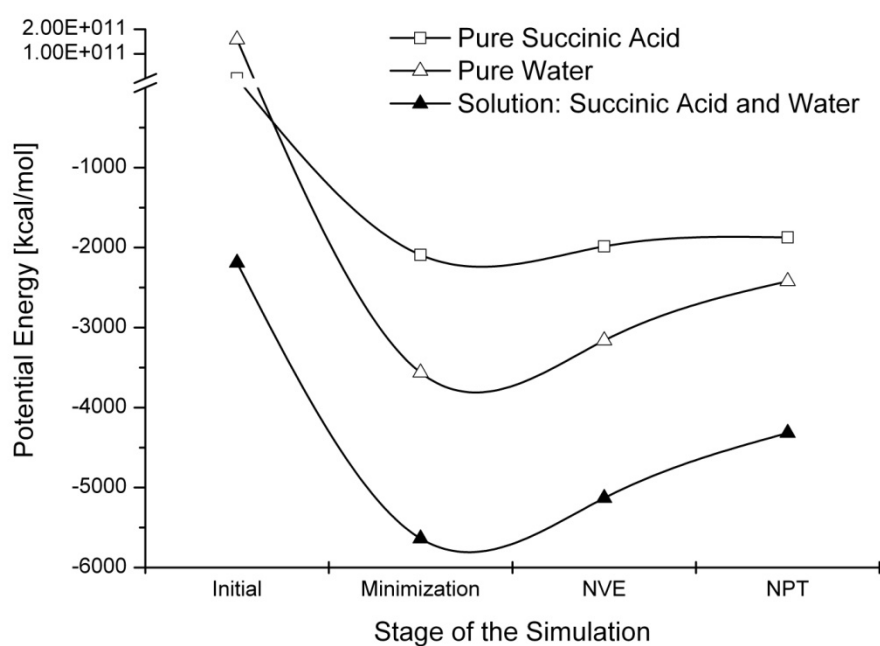
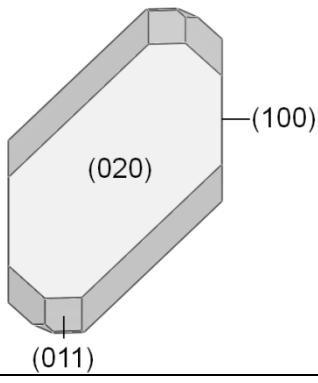
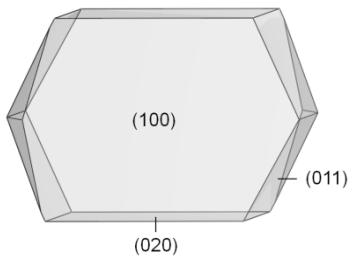
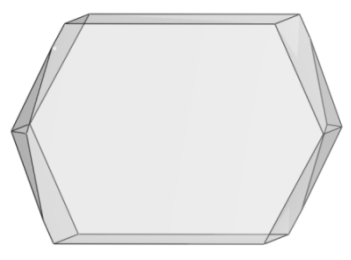

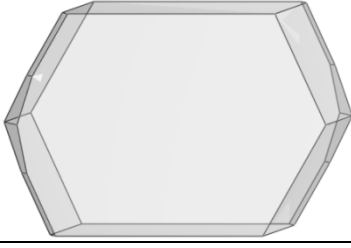
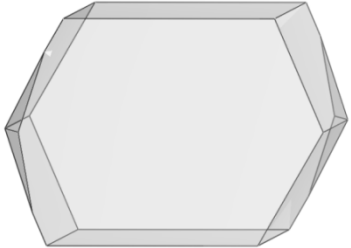
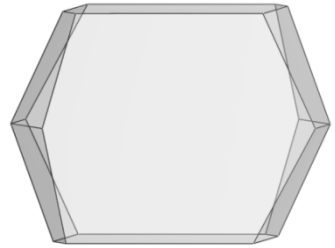
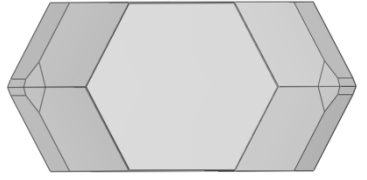
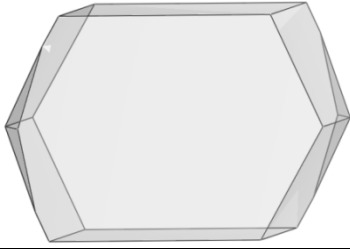


Figure 4-7 Potential energy of the amorphous cell at various simulations stages in the optimization procedure.

*Table 4-5 Predicted morphologies of succinic acid crystals in the presence of water [Sch11a].*

Pure Morphology		
		
	Constraint	
Watermodel	flexible	rigid
	DFT	
Nosé		
Velocity Scale		
	TIP3P	
Nosé		
Velocity Scale		



### The liquid and the solid side

The graphs presented in Figure 4-8 show the characteristic slope of the diffusion coefficient within the simulation time. The first third of the simulation time is characterized by slight fluctuations due to the equilibration. In the last third of the simulation time the diffusion coefficient is intensively fluctuating. The final fluctuation is due to the mathematical approximation done for the calculation. To ensure a fast computation the values for the MSD are only approximated, but not calculated in detail. Thus, the fluctuation in the final part of the calculation is more and more increasing.

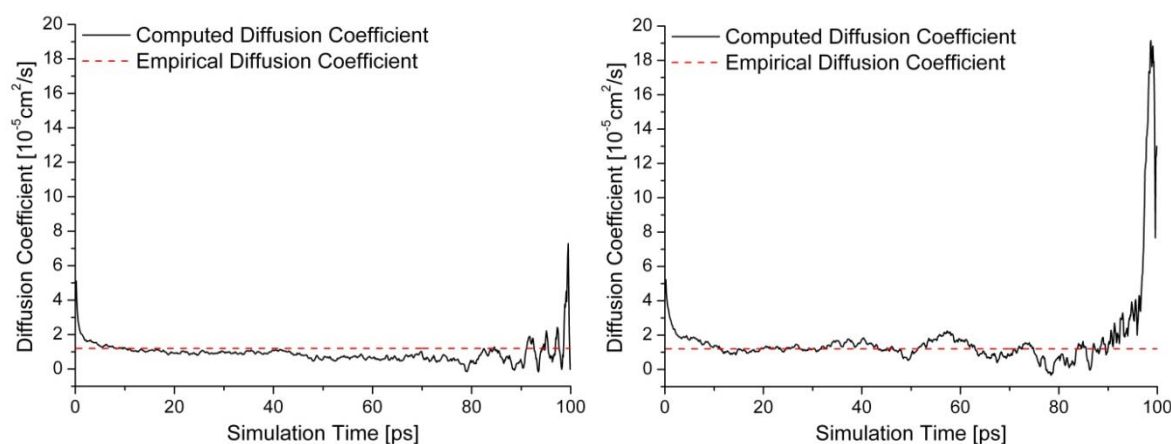


Figure 4-8 Diffusion coefficients computed for the faces (100) (left) and (011) (right) of a succinic acid crystal. Composition of the liquid side: DFT water and succinic acid molecules.

The data presented in Table 4-6 contains the average of the diffusion coefficient within the second third of the simulation time, here: from 33 to 66 ps. As seen from the graphs in Figure 4-8 the diffusion coefficients computed within the aforementioned limits of the simulation time is not identical for all surfaces. It can differ strongly depending on the surface. These variations are due to the surface structure. As an example the diffusion coefficient of face (020) is high. An illustration of the structure is seen in Table 4-6.

Table 4-6 Diffusion coefficients computed for the faces of a succinic acid crystal. Composition of the liquid side: DFT water and succinic acid molecules.

Face	(020)	(011)	(110)	(111)	(100)	(11-1)	(021)	(120)
$D_{hkl}$ [ $10^{-5} \text{ cm}^2 \text{ s}^{-1}$ ]	1.708	1.403	1.312	0.884	0.771	0.608	0.511	0.461
$D_{empirical}$	1.200							

### Morphology prediction

By means of the Layer Docking approach the modified morphology is calculated either with the established attachment energy approach or via the diffusion coefficient. The diffusion coefficient is related to the face growth rate. The morphologies predicted with these methods are presented in Figure 4-9.

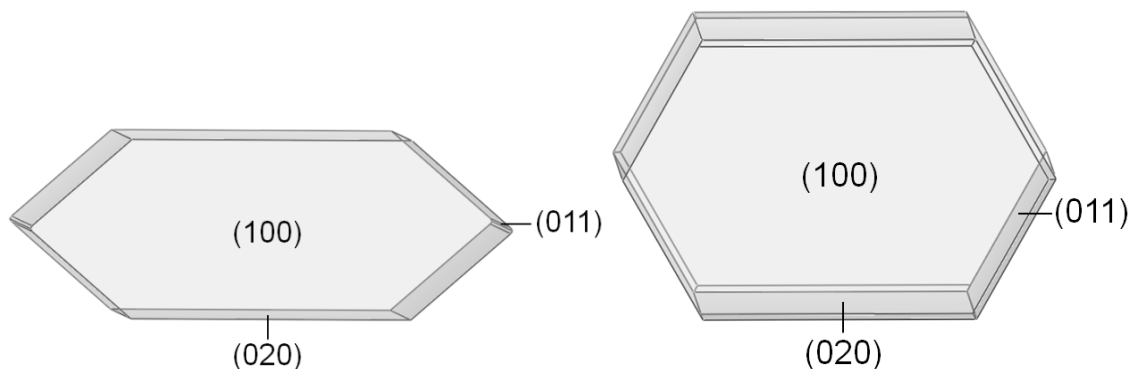


Figure 4-9 Morphologies of succinic acid crystals grown in from an aqueous solution predicted with the Layer Docking method. Right: via established attachment energy approach. Left: via diffusion coefficient.

### 4.4 Ascorbic Acid

The pure morphology of an ascorbic acid crystal is computed based on the method of Bravais, Friedel, Donnay and Harker and a subsequent use of the attachment energy method. The resulting morphologies are illustrated in Figure 4-10. The molecular conformation of selected surfaces is presented in Table 4-7. It is seen that the face (100) is strongly characterized by the presence of polar moieties. The faces (001) and (110) are covered by non-polar regions of the ascorbic acid molecules but predominantly exhibit a polar surface via the presence of polar moieties.

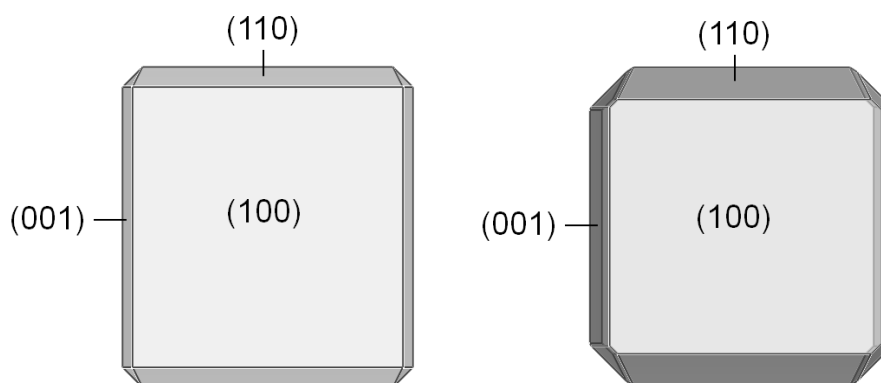
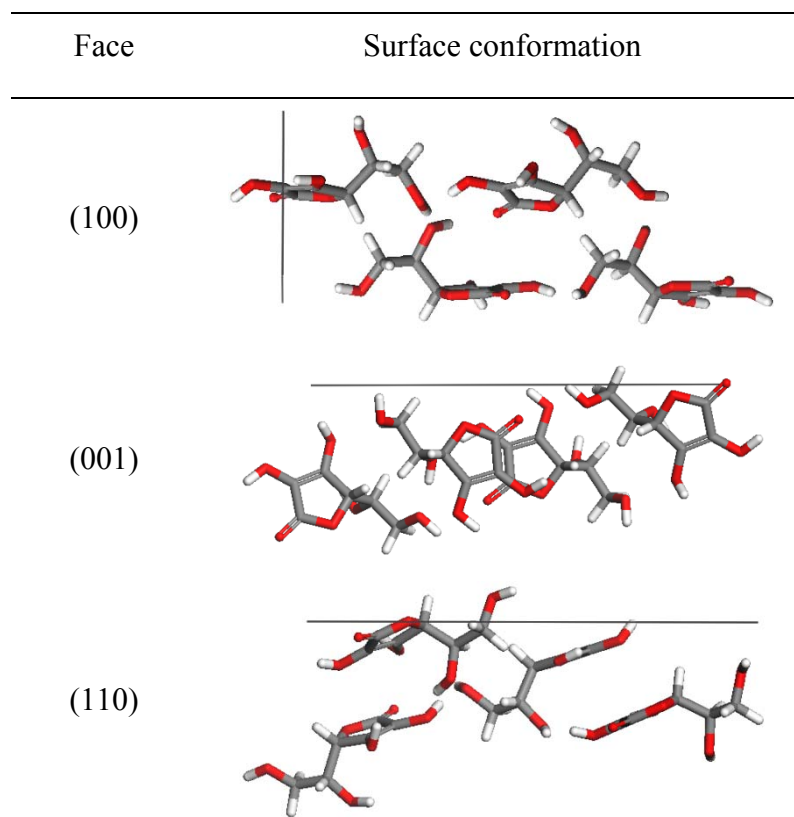


Figure 4-10 Pure morphology of a ascorbic acid crystal: BFDH (left) and Attachment Energy (right).

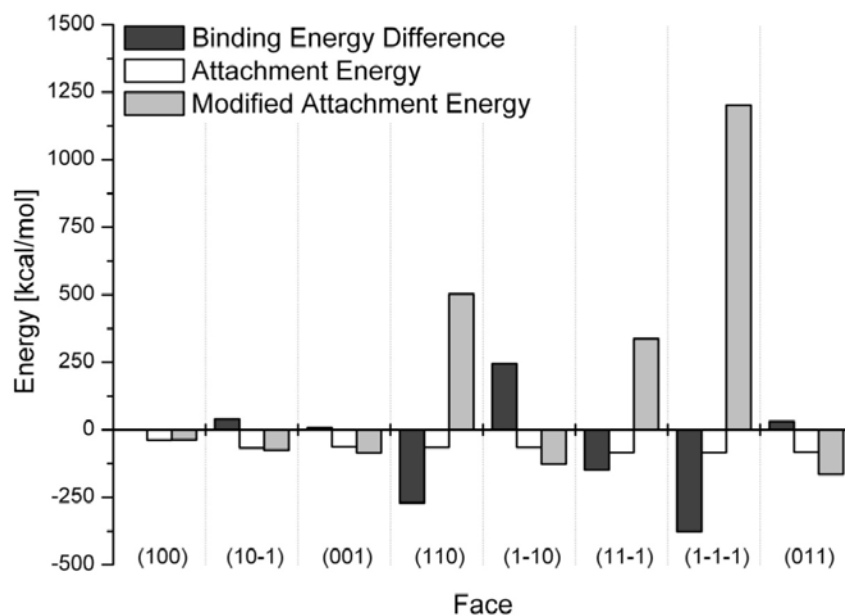
*Table 4-7 Molecular structure of selected surfaces of an ascorbic acid crystal.*



#### 4.4.1 Surface Docking Method

The energies computed for the presence of the DFT-water model are presented in the chart of Figure 4-11. The lowest absolute modified attachment energy is observed for the face (100). This face is covering the biggest share of the modified crystal in the presence of water. Consequently, the binding energy difference for this face is the lowest. The largest absolute attachment energy is observed for the face (100) and (1-1-1). The face (100) remains visible on the crystal surface, whereas the face (1-1-1) disappears.

The corresponding crystal morphology is presented in Table 4-8. Morphological changes in the presence of water are observed experimentally and in the modeling. The modelled morphology is obtained from the application of the Surface Docking method. The experimental crystal growth is induced by cooling crystallization from an aqueous solution.



*Figure 4-11 Binding energy differences, attachment energy of the pure morphology and modified attachment energy of the ascorbic acid crystal.*

*Table 4-8 Morphologies of ascorbic acid crystals pure and grown from aqueous solution.*

Pure Morphology	
Predicted Morphology	Experimental Morphology

#### 4.4.2 Layer Docking Method

The computation which is conducted in terms of the layer docking method comprised different steps. Step one is the amorphous cell construction, followed by an optimization procedure and the alignment of the optimized amorphous cell (liquid phase) and the crystal surface (solid phase). The results for ascorbic acid in an aqueous solution with the DFT water model are presented hereafter.

##### The liquid side

The results on the stepwise optimization of the amorphous cell as the liquid side are presented in the chart of Figure 4-12. The plot shows the potential energies at the single steps of the procedure. The chart shows different compositions of the cell: pure ascorbic acid molecules and the solution containing a mixture of ascorbic acid and water molecules. The initial energies for these compositions are clearly lowered in the minimization. Further optimization is achieved in the molecular dynamics. In the second NVE step (after the NPT) the energy is slightly lowered back to the level after the first NVE step. Thus, conducting a second NVE is not essential in terms of energetic optimization.

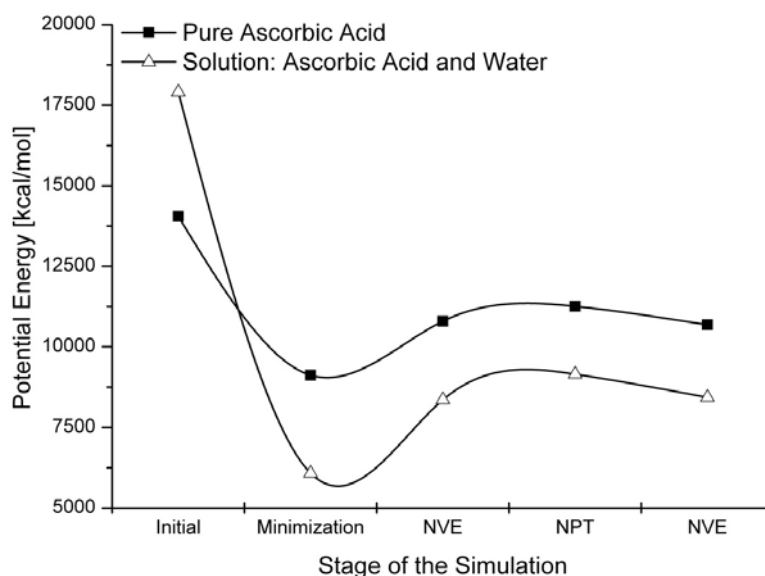


Figure 4-12 Potential energy of the amorphous cell at various simulations stages in the optimization procedure.

##### The liquid and the solid side

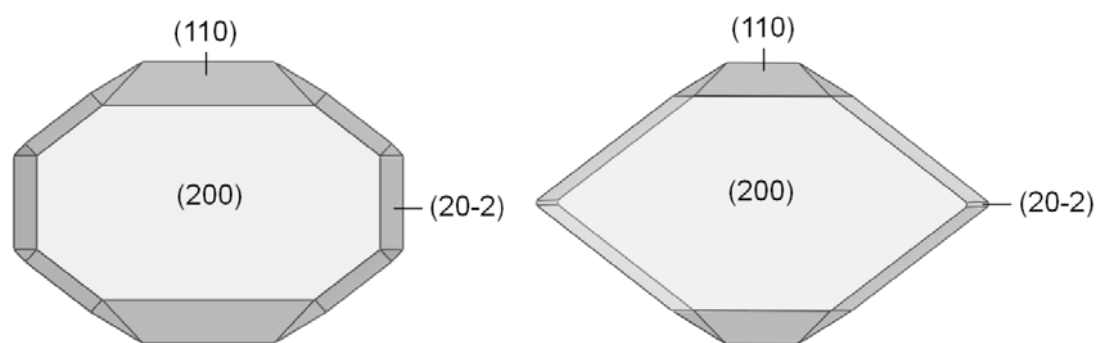
The simulations on the combined liquid and solid side could not be conducted for the present investigations. Building a layered system of the amorphous cell and the crystal surface

itself is possible. However, starting the subsequent molecular dynamics on the layered system is not possible. For this reason the diffusion coefficient is not determined.

#### 4.5 Caprolactam

The pure morphology of a caprolactam crystal is generated based on the method of Bravais, Friedel, Donnay and Harker and a subsequent use of the attachment energy method. The computed morphologies are illustrated in Figure 4-13.

The molecular conformation of selected surfaces is presented in Table 4-9. The face (200) is covered by a non-polar molecular arrangement. The faces (110) and (20-2) exhibit non-polar regions of the molecules but furthermore, the polar moieties of the molecules are accessible for interaction.

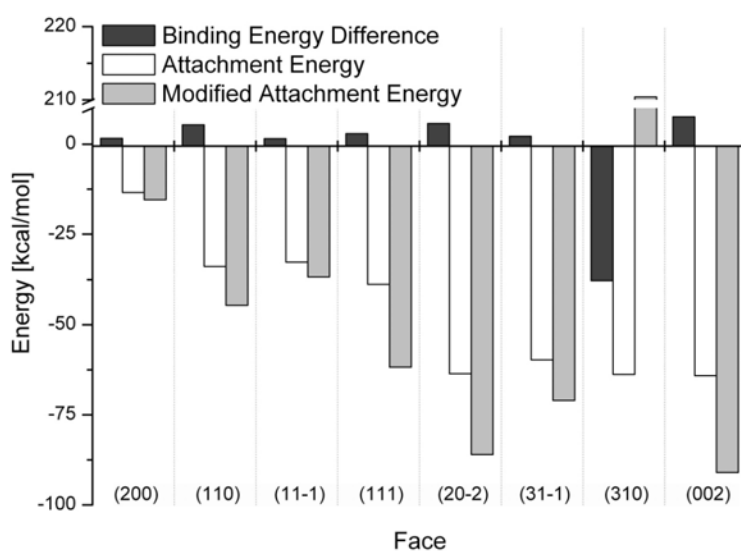
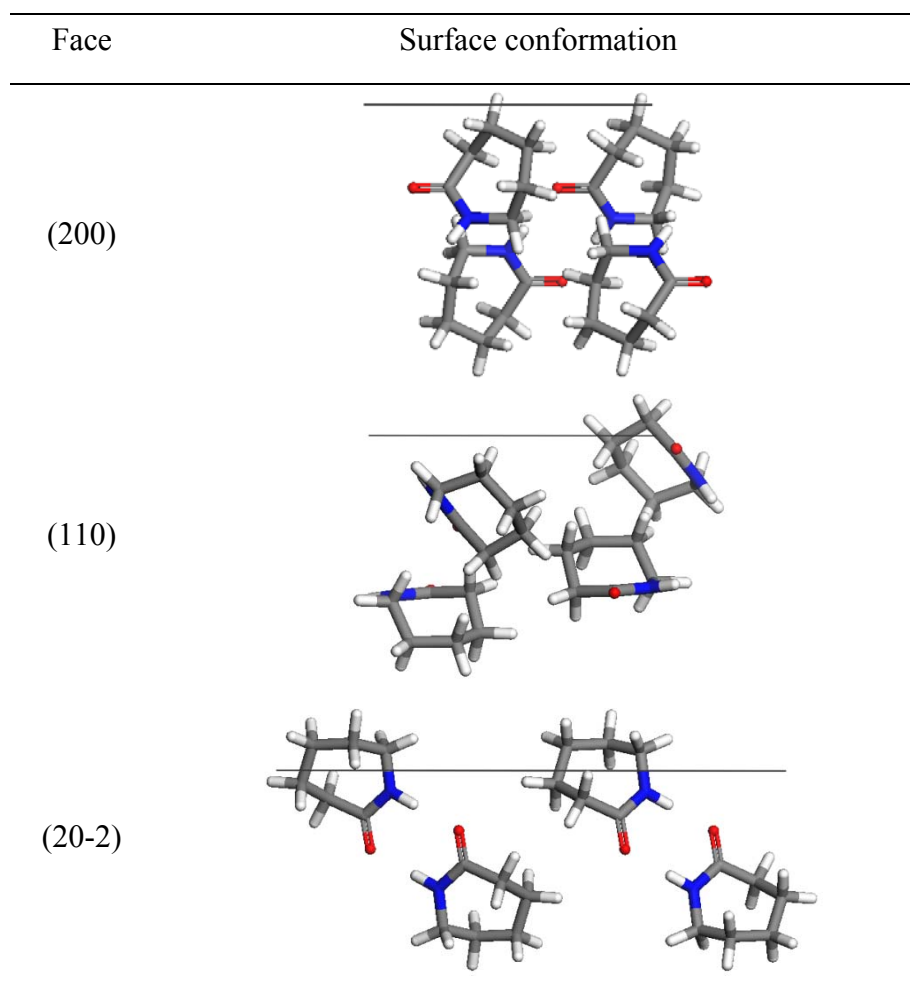


*Figure 4-13 Pure morphology of a caprolactam crystal: BFDH (left) and Attachment Energy (right).*

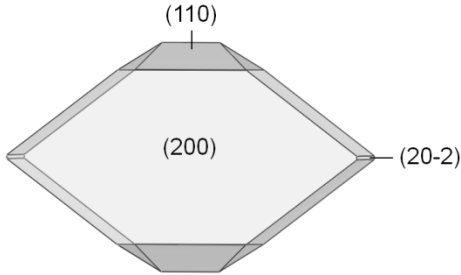
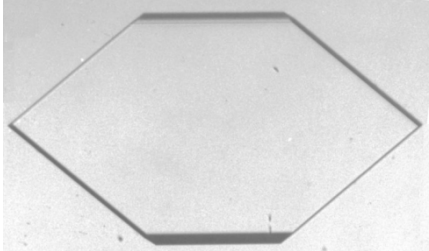
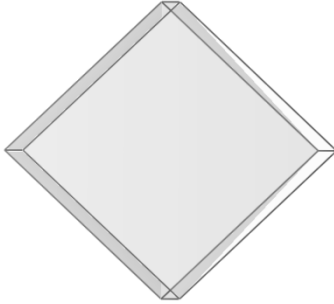
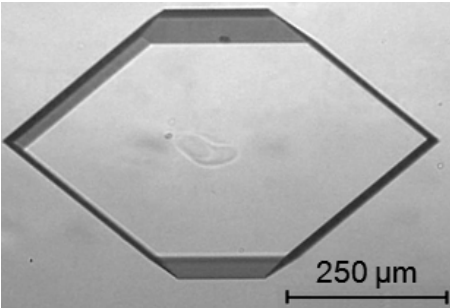
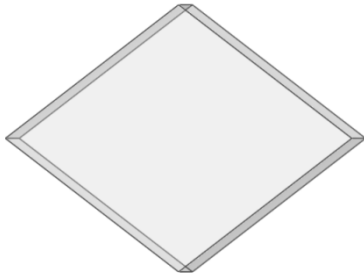
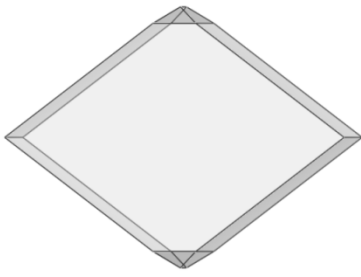
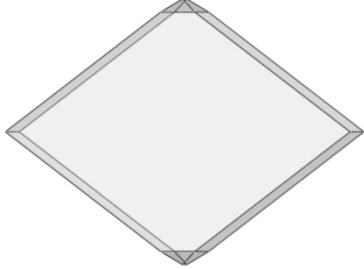
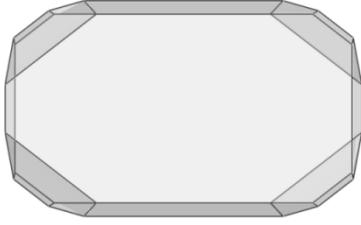
##### 4.5.1 Surface Docking Method

The energies computed for the presence of the DFT-water model are presented in the bar chart of Figure 4-14. The lowest absolute modified attachment energy is calculated for the face (200). Thus, the face covers the largest share of the modified crystal in the presence of water. The largest absolute attachment energy is observed for the faces (20-2) and (002). The faces do not remain visible on the crystal surface of the modified crystal.

The corresponding crystal morphology is presented in Table 4-10. Morphological changes in the presence of water are observed experimentally and in the modeling. The modelled morphology is obtained from the application of the Surface Docking method. The experimental crystal growth is induced by cooling crystallization from an aqueous solution.

*Table 4-9 Molecular structure of selected surfaces of a caprolactam crystal.**Figure 4-14 Binding energy differences, attachment energy of the pure morphology and modified attachment energy of the caprolactam crystal.*

*Table 4-10 Morphologies of caprolactam crystals: pure [Nie95] and in the presence of water.*

		Pure Morphology	
			
		Morphology	
Thermostat		Watermodel: DFT	Experimental
Velocity Scale			
		Watermodel: TIP3P	Watermodel: SPC
Nose			
Velocity Scale			



### 4.5.2 Layer Docking Method

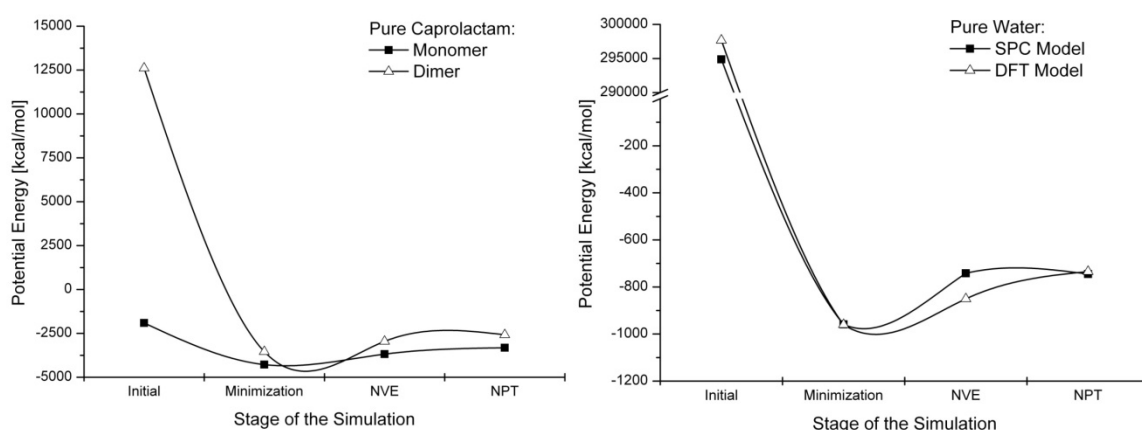
The layer docking approach is employed to predict the morphology of a caprolactam crystal. The results of the steps of the procedure are presented in the following chapter.

#### *The liquid side*

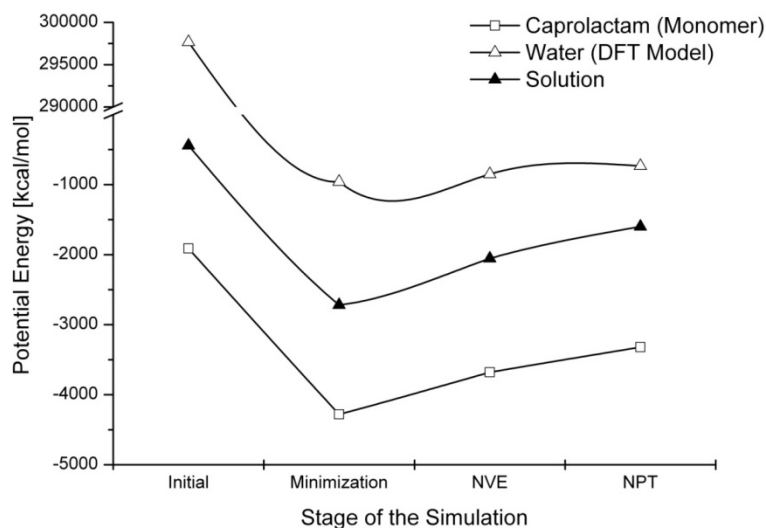
The optimization of the amorphous cell as the liquid side is conducted stepwise. The results from the cell construction to the dynamics are presented in the following graphs. Figure 4-15 (left) shows the potential energies for the optimized cell containing the pure caprolactam. The chart presents a comparison of a monomer and a dimer as initial input for the construction of the amorphous cell. In early steps of the modeling a significant difference in the energies is seen depending on the input molecule.

The plot in Figure 4-15 (right) gives the results on the optimization of an amorphous cell filled with pure water. The presented data is obtained from the simulation with the SPC and the DFT water model. At the last step of the optimization procedure the difference achieved for the corresponding total potential energy is neglectable.

The potential energies for the mixed state (solution) consisting of water and caprolactam is depicted in Figure 4-16. The graphs for the pure caprolactam and pure water are shifted in y-direction to the corresponding graph for the solution.



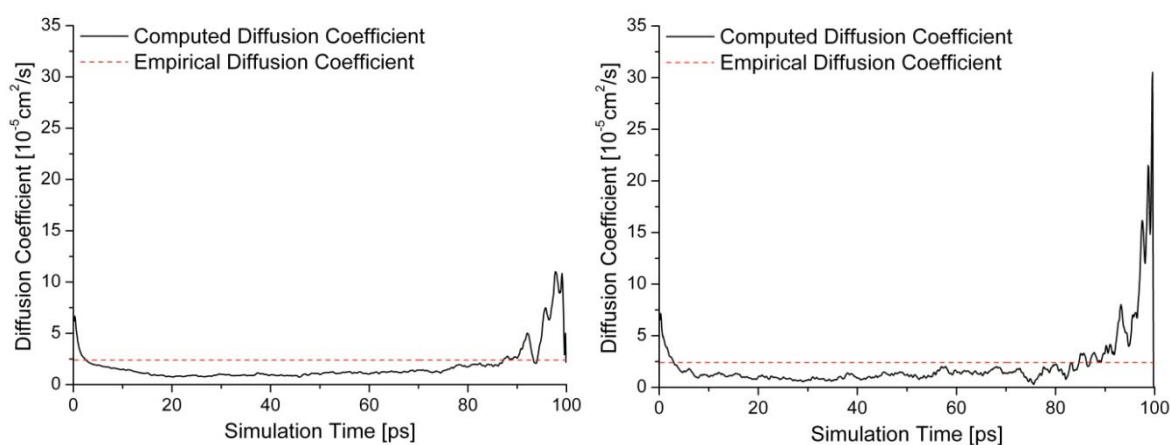
*Figure 4-15 Potential energy of the system at various stages of the optimization procedure for the amorphous cell. Molecular composition: pure caprolactam monomers and dimers (left); pure water, models: SPC and DFT (right).*



*Figure 4-16 Potential energy of the system at various stages of the optimization procedure for the amorphous cell. Comparison of the pure systems of caprolactam or water, respectively, as well as the system in the mixed state (solution).*

#### The liquid and the solid side

In the graphs in Figure 4-17 the diffusion coefficients for two different crystal faces is plotted versus the simulation time. Similar to the observations which are described in chapter 4.3.2 the presented graphs indicate three characteristic segments of the curve. Within the first third of the simulation time the diffusion coefficient rapidly decreases due to the equilibration. The second third is a period of low fluctuations and almost constant diffusion coefficient. In the last third of the simulation time the diffusion coefficient is intensively fluctuating and exponentially increasing.



*Figure 4-17 Diffusion coefficients for a layered system consisting of solid phase (crystal face) and liquid phase (solution of water and caprolactam).*

### Morphology prediction

The use of the Layer Docking approach enables to predict the modified morphology via the established attachment energy approach or by means of the diffusion coefficient. The diffusion coefficient is related to the face growth rate. The morphologies predicted with these methods are presented in Figure 4-18. The corresponding experimental morphologies are depicted in Table 4-10.

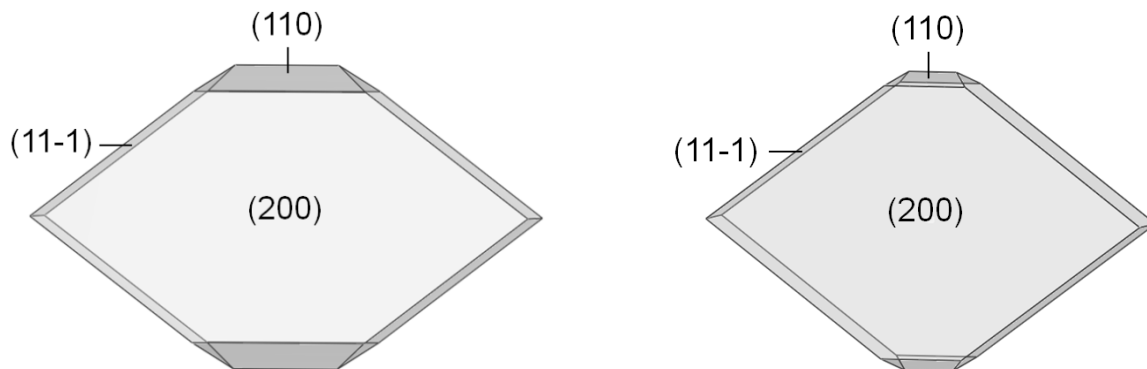


Figure 4-18 Morphologies of caprolactam crystals grown from an aqueous solution predicted with the Layer Docking method. Left: via established attachment energy approach. Right: via diffusion coefficient.

## 5. Discussion

### 5.1 Water

Water is used as solvent in all simulations which are conducted for the present investigations. Literature research revealed a wealth of existing water models with very different properties (e.g. charges, bond lengths, dummy atoms). The initial optimization of the water molecule aimed to investigate the characteristics of the molecules which are induced by the optimization methods. The study is conducted based on semi empirical, quantum mechanical and density functional methods. Representatively one optimized water molecule is chosen for further investigations in morphology predictions.

The findings in terms of the geometry and charges of the water molecule are employed in the established methods of morphology prediction. For the comparison various established water models (reference models, see Table 3-1) are employed with the same procedure. The subsequent, complex molecular dynamics simulations are conducted with the water model which is found by the use of the presented optimization methods. The findings are discussed hereafter.

#### 5.1.1 Molecular Optimization

For both, the ab initio electronic structure methods and the Density Functional Theory, the computation is independent from experimental data. However, the DFT methods are supposed to provide a higher accuracy. As a consequence, the B3PW91 63-1G optimized water molecule is selected for further applications in molecular dynamics. The method exposes results which are in good agreement with the TIP3P water model. The above mentioned DFT optimized water molecule has the bond lengths  $r(\text{OH})=0.973 \text{ \AA}$ , a HOH-angle of  $\alpha(\text{HOH})=108.647^\circ$  and hydrogen charges of  $q(\text{H})=0.371$ . In the following chapters, the optimized water molecule will be denoted as DFT.

### 5.2 Surface Docking Method

The morphological impact of the water molecules which is selected for the morphology prediction is demonstrated by use of the surface docking method (see Table 4-3, Table 4-5 and Table 4-10).

#### 5.2.1 Water Models

The investigations which focus on the application of water models in the morphology prediction using the surface docking method showed that [Sch11a]:

- 1) The presence of the rigid 3-site models DFT and TIP generate the extreme morphologies which are expected for the presence of a polar molecule. Whereas a flexible body of both models induced a rectangular habit.
- 2) The application SPC water in rigid or flexible state predicts a marginally modified attachment energy morphology of benzoic acid.
- 3) The presence of the TIP4P and TIP5P models the computed habits are similar to those which are predicted in the presence of 3-site TIP water. The water models are related via a similar geometry. The supplementary dummy atoms of the 4- and 5-site model are stabilizing the molecular geometries.
- 4) Evident differences between its flexible and rigid body results are observed. Only the flexible body approach allows atomic motion. The rigid (initial) model can not reach an energetic equilibrium by atomic movement. Minimum of equilibrium geometry can be reached by assuming flexibility of the water.

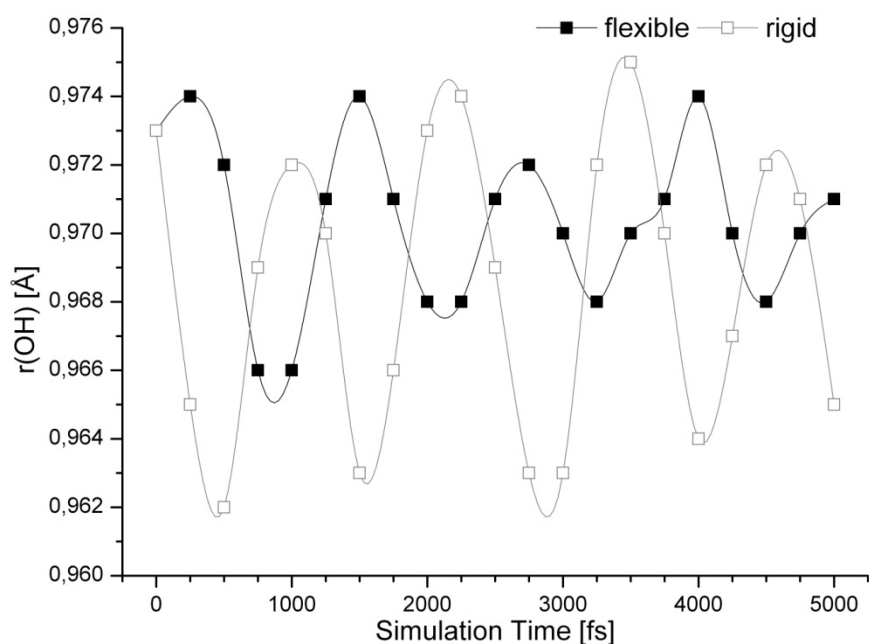
Consequently, the flexible approach reflects the influence of charges. Furthermore, the rigid body can additionally give information of habit modification caused by the initial geometry.

### 5.2.2 Constraints

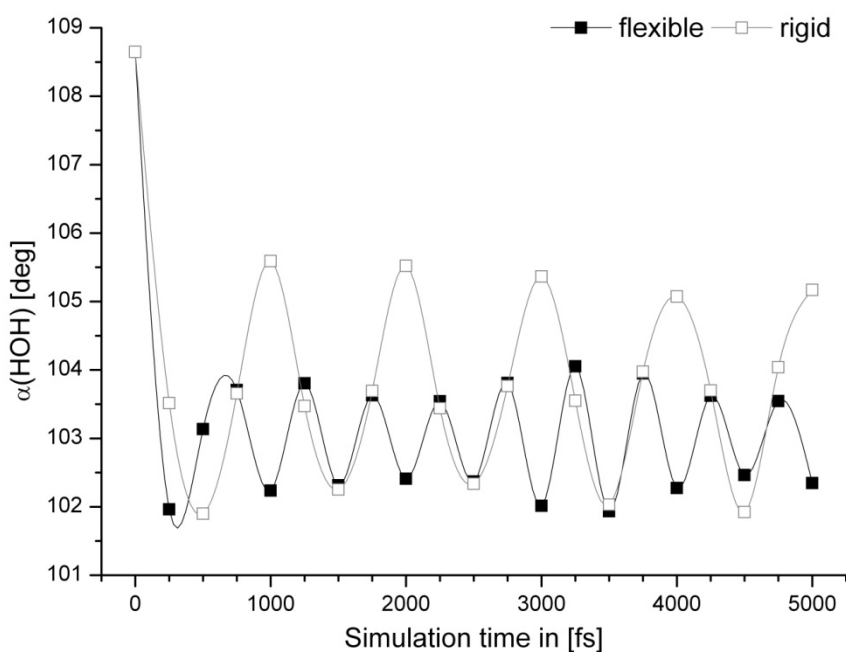
The software package MaterialStudios 4.0 (Accelrys Inc., USA) [Acc05] contains a function to make the molecule rigid during a simulation. For the rigid body considerations this tool is activated in order to suppress the change of the HOH-angle and the OH-bond lengths of water. The application of this function did not lead to the full preservation of the initial geometry of the water molecules. The plot in Figure 5-1 illustrates the fluctuation of the OH bond length within a water molecules. The fluctuations in the bond length are more intense when using the flexible water molecule. In the Figure 5-2 it is seen that the HOH-bond angle exhibits a higher frequency of fluctuation in a flexible molecule. The in both plots it is seen that despite of the constraints the rigid molecule shows fluctuations in the geometric properties, too. Consequently, applying the constraints merely limits the intramolecular change in the geometry than preventing it and the software MaterialsStudio does not fully restrict the geometric change of the constrained molecule. [Sch11b]

The obtained modified morphologies (Table 4-3) reflect the on one hand the impact of the charges of the employed model (constraint: flexible), and on the other hand the whole initial geometry as well as the charges (constraint: rigid). In case of the flexible water model an unhindered atomic motion (within the limits of non-bond and bonded

interactions) is possible for the atoms within one molecule. Limiting the atomic motion to the rigid constraint reduces the intermolecular motion of the atoms. Thus, the interaction of the molecule with the surface is affected. Even though the water molecule is widely assumed to be rigid, using a constraint in molecular dynamics for the purpose of morphology prediction is not enhancing the prediction results.



*Figure 5-1 The fluctuation of the OH bond length over the simulation time.*



*Figure 5-2 The fluctuation of the HOH bond angle over the simulation time.*

### 5.2.3 Thermostats

The method of temperature control used in the NVT dynamics has impact to the morphology prediction. Firstly it is the focus on the duration of the dynamics.

Due to the algorithm the Nosé thermostat produces a real canonical ensemble. The relation of the structure and the heat bath is represented by an additional degree of freedom in the algorithm. The additional degree of freedom is added to the equations of motion. Therefore, a fictitious mass  $Q$  is introduced as a predefined ratio. For a well chosen  $Q$  the Nosé algorithm will produce a real canonical ensemble.

In contrast, in the Velocity Scale thermostat the velocity of the atoms is scaled in order to keep the defined target temperature of the system. The Velocity Scale method is rapidly bringing the system to the equilibrium. But using this method suppresses natural fluctuations of the system and does not generate a realistic ensemble. In this context the computation time is shorter when employing the Velocity Scale method of temperature control at NVT runs.

## 5.3 Layer Docking Method

The advantages and drawbacks of the simulations conditions used in the Layer Docking approach are discussed in the present chapter. The results which are computed for the liquid side, the combined liquid and solid side and the subsequent morphology prediction examined.

### 5.3.1 Liquid Side

#### *Crystalline Input Molecules: Monomer vs. Dimer*

The focus is on the substance caprolactam. The results of the optimization presented in Figure 4-15 (left) reveal that a lower energy of the amorphous system is obtained when employing the monomer as molecular input for the cell construction. However, the necessity of taking into account that dimerization may occur is described in literature. The investigations conducted by Bennema et al. 1991 [Hei91] focus on the solvent-dependent dimerization of caprolactam and reveal water as a solvent which is not promoting dimerization of caprolactam. In contrast to this solvents as benzene and cyclohexane are strongly promoting the dimerization of caprolactam. Thus, the molecular input for the modeling of the amorphous cell does not need to be based on dimers when using water as solvent. Nonetheless, a change in the solvent requires a careful investigation on the corresponding dimerization constant. Moreover, the dilution of the solution causes further decreases in the dimerization constant.

### *Solvent Input Molecules: Monomer vs. Cluster*

Large scientific effort is put into the investigations on water clustering [Lud99, Wei98]. It is found that the imbalance of the charge distribution in the water molecule causes a strong hydrogen bonding and the cluster formation in non liquid phase. By means of quantum statistical thermodynamics cluster size distribution and cluster shapes are determined. In the Quantum cluster equilibrium theory of hydrogen-bonded liquids (QCE) quantum statistical methods are employed to model equilibria between clusters using the canonical ensemble (NVT). The QCE theory revealed that within the temperature range of 273.15 K to 300 K the fluid phase consists of 94% eight-membered clusters (w8), 4% five-membered clusters (w5) and 2% dimmers (Figure 5-3). The possible cluster shapes are illustrated in Figure 5-4.

In order to ensure the relevance of the clustering can be neglected in molecular dynamics the Layer Docking method is used with a water ring-shaped octamer instead of a monomer. The obtained results did not exhibit differences (in terms of energy and morphology).

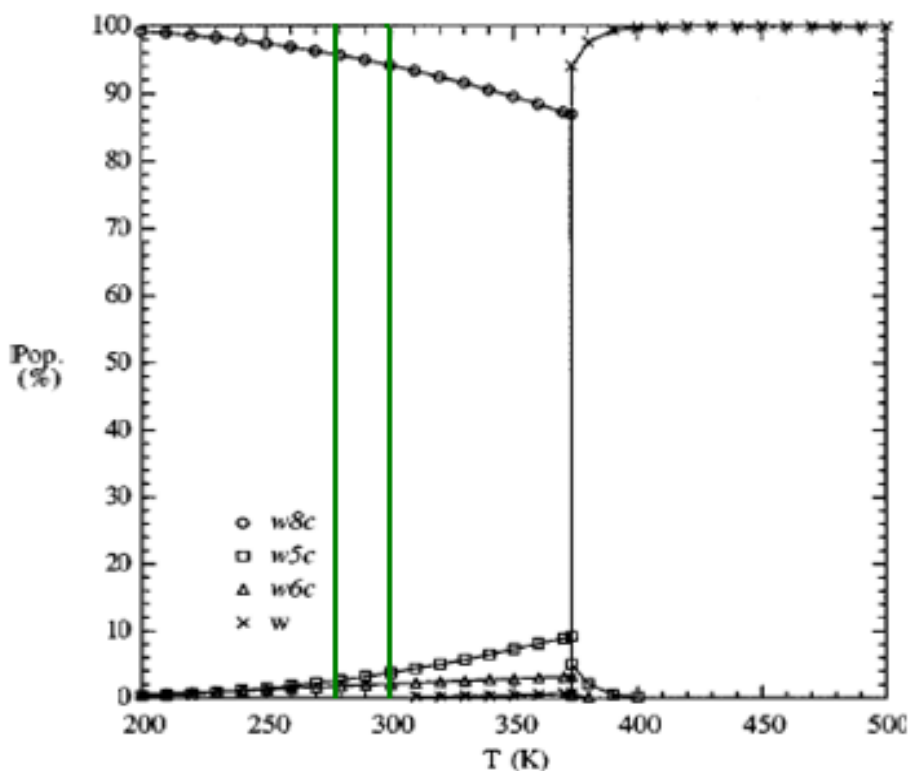
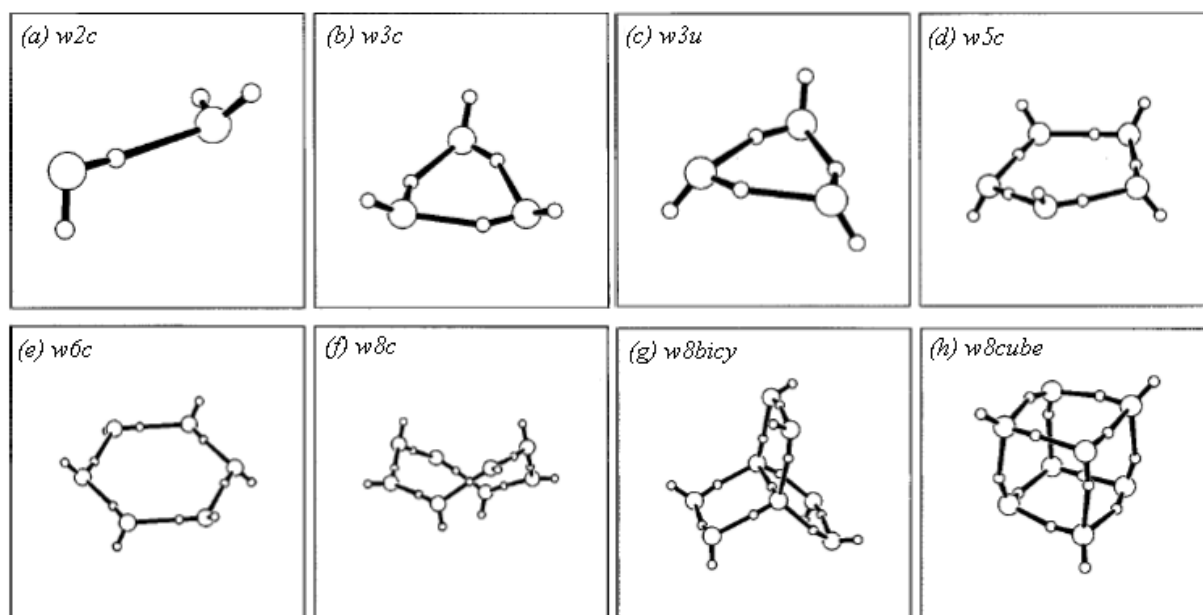


Figure 5-3 Population of water clusters over the temperature [Wei99]. The green lines represent the limit of atmospheric conditions (temperature range of 273.15 to 300 K).





*Figure 5-4 Optimized RHF/3-21G structures for water clusters [Wei99].*

### 5.3.2 Liquid and Solid Side

When using of the Nosé temperature control [Nos80] the estimation of the diffusion coefficient is not accomplished in agreement with empirical coefficient according Wilke-Chang [Wil55]. Augmenting the duration of the MD simulations can overcome this drawback, but is time consuming.

#### *Diffusion coefficient*

The focus in the diffusion coefficient consideration is on the substance benzoic acid. The new method for the morphology prediction of crystals in presence of solvents or additives is presented which allows the consideration of the concentration of the solute in the solvent. The modified morphology of benzoic acid crystals grown from aqueous solution as a case study is calculated by means of the diffusion coefficient. The modelled morphology is given proof by experiments.

The diffusion coefficients are successfully estimated within a 100 ps NVT simulation when the Velocity Scale algorithm is employed for temperature control. An increase of the simulation time may finally bring the results of the Nosé temperature control to a similar value, but is much more time consuming.

The presented new method for MD based morphology prediction allows the implementation of the solvent as well as the temperature effect on crystalline systems. The predicted results could be improved while keeping the simplicity and user-friendliness.

Morphology prediction by estimating the growth rate out of diffusion coefficient is possible and gives a good approach the empirical coefficient.

## 6. Conclusion

The scientific discussions and evaluations in modeling with the different morphology prediction methods leads to the following recommendations:

- The crystalline compound is selected. Once the choice is to predict the impact of an additive the user should apply *empirical methods* as the surface docking or the build-in method. If the solvent is of interest the layer docking methods is recommended for a known concentration. In case the concentration is not known the use of the surface docking method can supply with an alternative result. The modeling at known concentration of solute and solvent with implemented consideration of an additive can also be achieved by use of the layer docking method. The illustration which is presented in Figure 6-1 serves as decision tree for the choice of a method.
- If the solvent modeling is desired and the focus is on the *solvent water* it is not nessecary to condut a exhausting literature survey on the appropriate model. It is sufficient to use a simple DFT optimization method to conduct a moleculer optimization on the water molecule. The geometry of the molecule play a minor role, while the charges are more relevant in a morphology prediction.
- The modeling requires in any case the use of a *thermostat* in constat temperature dynamics. Herein, the thermostat Nosé or Velocity Scale should be used. While, the general preference should be Nosé.
- For the layer docking method the thickness of modeled solution layer should not fall below 5 Å. The aim is to ensure a sufficient *layerthickness* for the molecular motion within the layer. Furthermore, a realistic modeling requires a minimum layer for the interaction of solution and the crystal surface.
- The *minimization* of large systems of several thousands of atoms should be conducted at a minimum of 10.000 iterations.
- The *diffusion coefficient* which is obtained can be compared to the empirical diffusion coefficient according to the Wilke-Chang equation [Wil55]. The computed diffusion coefficient is used to scale the attachment energies of the faces of the pure crystal. The thereby modified attachment energy is directly related to the *face growth rate* and predicted the modified morphology is taking the concentration in the growth environment into account.

These important points are all considered and illustrated in the usermanual which is

found attached to this work as Appendix B (Userguide).

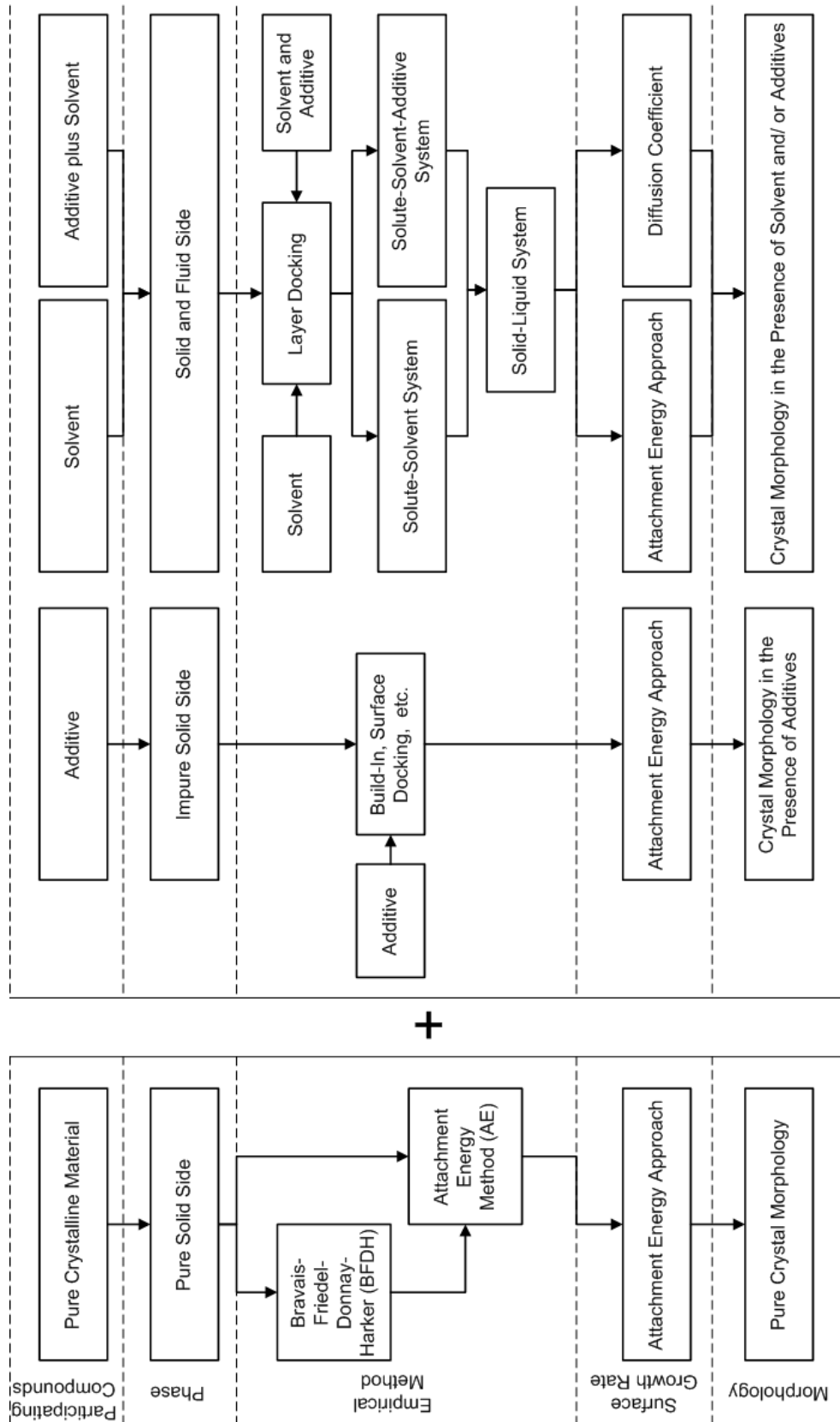


Figure 6-1 Schematic decision tree for modeling approaches.

## 7. Summary

The present work introduces a computational method for the prediction of the crystal morphology in the presence of a solution. The implementation of the concentration of the solute and the solvent molecules in the solution is conducted. The obtained prediction results are in agreement with experiments.

On the basis of the preceding research conducted by Niehörster [Nie97b], Mattos [Mat99], Schmiech [Sch05], Lu [Lu04b], Fiebig [Fie07a] and Yürüdü [Yür10] the “layer docking method” as a modeling method for the prediction of crystal morphology growth from a solution is developed.

The approach uses the therein presented fundamental findings in terms of calculating the binding and the attachment energy in order to obtain the morphology in presence of a solution as growth environment. In extend to this the approach of the face growth rate via the diffusion coefficient of each specific surface is provided. The modelling preformed for the substances benzoic acid, succinic acid, ascorbic acid and caprolactam in aqueous solution is confirmed in experimental work.

The comparison of the results computed by use of the conventional surface docking method, which does not allow the consideration of the concentration, is presented. The computed morphologies derived via the surface docking and the layer docking methods as well as the experimentally obtained crystals are illustrated. The obtained results gave proof to the applicability of the new method. Furthermore, the presented simulated diffusion coefficient is in agreement with the empirical diffusion coefficients [Wil55].

By the application of the presented modeling methods is possible to achieve reliable results if considering the appropriate solvent and carefully selecting the simulation conditions. The number of possible settings may have strong impact on the generated results. Thus, a clear user manual for both methods, the surface docking and the layer docking method, is given in the Appendix B.

The use of the layer docking method enables to implement the concentration of solute and solvent in the liquid phase. The therewith conducted modeling provides with the diffusion coefficient. The new achievement is the possibility to relate the diffusion coefficient directly to the crystal face growth rates. In extend to this the classical attachment energy approach can still be used with the same method of computation.

## 8. Zusammenfassung

Die Vorliegende Arbeit stellt eine computergestützte Methode der Morphologievorhersage für das Wachstum von Kristallen im Lösungsumfeld vor. Dabei ist die Konzentration der Moleküle des gelösten Stoffes zu denen des Lösungsmittels berücksichtigt. Die dadurch erzielten Ergebnisse sind in Übereinstimmung mit den experimentell erzielten.

Auf Basis der vorangegangenen Forschungsarbeiten von Niehörster [Nie97b], Mattos [Mat99], Schmiech [Sch05], Lu [Lu04b], Fiebig [Fie07a] und Yürüdü [Yür10] wurde die vorgestellte "Layer Docking Methode" als seine Modellierungsmethode zur Vorhersage der Kristallmorphologie aus einem Lösungsumfeld entwickelt.

Die Methode verwendet die grundlegenden Termini aus vorangegangenen Arbeiten in Bezug auf Bindungs- und Anlagerungsenergie um die Morphologievorhersage aus einer Lösung als Wachstumsumgebung zu berechnen. Darüber hinaus ist es möglich die Flächenwachstumsraten des Kristalles über den flächenspezifischen Diffusionskoeffizienten zu bestimmen. Diese Modellierungsmethode wurde mit den Stoffen Benzoesäure, Bernsteinsäure, Ascorbinsäure und Caprolactam aus wässrigem Lösungsumfeld durchgeführt und in experimentellen Arbeiten bestätigt.

Ein Vergleich der mit der neuen Layer Docking Methode und der konventionellen Surface Docking Methode (die keine Berücksichtigung der Konzentrationen gestattet) erzielten Ergebnisse ist präsentiert. Die Morphologien, die mit Hilfe der beiden Modellierungsmethoden vorhergesagt wurden sind den experimentellen Morphologien vergleichend gegenübergestellt. Es zeigte sich dass die vorgestellte neue Methode zu zuverlässigen Vorhersageergebnissen führt. Darüber hinaus sind die dargestellten modellierten Diffusionskoeffizienten in guter Näherung mit dem empirischen Diffusionskoeffizienten nach Wilke-Chang [Wil55].

Unter Zuhilfenahme der vorgestellten Modellierungsmethoden ist es möglich zuverlässige Ergebnisse zur erzielen, sofern das geeignete Lösungsmittel verwendet wird und die Simulationsbedingungen günstig gewählt sind. Da die Vielzahl der möglichen Einstellungen zum Teil sehr gravierende Auswirkungen auf die Ergebnisse haben kann, ist dieser Arbeit (siehe Anhang Appendix B) eine eindeutige und gut nachvollziehbare Anleitung für den Anwender der Methoden beigefügt.

Die Anwendung der Layer Docking Methode gestattet es dem Nutzer die Konzentration der Moleküle des gelösten Stoffes und die des Lösungsmittels in der flüssigen Phase zu Berücksichtigen. Die durchgeführte Modellierung erlaubt die Berechnung des Diffusionskoeffizienten. Die Neuerung ist die direkte Relation zwischen dem modellierten

Diffusionskoeffizienten und der Wachstumsgeschwindigkeit der Kristallflächen. Zudem kann aus der Modellierung der Layer Docking Methode die Morphologievorhersage über klassische Annäherung der Anlagerungsenergie durchgeführt werden.

## 9. List of Symbols and Abbreviations

### *Symbols*

Symbol	Description	Unit	Conversion to SI-Unit
$B_{hkl}$	Increase of MSD	-	-
$D_{1,2}$	Empirical diffusion Coefficient	$\text{m}^2/\text{s}$	-
$D_{hkl}$	Diffusion Coefficient	$\text{m}^2/\text{s}$	-
$d_{hkl}$	Interplanar spacing	Å	$1 \text{ Å} = 1 \times 10^{-10} \text{ m}$
$E^{cr}$	Crystallization energy	kcal/mol	$1 \text{ kcal/mol} = 4,186.8 \text{ J/mol}$
$E_{hkl}^{att}$	Attachment energy	kcal/mol	$1 \text{ kcal/mol} = 4,186.8 \text{ J/mol}$
$E_{hkl}^{sl}$	Slice Energy	kcal/mol	$1 \text{ kcal/mol} = 4,186.8 \text{ J/mol}$
$E_{Kinked}^{att}$	Attachment energy (kinked face)	kcal/mol	$1 \text{ kcal/mol} = 4,186.8 \text{ J/mol}$
$E_{Stepped}^{att}$	Attachment energy (stepped face)	kcal/mol	$1 \text{ kcal/mol} = 4,186.8 \text{ J/mol}$
$E_{Flat}^{att}$	Attachment energy (flat face)	kcal/mol	$1 \text{ kcal/mol} = 4,186.8 \text{ J/mol}$
$MSD$	Mean Squared Displacement	$\text{Å}^2/\text{s}$	-
$R_G$	Growth rate	$\text{m}^2/\text{s}$	-

### *Abbreviations*

Abbreviation	Description
AC	Amorphous cell
MD	Molecular Dynamics
MI	Morphological importance
MSD	Mean Squared Displacement
NVE	Constant number of particles, constant volume, constant energy
NpT	Constant number of particles, constant pressure, constant temperature
NVT	Constant number of particles, constant volume, constant temperature



## 10. Literature

- [Acc05] Accelrys Software Inc., MaterialsStudio 4.0, San Diego, USA, 2005.
- [Add82] Addadi, L., Berkovitch-Yellin, Z., Domb, N. Gati, E., Lahav, M., Leiserowitz, L., "Resolution of conglomerates by stereoselective habit modifications", *Nature*, **306** (1982) 21-26.
- [Asm09] Asmadi, A., Neumann, M.A., Kendrick, J., Girard, P., Perrin, M.-A., Leussen, F.J.J., "Revisiting the Blind Tests in Crystal Structure Prediction: Accurate Energy Ranking of Molecular Crystals", *J. Chem. Phys. B*, **113** (2009) 11313-11323.
- [Ben92] Bennema, P., Liu, X.Y., Lewtas, K., Tack, R.D., Rijpkema, J.J.M., Roberts, K.J., "Morphology of orthorhombic long chain normal alkenes: theory and observations", *J. Cryst. Growth*, **121** (1992) 679-696.
- [Ber81] Berendsen, H.J.C., Postma, J.O.M., van Gunstern, W.F., *Intermolecular Forces*, Pullmann, B., ed. Reidel, B. Pub. Company Netherlands, 1981, 331-342.
- [Ber82] Berkovitch-Yellin, Z., Addadi, L., Idelson, M., Lahav, M., Leiserowitz, L., Absolute configuration of chiral polar crystals", *Nature*, **306** (1982) 28-35.
- [Ber85] Berkovitch-Yellin, Z., "Toward an ab Initio Derivation of Crystal Morphology", *J. Am. Chem. Soc.*, **107** (1985) 3211-3222.
- [Boe92] Boek, E.S., Briels, W.J., van Erden, J., Feil, D., "Molecular-dynamics simulations of interfaces between water and crystalline urea", *J. Phys. Chem.*, **96** (1992) 7010-7018.
- [Boe93] Boek, E.S., Briels, W.J., "Molecular dynamics simulations of aqueous urea solutions: Study of dimer stability and solution structure, and calculation of the total nitrogen radial distribution function  $G_N(r)$ ", *J. Chem. Phys.*, **98** (1993) 1433-1438.
- [Boe94] Boek, E.S., Briels, W.J., Feil, D., "Interfaces between a Saturated Urea Solution and Crystalline Urea: A Molecular Dynamics Study", *J. Phys. Chem.*, **98** (1994) 1674-1681.
- [Bra66] Bravais, A., "Etudes Crystallographiques", Ed. Gauthier-Villars, Paris, France, 1866.
- [Bun91] Bunyan, J.M.E., Shankland, N., Sheen, D.B., "Solvent effects on the morphology of ibuprofen", *AIChE Symp. Ser.*, **87** (1991) 45-57.

- [Bur51] Burton, W.K., Cabrera, N., Frank, F.C., “The Growth of Crystals and the Equilibrium Structure of their Surfaces”, *Phil. Transact. Roy. Soc.*, **A244** (1951) 309-368.
- [Cly91] Clydesdale, G., Roberts, K.J., Docherty, R., “HABIT – a program for predicting the morphology of molecular crystals”, *Comp. Phys. Comm.*, **64** (1991) 321-338.
- [Cly94a] Clydesdale, G., Roberts, K.J., Docherty, R., “Modeling the morphology of molecular crystals in the presence of disruptive tailor-made additives”, *J. Cryst. Growth*, **136** (1994) 341-351.
- [Cly94b] Clydesdale, G., Roberts, K.J., Lewtas, K., Docherty, R., “Modeling the morphology of molecular crystals in the presence of blocking tailor-made additives”, *J. Cryst. Growth*, **142** (1994) 453-460.
- [Csd09] Cambridge Structural Database Version 5.31, Cambridge Crystallographic Data Centre, Cambridge, UK, 2009.
- [Dav76] Davey, R.J., “Effect of impurity adsorption on the kinetics of crystal growth”, *J. Cryst. Growth*, **35** (1976) 109-119.
- [Dav82] Davey, R.J., Mullin, J.W., Whiting, M.J.L., “Habit modification of succinic acid crystals grown from different solvents”, *J. Cryst. Growth*, **58** (1982) 314-322.
- [Don38] Donnay, J.D., Harker, D., “A New Law for Crystal Morphology Extending the Law of Bravais”, *Am. Mineral.*, **22** (1938) 457-477.
- [Fie07a] Fiebig, A., “Prediction of crystal morphology for a limited range of impurity concentrations”, *PhD Thesis*, Martin-Luther-Universität Halle-Wittenberg, Shaker Verlag, Aachen (2010).
- [Fie07b] Fiebig, A., Jones, M.J., Ulrich, J., “Predicting the effect of impurity adsorption on crystal morphology”, *Cryst. Growth Des.*, **7** (2007) 1623-1628.
- [Fel81] R. Feld, M.S. Lehmann, K.W. Muir, K.S. Speaksman, *Z. Kristallogr. Kristallgeom. Kristallphys., Kristallchem.*, **157**, 215 (1981).
- [For96] Foresman, J.B., Frisch, Æ., “Exploring Chemistry with Electronic Structure Methods”, Gaussian Inc., Pittsburgh, USA 1996.
- [Fri07] Friedel, M.G., “Etudes Sur la Loi de Bravais”, *Bull. Soc. Franc. Mineral.*, **31** (1907) 336-465.
- [Ges12] GESTIS – Substance Database, Institute for Occupational Safety and Health

- of the German Social Accident Insurance (IFA), Alte Heerstr. 111, 53757 Sankt Augustin, Germany (2012).
- [Gui02] Guillot, B., “A reappraisal of what we have learnt during three decades of computer simulations on water”, *J. Mol. Liqu.*, **101** (2002) 219-260.
- [Har55] Hartman, P., Perdok, W.G., “On the Relations between Structure and Morphology of Crystals I, II and III”, *Acta. Cryst.*, **8** (1955) 49-52, 521-524, 525-530.
- [Har80] Hartman, P., Bennema, P., “The Attachment Energy as a Habit Controlling Factor I-III”, *J. Cryst. Growth*, **49** (1980) 146-156, 157-165, 166-170.
- [Hei91] Van der Heijden, A.E.D.M., Geertman, R.M., Bennema, P., “Solvent-dependent growth morphology of caprolactam”, *J. Phys. D: Appl. Phys.*, **24** (1991) 123-126.
- [Hen09] Hengsterman, A., Kadam, S., Jansens, P.J., “Influence of Supercooling and Water Content on Crystal Morphology of Acrylic Acid”, *Cryst. Growth Des.*, **9** (2009) 2000-2007.
- [Hol99] Holmbäck, X., Rasmuson, Å.C., “Size and morphology of benzoic acid crystals produced by drowning-out crystallization”, *J. Cryst. Growth*, **198** (1999) 780–788.
- [Jac58] Jackson, J.A., “Mechanism of Growth”, in: *Liquid Materials and Solidification*, American Society for Metals, Cleveland (1958) 174-186.
- [Jor83] Jorgensen, W.L., Chandrasekhar, J., Madura, J.D., Impey, R.W., Klein, M.L., “Comparison of simple potential functions for simulating liquid water”, *J. Chem. Phys.*, **79** (1983) 926-935.
- [Lea01] Leach, A.R., “Molecular Modeling – Principles and Applications”, Pearson Education Ltd., Essex, UK 2001.
- [Lev81] Leviel, J.-L., Auvert, G., Savariault, J.-M., “Hydrogen Bond Studies. A Neutron Diffraction Study of the Structures of Succinic Acid at 300 K and 70 K”, *Acta Cryst.*, **37** (1981) 2185-2189.
- [Liu92] Liu, X.Y., Bennema, P., “The equilibrium state of solid-liquid interfaces of aliphatic compounds”, *J. Chem. Phys.*, **97** (1992) 3700-3709.
- [Liu96a] Liu, X.Y., Bennema, P., “Theoretical consideration of the growth morphology of crystals”, *Phys. Rev. B*, **53** (1996) 2324-2335.
- [Liu96b] Liu, X.Y., Bennema, P., “Prediction of the growth morphology of crystals”, *J. Cryst. Growth*, **166** (1996) 117-123.

- [Lu04a] Lu, J.J., Ulrich, J., "Improved understanding of molecular modelling-the importance of additive incorporation", *J. Cryst. Growth*, **280** (2004) 203-210.
- [Lu04b] Lu, J.J., "Predicting Crystal Morphology in the Presence of Additives by Molecular Modeling", *PhD Thesis*, Martin-Luther-Universität Halle-Wittenberg, Shaker Verlag, Aachen (2004).
- [Lud99] Ludwig, R., Weinhold, F., "Quantum cluster equilibrium theory of liquids: Freezing of QCE/3-21G water to tetrakaidecahedral "Bucky-ice"", *J. Chem. Phys.*, **110** (1999) 508-515.
- [Mag11] Mangin, D., Baltes, D., Klein, J.P., Monnier, O., "Antisolvent Crystallization in Supercritical Fluid: An Interesting Technique for Polymorph Screening", in Proceedings of 18<sup>th</sup> International Symposium on Industrial Crystallization (ISIC) 2011, Ed. M. Mazzotti, AIDIC, Milan, Italy, 2011, 63-64.
- [Mah01] Mahoney, M.W., Jorgensen, W.L., "Diffusion constant of the TIP5P model of liquid water", *J. Chem. Phys.*, **114** (2001) 363-366.
- [Map88] J.R. Maple, U. Dinur, A.T. Hagler, „Derivation of force fields for molecular mechanics and dynamics from ab initio energy surfaces”, *Proc. Natl. Acad. Sci.*, **85** (1988) 5350-5354.
- [Mat96] Mattos, M.V.C., Niehörster, S., Wangnick, K., Ulrich, J., "Comparison Between Theoretical and Experimental Habit Modification of Crystalline Stabilizers for Foods", in Proceedings of 13<sup>th</sup> International Symposium on Industrial Crystallization (ISIC) 1996, Eds. B. Biscans, N. Gabas, Toulouse, France, 19-24.
- [Mat99] Mattos, M.V.C., "Zur Übertragung der Einbau-Annäherung auf die Kristallhabitusänderung durch Adsorption", *PhD Thesis*, Universität Bremen, Shaker Verlag, Aachen (1999).
- [Mye95] Myerson, A.S., Jang, S.M., „A comparison of binding energy and metastabile zone width for adipic acid with various additives“, *J. Cryst. Growth*, **156** (1995) 469-476.
- [Mye99] Myerson, A.S., "Molecular Modeling Applications in Crystallization", Cambridge University Press, New York, USA 1999.
- [Nie95] Niehörster, S., Ulrich, J., „Designing Crystal Morphology by a Simple Approach“, *Cryst. Res. Technol.*, **30** (1995) 389-395.
- [Nie96] Niehörster, S., Mattos, M., Ulrich, J., "An Approach to Design the Habit of

- Organic Crystals-Modelling and Verification”, in Proceedings of 13<sup>th</sup> International Symposium on Industrial Crystallization (ISIC) 1996, Eds. B. Biscans, N. Gabas, Toulouse, France, 1996, 25-31.
- [Nie97a] Niehörster, S., Mattos, M.V.C., Ulrich, J., „A Modelling Study of Caprolactam’s Crystal Habit Modification“, *Bull. Soc. Sea Water Sci. Jpn.*, **51** (1997) 29-34.
- [Nie97b] Niehörster, S., “Der Kristallhabitus unter Additiveinfluss”, *PhD Thesis*, Universität Bremen, Bremen (1997).
- [Nos84] Nosé, S., “A molecular dynamics method for simulations in the canonical ensemble”, *Mol. Phys.*, **52** (1984) 255-268.
- [Oha73] Ohara, M., Reid, R.C., “Modeling Crystal Growth Rates from Solution”, Prentice-Hall, Eaglewood Cliffs, NJ 1973.
- [Par80] Parrinello, M., Rahman, A., “Crystal Structures and Potentials: A Molecular-Dynamics Study”, *Phys. Rev. Lett.*, **45** (1980) 1196-1199.
- [Par81] Parrinello, M., Rahman, A., “Polymorphic transitions in single crystals: A new molecular dynamics method”, *J. Appl. Phys.*, **52** (1981) 7182-7190.
- [Rap91] Rappé, A.K., Goddard, W.A., “Charge Equilibration for Molecular Dynamics”, *J. Phys. Chem.*, **95** (1981) 3358-3363.
- [Rie11] Rieger, J., “Precursor Structures in Crystallization and Precipitation and Control of Particle Formation by Polymers”, in Proceedings of 18<sup>th</sup> International Symposium on Industrial Crystallization (ISIC) 2011, Ed. M. Mazzotti, AIDIC, Milan, Italy, 2011, 28.
- [Sch04] Schmiech, P., Ulrich, J., “Improvement of a Model for the Crystal Habit Prediction by Use of PBC-Vectors”, *Chem. Eng. Technol.*, **28** (2004) 734-737.
- [Sch05] Schmiech, P., “Zur Vorhersage des Kristallhabitus unter Fremdstoffeinfluss mittels PBC-Vektoren”, *PhD Thesis*, Martin-Luther-Universität Halle-Wittenberg, Shaker Verlag, Aachen (2005).
- [Sch11a] Schmidt, C., Yürüdü, C., Wachsmuth, A., Ulrich, J., “Modeling the morphology of benzoic acid crystals grown from aqueous solution”, *CrystEngComm*, **13** (2011) 1159-1169.
- [Sch11b] Schmidt, C., Ulrich, J., “Morphology Prediction of Benzoic Acid Crystals – Thermostats”, *Chem. Eng. Technol.*, **35** (2011) 563-570.
- [Sch11c] Schmidt, C., Ulrich, J., “Predicting crystal habits grown from aqueous multi-

- component solutions - Method of Computation involving multiple Solvents”, in Proceedings of 18<sup>th</sup> International Workshop on Industrial Crystallization (BIWIC) 2011, Eds. S.S. Kadam, S.A. Kulkarni, J.H.T. Horst, Delft University of Technology, Delft, Netherlands, 2011, 288-293.
- [Sch11d] Schmidt, C., Ulrich, J., “Crystal Habit Prediction Including the Liquid as well as the Solid Side”, in Proceedings of 18<sup>th</sup> International Symposium on Industrial Crystallization (ISIC) 2011, Ed. M. Mazzotti, AIDIC, Milan, Italy, 2011, 96-97.
- [Sch11e] Schmidt, C., Ulrich, J., “Molecular Modeling – Scientific Toy or Industrial Tool”, in: Proceedings of 20<sup>th</sup> Nisshin Engineering Particle Technology International Seminar (NEPTIS), Otsu, Japan, 2011, 1-10.
- [Sch12] Schmidt, C., Ulrich, J., “Crystal Habit Prediction – Including the Solid as well as the Liquid Side”, *Cryst. Res. Technol.*, (2012), accepted.
- [Wei98] Weinhold, F., “Quantum cluster equilibrium theory of liquids: Illustrative application to water”, *J. Chem. Phys.*, **109** (1998) 373-384.
- [Wil55] Wilke, C.R., Chang, P., “Correlation of Diffusion Coefficients in Dilute Solutions” *AIChE Journal*, **1** (1955) 264-270.
- [Win75] Winkler, F.K., Dunitz, J.D., “Medium Ring Compounds. XIX. Caprolactam: Structure Refinement”, *Acta Cryst.*, **B35** (1975) 268-269.
- [Win98] Winn, D., Docherty, M.F., “A New Technique for Predicting the Shape of Solution-Grown Organic Crystals”, *AIChE Journal*, **45** (1998) 2501-2514.
- [Win00] Winn, D., Docherty, M.F., “Modeling Crystal Shapes of Organic Materials Grown from Solution”, *AIChE Journal*, **47** (2000) 1359-1377.
- [Win02] Winn, D., Docherty, M.F., “Predicting shape of organic crystals grown from polar solvents”, *Chem. Eng. Sc.*, **57** (2002) 1805-1813.
- [Wir87] Wireko, F.C., Shimon, L.J.W., Frolow, F., Berkovitch-Yellin, Z., Lahav, M. Leiserowitz, L., “Effect of solvent on the growth of organic crystals: 1. The riddle of  $\alpha$ -resorcinol”, *J. Phys. Chem.*, **91** (1987) 484-491.
- [Woo75] Woodcock, L.V., *Advances in Molten Salt Chemistry*, Plenum: New York 1975.
- [Yür08] C. Yürüdü, M.J. Jones, J. Ulrich, “Determination of the effect of external environment on growth kinetics using molecular modeling – Calculating diffusion coefficients”, in: Proceedings of 17<sup>th</sup> international Symposium on

Industrial Crystalization (ISIC), Maastricht, The Netherlands, 2008, Vol. 1, pp. 431-438.

- [Yür10] Yürüdü, C., “Predicting crystal Growth Rates Using Molecular Modelling Techniques with Explicit Consideration of the Driving Force”, *PhD Thesis*, Martin-Luther-Universität Halle-Wittenberg (2010), urn:nbn:de:gbv:3:4-3409.
- [Yür12] Yürüdü, C., Jones, M.J., Ulrich, J., “Modelling of diffusion for crystal growth”, *Soft Materials*, **10** (2012) 257-284.

## 11. Appendix A

*Table 11-1 Overview on available modeling approaches.*

Model	Methodology	Literature
<b>Pure Substance</b>		
<ul style="list-style-type: none"> <li>Bravais-Friedel-Donnay-Harker Method (A. Bravais)</li> </ul>	Geometric	[Bra66] [Don38] [Fri07]
<ul style="list-style-type: none"> <li>Attachment Energy Theory (P. Hartman)</li> </ul>	Chemical	[Har80]
<ul style="list-style-type: none"> <li>Periodic Bond Chain Theory (P. Hartman)</li> </ul>	Chemical	[Har55]
<b>Additives</b>		
<ul style="list-style-type: none"> <li>Disruptive and Blocking Tailor Made (K.J. Roberts, R. Docherty)</li> </ul>	Chemical interaction with additive	[Cly94a] [Cly94b]
<ul style="list-style-type: none"> <li>Build In (Z. Berkowitch-Yellin, M. Lahav, L. Leiserowitz)</li> </ul>	Chemical interaction: one additive molecule within unit cell; based on attachment energy calculation	[Ber85]
<ul style="list-style-type: none"> <li>Connected nets (P. Bennema)</li> </ul>	Chemical interaction: one additive, based on internal structure; theory of roughening transition.	[Ben92] [Liu96a,b]
<b>Additives (related methods)</b>		
<ul style="list-style-type: none"> <li>Build In (J. Ulrich)</li> </ul>	Chemical interaction: one additive molecule within unit cell; based on attachment energy calculation	[Nie95,Nie96] [Mat96]
<ul style="list-style-type: none"> <li>Build In (J. Ulrich)</li> </ul>	Chemical interaction: one additive molecule within unit cell; based on PBC theory	[Sch04]



- 
- Additive adsorption (A.S. Myerson, J. Ulrich)      Chemical interaction: one additive molecule on crystal surface; based on attachment energy calculation      [Mye95] [Lu04a] [Sch11a,b]

---

### Solvents

---

- Adsorption from liquid layer (J. Ulrich)      Chemical interaction: fluid solution layer on crystal surface; based on attachment energy calculation      [Yür12] [Sch11c,d]
  - Morphology prediction of crystals grown in presence of solvents (R. Docherty)      No fluid phase simulations, uses physical properties of solvent for (organic) crystals grown from polar solvents      [Win98] [Win00] [Win02]
-

**12. Appendix B (Userguide)**

See attachment.

## Curriculum Vitae

### *Personal*

Name: Christiane Schmidt  
Date of Birth: 19.07.1983 in Lutherstadt Eisleben  
Nationality: German

### *Education*

04/2009 – 04/2012 Martin Luther University Halle-Wittenberg  
Zentrum für Ingenieurwissenschaften, Verfahrenstechnik/TVT  
Scientific assistant

04/2004 – 03/2009 Martin Luther University Halle-Wittenberg  
Studies in Business and Engineering (Wirtschaftsingenieurwesen)  
Graduated as Diplom Wirtschaftsingenieur

01/2008 – 05/2008 Grenoble École de Management (GEM), France  
Studies in Marketing and Finances

## List of Publications

### *Peer Reviewed Publications in Journals and Proceedings*

1. Schmidt, C., Yürüdü, C., Wachsmuth, A., Ulrich, J., “Modeling the morphology of benzoic acid crystals grown from aqueous solution”, *CrystEngComm*, **13** (2011) 1159-1169.
2. Buchfink, R., Schmidt, C. Ulrich, J., “Fe<sup>3+</sup> as an example of the effect of trivalent additives on the crystallization of inorganic compounds, here ammonium sulfate ”, *CrystEngComm*, **13** (2011) 1118-1122.
3. Schmidt, C., Ulrich, J., “Morphology Prediction of Benzoic Acid Crystals – Thermostats”, *Chem. Eng. Technol.*, **34** (2011) 563-570.
4. Schmidt, C., Ulrich, J., “Morphology Prediction of Benzoic Acid Crystals – Thermostats”, Proceedings of 17<sup>th</sup> International Workshop on Industrial Crystallization (BIWIC) 2010, Halle (Saale), Germany, Eds. T. Stelzer, J. Ulrich, Cuvillier Verlag, Göttingen, Germany, 7-12.
5. Schmidt, C., Ulrich, J., “Predicting crystal habits grown from aqueous multi-component solutions - Method of Computation involving multiple Solvents”, Proceedings of 18<sup>th</sup> International Workshop on Industrial Crystallization (BIWIC) 2011, Delft, Netherlands, Eds. S.S. Kadam, S.A. Kulkarni, J.H. Ter Horst, University of Technology, Delft, Netherlands, 278-283.
6. Schmidt, C., Ulrich, J., “Crystal Habit Prediction Including the Liquid as well as the Solid Side”, Proceedings of 18<sup>th</sup> International Symposium on Industrial Crystallization (ISIC) 2011, Zurich, Switzerland, Ed. M. Mazzotti, Associazione Italiana di Ingegneria Chimica (AIDIC), Milano, Italy 96-97.
7. Schmidt, C., Ulrich, J., “Molecular Modeling – Scientific Toy or Industrial Tool”, Proceedings of 20<sup>th</sup> Nisshin Engineering Particle Technology International Seminar (NEPTIS) 2011, Kyoto, Japan.
8. Schmidt, C., Ulrich, J., “Crystal Habit Prediction – Including the Solid as well as the Liquid Side”, *Cryst. Res. Technol.*, (2012), accepted.
9. Schmidt, C., Ulrich, J., “Predicting the Crystal Morphology Grown from Solution”, *Chem. Eng. Technol.*, (2012), accepted.

10. Schmidt, C., Ulrich, J., “Molecular Modeling Scientific Toy or Industrial Tool – An Evaluation of the State of the Art”, *J. Cryst. Growth*, (2012), submitted.
11. Schmidt, C., Jones, M.J., Ulrich, J., “Influence of Additives and Impurities on Crystallization” in “Crystallization - From Basic Concepts to Industrial Applications”, Ed. W. Beckmann, Wiley-VCH Verlag GmbH, Weinheim, Germany, (2012), accepted.

#### *Contributions in Conferences*

1. Schmidt, C., Yürüdü, C., Ulrich, J., “What about Water in Modeling the Morphology of Crystals”, ProcessNet Working Party „Molecular Modeling and Simulation for Process and Product Design“, poster presentation, Würzburg, Germany (2010).
2. Schmidt, C., Ulrich, J., “Morphology Prediction of Benzoic Acid Crystals – Thermostats”, Proceedings of 17<sup>th</sup> International Workshop on Industrial Crystallization (BIWIC), oral presentation, Halle (Saale), Germany (2010).
3. Schmidt, C., Ulrich, J., “Morphology of succinic acid crystals grown from aqueous solution”, Fachausschuss Kristallisation, poster presentation, Bad Dürkheim, Germany (2011).
4. Schmidt, C., Ulrich, J., “Predicting crystal habits grown from aqueous multi-component solutions - Method of Computation involving multiple Solvents”, Proceedings of 18<sup>th</sup> International Workshop on Industrial Crystallization (BIWIC), poster presentation, Delft, Netherlands (2011).
5. Schmidt, C., Ulrich, J., “Crystal Habit Prediction Including the Liquid as well as the Solid Side”, Proceedings of 18th International Symposium on Industrial Crystallization (ISIC), oral presentation, Zurich, Switzerland (2011).
6. Schmidt, C., Ulrich, J., “Molecular Modeling – Scientific Toy or Industrial Tool”, Proceedings of 20th Nisshin Engineering Particle Technology International Seminar (NEPTIS), oral presentation by J. Ulrich, Kyoto, Japan (2011).

Halle (Saale), 27.03.2012

Christiane Schmidt



# Userguide

for the

## Prediction of Crystal Morphology

in the

## Presence of Additives and/ or Solvents

for

## Organic Compounds and Water

with

## MaterialsStudio 4.0

and

## Cerius<sup>2</sup> 4.5/ 4.7





**Content**

1. Introduction	1
1.1 Precondition	1
1.2 Computational I: Crystallographic Structure Data	1
1.3 Computational I: Hardware	1
1.4 Computational III: Software	2
1.5 Computational IV: Method	2
2. Crystallographic Structure Data (CSD)	4
2.1 The Cambridge Crystallographic Data Centre (CCDC)	4
2.2 The RCSB Protein Data Bank (PDB)	9
2.3 The American Mineralogist Crystal Structure Database (AMCSD)	9
3. MaterialsStudio 4.0	11
3.1 The Surface Docking Method	13
3.1.1 The Solid Side (Crystal Surface)	13
3.1.2 Combined Crystal Surface and Additive	22
3.1.3 The Modified Morphology	30
3.2 The Layer Docking Method	33
3.2.1 The Liquid Side (Solution)	33
3.2.2 Combined Surface and Solution	38
3.2.3 The Modified Morphology	45
4. Cerius <sup>2</sup> 4.5 and 4.7	49
4.1 Command Tracing and Non-graphical simulation start	50
4.2 The Surface Docking Method	51
4.2.1 The Solid Side (Crystal Surface)	52
4.2.2 Combined Crystal Surface and Additive	66
4.2.3 The Modified Morphology	72
4.3 The Layer Docking Method	74
4.3.1 The Liquid Side (Solution)	74
4.3.2 Combined Surface and Solution	78
4.3.3 The Modified Morphology	84
5. References	85

## **1. Introduction**

The present manual aims to guide the user through selected methods of morphology prediction which have been developed in the past years. The presented methods are specified for additives on the one hand and solvents on the other. The methods are used with the software “MaterialsStudio 4.0” and “Cerius<sup>2</sup>” (Versions 4.5 and 4.7).

The requirements for the application of the methods are introduced in the following paragraph.

### **1.1 Precondition**

Before getting started it is essential to obtain information on the substances and the conditions of the crystallization process. Parameters such as the temperature of the crystallization and the concentration of the relevant compounds are necessary in order to conduct a reliable computer modeling. In the present user guide it is focused on the computer chemical aspects of the procedure. For experimental data, such as solubility, concentration or temperature the reader is referred to literature [Lin58, Lin65].

### **1.2 Computational I: Crystallographic Structure Data**

Once the decision of the participating compounds is taken the crystallographic structure data (also crystal structure data or crystal unit cell) is required. The data can be obtained from established databases as presented in chapter 2. The chapter is entitled Crystallographic Structure Data (CSD) and presents the first step which is to be conducted prior to the modeling – the downloading of the crystallographic structure data (crystal unit cell).

The Cambridge Crystallographic Data Centre [Csd09] is an established supplier for crystallographic structure data for organic compounds and is presented in chapter 2.1. The structure of proteins can be obtained from the RCSB Protein Databank (PDB) [Pdb11] as seen in chapter 2.2. Data for minerals is supplied by the American Mineralogist Crystal Structure Database (AMCSD) [Dow03] which is introduced in chapter 2.3.

### **1.3 Computational I: Hardware**

The computational procedures for the morphology prediction rely on the use of powerful computers. The general rule is the more powerful the hardware the faster proceed the computer experiments. Concerning the time and cost effectiveness it is desired to lower the computation time.

The modeling software requires the use of license servers and gateways. Thus, the hardware which is used in terms of this user manual is based on two sgi silicon graphics tezero workstations. The operating system is Irix65 Release 6.4.

#### **1.4 Computational III: Software**

A further requirement prior to the simulation is the modeling software. The user friendliness and the costs are dominating the choice of the software. The Accelrys Inc. modeling software supplies a user interface which is easy to handle and a number of simple methods of morphology prediction can be used with the software. Thus, the packages MaterialsStudio 4.0 [Acc05] and Cerius<sup>2</sup> 4.5 and 4.7 have been employed for the modeling which is conducted for the present user manual.

The chapter 3 introduces the software MaterialsStudio 4.0 and how to proceed with the use of empirical modeling methods as the Surface Docking and the Layer Docking method. The use of these methods with the software Cerius<sup>2</sup> 4.5 and 4.7 is introduced in the chapter 4.

#### **1.5 Computational IV: Method**

Upon the real (experimental) conditions is required to take a decision whether an additive or impurity (presence of even ppm is relevant) may modify the morphology of the pure compound or a solvent (high concentration of non-crystalline substance) is relevant in participating in the crystallization process.

The decision tree which is depicted in Figure 1-1 enables to choose the most appropriate method for the morphology prediction. The method should be chosen according to the concentration of the particles of each compound which is participating in the crystallization process. In the illustration it is seen an increasing amount of foreign particles from the low concentration of an additive or impurity up to high concentration of a solvent. The concentration is related to the modeling method. Thus, different concentration implies a variation in the consideration of the participating compounds.

The morphology prediction for pure compounds (seen in Figure 1-1 left) is available from a software routine. The presence of any foreign particle (additive, impurity or solvent) is considered in existing software packages via manual steps. The use of the Surface Docking method [Lu04] or the Build-In method [Nie95] as empirical methods is essential to model the presence of additives or impurities in a melt (Figure 1-1 middle). The impact of the presence of a solvent can be predicted by means of the Layer Docking Method [Sch11a] (Figure 1-1 right).

Each of these methods requires an own procedure in the modeling software. The attached user manual illustrates the manual steps to be performed in order to predict the crystal morphologies in the presence of additives, impurities and solvents, respectively.

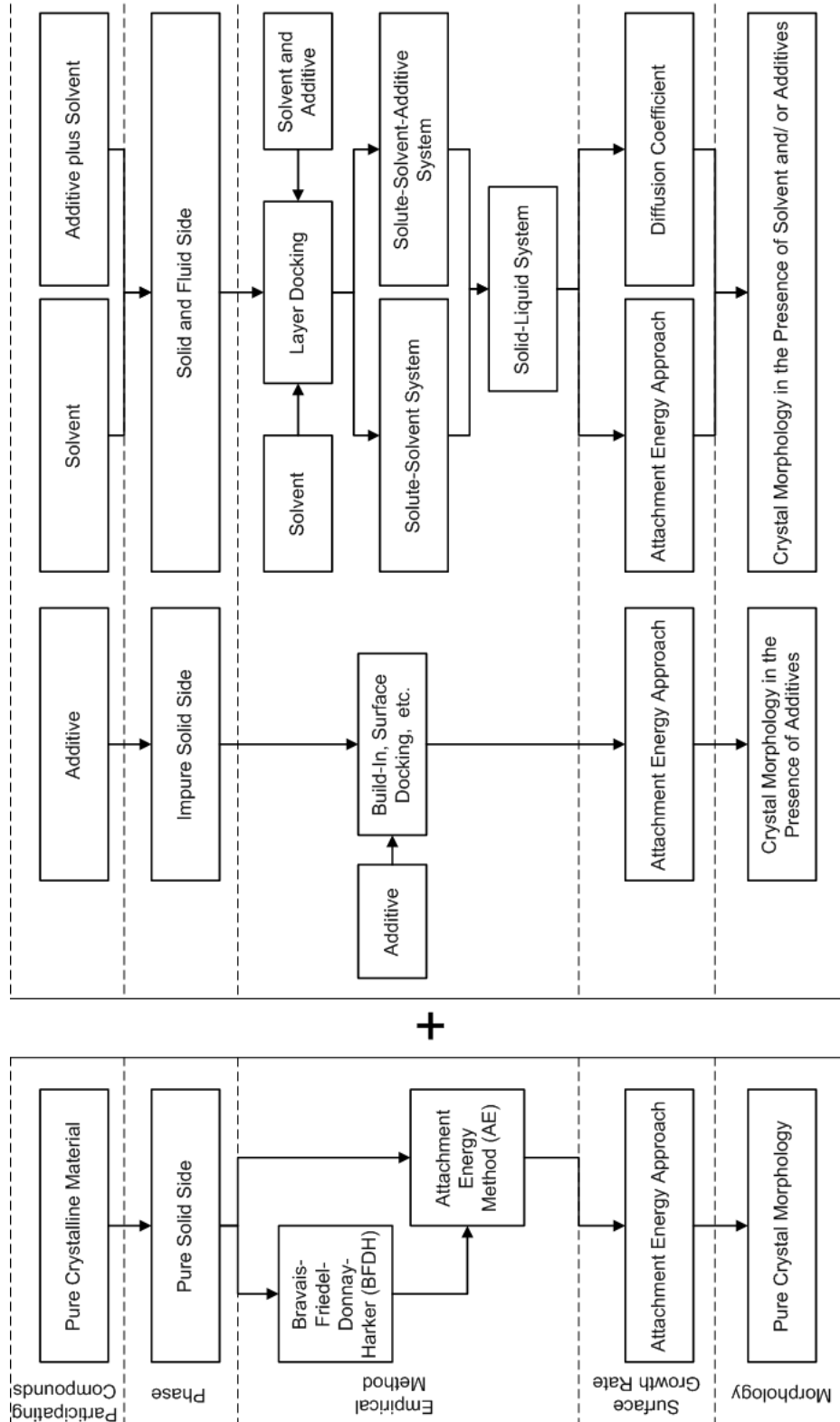


Figure 1-1 Decision tree for the choice of the empirical modeling method.

## 2. Crystallographic Structure Data (CSD)

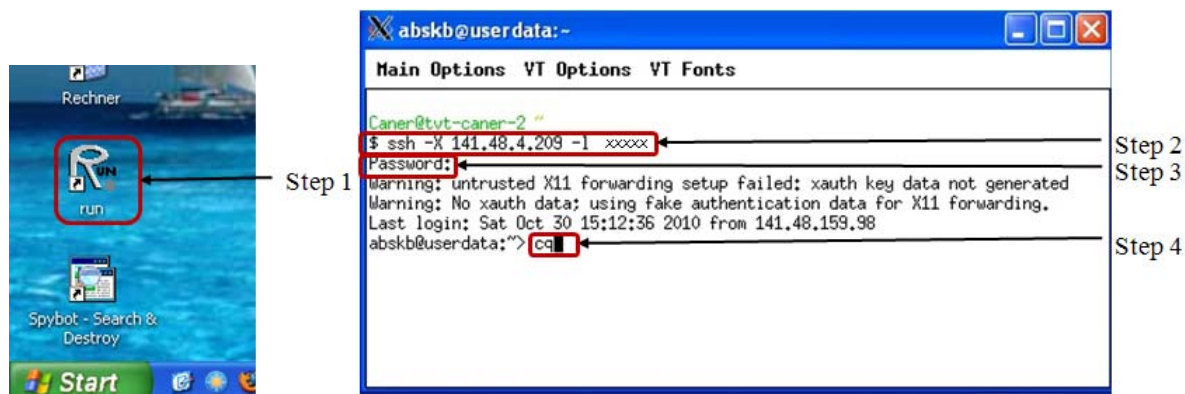
### 2.1 The Cambridge Crystallographic Data Centre (CCDC)

The downloading of crystallographic structure data (CSD) for organic substances is obtained from the Cambridge Crystallographic Data Centre (CCDC). The following steps describe how to get access to the Cambridge Crystallographic Data Centre (CCDC).

The user should open the program “Run” from the desktop as seen in the left illustration of Figure 2-1 (Step 1). The subsequent steps 2 to 4 are illustrated in Figure 2-1 (right) for a user from the Martin-Luther University. The program welcomes the user in the command line with “pcuser@pc-name”. In the command line below the following command should be typed (Step 2):

```
$ ssh -X 141.48.4.209 -l username
```

The program will now ask for the password (Step 3) and the user should type the password for the account. After the password was successfully entered the user is connected to the CCSD and the command line indicates “username@userdata~”. The graphical CCSD user interface is accessed when typing the command “cq” (Step 4). The graphical CCSD user interface will open with the start screen as it is depicted in Figure 2-2.



*Figure 2-1 “Run.exe”-icon on the desktop (left) and “Run.exe” dialogue (right).*



*Figure 2-2 Start screen of the CCDC database.*

In order to search the Crystal Structure Data (CSD) from the CCSD the subsequent steps are to be proceeded.

For conducting the search for a compound name the user should click on “Name/Class” (Step 1). Now the dialogue “Name/Class” will open (Step 2). Here, the compound name should be typed and a click on the “Add”-button will confirm the choice. The compound name will appear in the field “Contains”. By a click on the “Search”-button the dialogue “Search Setup” will be opened (Step 3). Pressing the “Start Search” button will start the search (Step 4). When the search is finished, the screen as depicted in Figure 2-5 is seen. Clicking on the “All text” index card (Figure 2-5) in the menu on the left enables the user to see details on the structure (Step 5). A structure with the property of interest should be selected according to the given information (see Figure 2-6). As an example the temperature should match the experimental temperature; furthermore, a recently published structure should be preferred.

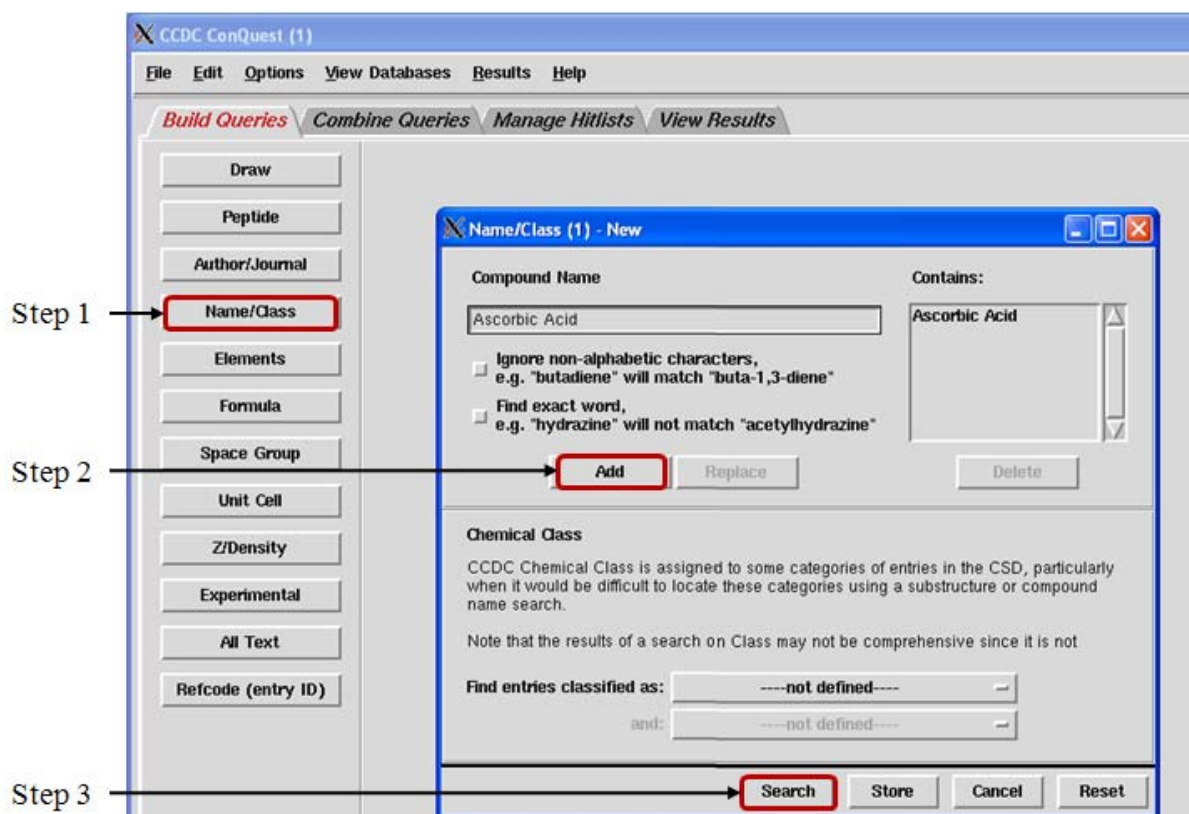


Figure 2-3 Build a query via entering the compound name.

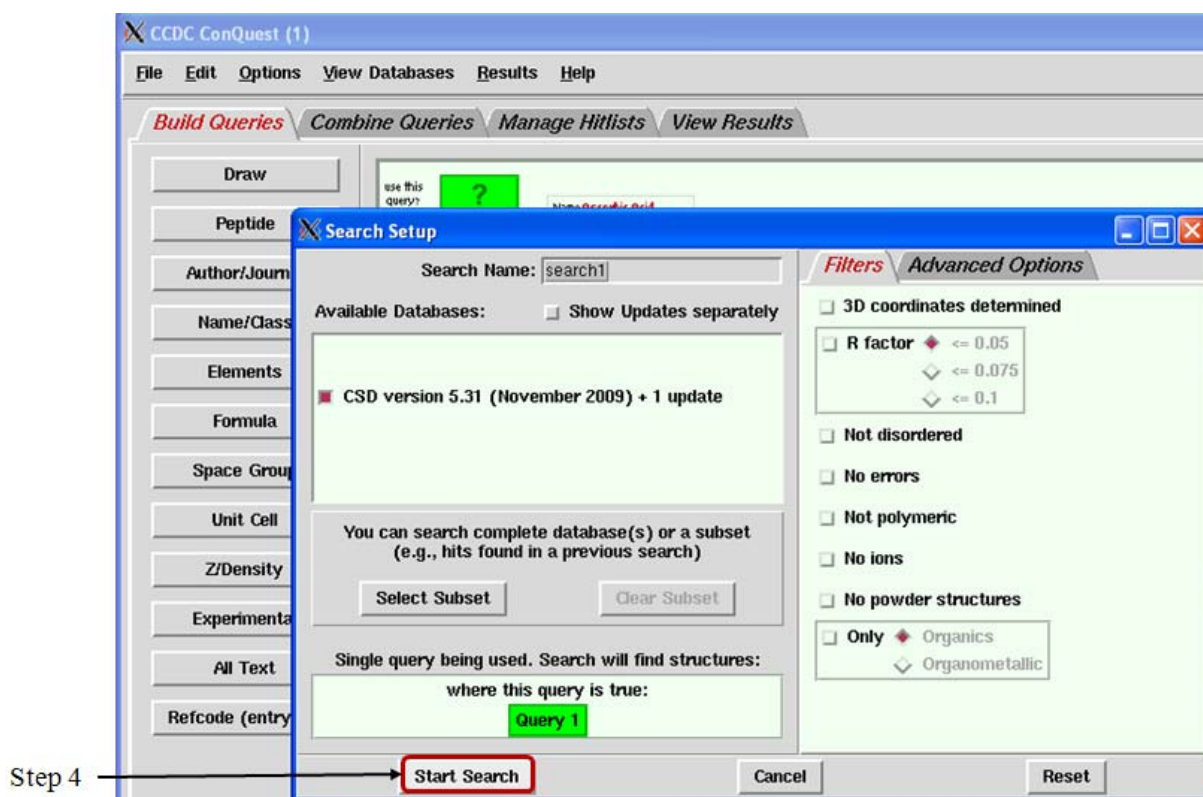


Figure 2-4 Starting the search.

Step 5 →

CCDC ConQuest (1) : search1 [Search]

File Edit Options View Databases Results Help

Build Queries Combine Queries Manage Hitlists View Results

Refcode: AMOBEJ CSD version 5.31 (November 2009)

PhCH<sub>2</sub>—O—C=C—O—CH<sub>2</sub>Ph

AMOBEJ

Analyse Hitlist

- ✓ AMOBEJ
- ✓ AMOBIN
- ✓ BAGSAE
- ✓ BAGSEI
- ✓ BEYMOH
- ✓ BIZDUK
- ✓ DASCBH
- ✓ DHASCB10
- ✓ DOCASC
- ✓ ERAVAU
- ✓ FAKSUF
- ✓ IASCOR10
- ✓ IWODIH
- ✓ LASCAC01
- ✓ LASCAC02
- ✓ LASCAC10
- ✓ LASCAC11

*Figure 2-5 Results of the search.*

CCDC ConQuest (1) : search1 [Search]

File Edit Options View Databases Results Help

Build Queries Combine Queries Manage Hitlists View Results

Refcode: LASCAC13 CSD version 5.31 (November 2009)

Author(s) B. Dittlich, M. Strumpel, M. Schafer, M. A. Spackman, T. Koritsanzky

Reference Acta Crystallogr., Sect. A Found Crystallogr. (2006), 62, 217

Publication DOI 10.1107/S0108767306010336

Deposition IUCr CN5008

Formula C<sub>6</sub> H<sub>8</sub> O<sub>6</sub>

Compound L-Ascorbic acid

Synonym Vitamin C

Spacegroup Name: P21 Number: 4

Cell a: 6.395(2) b: 6.240(2) c: 17.095(3)  
alpha: 90.00 beta: 99.34(<1) gamma: 90.00  
Volume: 673.127

Reduced Cell a: 6.240 b: 6.395 c: 17.095  
alpha: 99.34 beta: 90.00 gamma: 90.00  
Volume: 673.127

Molecular Volume 168.282

Chemical Units 1

Z, Z' Z: 4.0 Z': 2.0

R-Factor (%) 1.86

Temperature (K) Room Temp. (283-303)

Density CCDC: 1.738

Intensity Meas diffractometer

Average Sigma (C-C) not recorded

LASCAC13

Analyse Hitlist

- ✓ AMOBEJ
- ✓ AMOBIN
- ✓ BAGSAE
- ✓ BAGSEI
- ✓ BEYMOH
- ✓ BIZDUK
- ✓ DASCBH
- ✓ DHASCB10
- ✓ DOCASC
- ✓ ERAVAU
- ✓ FAKSUF
- ✓ IASCOR10
- ✓ IWODIH
- ✓ LASCAC01
- ✓ LASCAC02
- ✓ LASCAC10
- ✓ LASCAC11
- ✓ LASCAC12
- ✓ LASCAC13
- ✓ LASCAC14
- ✓ NETROT
- ✓ SERASC10
- ✓ SUHTOE
- ✓ SUPVOO
- ✓ VADZUV
- ✓ VECLAR
- ✓ VECLIV
- ✓ XEVKIS
- ✓ ZZZDSW
- ✓ ZZZIMQ
- ✓ ZZZVIO

*Figure 2-6 Analysing the results of the search.*

For the *downloading of the desired structure* the user should follow the steps according to Figure 2-7.

The user should follow the path in the main menu “File/Export Entry as...” (Step 1). As a second step the settings should be chosen as follows: in “Export as” the format “cif” and the boxes “Additional CIF data items”, “One file per entry”, “Include defined parameters” and “Include bonds” are to be checked. To confirm the choice the user should click on the “save” button. The crystallographic structure data will be saved in the network drive for the corresponding user account “username” in the selected folder. The CCDC program is to be closed via the main menu path File/Exit (Step3). The connection to the CCDC host is stopped



from the main menu in the “run.exe” dialogue by clicking on the main menu path “Main/Send KILL Signal” (Step 4). An illustration is seen in Figure 2-8.

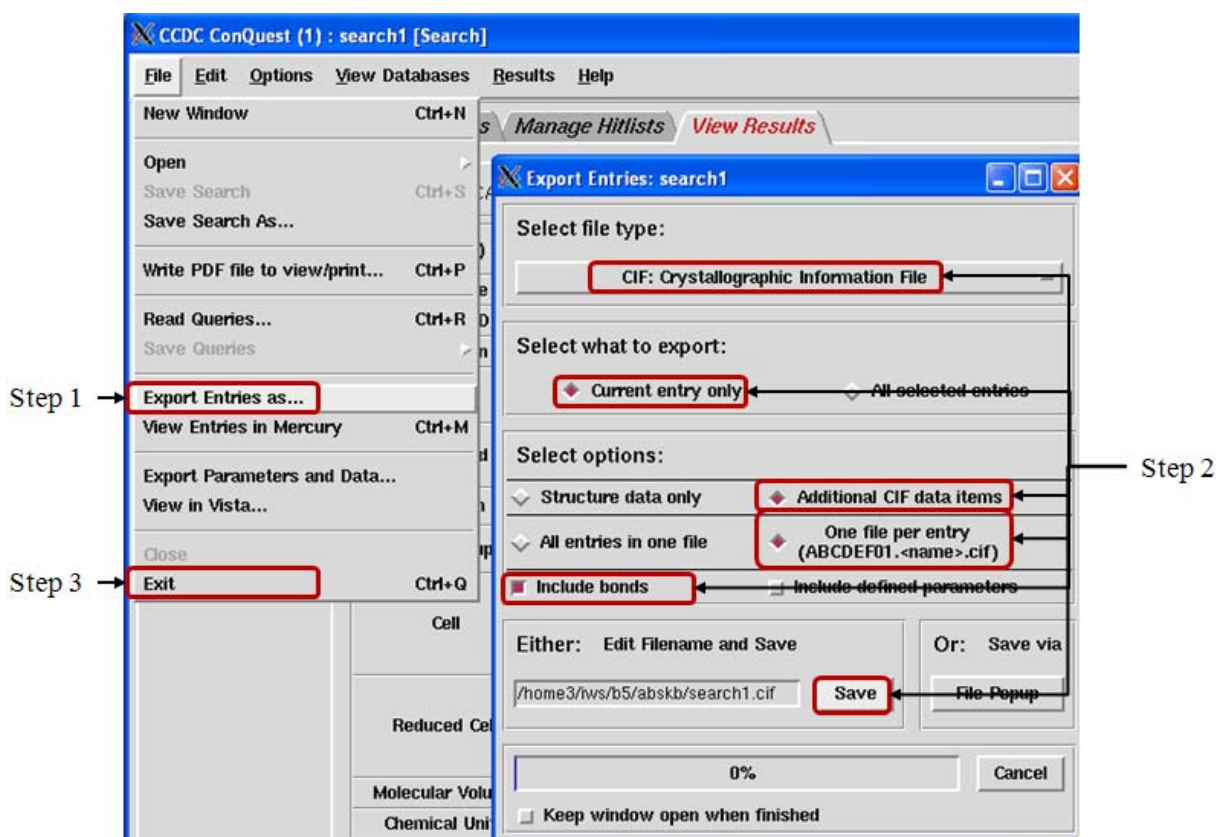


Figure 2-7 Downloading the results of the search.

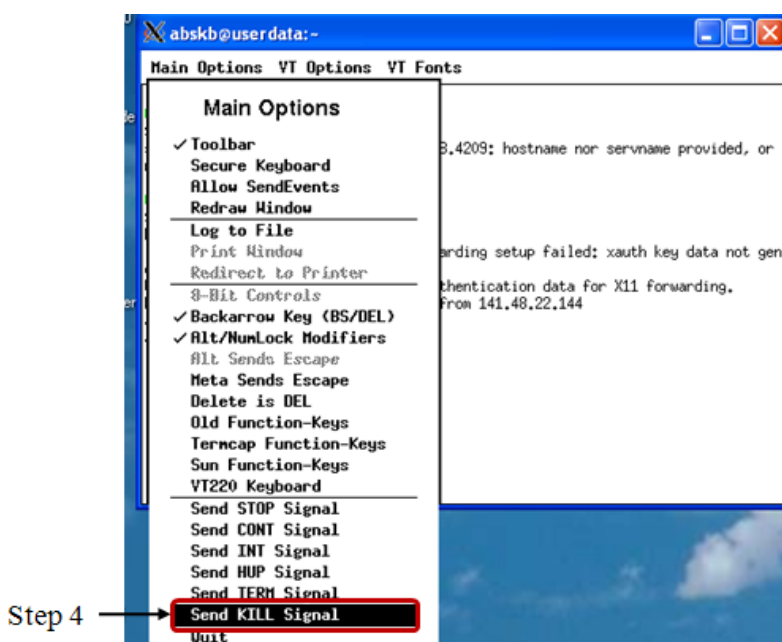


Figure 2-8 Stopping the connection to the CCDC.

## 2.2 The RCSB Protein Data Bank (PDB)

The download of protein structures can be achieved via the RCSB Protein Data Bank (PDB). The search mask is depicted in Figure 2-9. By typing the name of the desired protein the search can be started.

The screenshot shows the RCSB Protein Data Bank (PDB) search mask. At the top left is the PDB logo and a search bar containing 'PDB-101'. To the right, it says 'An Information Portal to Biological Macromolecular Structures' and 'As of Tuesday Jan 24, 2012 at 4 PM PST there are 78867 Structures'. Below the search bar is a navigation menu with categories: 'All Categories', 'Author', 'Macromolecule', 'Sequence', and 'Ligand'. The main content area is titled 'Biological Macromolecular Resource' and includes sections for 'Featured Molecules', 'Molecule of the Month' (Messenger RNA Capping), and 'Protein Structure Initiative Featured System' (Disordered Proteins). A sidebar on the left contains navigation links for 'MyPDB', 'Home', 'Deposition', 'Tools', and 'PDB-101'.

Figure 2-9 Search mask of the RCSB Protein Data Bank.

## 2.3 The American Mineralogist Crystal Structure Database (AMCSD)

The structure of inorganic compounds is obtained from the American Mineralogist Crystal Structure Database (AMCSD). The search mask of the database (see Figure 2-10) is accessed via the internet browser. The search can be conducted for a specific mineral (if the name is known), for the author, via the contained elements, cell parameters diffractions data or by entering any keyword.

**American Mineralogist Crystal Structure Database**

This site is an interface to a crystal structure database that includes every structure published in the American Mineralogist, The Canadian Mineralogist, European Journal of Mineralogy and Physics and Chemistry of Minerals, as well as selected datasets from other journals. The database is maintained under the care of the Mineralogical Society of America and the Mineralogical Association of Canada, and financed by the National Science Foundation.

<input style="width: 95%;" type="text"/>	<b>Mineral</b>
<input style="width: 95%;" type="text"/>	<b>Author</b>
<input style="width: 95%;" type="text"/>	<b>Chemistry Search</b>
<input style="width: 95%;" type="text"/>	<b>Cell Parameters and Symmetry</b>
<input style="width: 95%;" type="text"/>	<b>Diffraction Search</b>
<input style="width: 95%;" type="text"/>	<b>General Search</b>
	<a href="#">Search Tips</a>






**Logic interface**       AND     OR

**Viewing** (About [File Formats](#))     amc long form     amc short form     cif

**Download**       amc     cif     diffraction data

---

People

Extra

**Number of Files downloaded since Apr 1, 2003:** 241681709  
**Data Last Updated:** January 26, 2012  
**Web Page Last Updated:** September 22, 2008  
 This page has been accessed 1391913 times.

Also see our [complete list of minerals](#) and [complete list of authors](#).

This material is based upon work supported by the National Science Foundation under Grant Nos. EAR-0112782, and EAR-0622371. Any opinions, findings, and conclusions or recommendations expressed in this material are those of the authors and do not necessarily reflect the views of the National Science Foundation.

Should the use of the database require a citation, then please use: Downs, R.T. and Hall-Wallace, M. (2003) The American Mineralogist Crystal Structure Database. American Mineralogist 88, 247-250. ([pdf file](#))

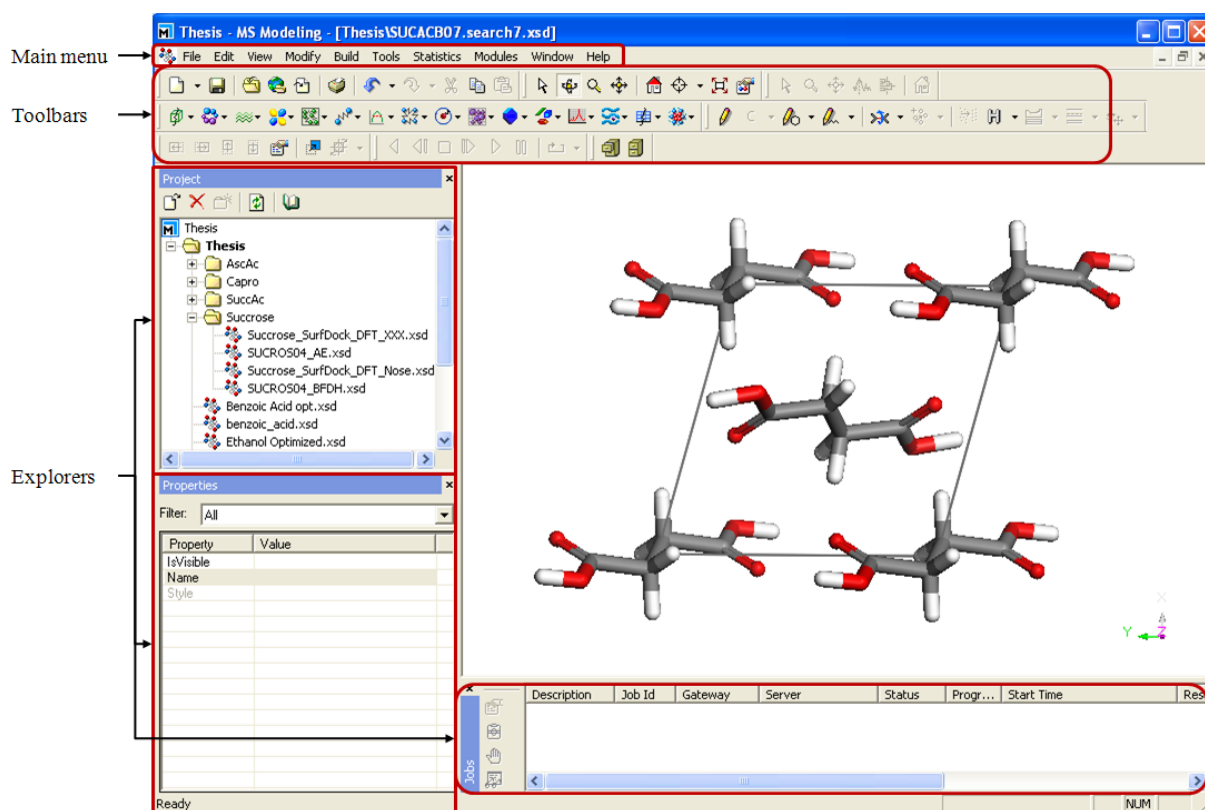
Contact [Robert T Downs](#) for suggestions and corrections.

*Figure 2-10 Search mask of the American Mineralogist Structure Database.*

### 3. MaterialsStudio 4.0

In the present section some frequently used terms are introduced in order to get familiar with the software Materials Studio 4.0.

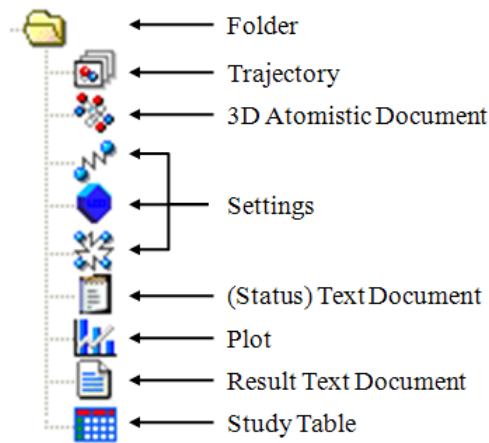
Figure 3-1 shows a screen shot of a Materials Studio dialogue. In general for components of the dialogue are seen: the main menu, toolbars, the explorers and the graphical visualization of a file. There is a wide range of toolbars available, here, only a small selection is depicted. The available explorer types are the “Project Explorer” (on the left top), the “Properties Explorer” (on the left bottom) and the “Job Explorer” (on the right bottom). All of the explorers are useful tools to see the content of the project, the properties of the molecular structure which is seen in the visualization and to see the status of jobs (simulations) which are currently running.



*Figure 3-1 Screenshot of MaterialsStudio 4.0.*

In the project explorer a number of icons are seen. A selection of the most important icons is depicted in Figure 3-2. The 3D graphical visualization is given in the trajectory and the 3D atomistic documents. The settings of all calculations are saved and can be opened via double clicking on the icons. The icons are identical to the symbol of the module which was used for the calculation. The text documents can be either used for notes, or provide with the status information on the running job. Plot documents can be created by the user via one of the

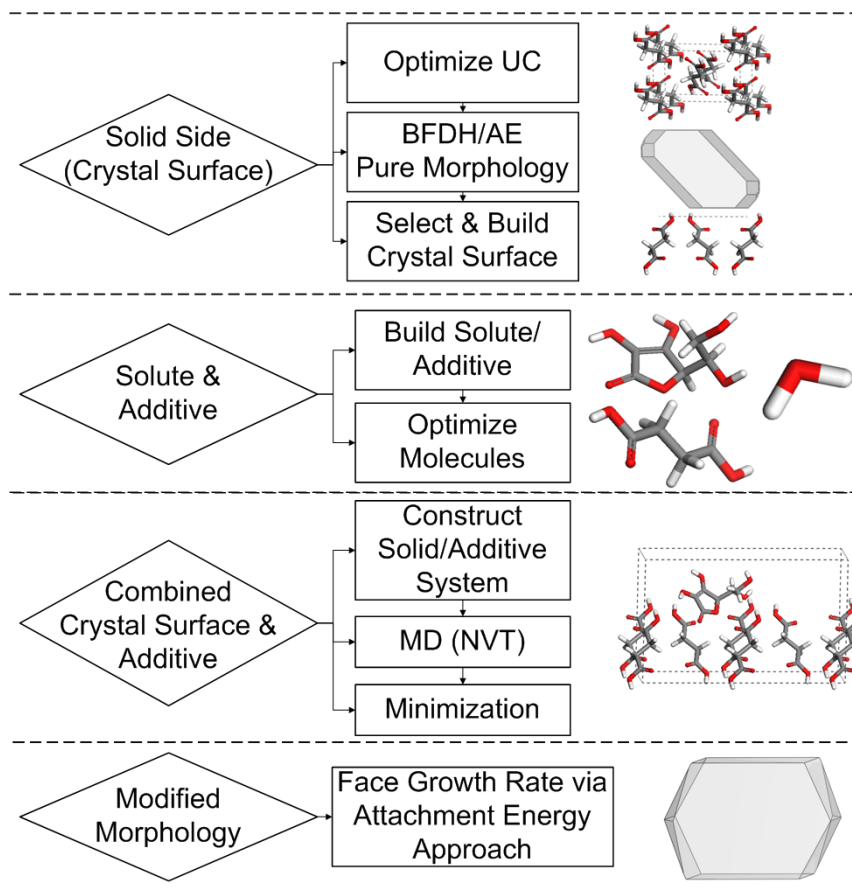
analysis tool or automatically produced as a supplementary output file. The result text document provides with data from the simulations (e.g. cell parameters, energies and densities). The study table is an important output file from the BFDH and the attachment energy calculation.



*Figure 3-2 Document icons in MaterialsStudio 4.0.*

### 3.1 The Surface Docking Method

The Surface Docking method is an established method in morphology prediction for crystals grown in presence of additives. The illustration of the procedures is given in Figure 3-3. In the subsequent chapter all these procedures are introduced in detail.



*Figure 3-3 Schematic representation of the Surface Docking method.*

#### 3.1.1 The Solid Side (Crystal Surface)

##### 3.1.1.1 Step 1: Importing the Crystallographic Structure

In order to import a structure go to the main menu and follow the path “File/Import” (illustrated in Figure 3-4). A dialogue will open which enables to select the desired data.



*Figure 3-4 Importing a structure file.*

### 3.1.1.2 Step 2: Force Field and Charge Calculation

Follow the path depicted in Figure 3-5. To open the tool “Discover” click on the corresponding symbol in the toolbar. From the drop down menu select “Setup”. The dialogue with five index cards will open as depicted on the right. Some of the default settings are to be modified and highlighted with a red frame. The charge and the force field calculation are started when pressing the button on the index card “Typing” (Figure 3-5 bottom right).

In order to see the charges and force field types an atom labeling should be conducted. By clicking on the right mouse button and a drop down menus is opened, here click on “Label”. The appearing dialogue enables to select the property of interest. A visualization is obtained when click on “Apply”. An illustration of these steps is seen in Figure 3-6.

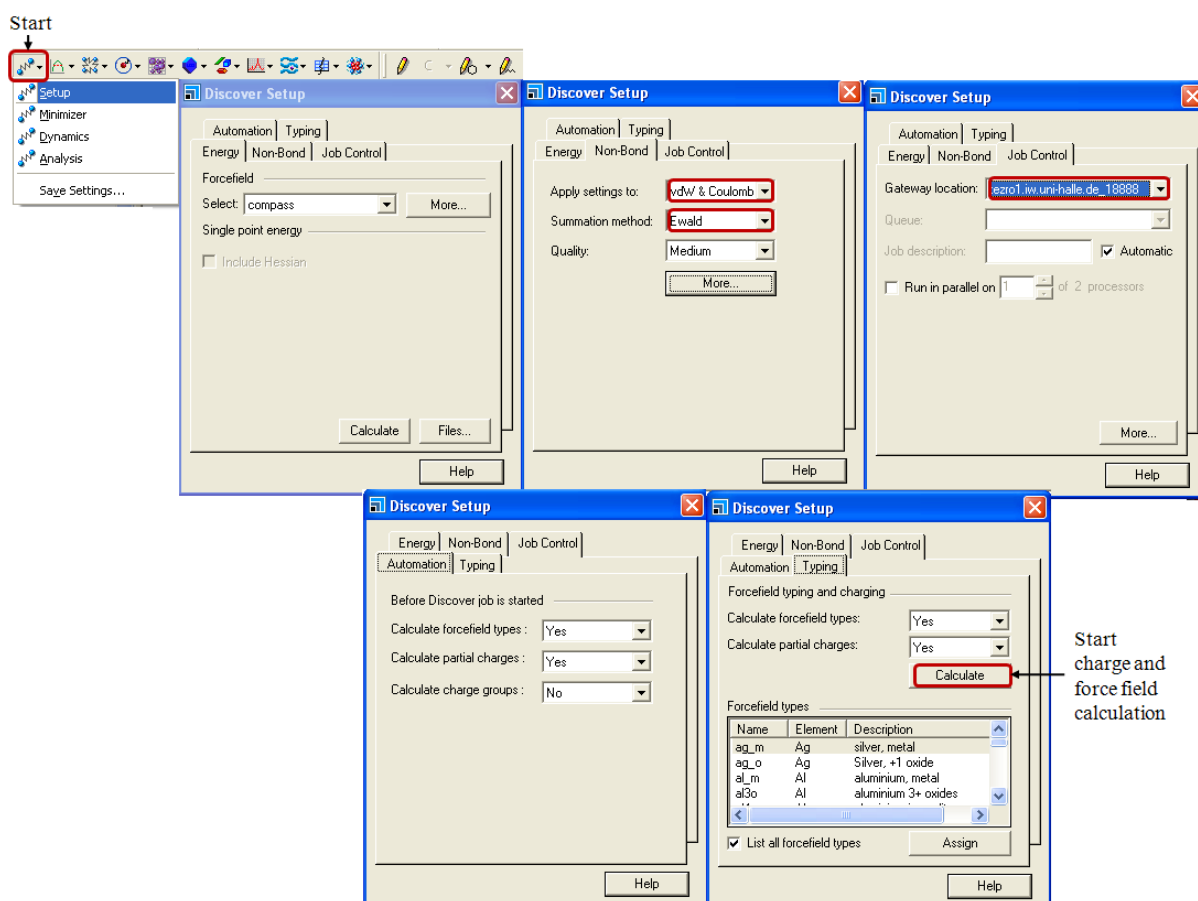
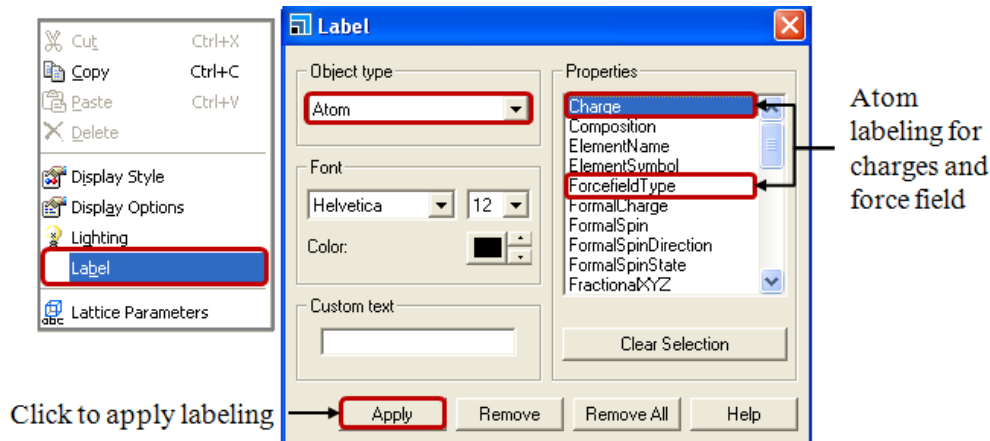


Figure 3-5 Applying the force field and charge calculation with the tool Discover.

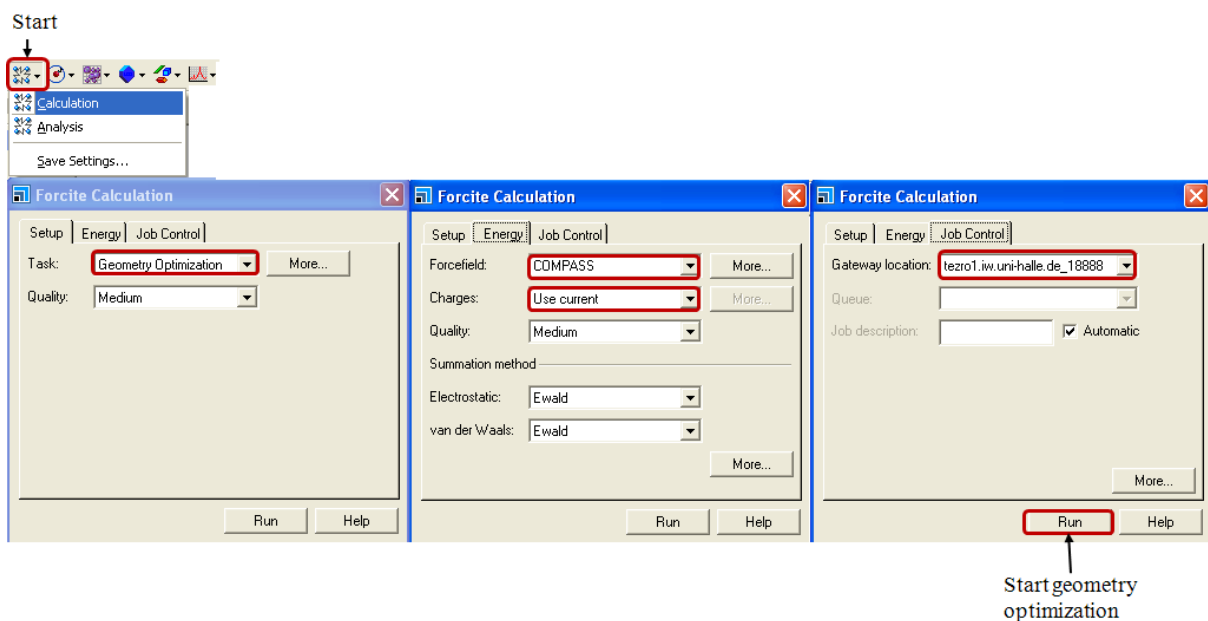




*Figure 3-6 Labeling of atoms.*

### 3.1.1.3 Step 3: Geometry Optimization for Crystal Structure Data or Molecules

After the charges and the force field is calculated the structure needs to be optimized. The calculation can be performed with the tool “Forcite” which is also found in the toolbar as illustrated in Figure 3-7. A change of the default settings is required in all of the three index cards. Firstly the “Task” in the “Setup” index should be set to “Geometry Optimization”. In the index card “Energy” the force field is selected (here: COMPASS) and the charge calculation should be set to “Use Current”, since, the charge calculation was performed in chapter 3.1.1.2. Another reason for not repeating the charge calculation is the additional computation time which would be required.

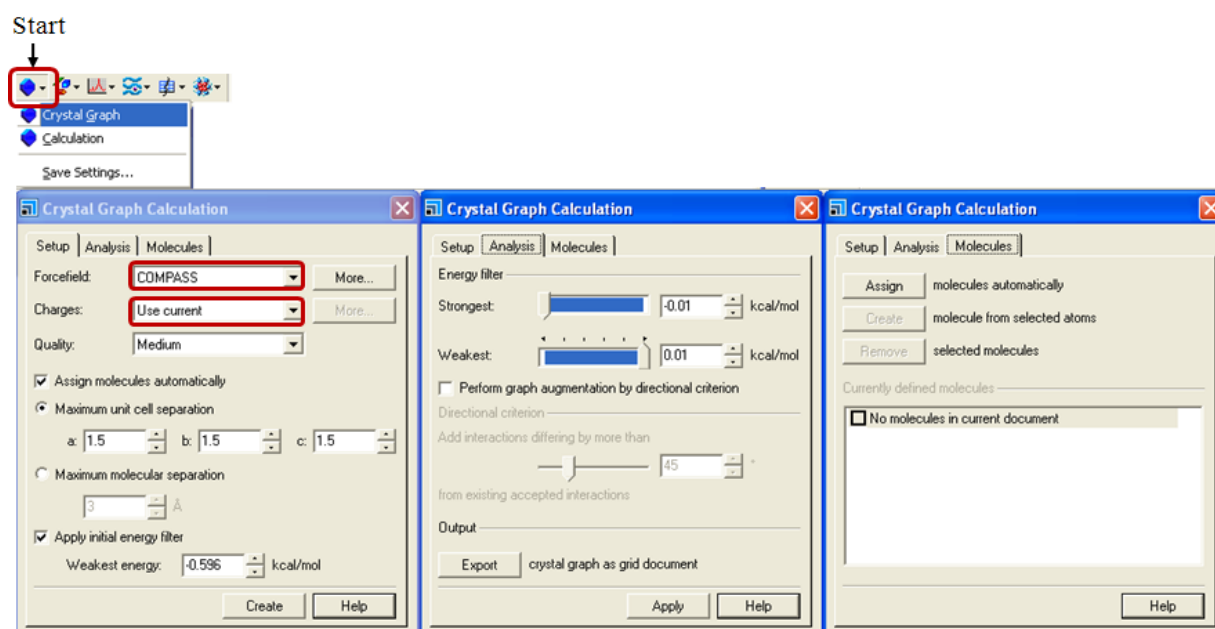


*Figure 3-7 Geometry optimization with the module “Forcite”.*

### 3.1.1.4 Step 4: BFDH and Attachment Energy

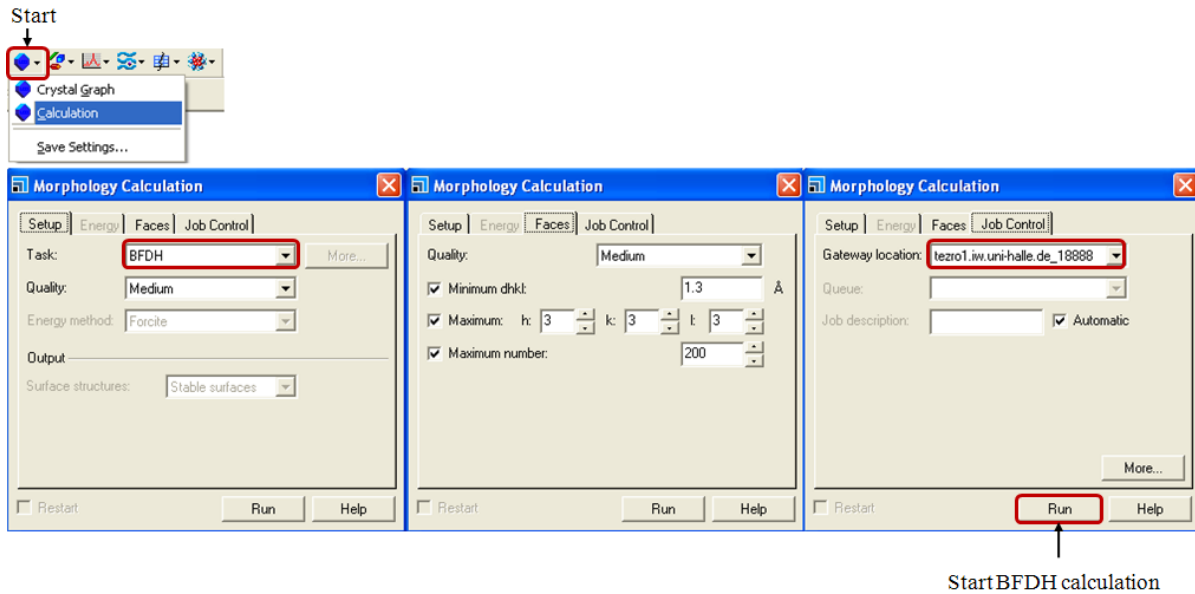
The required calculations are performed with the module “Morphology” which is available in the toolbar.

The illustrations in Figure 3-8 gives an overview on the settings which are recommended for the calculations. These are to be set prior to the BFDH and attachment energy calculations. The settings comprise the choice of the force field (here: COMPASS) and the charge calculation. Since the charges are calculated prior to the geometry optimization this step can be skipped. The corresponding drop down menu for the “Charges” in the index card “Setup” is set to “Use current”. The change of any other settings in the “Crystal Graph Calculation” dialogue is not recommended. The settings are saved automatically when the dialogue is closed.



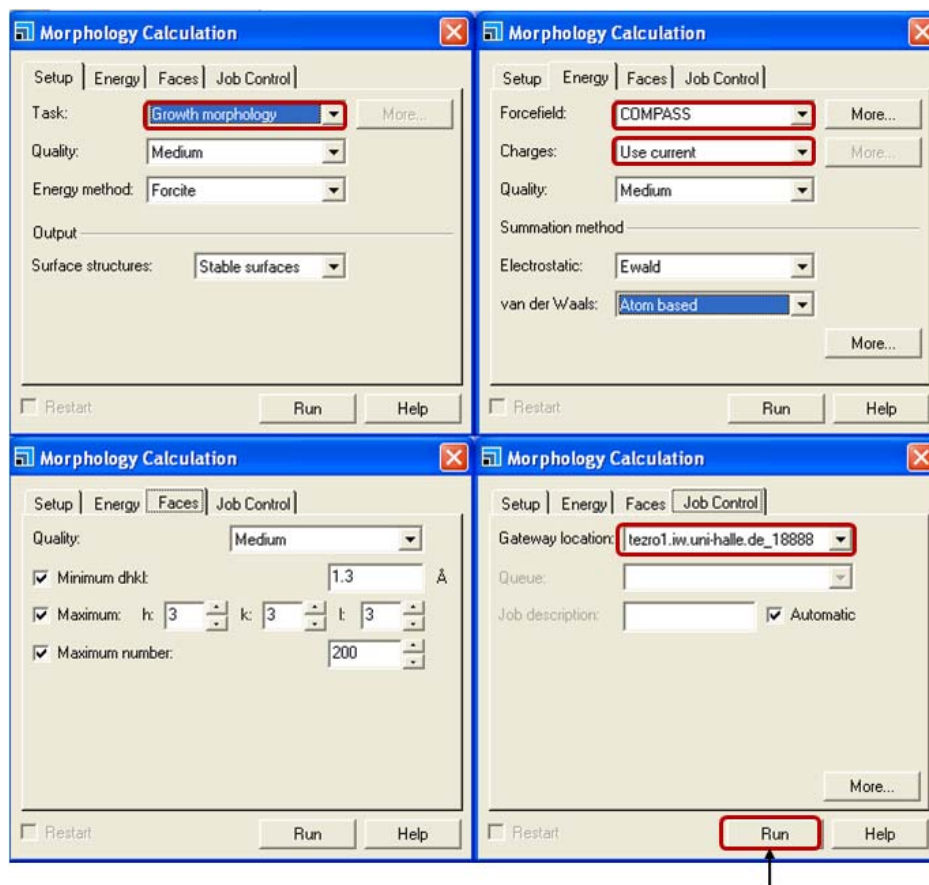
*Figure 3-8 Settings in the module “Morphology”.*

The menu for the *BFDH* calculations is accessed via the submenu “Calculation” in the module “Morphology” (see Figure 3-9). The dialogue “Morphology Calculation” is displayed. In the first index card the “Task” “BFDH” is selected from the drop down menu. From the index card “Job Control” the gateway is selected. In order to start the calculation, open the 3D atomistic file of the optimized unit cell and press the button “Run”. The BDFH calculation usually proceeds within two minutes. The corresponding result files will be automatically displayed at end. A new document folder (seen in the “Project Explorer”) in which these files are stored will be created (see Figure 3-11).



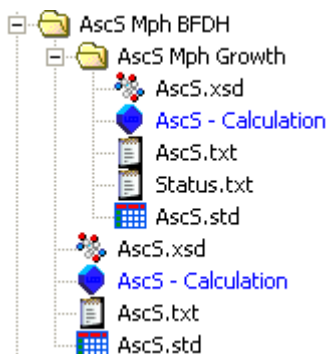
*Figure 3-9 BFDH calculation in the module “Morphology”.*

The *attachment energy* calculation is started from the same dialogue which is accessed via the submenu “Calculation” in the module “Morphology” (see Figure 3-10). The first index card provides to choose the “Task” “Growth morphology” from a drop down menu. The second index card is entitled “Energy” and allows the choice of the force field (here: COMPASS) and the charge calculation. Since the charges are calculated prior to the geometry optimization this step can be skipped and drop down menu for the “Charges” is set to “Use current”. From the index card “Job Control” the gateway is selected. The change of any other settings in the “Morphology Calculation” dialogue is not recommended. In order to start the calculation, open the 3D atomistic file which is produced in the BFDH and press the button “Run”. The attachment energy calculation proceeds within ten minutes. The corresponding result files will be automatically displayed at end. A new document folder (seen in the “Project Explorer”) in which these files are stored will be created (see Figure 3-11).



Start attachment energy calculation

*Figure 3-10 Attachment energy calculation in the module “Morphology”.*



*Figure 3-11 Illustration of the folder structure seen in the Project Explorer after the BFDH and Attachment Energy calculation.*

### 3.1.1.5 Step 5: Important Crystal Surfaces

The 8 most important crystal faces (morphological importance corresponds to visibility) are to be selected and surface boxes are prepared by cleaving a face, creating a supercell and adding the vacuum slab.

Open the study table which is a result file of the attachment energy calculation. Select the faces 1 to 8 from the top of the list (see Figure 3-12). Note the miller indices of the faces and the corresponding attachment energies.

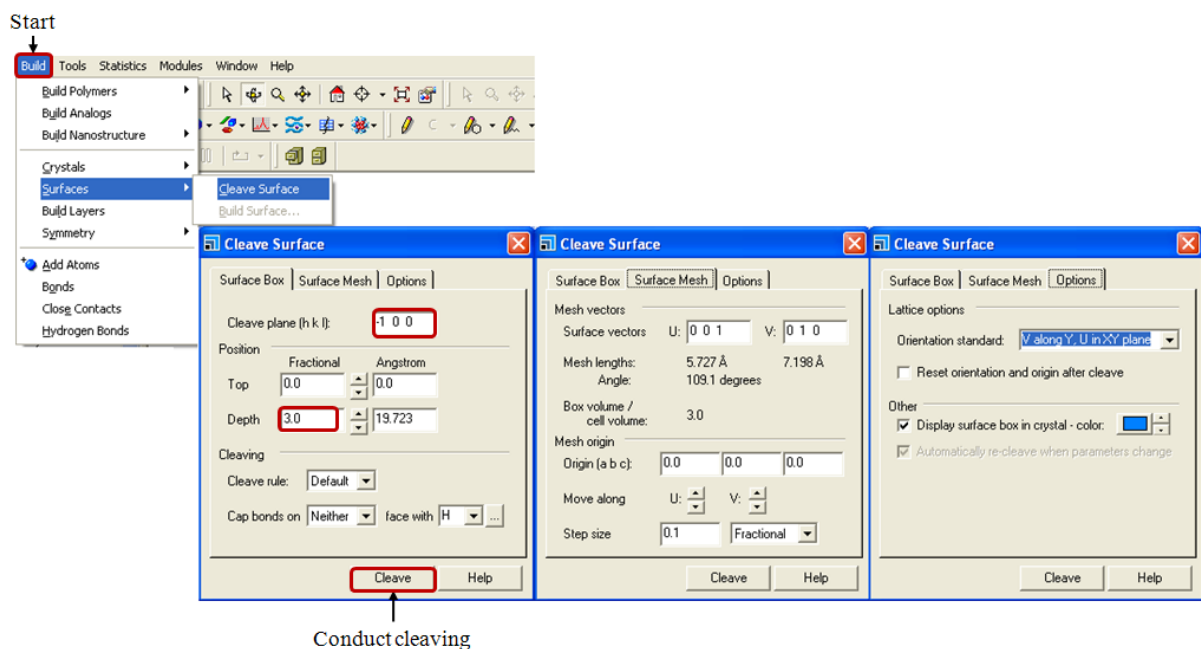
Start: Open study table

Select 8 most important surfaces

	A	B	C	D	Open surface structure	F	J	K	L
	hkl	Multiplicity	dhkl	Surface area	Surface	Eatt(Total)	Distance	Total facet area	% Total facet ar
1	{ 2 0 0 }	2	8.84122757	74.43414848	Surface (2 0 0)	-33.24651416	33.24651416	2.282290e+004	43.344154
2	{ 1 1 0 }	4	6.95748680	94.58720722	Surface (1 1 0)	-54.72018810	54.72018810	7.037205e+003	13.364722
3	{ 1 1 -1 }	4	5.97079296	110.21806484	Surface (1 1 -1)	-56.11322356	56.11322356	2.253080e+004	42.789425
4	{ 1 1 1 }	4	5.18150493	127.00735684	Surface (1 1 1)	-75.40078357	75.40078357		
5	{ 2 0 -2 }	2	4.85868989	135.44582182	Surface (2 0 -2)	-90.06345074	90.06345074	264.17126695	0.501701
6	{ 3 1 -1 }	4	4.74366354	138.73016925	Surface (3 1 -1)	-67.31094763	67.31094763		
7	{ 3 1 0 }	4	4.65018329	141.51899056	Surface (3 1 0)	-86.25481328	86.25481328		
8	{ 0 0 2 }	2	4.56623178	72.06042939	Surface (0 0 2)	-110.43711582	110.43711582		
9	{ 1 1 -2 }	4	4.10227824	160.42043147	Surface (1 1 -2)	-115.51378720	115.51378720		

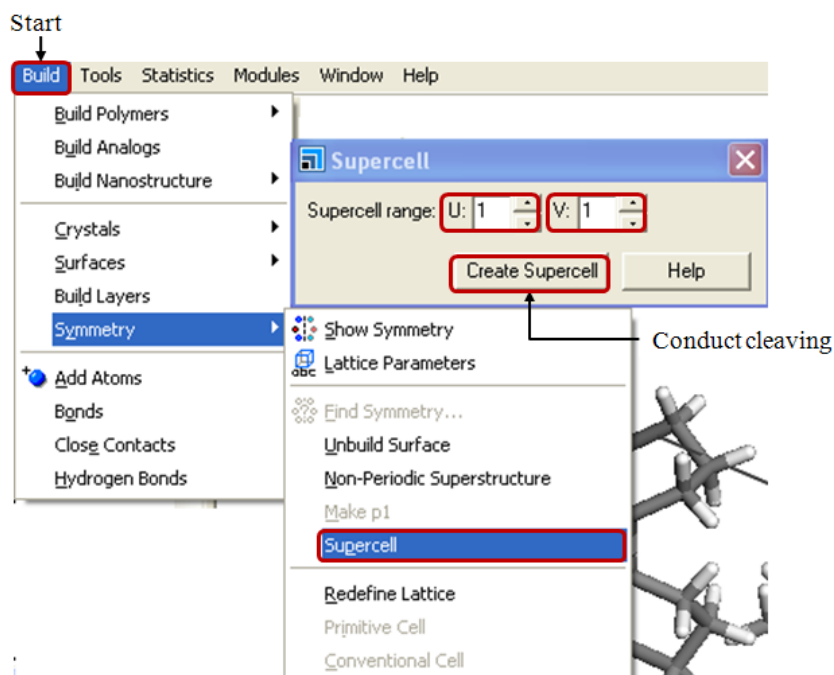
*Figure 3-12 Study table resulting from the attachment energy calculation.*

Prior to the *cleaving* of a surface a crystal structure should be visible. The structure is available either by clicking on the symbol in the column E of the study table (Figure 3-12) or when opening the 3D result file from the attachment energy calculation. In order to cleave a surface for a crystal surface box follow the procedure as illustrated in Figure 3-13. In the main menu follow the path Build/Surfaces/Cleave Surface. The dialogue “Cleave surface will be opened. In the index card “Surface Box” the “Cleave Plane {h k l}” is the one you cleave. Set the fractional value for “Position” “Depth” to 3.0. Any other settings should remain as default. The cleaving is conducted when pressing the button “Cleave”.



*Figure 3-13 Cleaving a crystal surface.*

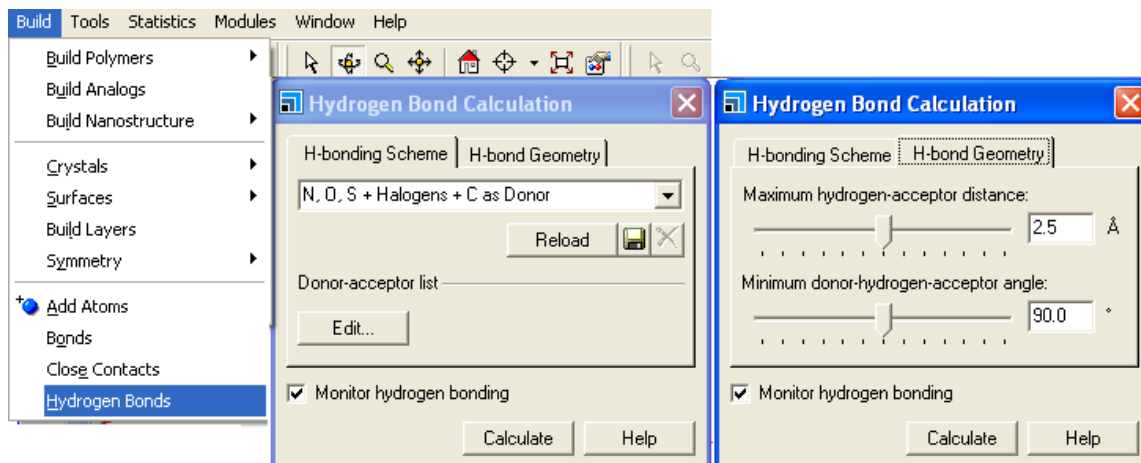
The construction of a *supercell* is the next task which is achieved when following the main menu path Build/Symmetry/Supercell (illustrated in Figure 3-14). The Supercell dialogue allows the change of the “Supercell range”, here, set U: 4 and V: 6. Depending on the surface structure it is even possible to select U: 2 and V: 3. Press the button in order to create a supercell.



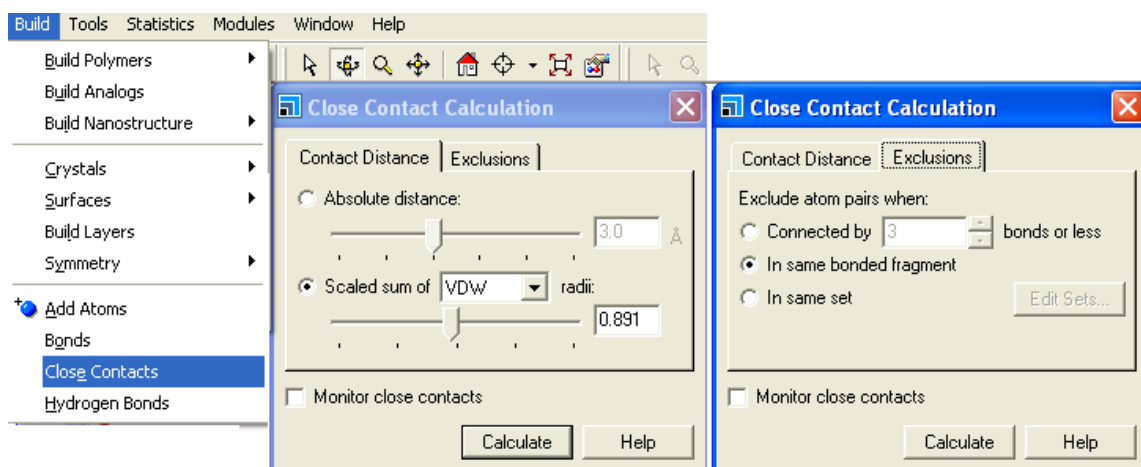
*Figure 3-14 Building a supercell.*



Repeat the procedure for each of the surfaces of the first set e.g. with the additive molecule and again for the second set where host the molecule is attached to the crystal surface. At the end of the procedure there should be a total of 16 faces.



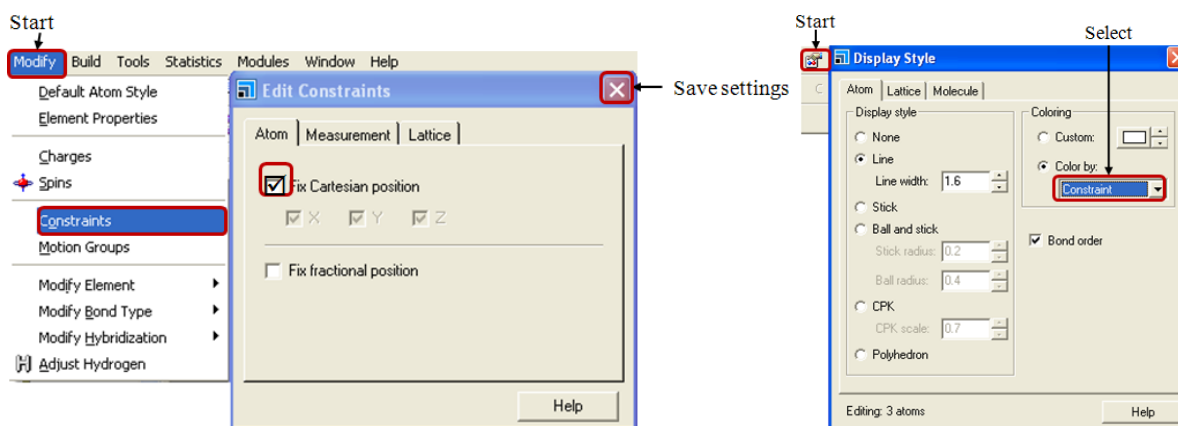
*Figure 3-16 Display hydrogen bonds.*



*Figure 3-17 Display close contacts.*

In order to prevent the movement of the surface molecules it is required to set constraints and fix the surface atoms. Therefore, the atoms of the surface are to be selected. Open the path Modify/Constraints from the main menu and on the index card “Atom” check the option “Fix Cartesian Position” (see Figure 3-18 left). To ensure the surface atoms are fixed it is possible to color the atoms by constraint. Get access to the tool “Display Style” via the button in the tool bar or by clicking on the right mouse button. In the dialogue “Display Style” select in the index card “Atom” in “Coloring” “Color by Constraint” from the drop down menu (Figure 3-18 right). When finished save your file.





*Figure 3-18 Left: Setting the constraints prior NVT molecular dynamics. Right: Display colouring by constraint.*

### 3.1.2.2 Step 7: Molecular Dynamics (NVT)

Before starting the molecular dynamics all “Discover” settings (such as the selection of a gateway and force field) are to be made. This is done in the “Discover Setup” dialogue which is accessed via the toolbar Discover/Setup. The illustration in Figure 3-19 gives a listing of all required settings. The “Forcefield” is selected in the index card “Energy”. The general settings are similar to those depicted in Figure 3-5, but the main difference is the settings in the index cards “Automation” and “Typing” which should explicitly avoid the charge calculation. The calculation of the charges is not necessary since it was conducted in chapter 3.1.1.2. The settings are saved automatically when closing the dialogue.

In order to perform the molecular dynamics simulations follow the path Discover/Dynamics from the toolbar. The dialogue “Discover Molecular Dynamics” will be opened. The settings in the index card “Dynamics” are to be changed as follows. Set the “Ensemble” as “NVT”, the “Temperature” to “300 K”, and “Number of steps” to “5000” with a “Dynamics time ”of“ 5 ps. “Save” the trajectory as “Full” at the “Frame output every” 50 steps. In order to change the thermostat, click on the “Thermostat” button. The dialogue “Thermostat” will be opened where it is possible to select the thermostat as Nosé, Velocity Scale, Andersen or Berendsen. According to the selected temperature control method the option of changing the factor for the temperature control is given, which is with Velocity Scale the “Temperature difference” (default is “10 K”) and with Nosé the “Q ratio” (default is “1.0”). These default values should not be modified. As a thermostat the Nosé method is recommended. Press the “OK” button in the “Thermostat” dialogue in order to save the settings and close the dialogue. If all the settings are made press the “Run” button in the “Discover Molecular Dynamics” dialogue.

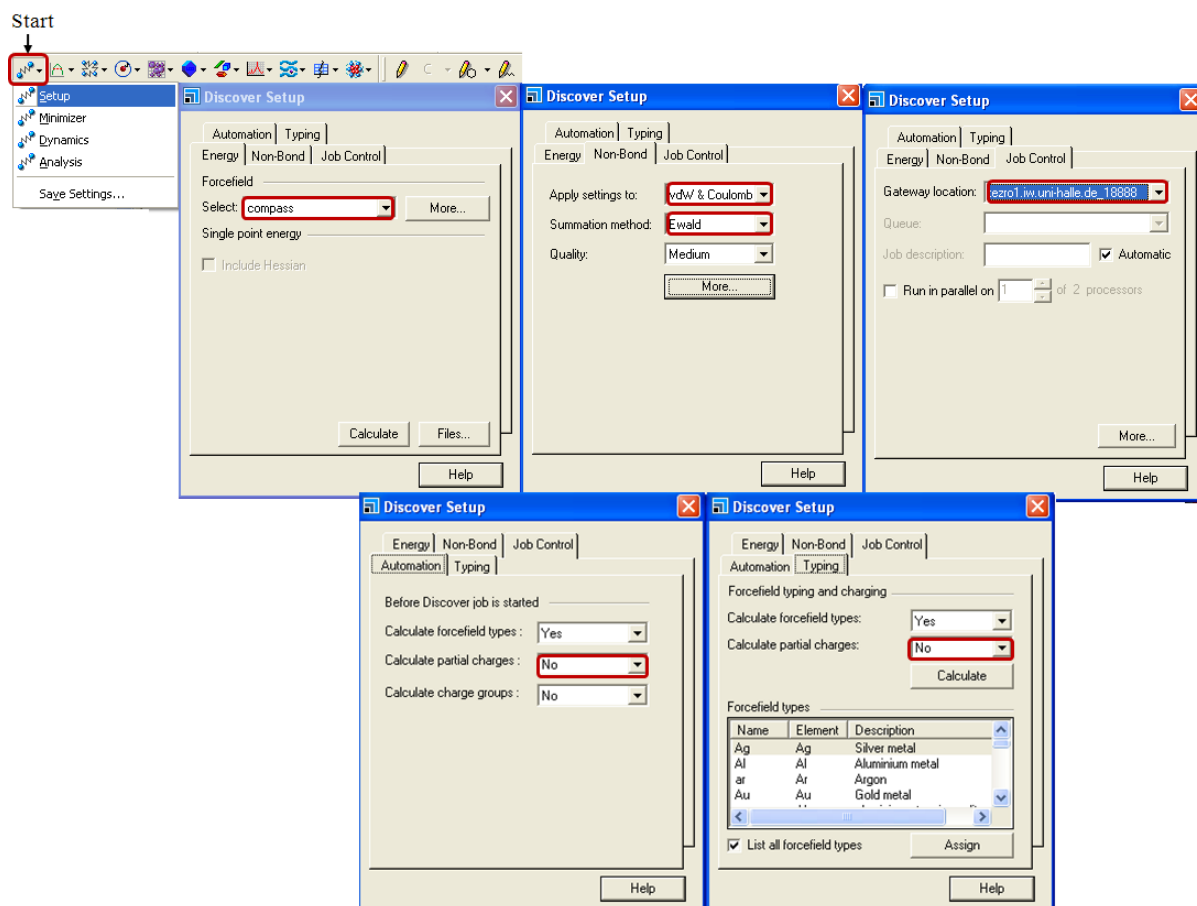
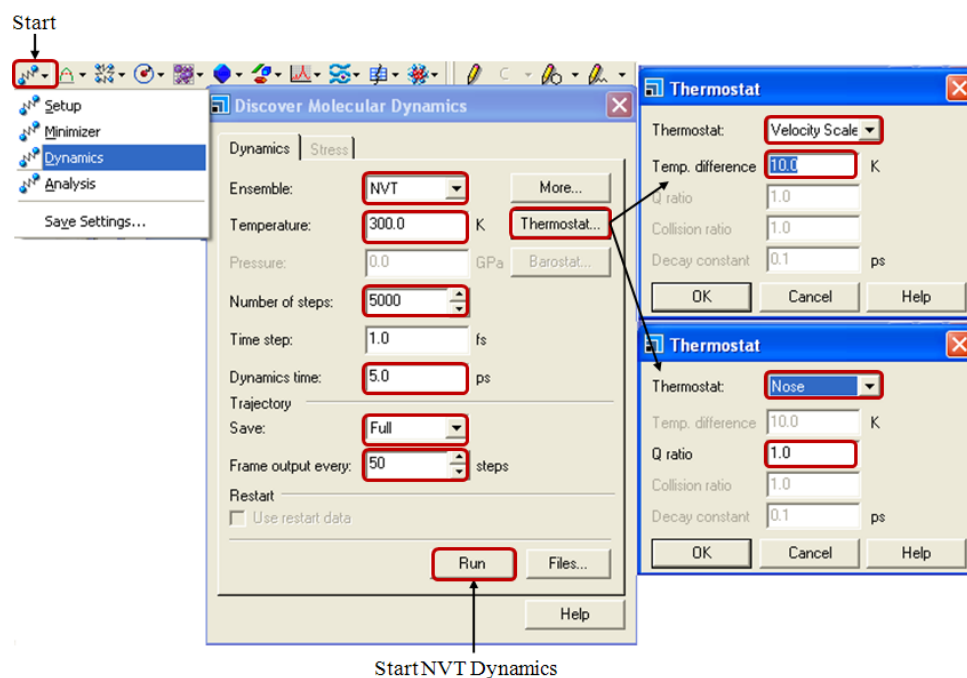


Figure 3-19 Settings in the “Discover Setup” dialogue.

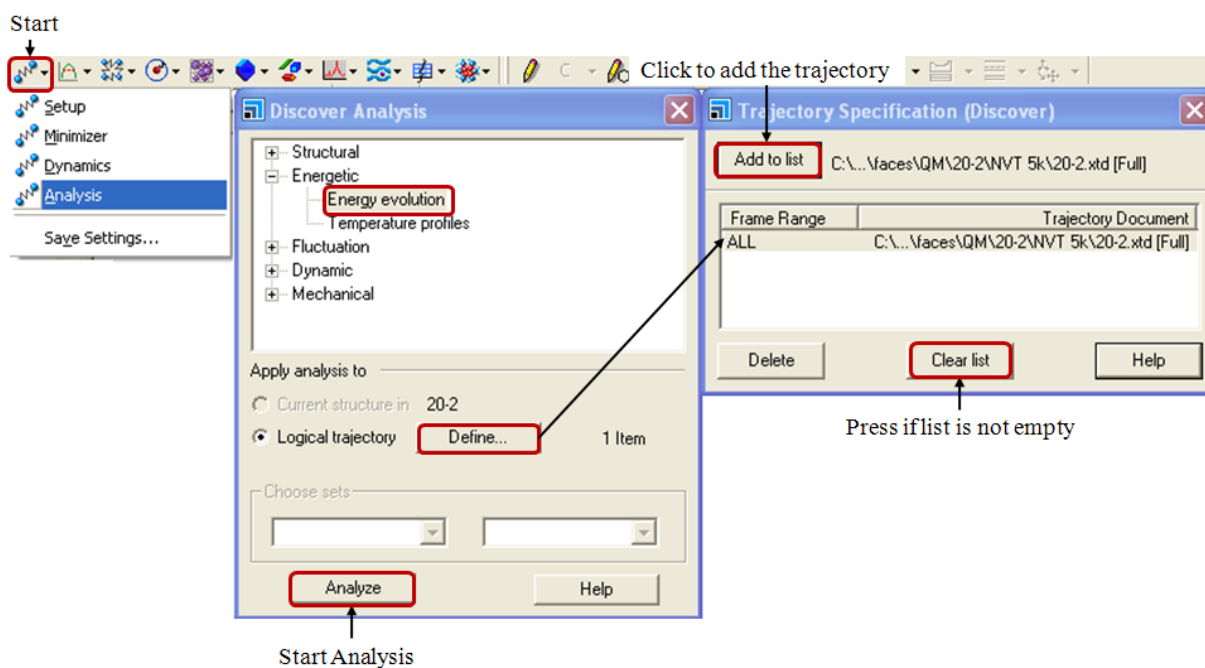


StartNVT Dynamics

Figure 3-20 Molecular dynamics settings (NVT).

### 3.1.2.3 Step 8: Trajectory Analysis

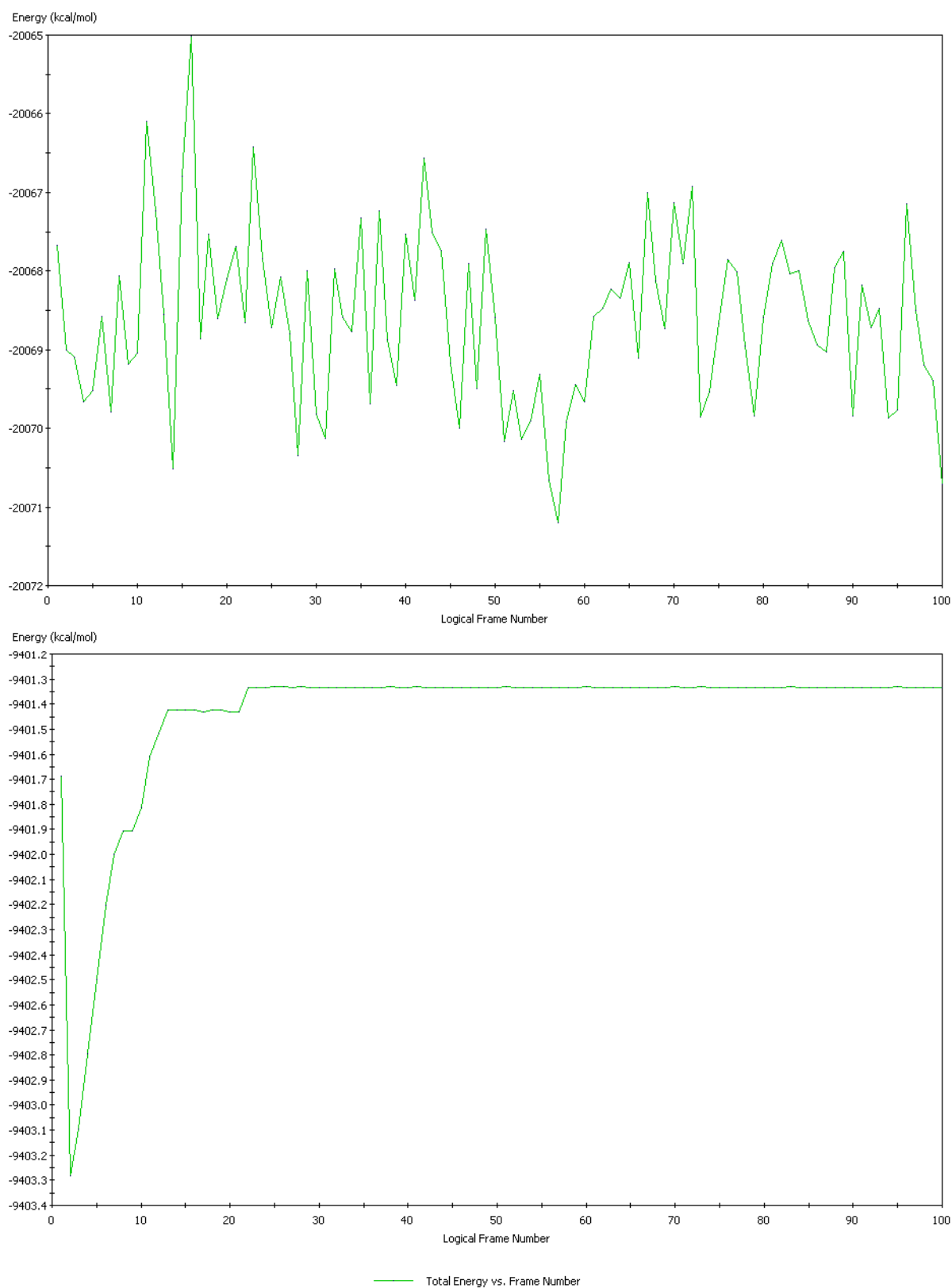
The *analysis* of the resulting molecular trajectory file is carried out with the “Discover Analysis” accessed via the toolbar path Discover/Analysis. Select “Energetic” and “Energy evolution” the root structure which is seen in the dialogue. The selection of a trajectory to be analyzed is done in the “Trajectory Specification (Discover)” dialogue which is accessed when clicking on the “Define...” button as illustrated in Figure 3-21. The dialogue which is opened consists of a list and several buttons. The list may contain files which are previously analyzed, in this case press the “Clear list” button. In case the list is empty directly press the “Add to list” button. If there is no path for the document indicated right of the “Add to list” button there is no trajectory files active or open. In this case open a trajectory file and follow the procedure. Close the “Trajectory Specification (Discover)” dialogue and start the analysis by pressing the “Analyze” button. Within several seconds the result from the analysis is created. The file is a plot of the total energy vs. simulation time (examples are presented in Figure 3-22). Herein, search for the frame (or time step) with the lowest energy (write down the frame number and the total energy). Save and close the file containing the plot.



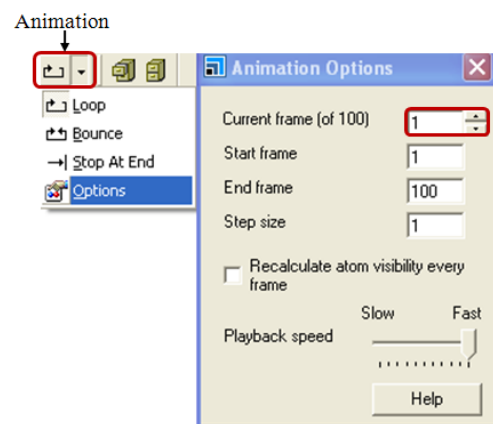
*Figure 3-21 Discover analysis of a trajectory document.*

Open the trajectory file and skip the frames to the frame of the lowest total energy. The molecular conformation in this frame is achieved with the tool “Animation”. The tool is accessed via the toolbar path “Animation/Options” (see Figure 3-23). In the dialogue “Animation Options set the “Current frame” to the lowest energy frame and press the Tab key on your keyboard. As the molecules moved, copy the molecular conformation in this frame

(via Ctrl+C and Ctrl.+V) to an empty 3D atomistic document and save it as “lowest energy frame” (lef).

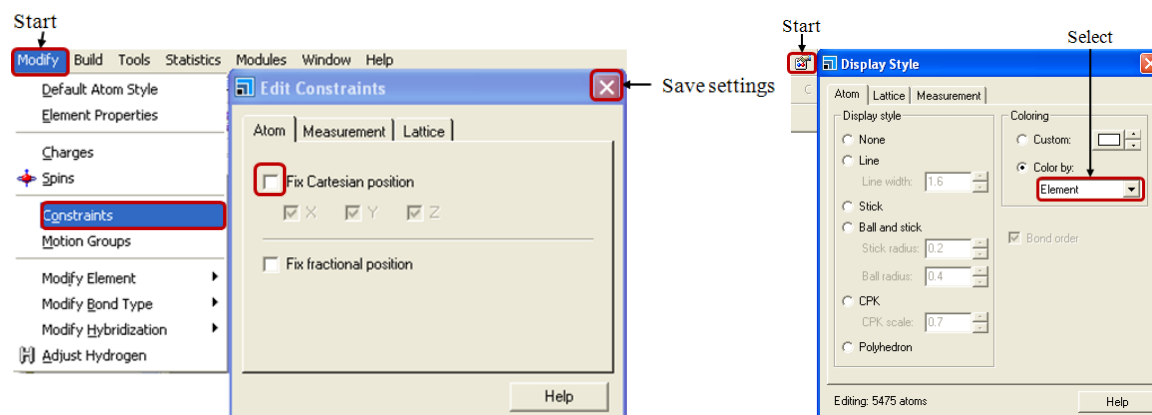


*Figure 3-22 Plots of the total Energy vs. Frame Number from the Discover Analysis.*



*Figure 3-23 Animation options of a trajectory document.*

Remove the constraints from the surface atoms prior to the next step as illustrated in Figure 3-24. Press Ctrl.+A to select all atoms and follow the path Modify/Constraints from the main menu. In the dialogue “Edit Constraints” deselect “Fix Cartesian Position” in the index card “Atom”. For a better visualization of these changed constraints change the coloring of the atoms to “Constraint”. If the atoms are all colored in grey the constraints are removed successfully and the coloring should be set to “Color by Element” (see Figure 3-24 right).

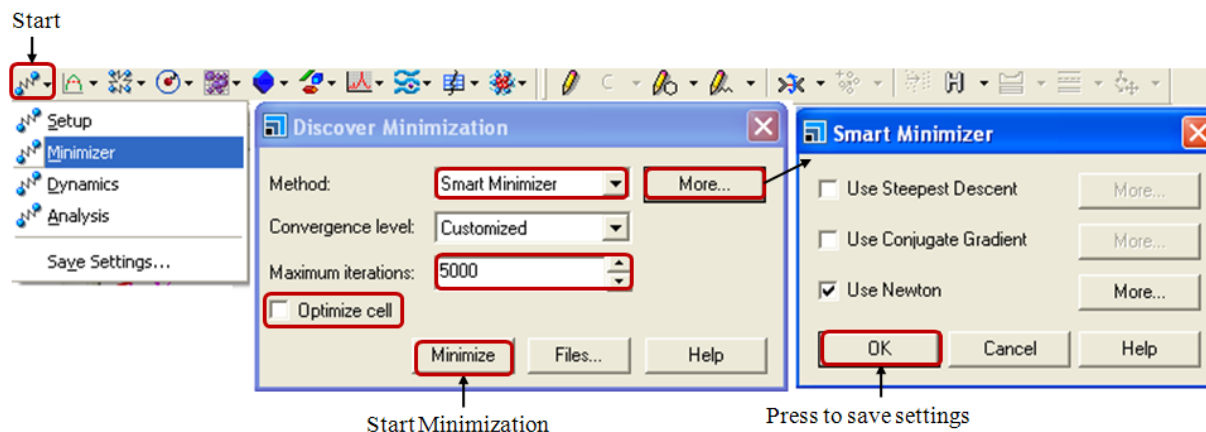


*Figure 3-24 Left: Removing the constraints from the surface atoms. Right: Atom coloring.*

### 3.1.2.4 Step 9: Minimization

Starting the minimization of the molecular conformation at the lowest energy level is achieved when following the path Discover/Minimizer” from the toolbar (Figure 3-25). The “Discover Minimization” dialogue enables to select the “Method” as “Smart Minimizer”, at the level of 5000 “Maximum iterations”. Make sure that the box “optimize cell” is not checked. When clicking the button “More...” the “Smart Minimizer” dialogue enables to choose the minimization algorithms. Here, “Use Steepest Descent” and “Use Conjugate

Gradient” should be deselected and “Use Newton” is checked. In order to start the minimizations press the “Minimize” button. One of the result files is a text file from which the total potential energy is obtained. Note the total potential energy after the minimization.



*Figure 3-25 “Discover Minimization” dialogue.*

### 3.1.2.5 Step 10: Calculating the Energy of Surface and Additive

Open the 3D atomistic document which is the result file from the minimization. Delete the molecule which is docked on the surface and save the file as “surface only”. (Take care not to overwrite the existing result file!) In order to calculate the current energy (total potential energy) of the structure follow the path Discover/Setup in the toolbar. The settings should remain the same as those which were set prior the dynamics and the corresponding minimization. In the index card “Energy” press the button “Calculate” (see Figure 3-26). The resulting text file supplies with the total potential energy of the surface.

The same procedure is to be conducted for the molecule which is docked on the surface. Thus, open the 3D atomistic document which is the result file from the minimization. Select and delete all atoms of the crystal surface, only the molecules on the surface should not be deleted. Save the file as “additive only” and calculate the current energy of the system according to the description which was given before. Note the total potential energies of the system.

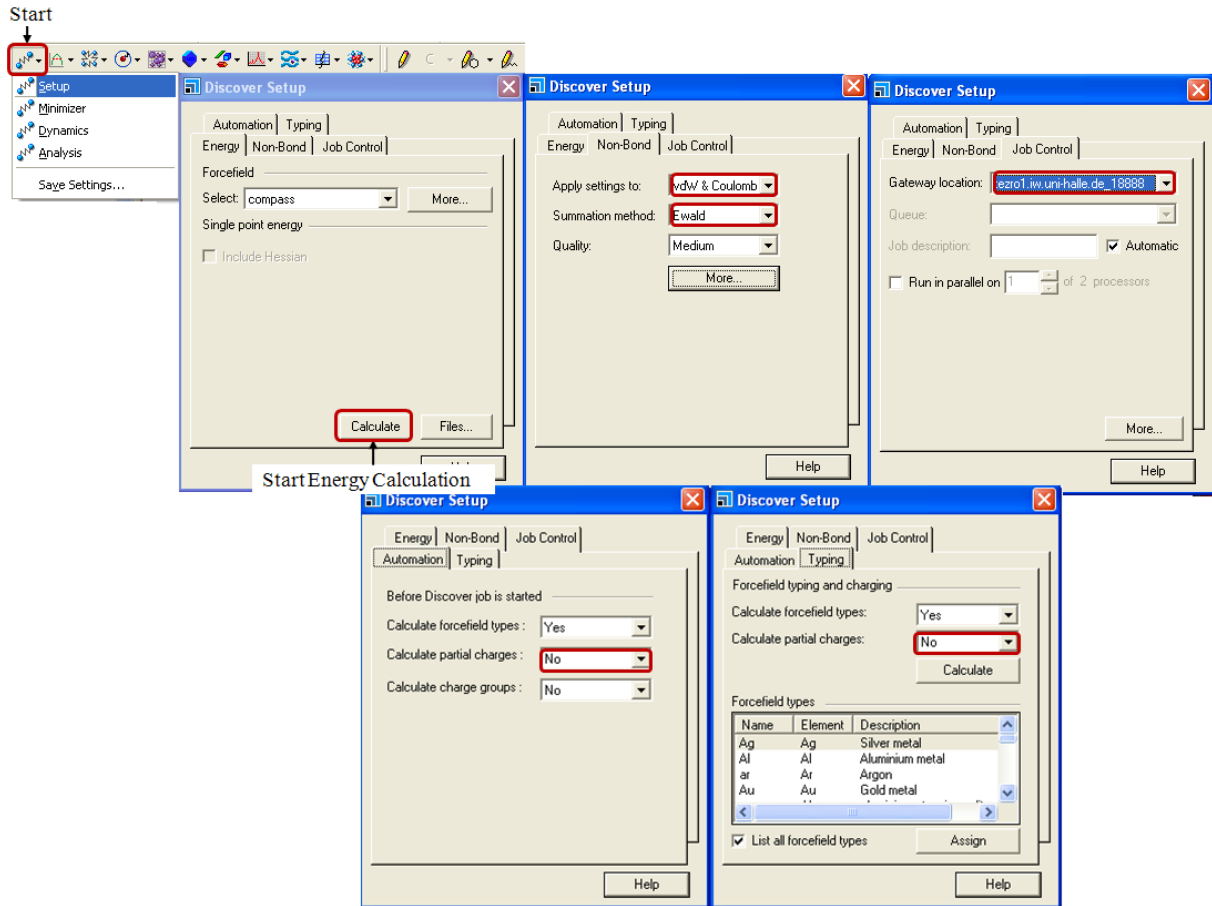


Figure 3-26 “Discover Setup” dialogue for the calculation of the current energy.

### 3.1.3 The Modified Morphology

#### 3.1.3.1 Step 11: Calculating the Modified Attachment Energy

- Binding energy of the host crystal molecule to the surface

$$E_b^{host} = E_{total} - (E_{surface} + E_{host}) \quad 3-1$$

- Binding energy of the additive molecule to the surface

$$E_b^{additive} = E_{total} - (E_{surface} + E_{additive}) \quad 3-2$$

- Binding energy difference

$$\Delta b = E_b^{additive} - E_b^{host} \quad 3-3$$


- Modified attachment energy according to Lu 2004

$$E_{hkl}^{att,mod} = E_{hkl}^{att} - \frac{E_{hkl}^{att} \times \Delta b}{E_b^{host}} \quad 3-4$$

### 3.1.3.2 Step 12: Calculating the Modified Morphology

Open a new study table file and copy face indices into the first column of this table. In the second column add the corresponding modified attachment energies (see Figure 3-27). Save the file in a new folder as “modified.std” or “mod.std”.

	A	B	C	D
	hkl	Eatt(Total)		
1	{ 2 0 0 }	-17.13051733		
2	{ 1 1 0 }	-51.94282414		
3	{ 1 1 -1 }	408.31946420		
4	{ 1 1 1 }	685.47435270		
5	{ 2 0 -2 }	120.32324530		
6	{ 3 1 -1 }	-74.42828087		
7	{ 3 1 0 }	-61.30168473		
8	{ 0 0 2 }	415.66559070		



*Figure 3-27 Left: Study table with Miller face indices and the corresponding modified attachment energies. Right: Document folder with study table and 3D atomistic file for the morphology.*

Open the attachment energy morphology of the pure crystal which was obtained in step 4 (chapter 3.1.1.4). Save a copy of the 3D atomistic document as “modified.xsd” or “mod.xsd”. The copy of this 3D atomistic document and the aforementioned study table need to have the same name and are to be saved in the same folder (seen in Figure 3-27 right).

In order to calculate the modified morphology open the study table (mod.std) and the 3D atomistic document (mod.xsd). Mark the first two columns which contain the face indices and the attachment energies (see Figure 3-28). For the morphology prediction follow the path Morphology/Calculation and in index card “Setup” of the dialogue “Morphology Calculation” select the “Task” “Generate Habit”. The morphology in the file modified.xsd will change to the modified morphology and in the study table modified.std additional columns will appear which contain information on the surface share of the faces. Save the new files.



Start

Morphology Calculation

Setup | Energy | Faces | Job Control

Task: **Generate habit** More...

Quality: Medium

Energy method: Forcite

Output

Surface structures: Stable surfaces

Restart Run Help

Start Habit Generation

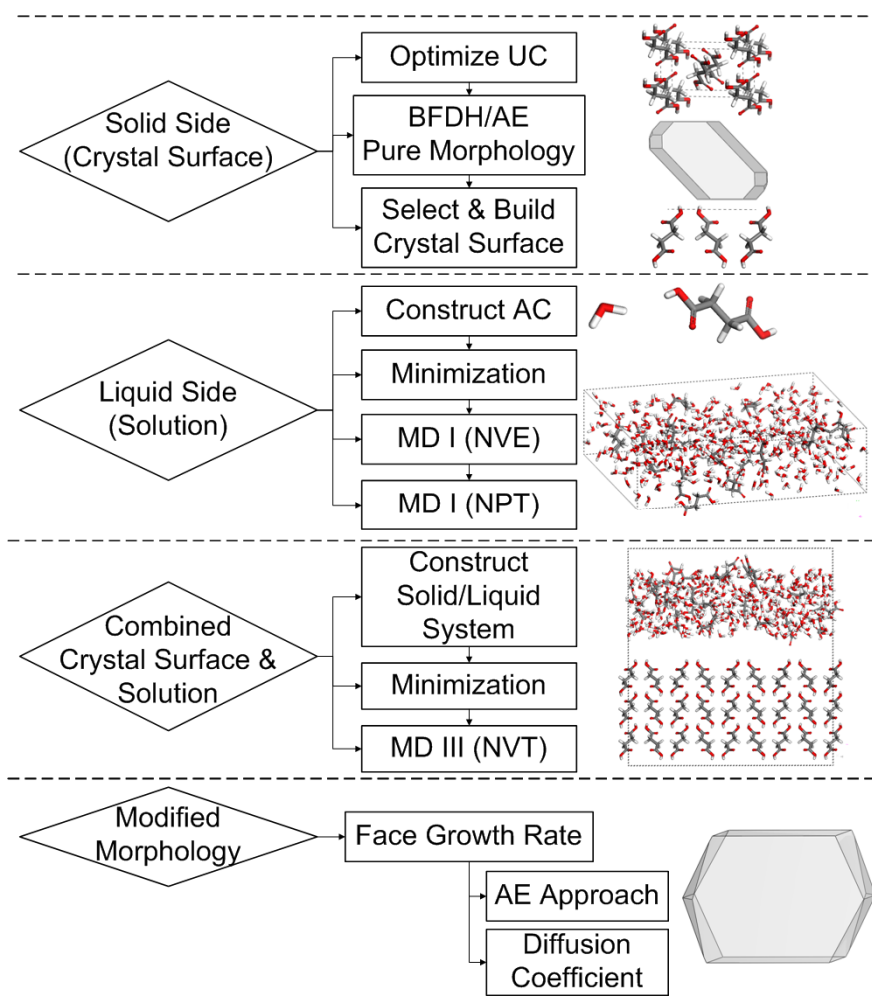
Select

	A	B
	hkl	Eatt(Total)
1	{ 2 0 0 }	-17.13051733
2	{ 1 1 0 }	-51.94282414
3	{ 1 1 -1 }	408.31946420
4	{ 1 1 1 }	685.47435270
5	{ 2 0 -2 }	120.32324530
6	{ 3 1 -1 }	-74.42626067
7	{ 3 1 0 }	-61.30168473
8	{ 0 0 2 }	415.66559070

Figure 3-28 “Morphology Calculation” dialogue to generate the modified morphology.

### 3.2 The Layer Docking Method

The Layer Docking method is developed for the prediction of crystal morphologies grown from a solution. The Layer Docking method proceeds in larger number of steps than the aforementioned Surface Docking method. The illustration of the procedure is given in Figure 3-29. Since the previous chapters 3.1.1 to 3.1.1.5 describe the proceeding for the modeling of the solid side (crystal surface) the subsequent chapter will enter the procedure at the modeling which is conducted for the liquid side.

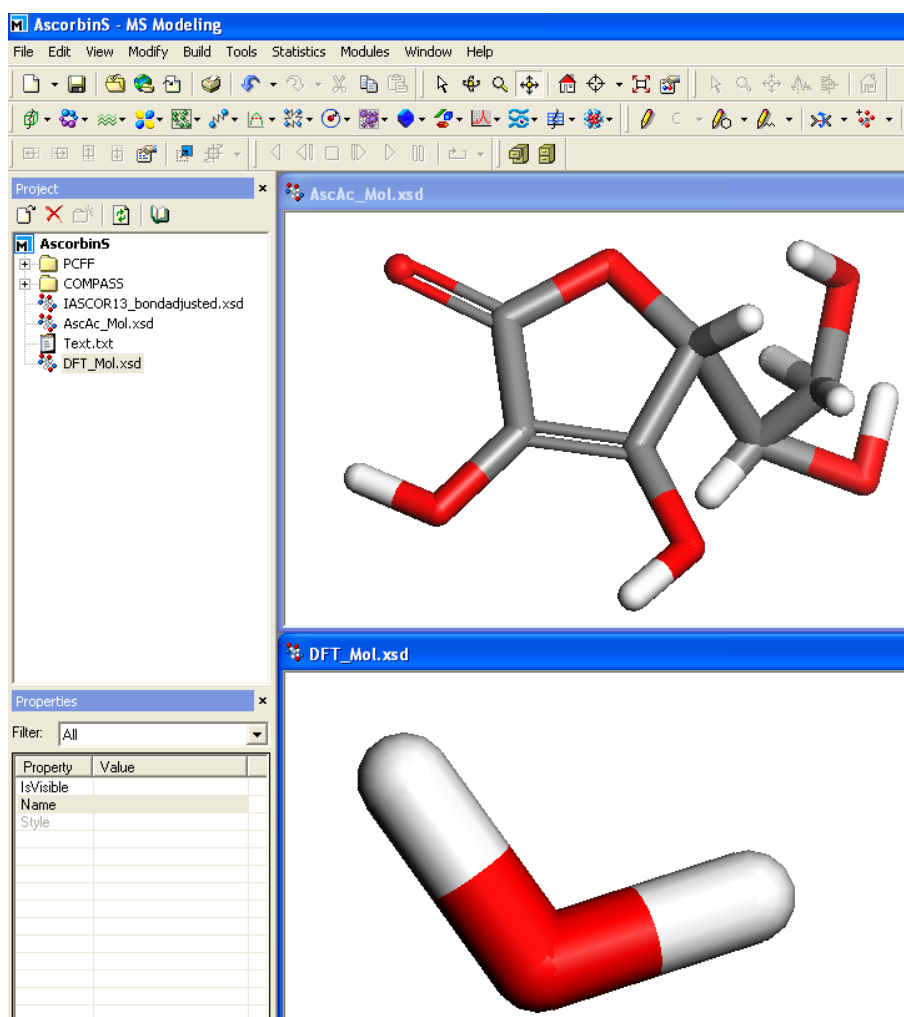


*Figure 3-29 Schematic representation of the Layer Docking method.*

#### 3.2.1 The Liquid Side (Solution)

##### 3.2.1.1 Step 1: Constructing an Amorphous Cell

In order to start the procedure the file(s) with the solute and solvent molecule(s) of interest should be opened (see Figure 3-30).



*Figure 3-30 Selected molecules for the amorphous cell construction.*

From the toolbar the module “Amorphous Cell” is accessed when clicking on the “Amorphous Cell”-button. As the drop down menu is opened should click on “Construction” (Figure 3-31). The depicted dialogue “Amorphous Cell Construction” will open.

The index card “Construct” will be clean in the “Constituent molecules” column. When pressing the button “Add”, which is located on the right, the active molecule will be added to the list. Thus, activate e.g. the solvent molecule and click on the “Add”-button in the dialogue “Amorphous Cell Construction”. The same procedure is to be repeated for the solute molecules. If the molecules of interest are given in the list the column “Number” of the molecules can be modified manually. Here a total of 10 molecules for 2 species are given in the list. Deleting of any molecule is achieved when pressing the “Delete” button which is located on the right.

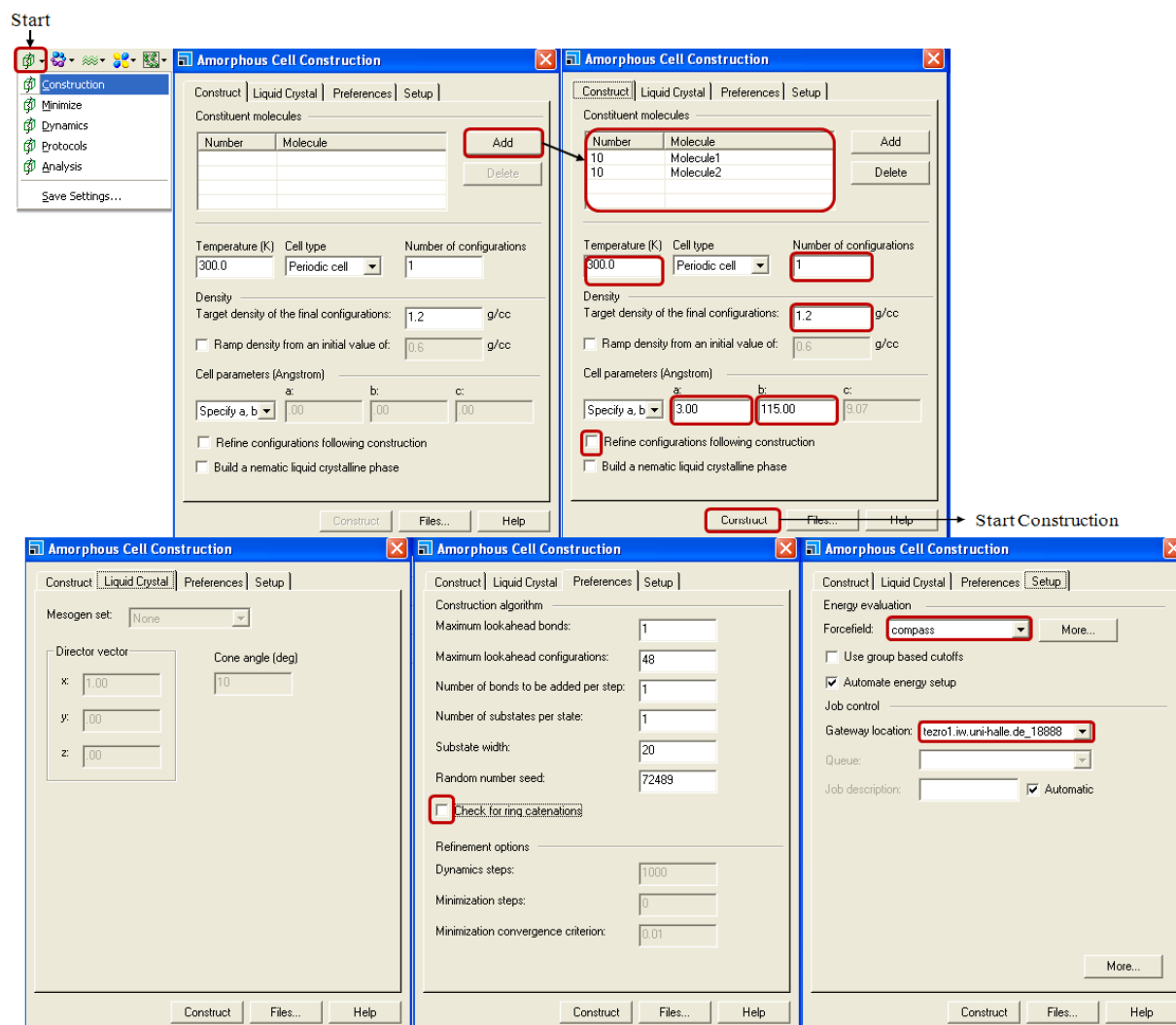


Figure 3-31 “Amorphous Cell Construction” dialogue.

The column “Temperature” is to be changed to 300 K (or the temperature which is used in the real crystallization process). The “Cell type” remains default as “Periodic Cell”. The number of configurations is to be set to “1” and the “Target density” should match the experimental density of the mixture. The “Cell parameters” “a” and “b” need to match the parameters of the corresponding surface which was constructed in chapter 3.1.1.5. The displaying of the cell parameters of the surface is obtained when pressing the right mouse button and following the menu “Lattice Parameters” (Figure 3-32). The values which are given for the “Lengths” “a” and “b” are those which are relevant for the construction of the amorphous cell. The remaining settings in the “Amorphous cell” dialogue should be as depicted in Figure 3-31. Special care is to be taken when choosing the force field, since the force field should match with the one used for building the corresponding surface. When all the settings are checked, press on the “Construct” button. The amorphous cell is constructed within one hour. A new folder will be created for the resulting data.

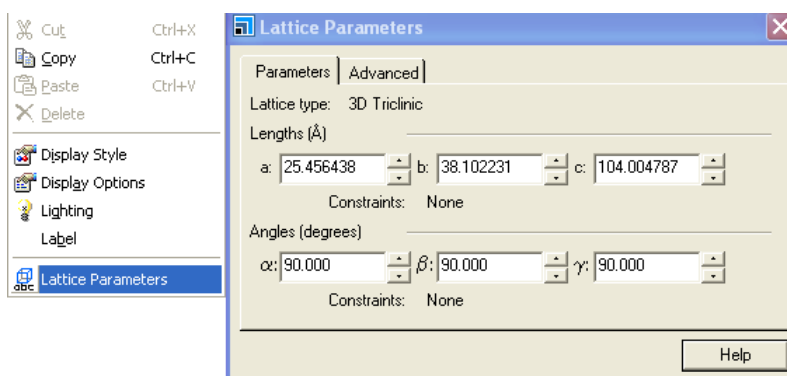


Figure 3-32 The “Lattice Parameters” dialogue.

### 3.2.1.2 Step 2: Minimization

The minimization step is conducted on the amorphous cell which is the resulting 3D atomistic file from the first step (chapter 3.2.1.1). The “Discover Minimization” dialogue is required to start the procedure (use the “Discover Setup” which is given in Figure 3-19). This is obtained via the toolbar path Discover/ Minimizer (see Figure 3-33). The chosen method is “Smart Minimizer” and at least “10.000” should be selected as “Maximum iterations”. The box “Optimize cell” is unchecked. Clicking on “More” enables to choose the specifications for the “Smart Minimizer”. In the corresponding dialogue deselect the boxes “Use Steepest Descent” and “Use Conjugate Gradient”, check “Use Newton”. Click on “More” in order to specify the “Newton” minimization. Select the algorithm “BFGS” and leave any other settings as default. Press “OK” to save the settings. Press the “Minimize” button to conduct the minimization of the amorphous cell. Depending on the number of molecules and the maximum iterations the simulation may have duration of several days.

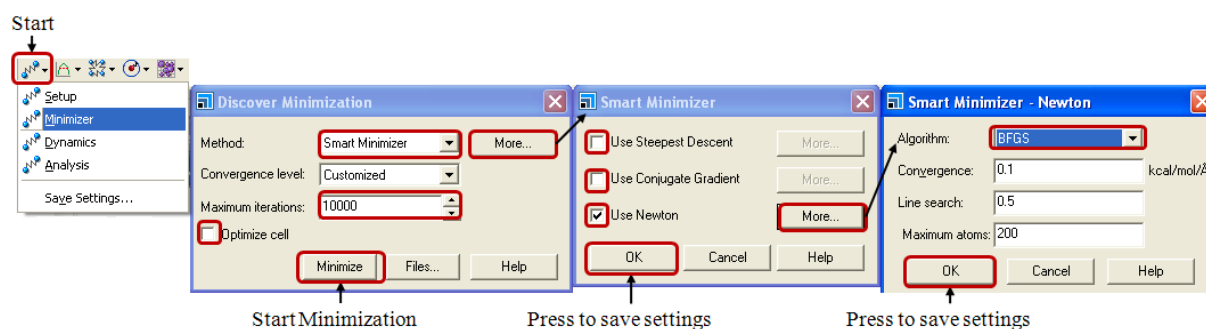
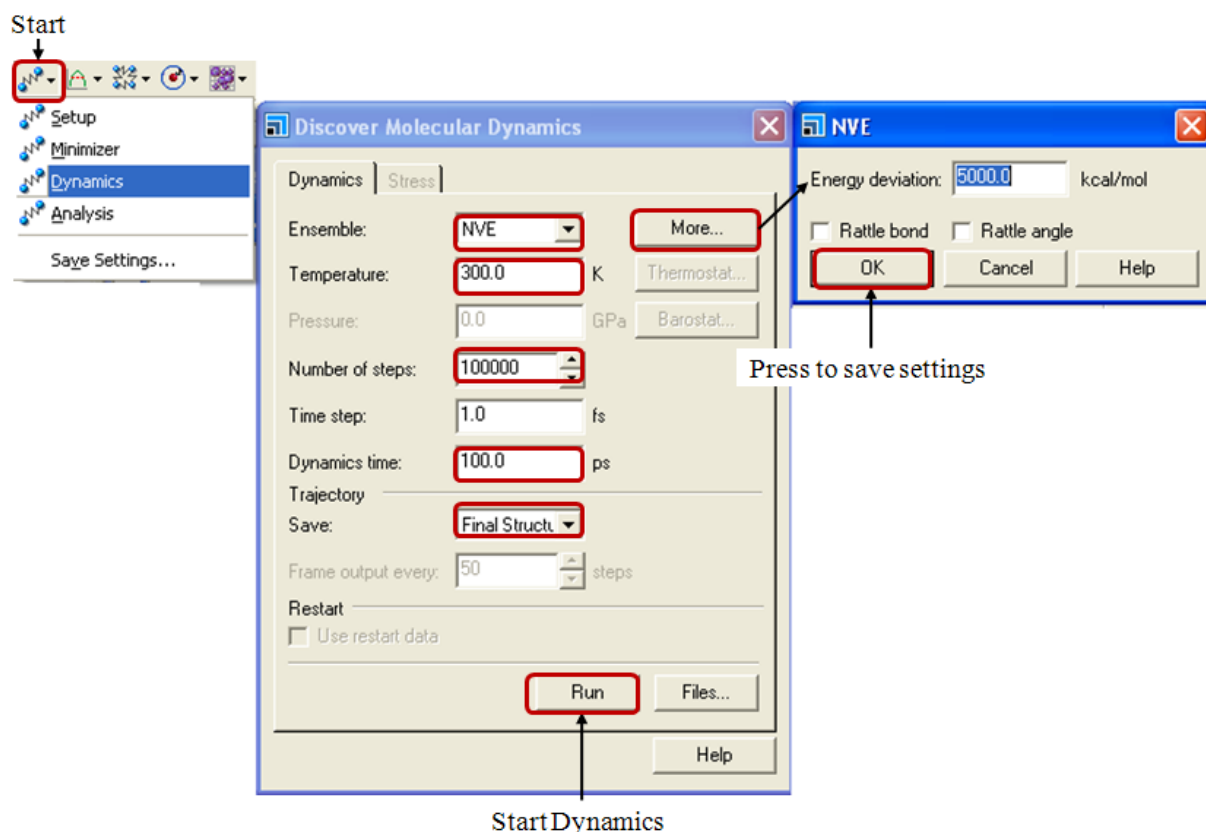


Figure 3-33 “Discover Minimization” dialogue.

### 3.2.1.3 Step 3: Molecular Dynamics I (NVE)

The basic settings for the molecular dynamics procedure are to be used as depicted in Figure 3-19. The specific settings are achieved by following the path “Discover/ Dynamics” from the toolbar (see Figure 3-34). Select the “Ensemble” “NVE”, a “Temperature” of “300 K”, the

“Number of steps” should be 100.000 at the “Dynamics time” of 100 ps. The trajectory should be saved as “Final Structure”. When pressing the button “More” the NVE “Energy deviation” can be modified. A change of this setting is not recommended. Press “OK” to save changes or just leave the menu without changing anything. Press the “Run” button to start the NVE molecular dynamics. The calculation may have duration for several days. The resulting data will be stored in a folder which is automatically created by the program.



*Figure 3-34 Molecular dynamics settings (NVE).*

#### 3.2.1.4 Step 4: Molecular Dynamics II (NpT)

Prior to the start of the molecular dynamics, it should be ensured that the Discover Settings are used as illustrated in Figure 3-19. The molecular dynamics settings are obtained by following the path “Discover/ Dynamics” from the toolbar (see Figure 3-35). Select the “Ensemble” “NPT”, the “Temperature” of “300 K”, the “Number of steps” should be 10.000 at the “Dynamics time” of 10 ps. The trajectory is to be saved as “Final Structure”. When pressing the button “More” the NPT “Energy deviation” can be modified but the change of these settings is not recommended. Thus, press “OK” to save changes or just leave the menu without changing anything. A click on the button “Thermostat...” will open the “Thermostat” dialogue where the thermostat “Nose” (or “Velocity Scale”) should be selected, any other

setting in this dialogue should remain as default and the “OK” button is pressed to save the settings. In the dialogue “Discover Molecular Dynamics” a click on the button “Barostat...” opens the dialogue “Barostat”. Here, only the “Barostat” “Parrinello” is to be selected and the choice should be confirmed by clicking on the “OK” button. Press the “Run” button in the dialogue “Discover Molecular Dynamics” to start the NPT molecular dynamics. The calculation may have duration for several hours. The resulting data will be stored in a folder which is automatically created by the program.

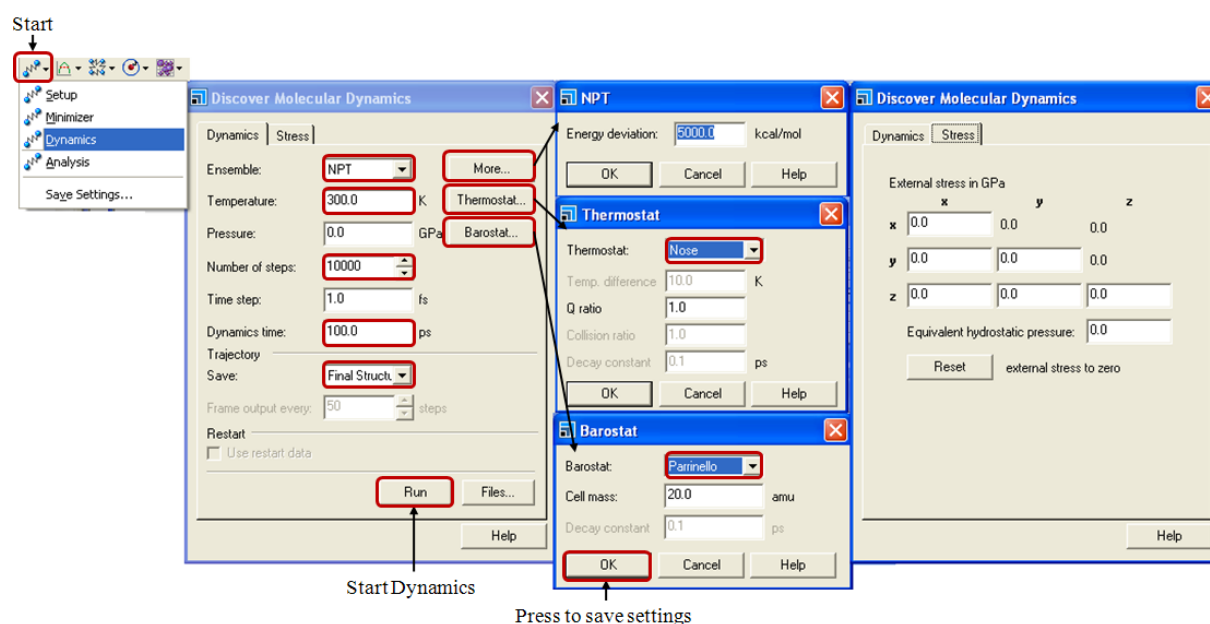


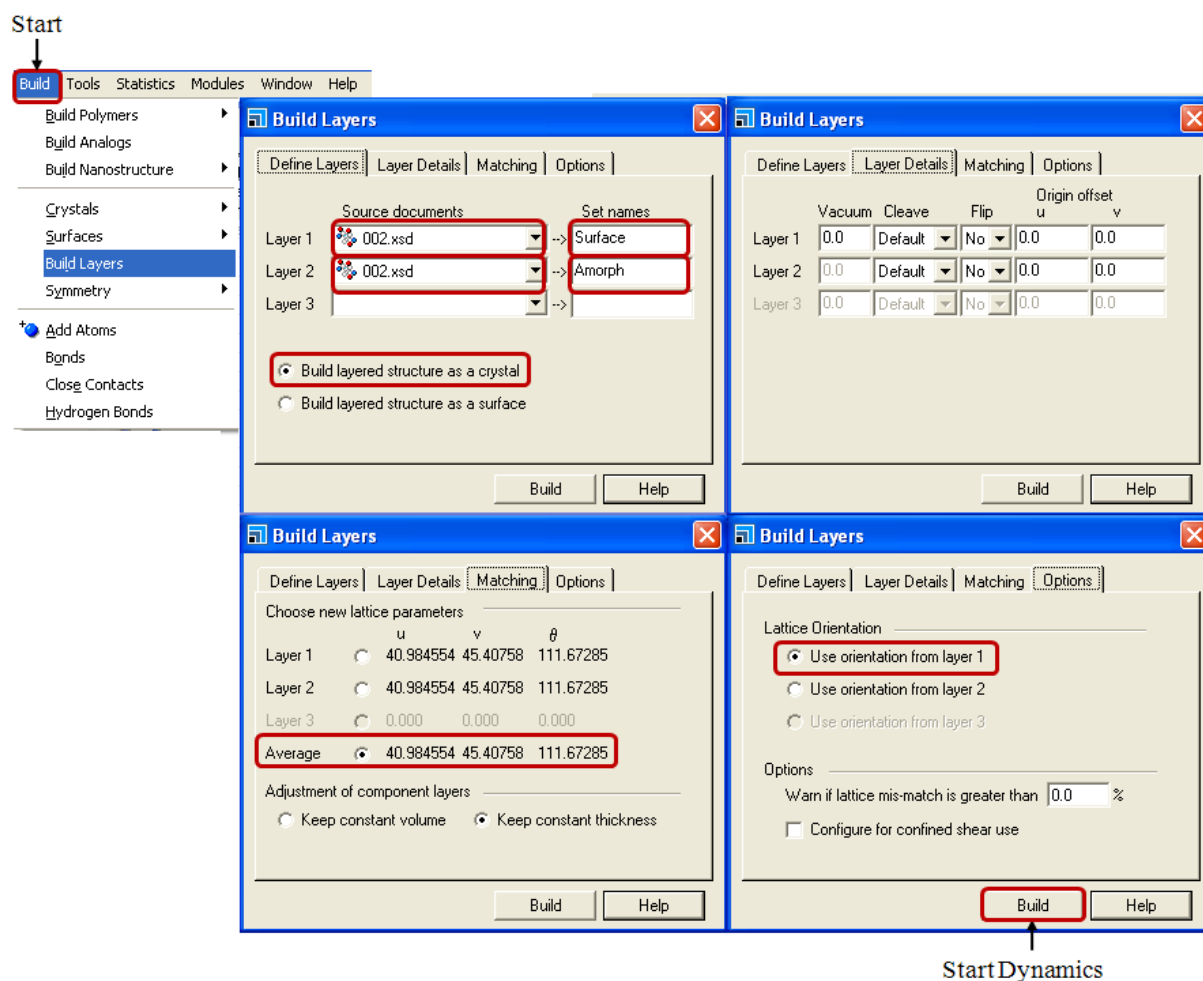
Figure 3-35 Molecular dynamics settings (NpT).

### 3.2.2 Combined Surface and Solution

The produced optimized amorphous cell is to be combined with the crystal surface in order to conduct a so-called production run of the molecular dynamics.

#### 3.2.2.1 Step 1: Constructing Solid/ Liquid System

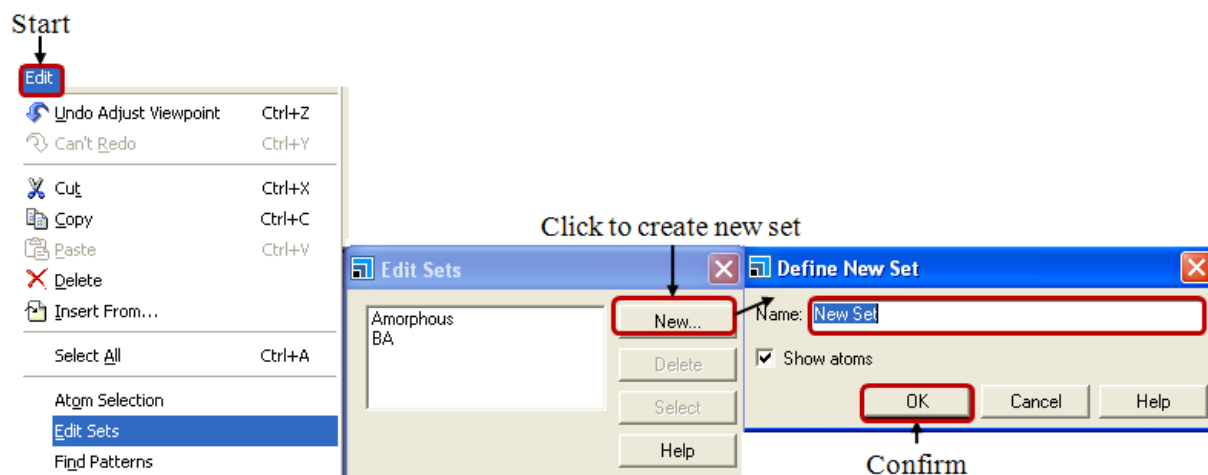
Prior to the molecular dynamics the amorphous cell and the surface are to be combined as layers. The corresponding menu is achieved when following the main menu path Build/ Build Layers (see Figure 3-36). Via the drop down menu in the index card “Define Layers” the “Layer 1” to “Layer 3” can be specified. The file which is to be defined as layer should be active in the background. Once the layer is selected the user is free to select as “Set name”. Here the names “Surface” and “Amorph” are chosen.



*Figure 3-36 The “Build Layers” dialogue.*

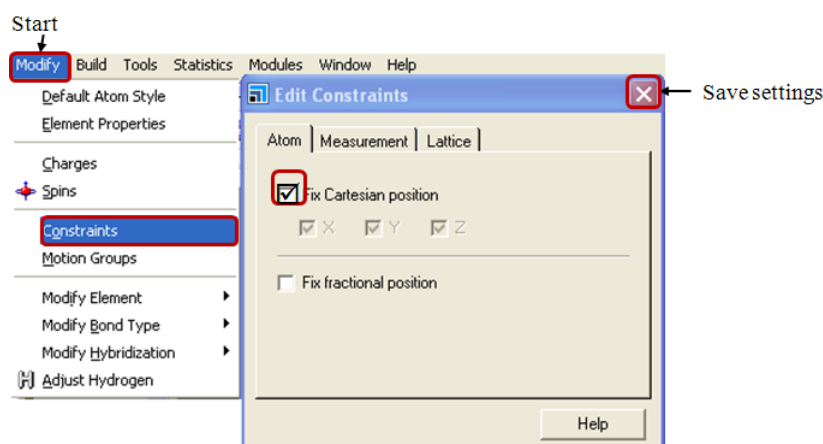
For the subsequent calculation of the diffusion coefficient it is required to specify sets for all solute molecules (optional: solvent). To achieve this select all solute molecules in the amorphous layer. When all molecules are selected follow the main menu path Edit/Edit Sets as illustrated in Figure 3-37. As the dialogue “Edit Sets” opened click on the “New...” button to define a new set in the corresponding dialogue. Select a “Name” for the new set and if preferred disable the “Show atoms” box. When finished confirm by pressing the “OK” button and save the file with the sets.





*Figure 3-37 “Edit Sets” dialogue.*

As any movement of the surface atoms is to be prevented in the NVT molecular dynamics the atoms of the surface are to be fixed in their Cartesian position. To achieve this, the atoms of the surface are to be selected. The path to the menu is Modify/Constraints and is accessed from the main menu. On the index card “Atom” the option “Fix Cartesian Position” should be checked (see Figure 3-38). In order to ensure the surface atoms are fixed it is possible to color the atoms by constraint. Get access to the corresponding menu via the tool bar. The hereby created file is to be saved.



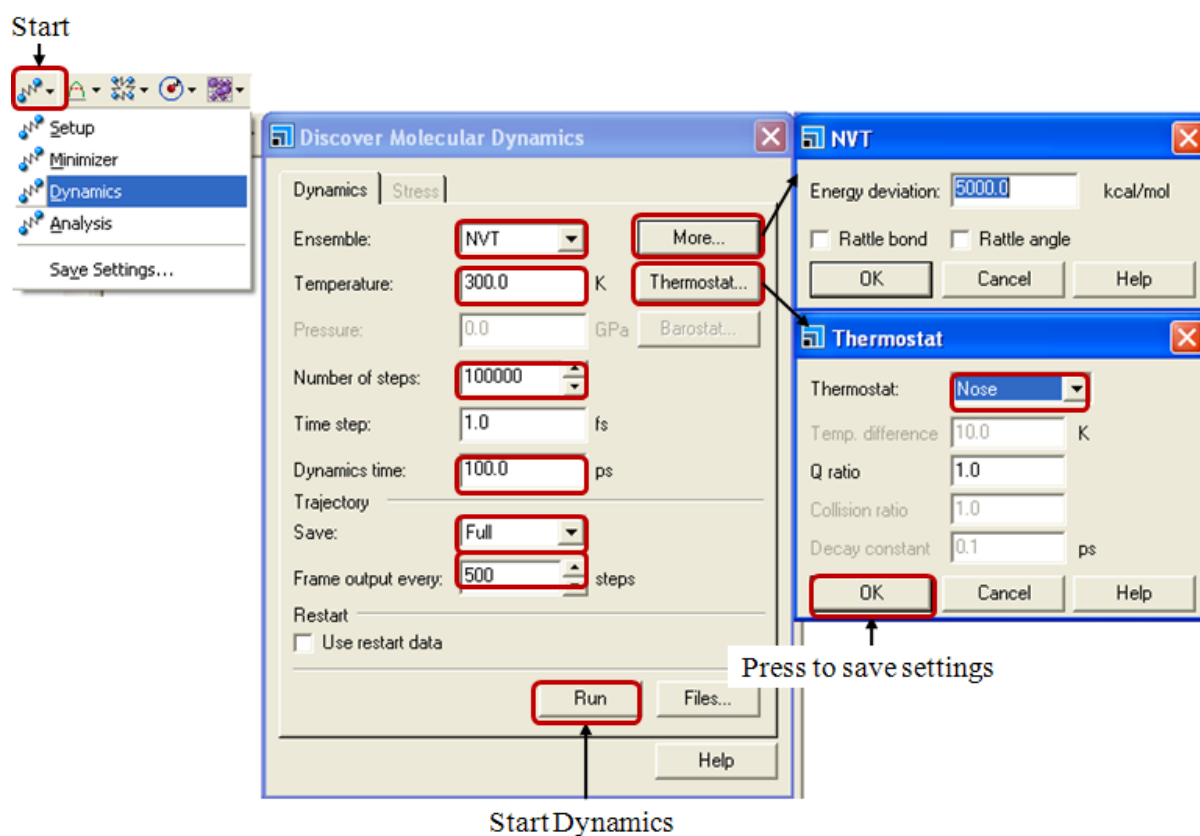
*Figure 3-38 Setting the constraints prior NVT molecular dynamics.*

### 3.2.2.2 Step 2: Molecular Dynamics III (NVT)

Before starting the molecular dynamics all “Discover” settings (such as the selection of a gateway and force field) are to be made. This is done in the “Discover Setup” dialogue which is accessed via the toolbar Discover/Setup. The illustration in Figure 3-19 gives a listing of all required settings and the corresponding detailed description is found in chapter 3.1.2.2.

In order to perform the molecular dynamics simulations follow the path Discover/Dynamics from the toolbar. The dialogue “Discover Molecular Dynamics” will be opened. The settings

in the index card “Dynamics” are to be changed as depicted in Figure 3-39. Set the “Ensemble” as “NVT”, the “Temperature” to “300 K”, and “Number of steps” to “100000” with a “Dynamics time” of “100 ps”. “Save” the trajectory as “Full” at the “Frame output every” 50 steps. In order to change the thermostat, click on the “Thermostat” button. The dialogue “Thermostat” will be opened where it is possible to select the thermostat as Nosé, Velocity Scale, Andersen or Berendsen. According to the selected temperature control method the option of changing the factor for the temperature control is given, which is with Velocity Scale the “Temperature difference” (default is “10 K”) and with Nosé the “Q ratio” (default is “1.0”). These default values should not be modified. As a thermostat the Nosé method is recommended. Press the “OK” button in the “Thermostat” dialogue in order to save the settings and close the dialogue. When the settings are made press the “Run” button in the “Discover Molecular Dynamics” dialogue.

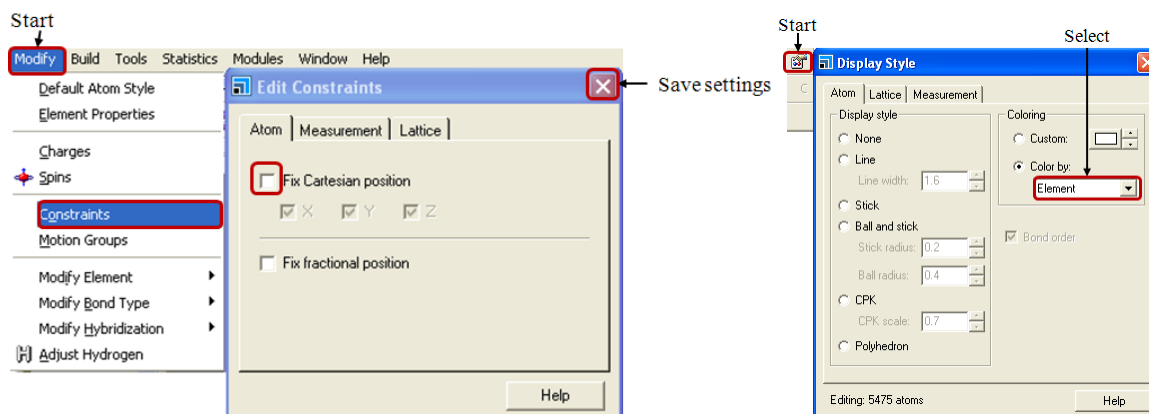


*Figure 3-39 Molecular dynamics settings (NVT).*

### 3.2.2.3 Step 3: Trajectory Analysis

The *analysis* of the resulting molecular trajectory file is carried out using the “Discover Analysis” as presented in chapter 3.1.2.3. By means of the therein presented method the lowest energy frame is detected which is required for the subsequent minimization (chapter 3.2.2.4).

For the calculation of the diffusion coefficient the “Mean squared displacement” (MSD) is required. Prior conducting the corresponding MSD analysis the constraints which are set to the surface are to be removed as illustrated in Figure 3-40. Press the keys Ctrl.+A to select all atoms and follow the path Modify/Constraints from the main menu. In the dialogue “Edit Constraints” deselect “Fix Cartesian Position” in the index card “Atom”. For the visualization change the coloring of the atoms to “Element” (see Figure 3-40 right).



*Figure 3-40 Left: Removing the constraints from the surface atoms. Right: Atom coloring.*

Open the trajectory file and start the *analysis* of the resulting molecular trajectory file with the “Discover Analysis”. The tool is accessed via the toolbar path Discover/Analysis. Select “Dynamic” and “Mean squared displacement” in the root structure which is custom in the dialogue. The selection of a trajectory to be analyzed is done in the “Trajectory Specification (Discover)” dialogue which is accessed when clicking on the “Define...” button as illustrated in Figure 3-41. The dialogue which is opened consists of a list and several buttons. The list may contain files which are previously analyzed, in this case press the “Clear list” button. In case the list is empty directly press the “Add to list” button. If there is no path for the document indicated right of the “Add to list” button there is no trajectory file active or open. In this case open a trajectory file and follow the procedure. Back in the “Discover Analysis” dialogue in “Choose sets” the selection of the set which is desired for the analysis (set which contains solute molecules) should be done via the drop down menu. For starting the analysis press the “Analyze” button.

The result from the analysis is the plot of the MSD vs. simulation time. From the plot select the graphs and copy paste the data to an origin worksheet. The transferred data consists of 8 columns. Four contain information on the time step of the simulation time (column 1, 3, 5 and 7) and the remaining columns are filled with the data for the MSD. Thus, the second column contains the total MSD, the columns 4, 6 and 8 contain the MSD in x-, y- and z-direction. The

data of the first two columns should be plotted and a linear fit is required to obtain the  $R^2$  and the B. The values should be noted for the calculation of the average diffusion coefficient.

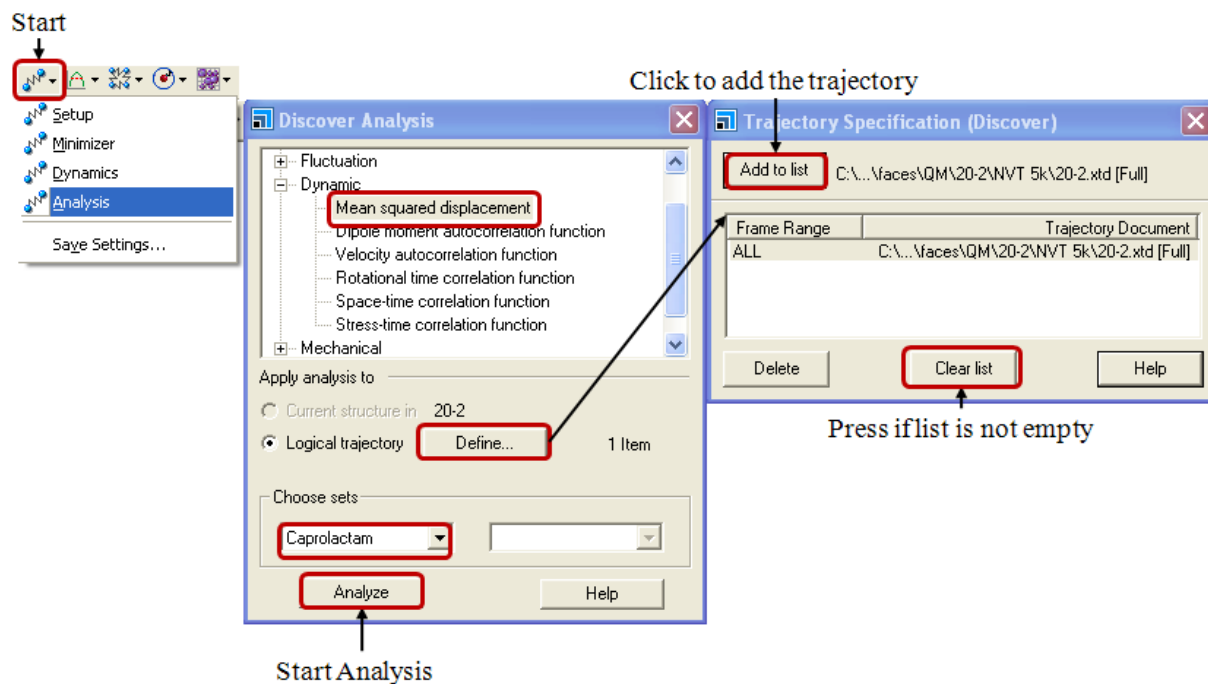


Figure 3-41 The “Discover Analysis” of the trajectory file.

### 3.2.2.4 Step 4: Minimization

Starting the minimization of the molecular conformation at the lowest energy level is achieved when following the path Discover/Minimizer” from the toolbar (Figure 3-42). The “Discover Minimization” dialogue the selection of the “Method” “Smart Minimizer”, at the level of 10.000 “Maximum iterations”. The box “optimize cell” is not checked. A click on the button “More...” the “Smart Minimizer” dialogue allows the choice of the minimization algorithms. Here, “Use Steepest Descent” and “Use Conjugate Gradient” should be deselected and only “Use Newton” is checked. In order to start the minimizations press the “Minimize” button. One of the result files is a text file from which the total potential energy is obtained. Note the total potential energy after the minimization.

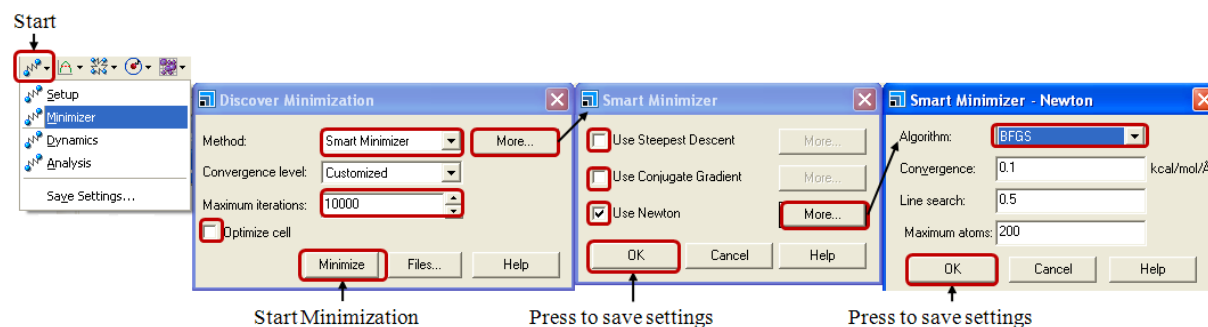


Figure 3-42 The “Discover Minimization” dialogue.

### 3.2.2.5 Step 5: Calculating the Energy of Surface and Amorphous Layer

Open the 3D atomistic document which is the result file from the minimization. Delete the molecules which are in the amorphous layer on the surface and save the file as “surface only”. (Take care not to overwrite the existing result file!) In order to calculate the current energy (total potential energy) of the structure follow the path Discover/Setup in the toolbar. The settings should remain the same as those which were set prior to the dynamics and the corresponding minimization. In the index card “Energy” press the button “Calculate” (see Figure 3-26). The resulting text file supplies with the total potential energy of the surface.

The same procedure is to be conducted for the amorphous layer which is covering the surface. Thus, open the 3D atomistic document which is the result file from the minimization. Select and delete all atoms of the crystal surface, only the molecules on the surface should not be deleted. Save the file as “amorphous only” and calculate the current energy of the system according to the description which was given for the calculation of the surface energy. Note the total potential energies of the system.

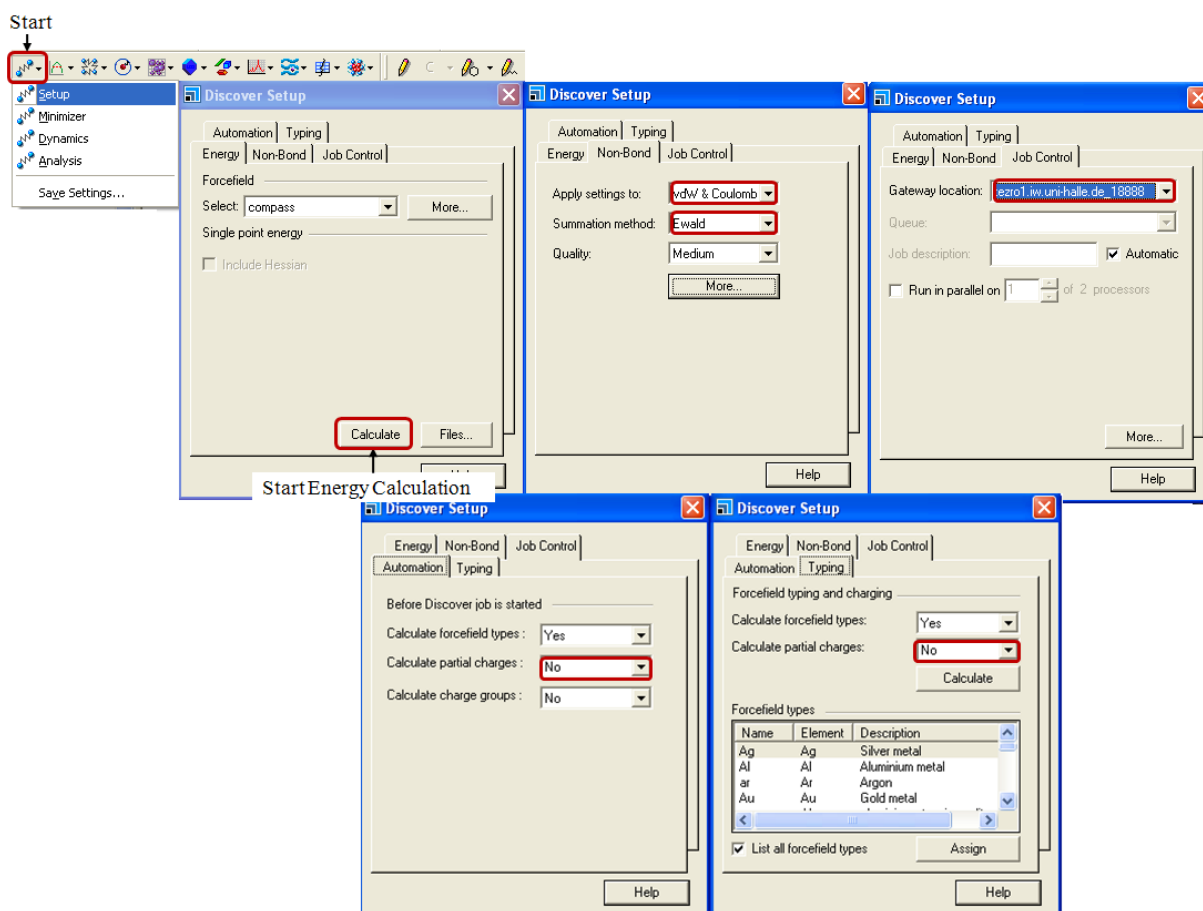


Figure 3-43 “Discover Setup” dialogue for the calculation of the current energy.

### 3.2.3 The Modified Morphology

The prediction of the modified morphology in presence of solvents (and additives) can proceed via 2 different methods when using the Layer Docking method. Both methods imply the use of the attachment energy which is derived from the calculation of the pure morphology. The first method is based on the approach of the modified attachment energy (the attachment energy of a crystal face in presence of the liquid side) which was originally introduced by Ulrich and Lu. The second method explicitly considers the enrichment of solute molecules in the liquid phase via the diffusion coefficient. The modified attachment energy is therein weighted with the diffusion coefficient in the presence of the liquid side.

#### 3.2.3.1 Step 6: Calculating the Modified Attachment Energy

In order to generate the morphology in presence of the liquid side the tool “Morphology” is used in the software MaterialsStudio 4.0. For the generation of the modified morphology knowledge of the modified attachment energy is required. The approach of the face growth rates is then conducted via the relation

$$R_{G,hkl} \sim E_{hkl}^{att,mod} \quad 3-5$$

##### 3.2.3.1.1 Attachment Energy Approach

From the energies calculated in the chapters 3.2.2.4 and 3.2.2.5 the binding energy of the solute (host crystal) molecules to the surface is calculated

$$E_b^{solute} = E_{total} - (E_{surface} + E_{solute}) \quad 3-6$$

The binding energy of the solvent molecules to the surface is defined as

$$E_b^{solvent} = E_{total} - (E_{surface} + E_{solvent}) \quad 3-7$$

The binding energy difference from binding energy of the solvent and the solute is

$$\Delta b = E_b^{solvent} - E_b^{solute} \quad 3-8$$

The original modified attachment energy based on Lu 2004 [Lu04] is modified according to Schmidt 2011 [Sch11b]

$$E_{hkl}^{att,mod} = E_{hkl}^{att} - \frac{E_{hkl}^{att} \times \Delta b}{E_b^{solute}} \quad 3-9$$

The obtained modified attachment energies for all important faces (see chapter 3.1.1.5) are used for the generation of the modified morphology in the presence of solvents (and additives) which is presented in chapter 3.2.3.2.

### 3.2.3.1.2 Diffusion Coefficient Approach

The data which is obtained from the MSD “Discover Analysis” following chapter 3.2.2.3 is in the focus of the present chapter. The MSD data for a crystal face  $hkl$  which was transferred to the Origin worksheet has been plotted and a linear fit of the curve supplied with the  $R^2$  and the  $B$ , respectively. By means of the  $B$  it is possible to calculate the diffusion coefficient in accordance with [Boe92]) via the equation

$$D_{hkl} = \frac{B_{hkl}}{6} \cdot 10 \quad 3-10$$

The diffusion coefficient is intensively fluctuating within the simulation time. Thus the average value can be determined using the  $B$  derived from the linear fit over the whole simulation time. In this case the  $R^2$  may be lower than 0.998 which is not a desired case. In the help of the latest version of the software “MaterialsStudios 5.0” it is recommended to use of the data which is obtained from the beginning of the second third of the simulation time until half of the simulation time has passed. The remaining results should not be used since due to the algorithms used in the simulations the therein produced data is only roughly approached based on the results of the first half of the simulation time (private communication [Men11] and [All87]).

Consequently the best approximation of the diffusion coefficient from the NVT molecular dynamics which comprises a total of 100 ps is achieved when using the average diffusion coefficient out of the time range of 33 ps to 50 ps. The diffusion coefficient is to be calculated for all the important faces (see chapter 3.1.1.5).

The obtained coefficients are then used as weighting factors for the attachment energies of the corresponding faces of the pure substance. The modified attachment energy for each of these faces is calculated as follows

$$E_{hkl}^{att,mod} = E_{hkl}^{att} \cdot D_{hkl} \quad 3-11$$


The modified attachment energies for all important faces (see chapter 3.1.1.5) which are weighted by means of the diffusion coefficient are used for the generation of the modified

morphology in the presence of solvents (and additives). The further steps for the morphology generation are presented in chapter 3.2.3.2.

### 3.2.3.2 Step 12: Calculating the Modified Morphology

Open a new study table file and copy face indices into the first column of this table. In the second column add the corresponding modified attachment energies (see Figure 3-44). Save the file in a new folder as “modified.std” or “mod.std”.

	A	B	C	D
	hkl	Eatt(Total)		
1	{ 2 0 0 }	-17.13051733		
2	{ 1 1 0 }	-51.94282414		
3	{ 1 1 -1 }	408.31946420		
4	{ 1 1 1 }	685.47435270		
5	{ 2 0 -2 }	120.32324530		
6	{ 3 1 -1 }	-74.42828087		
7	{ 3 1 0 }	-61.30168473		
8	{ 0 0 2 }	415.66559070		



*Figure 3-44 Left: Study table with Miller face indices and the corresponding modified attachment energies. Right: Document folder with study table and 3D atomistic file for the morphology.*

Open the attachment energy morphology of the pure crystal which was obtained according to chapter 3.1.1.4. Save a copy of the 3D atomistic document as “modified.xsd” or “mod.xsd”. The copy of this 3D atomistic document and the aforementioned study table need to have the same name and are to be saved in the same folder (seen in Figure 3-44 right).

In order to calculate the modified morphology open the study table (mod.std) and the 3D atomistic document (mod.xsd). Mark the first two columns which contain the face indices and the attachment energies (see Figure 3-45). For the morphology prediction follow the path Morphology/Calculation and in index card “Setup” of the dialogue “Morphology Calculation” select the “Task” “Generate Habit”. The morphology in the file modified.xsd will change to the modified morphology and in the study table modified.std additional columns will appear which contain information on the surface share of the faces. Save the new files.



Start

Morphology Calculation

Setup | Energy | Faces | Job Control

Task: **Generate habit** More...

Quality: Medium

Energy method: Forcite

Output

Surface structures: Stable surfaces

Restart Run Help

Start Habit Generation

Select

	A	B
	hkl	Eatt(Total)
1	{ 2 0 0 }	-17.13051733
2	{ 1 1 0 }	-51.94282414
3	{ 1 1 -1 }	408.31946420
4	{ 1 1 1 }	685.47435270
5	{ 2 0 -2 }	120.32324530
6	{ 3 1 -1 }	-74.42626067
7	{ 3 1 0 }	-61.30168473
8	{ 0 0 2 }	415.66559070

Figure 3-45 “Morphology Calculation” dialogue to generate the modified morphology.

#### 4. Cerius<sup>2</sup> 4.5 and 4.7

In order to get access to the program Cerius<sup>2</sup> 4.5 or 4.7 the sgi work stations tezro1 or tezro2. Log in as a user who has the privileges to use Cerius<sup>2</sup>. On the screen the “Toolchest” is seen on the left. Follow the path via Toolchest/Dektop/Open unix shell. The unix shell (“winterm” dialogue) will open as illustrated in Figure 4-1. In the command line of the “winterm” dialogue the user should enter the command “cerius2” (or “cerius245” for Cerius<sup>2</sup> 4.5). The program Cerius<sup>2</sup> 4.7 is started and the screen as depicted in Figure 4-2 is seen.

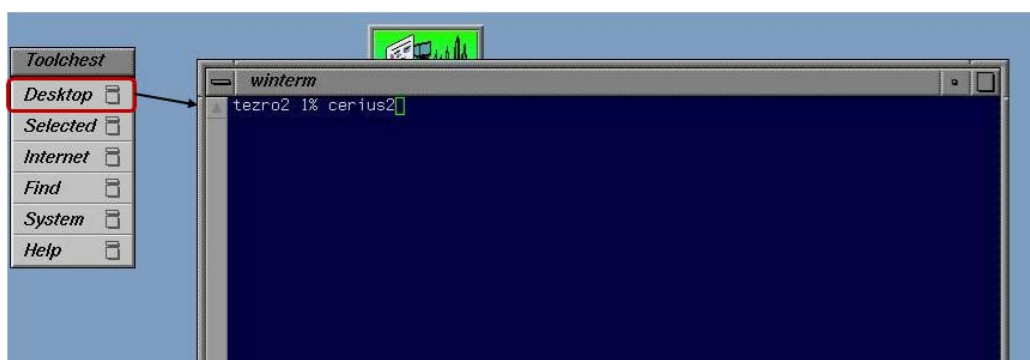


Figure 4-1 “winterm” dialogue in the system IRIX65 Release 6.4.

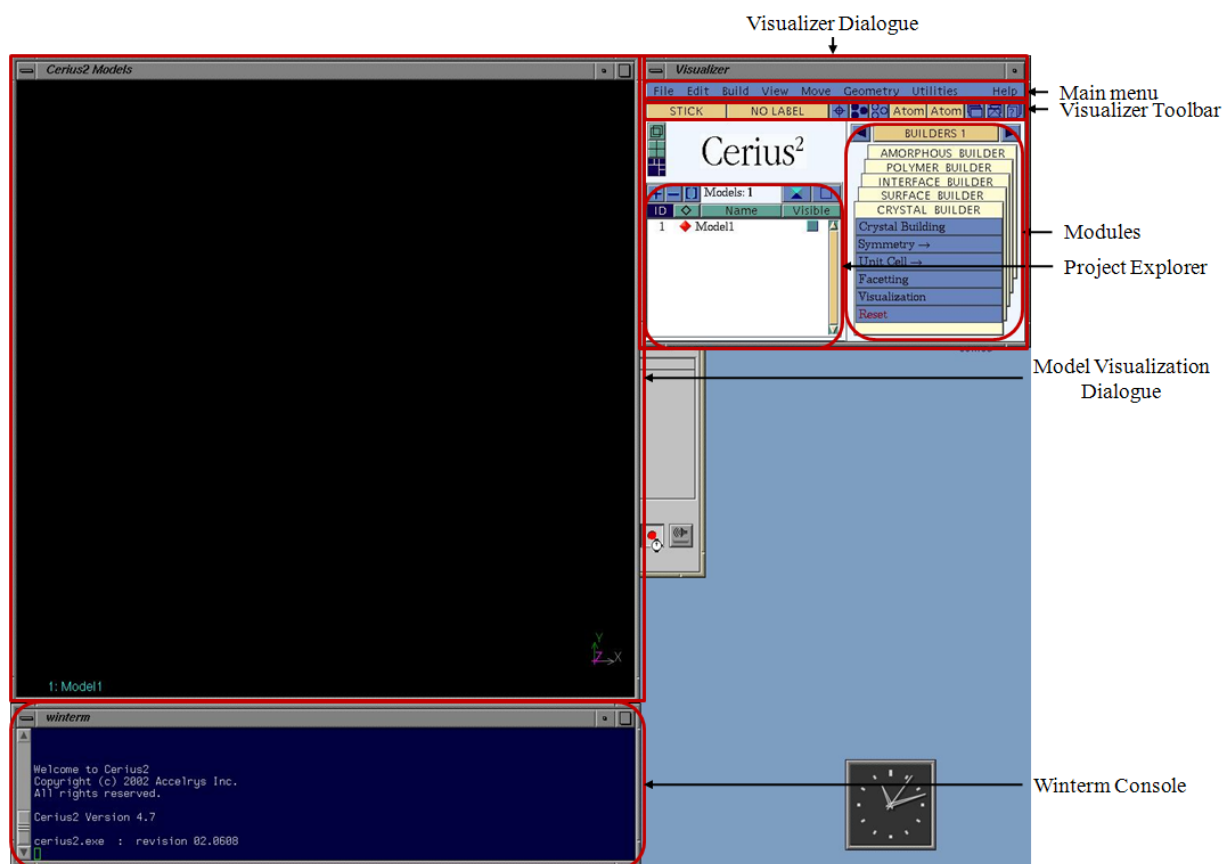
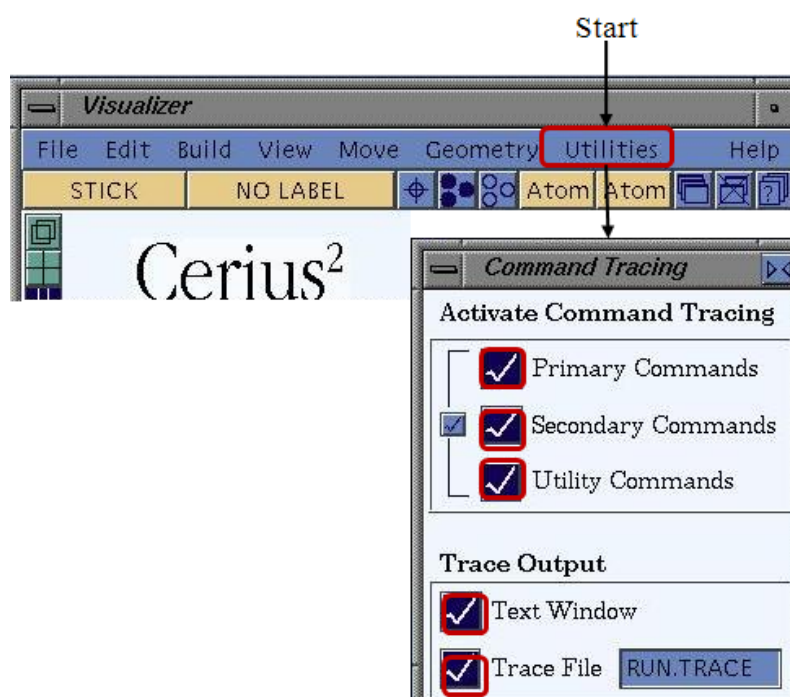


Figure 4-2 Start screen of the program Cerius<sup>2</sup> 4.7.

#### 4.1 Command Tracing and Non-graphical simulation start

The command tracing is recording all the procedures which are carried out by the user. Thus, it is to be started prior any modeling activity.

As the program Cerius<sup>2</sup> is started go to the main menu and follow the path Utilities/Command Tracing which is opened by a click. The “Command Tracing” dialogue will appear. In the section “Activate Command Tracing” the boxes “Primary Commands”, “Secondary Commands” and “Utility Commands” are to be checked. In the section “Trace Output” check the boxes “Text Window” and “Trace File”. As seen in the Figure 4-3 the tracing process of all commands is switched on.



*Figure 4-3 The “Command Tracing” dialogue.*

Saving the tracing file is achieved when closing the software Cerius<sup>2</sup>. The user is asked if it is desired to save the \*.log file. Confirm this by a click on the “Yes” button. Store the file in the preferred location and change the name.

In case Cerius<sup>2</sup> has been left without saving the trace file follow the procedure as follows. Open a unix-shell and enter the command “ls -l”. The command will give a list of the files in the current directory. Search for “run.log” to find the tracing file, once the file was found go on with closing the unix-shell. Open the folder “Schmidt” (or any other folder which contains the file) in the graphical interface and open the \*.log file with the program “nedit”. Save the file in the preferred location and change the name. Note: When restarting the tracing with cerius2 the existing file “run.log” will be overwritten.

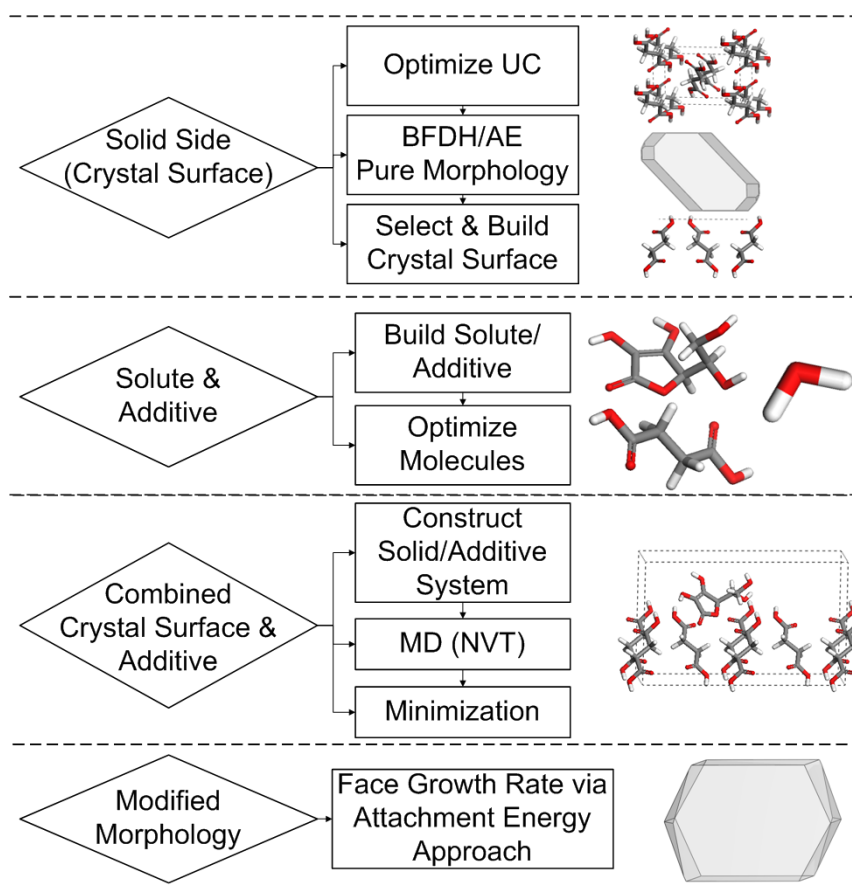
The testing of your log-file is achieved as follows. Open the log file with the program “nedit” and mark the text which needs to be copied. Open cerius2 and move the mouse cursor to the winterm dialogue. In order to insert the text to the winterm window click on the middle mouse button and the text will be pasted to the unix-shell. For a start of the process according to the scripting/tracing file press “enter”. Close Cerius<sup>2</sup> if no error comes up.

Conducting the start of a simulation without graphical user interface proceeds as described in the following. Open a unix-shell. Note: The log-file which is to be started needs to be in the same folder as the current directory, in which the user is located. The simulation is started via typing “cerius2 -b output.txt -n input.log” (where “output” and ”input” shall be the file-names). In order to check if the process is still running type “ps -ef | grep username“ (“username” eg “schmidt”).

The advantage of the non-graphical simulation is the strong decrease of simulation duration. Care should be taken concerning the compatibility of the log-files, since, the log-files are not compatible with other versions of Cerius<sup>2</sup>, e.g. Cerius<sup>2</sup> 4.5 file cannot be used in Cerius<sup>2</sup> 4.7 and vice versa.

## 4.2 The Surface Docking Method

The Surface Docking method is an established method in morphology prediction for crystals grown in presence of additives. The illustration of the procedures is given in Figure 4-4. In the subsequent chapter all these procedures are reflected in detail.

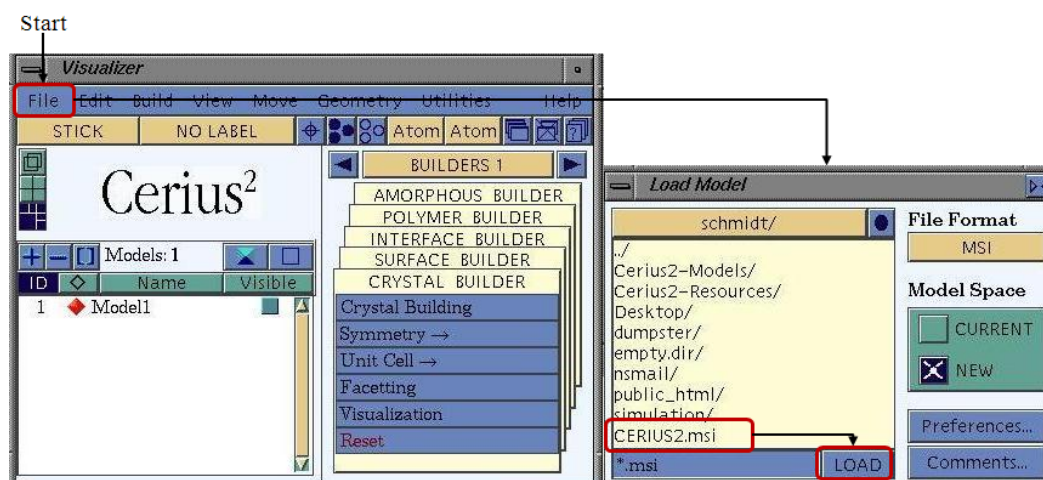


*Figure 4-4 Schematic representation of the Surface Docking method.*

## 4.2.1 The Solid Side (Crystal Surface)

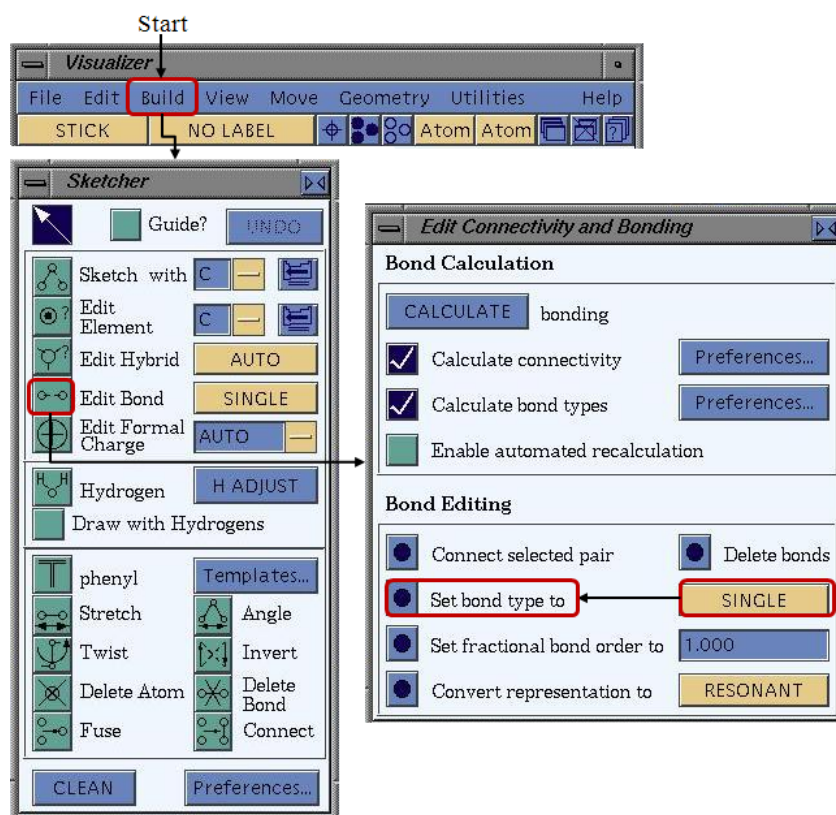
### 4.2.1.1 Step 1: Importing the Crystallographic Structure

In order to import a crystallographic structure (crystal unit cell) load model of the unit cell follow the main menu path File/Load Model. In the “Load Model” dialogue select the model (e.g. with the file format “.msi”) and click on the “LOAD” button as illustrated in Figure 4-5. Once the file is loaded it is seen in the model visualization dialogue “Cerius<sup>2</sup> Models” (see Figure 4-2).



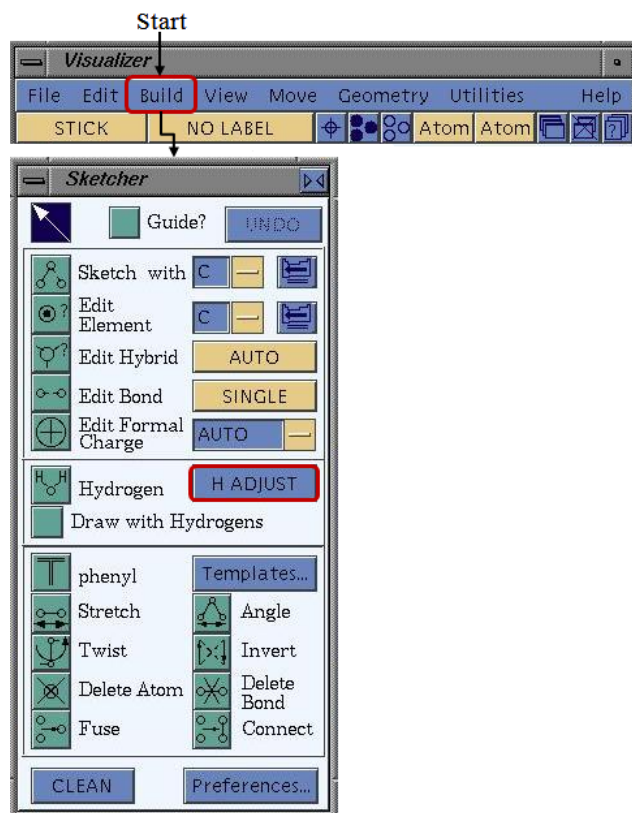
*Figure 4-5 Loading a crystallographic structure via the “Load Model” dialogue.*

In the crystallographic structure it should be checked if the bonds within the molecules are set, since in most of the cases the double bonds are missing. For the modification of the intramolecular bonds follow the main menu path Build/3D Sketcher here, click on “Modify the bonds”. The “Edit Connectivity and Bonding” dialogue will open as illustrated in Figure 4-6.



*Figure 4-6 Modification of intramolecular bonds via the “Edit Connectivity and Bonding” dialogue.*

Since the hydrogen atoms of the molecules are not attached in most of the downloaded crystallographic structure files it is necessary to check if the hydrogen atoms are added to the molecules. In case of missing hydrogen atoms follow the main menu path Build/3D Sketcher and as the “Sketcher” dialogue is opened click on the “H ADJUST” button (seen in Figure 4-7).

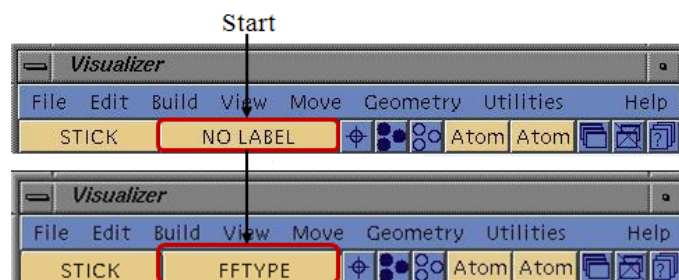


*Figure 4-7 Adding the hydrogen atoms via the “Sketcher” dialogue.*

#### 4.2.1.2 Step 2: Force Field and Charge Calculation

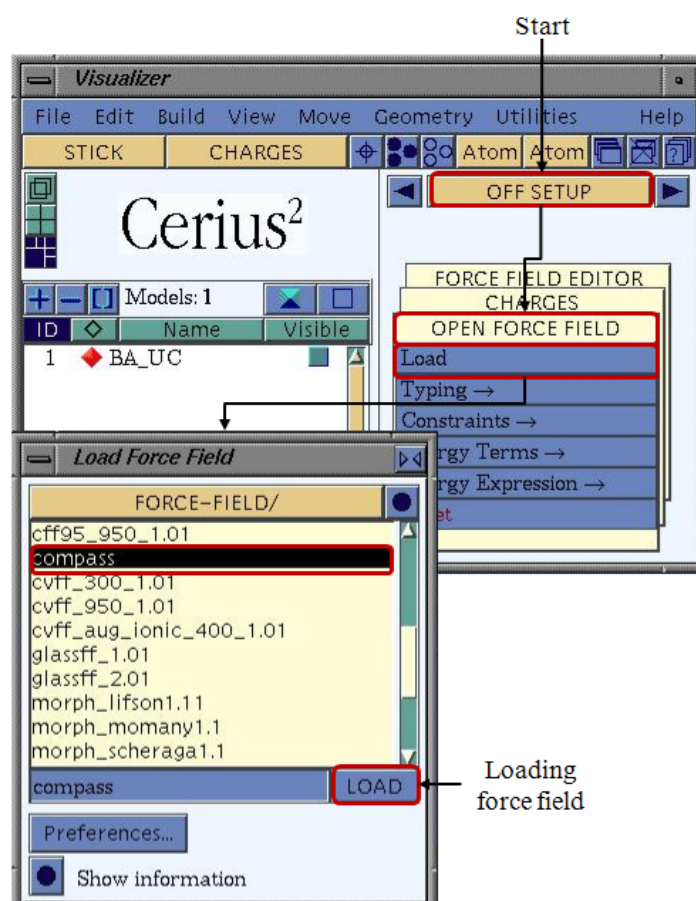
Before conducting any further step of the computational procedure it is a basic requirement to apply the force field on the atoms. Initially it can be checked if any force field has been applied so far by using the labeling function. The function is available from the visualizer toolbar as seen in Figure 4-8. Default setting in the toolbar is “NO LABEL” this should be changed to “FFTYPE”.





*Figure 4-8 Labeling of the force field type via the visualizer toolbar.*

If no force field type is displayed the application should be started via the “OFF SETUP” which is accessed from the modules in the “Visualizer” dialogue. As illustrated in Figure 4-9 the index card “OPEN FORCE FIELD” is to be selected and the click on “Load” will open the “Load Force Field” dialogue. Here, the force field should be selected (recommended is compass or pcff) and the choice is confirmed by a click on the “LOAD” button. The “Load Force Field” dialogue can be closed.



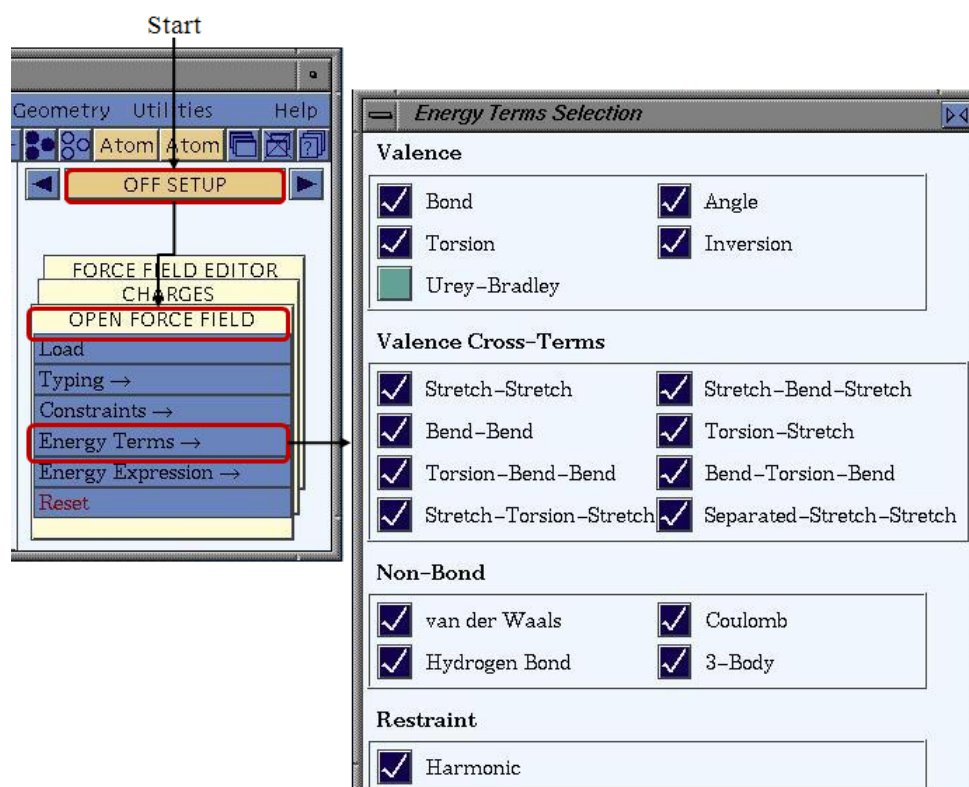
*Figure 4-9 Loading the force field via the “Load Force Field” dialogue.*

The choice of the considered in energy terms selection is crucial for the subsequent modeling. The selection menu is obtained via the path OFF SETUP/OPEN FORCE FIELD/Energy

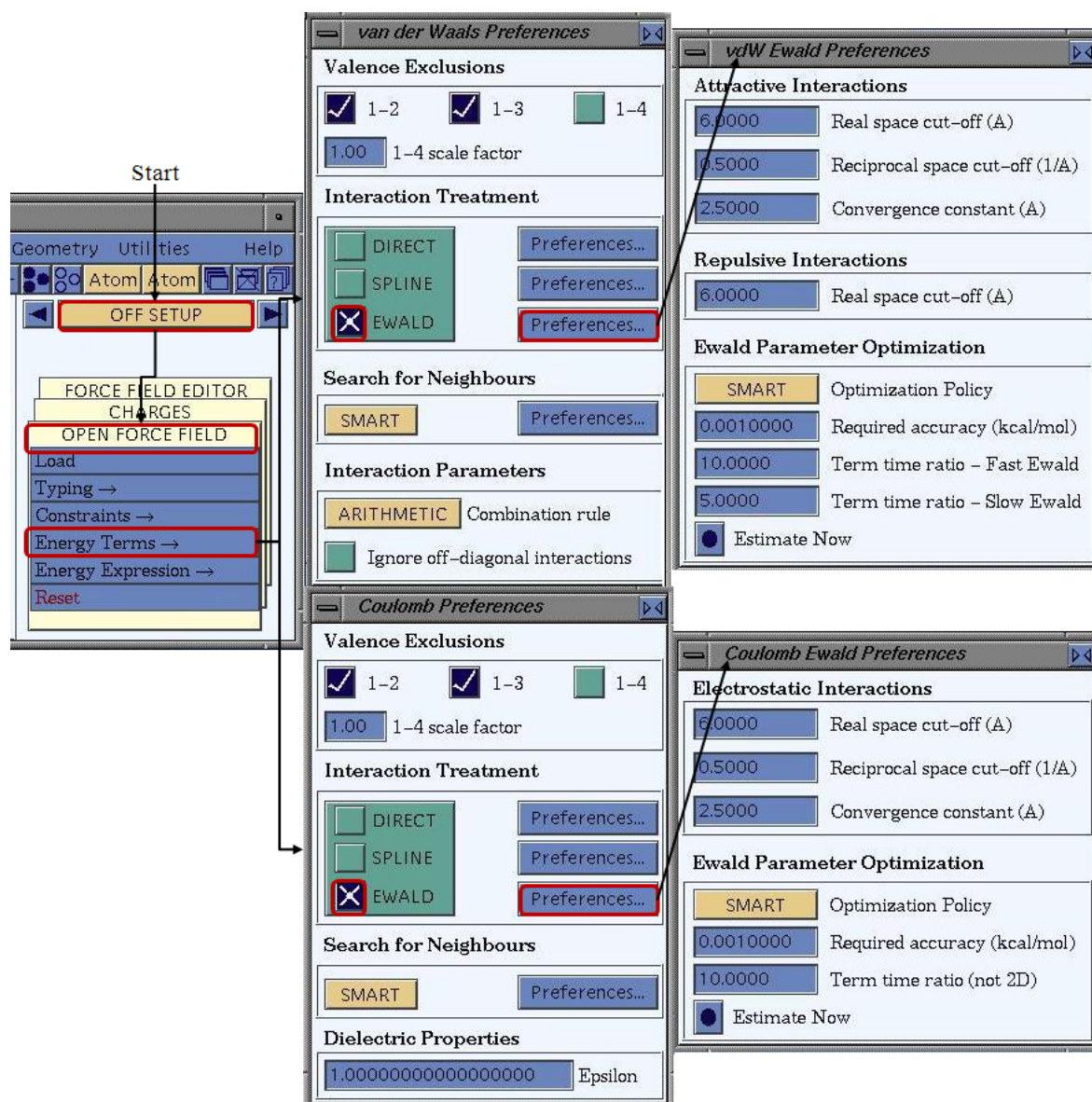


Terms/Selection and the dialogue “Energy Terms Selection” appears. The dialogue should be modified as depicted in Figure 4-10.

Furthermore, it is essential to select a calculation method for energy terms. The path from the module OFF SETUP/OPEN FORCE FIELD/Energy Terms/van der Waals and Coulomb enables to change the settings. The corresponding dialogues are depicted in Figure 4-11. The “van der Waals Preferences” and the “Coulomb Preferences” dialogues open. In both of the dialogues the “Interaction Treatment” is set to “Ewald” by checking the corresponding box (see Figure 4-11). Further settings are not recommended but can be accessed when clicking on the “Preferences...” button next to the selected method of interaction treatment. If necessary the settings in “vdW Ewald Preferences” and “Coulomb Ewald Preferences” should be set to the values as given in the illustration below.



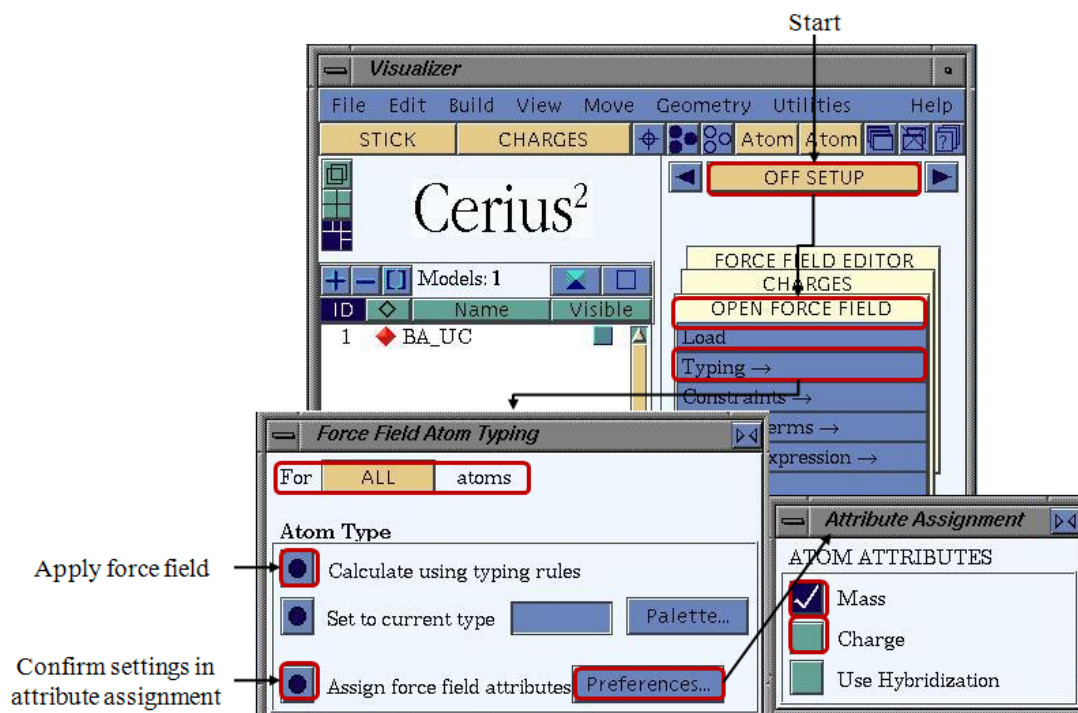
*Figure 4-10 The “Energy Terms Selection” dialogue.*



*Figure 4-11 The “van der Waals Preferences” and “Coulomb Preferences” dialogues for “Energy Terms” settings.*

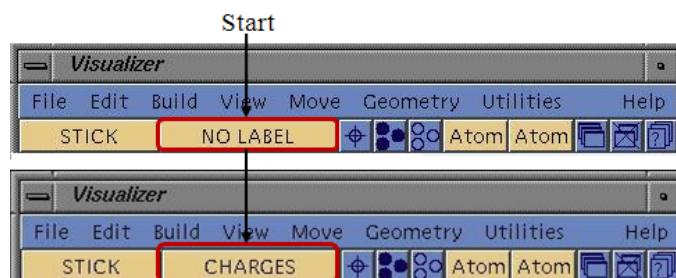
The force field parameters which are applied to the atoms are selected in the next step (atom typing). In order to achieve the typing menu follow the path from the module OFF SETUP/OPEN FORCE FIELD/Typing/Atoms (Figure 4-12). The dialogue “Force Field Atom Typing” is opened and setting to conduct the typing “For ALL atoms” should be chosen. By a click on the “Preferences...” button which is located at the bottom right. The dialogue “Attribute Assignment” will appear in which the box for “Mass” should be checked and the boxes “Charge” and “Hybridization” are deselected. The step is important since the default settings are changed here. Confirm the settings done in the “Attribute Assignment” dialogue by clicking on the button at the bottom left (next to the text “Assign force field attributes”) in

the dialogue “Force Field Atom Typing”. The force field is then applied to the atoms by a click on the button located left to the text “Calculate using typing rules” in the same dialogue. After applying the force field the labeling of the atoms should be checked, if the step was performed successfully the force field labels are displayed and the dialogues can be closed.



*Figure 4-12 The “Force Field Atom Typing” dialogue.*

The next task is the charge calculation. Prior conducting the actual calculation it should be checked if the charges are assigned to the atoms via the labeling function which is available from the visualizer toolbar. The steps for the labeling procedure are depicted in Figure 4-13. The default setting in the toolbar “NO LABEL” is to be changed into “CHARGES”. The charges should be “0.0000” for a downloaded crystallographic structure file. In case the charges are displayed as none zero the charge calculation as described hereafter can be skipped.



*Figure 4-13 Labeling of the charges via the visualizer toolbar.*

As all atomic charges are displayed “0.0000” the calculation can be performed. In order to calculate the charges follow the path from the module “OFF SETUP” and click on “Charges”.



As the Dialogue “Charges opens check the box “Charge-Equilibration” and click on the “Preferences...” button which is located right to the chosen “Calculation Method”. The “Charge Equilibration preferences” dialogue is displayed as depicted in Figure 4-14. In the dialogue it is required to choose the parameter set which will be employed for the subsequent charge calculation. The selection of “QEq\_charged1.1” is recommended and should be confirmed by clicking on the “LOAD” button. The “Charge Equilibration preferences” dialogue can be closed. Back in the “Charges” dialogue all settings are applied and the button “CALCULATE” is pressed for conducting the charge calculation.

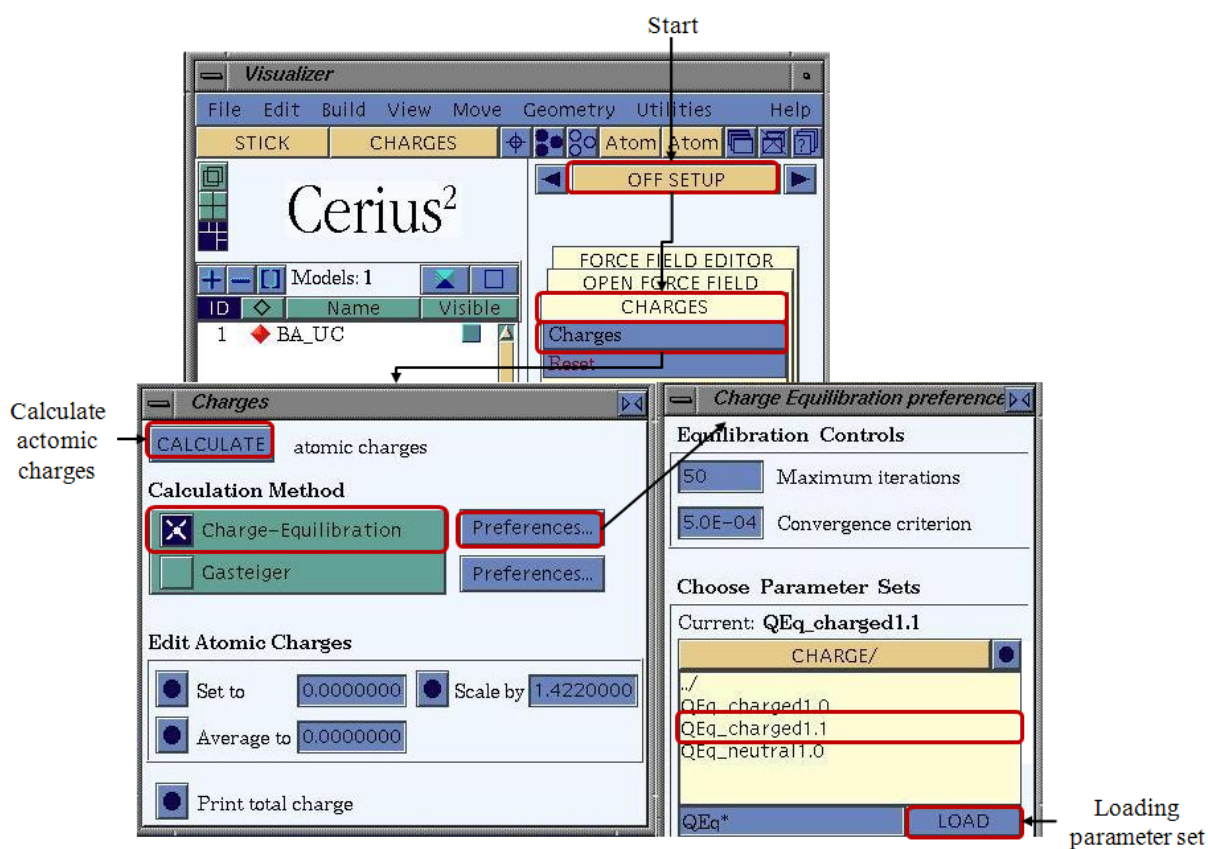
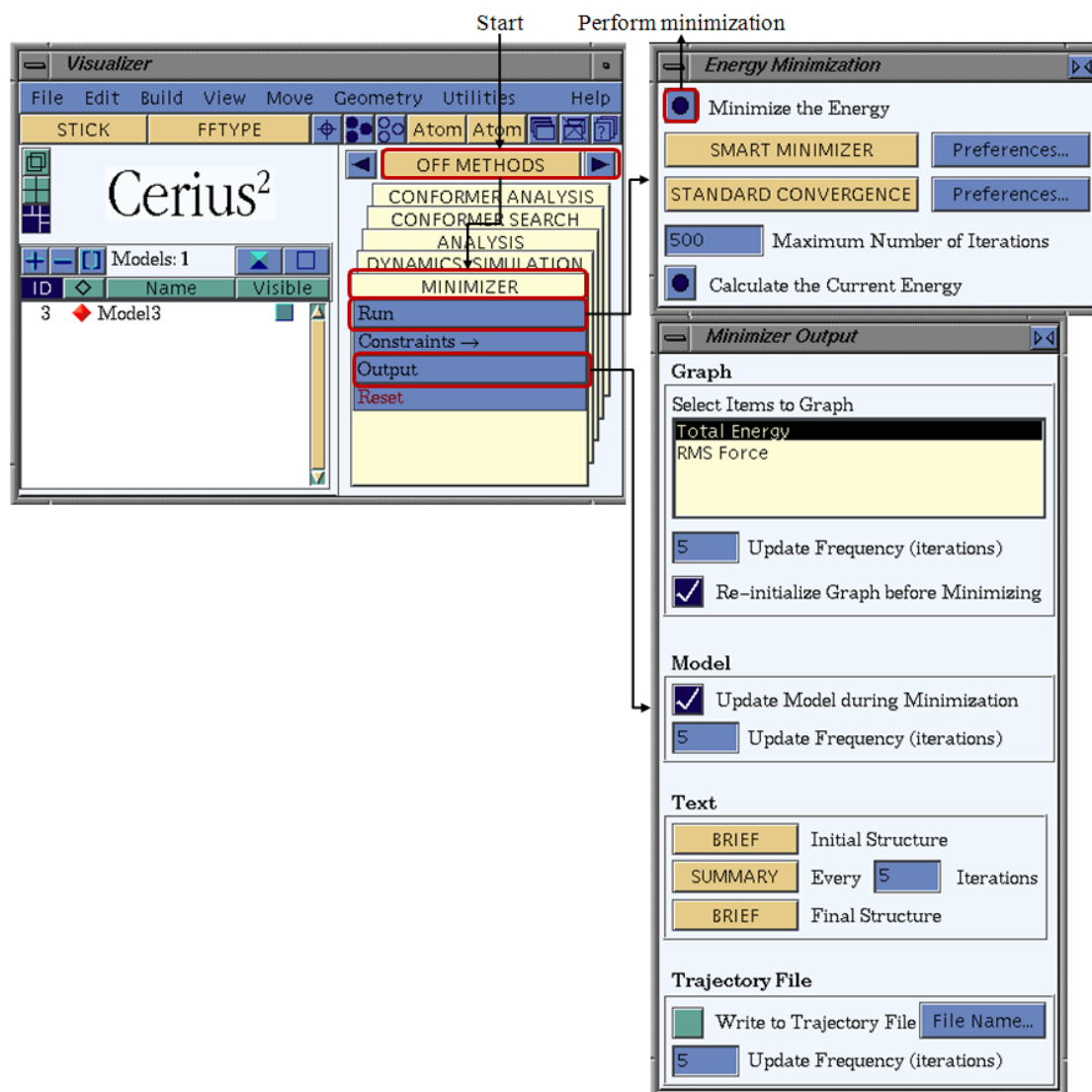


Figure 4-14 Dialogues for the charge calculation accessed via “OFF-SETUP”.

#### 4.2.1.3 Step 3: Geometry Optimization for Crystal Structure Data or Molecules

Once the force field has been applied and the charges are calculated according to the aforementioned steps the geometry optimization is conducted via the “Energy Minimization” dialogue. To perform the minimization the module OFF METHODS/MINIMIZER is used. A click on the path OFF METHODS/MINIMIZER/Run will open the “Energy Minimization” dialogue. If necessary the settings should be changed as depicted in Figure 4-15. Furthermore, the menu which is accessed via OFF METHODS/MINIMIZER/Output may require the change of the settings. If all settings are in accordance with those which are seen in the illustration (Figure 4-15), the “Minimize Energy” button in the “Energy Minimizer” dialogue

can be pressed in order to start the minimization. Once the minimization has been performed it is optional to recalculate charges via the module path OFF SETUP/Charges/Charges as described in the past chapter.



*Figure 4-15 The “Energy Minimization” dialogue.*

#### 4.2.1.4 Step 4: BFDH and Attachment Energy Calculation

After the successful performance of the past steps the pure crystal morphology can be calculated. This is obtained when following the module path OFF INSTRUMENTS I/ MORPHOLOGY/Calculate. The dialogue “Calculate Morphology” appears (see Figure 4-16 top). Here, the BFDH calculation and/ or the Growth Morphology (Attachment energy) calculation can be performed. If only the BFDH morphology is desired a click on the “Calculate” button in the “Bravais-Friedel-Donnay-Harker” section of the dialogue will start the BDFH calculation. For the subsequent calculation of the attachment energy the graphical result file which is obtained from the BFDH calculation is used. In order to perform the

attachment energy calculation start in the section “Growth Morphology” of the dialogue “Calculate Morphology”. Herein, “bond energy list” is to be used and in order to skip the BFDH calculation the box “Do BFDH first” should be deselected. Clicking on the “Calculate” button starts the calculation of the attachment energy morphology. In case both, the BFDH and the attachment energy morphologies are desired the user should move to the “Growth Morphology” section as described before, check the box “Do BFDH first” and start the calculation by pressing the “Calculate” button.

The resulting graphical files should display the morphology and the crystal unit cell. If desired the visualization of the morphology can be changed via the “Morphology Display” dialogue which is accessed via the path OFF INSTRUMENTS I/ MORPHOLOGY/Display (Figure 4-16 bottom).

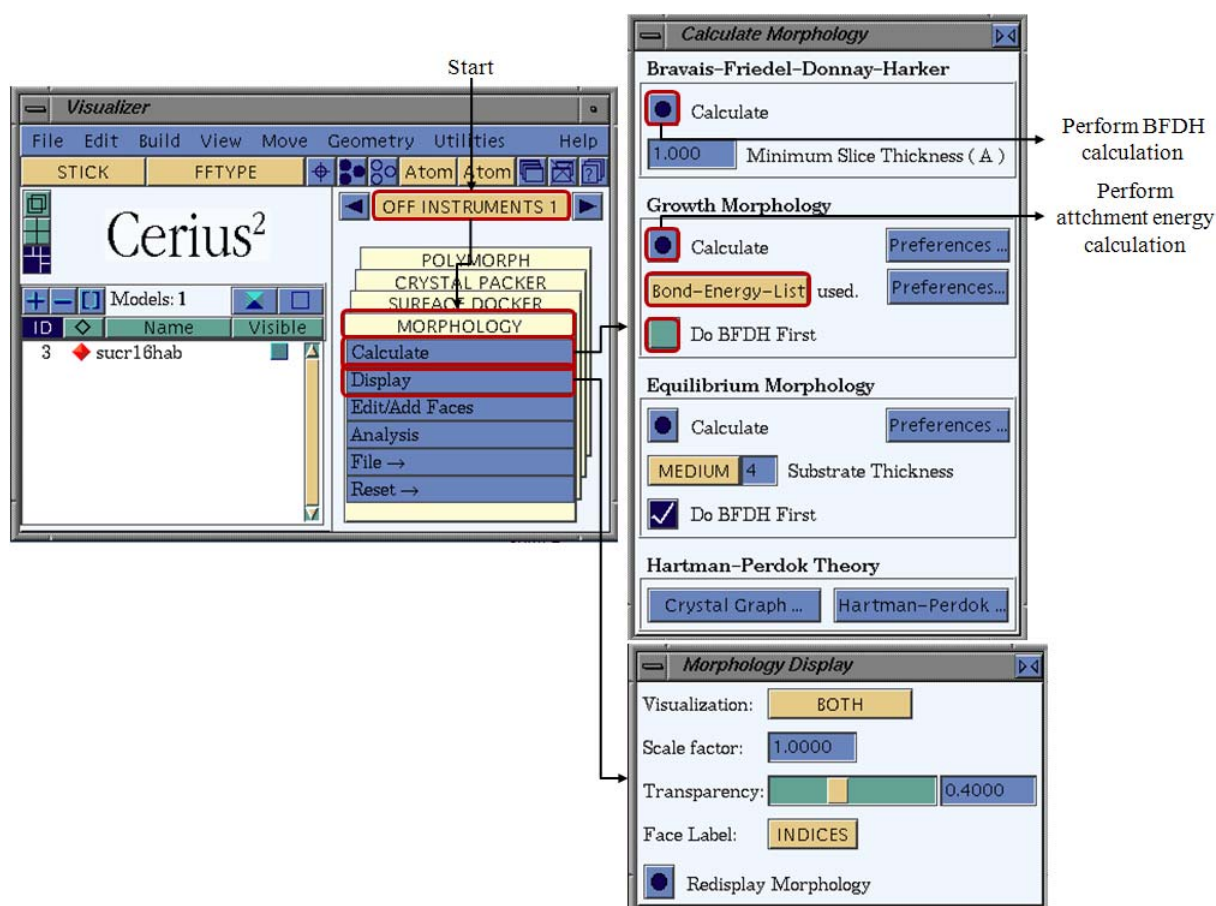


Figure 4-16 The “Calculate Morphology” and the “Morphology Display” dialogues.

#### 4.2.1.5 Step 5: Important Crystal Surfaces

After the BFDH and attachment energy calculation has been performed it is possible to display the miller indices of the visible crystal surfaces via OFF INSTRUMENTS I/

MORPHOLOGY/Display in the appearing “Morphology Display” dialogue the “Face Label” should be set to “Indices” by default. The path is illustrated in Figure 4-17 on the top right.

The listing of all (visible and invisible) crystal surfaces is accessed via the path OFF INSTRUMENTS I/ MORPHOLOGY and the click on Edit/Add Faces. It is recommended to note the Miller indices of the 8 most important faces and the corresponding attachment energies. In order to obtain a complete listing of the crystal surfaces follow the path OFF INSTRUMENTS I/ MORPHOLOGY/ and click on “Edit/Add Faces”. The “Edit/Add Faces” dialogue is opened where a click on the “List All Faces to Text Window” button will start the plot of the face list to the winterm console. The list gives the miller indices and the interplanar spacing  $d_{hkl}$ . Note:  $d_{hkl} \sim |E_{hkl}^{att}|$ . The procedure is depicted in Figure 3-44 at the bottom right.

In order to save the list open a unix-shell and enter the command “ls -l”. A list of all files in the current directory will be given. Here the user should search the file which has been recently created (check system time by entering: “date”). In order to see first lines of the chosen file, enter the command “more filename.extension” and press [F1] to interrupt the list. If the desired file has been detected a jot-file of the file should be created in order to save the data by entering. Therefore enter the command “jot filename.extension”.

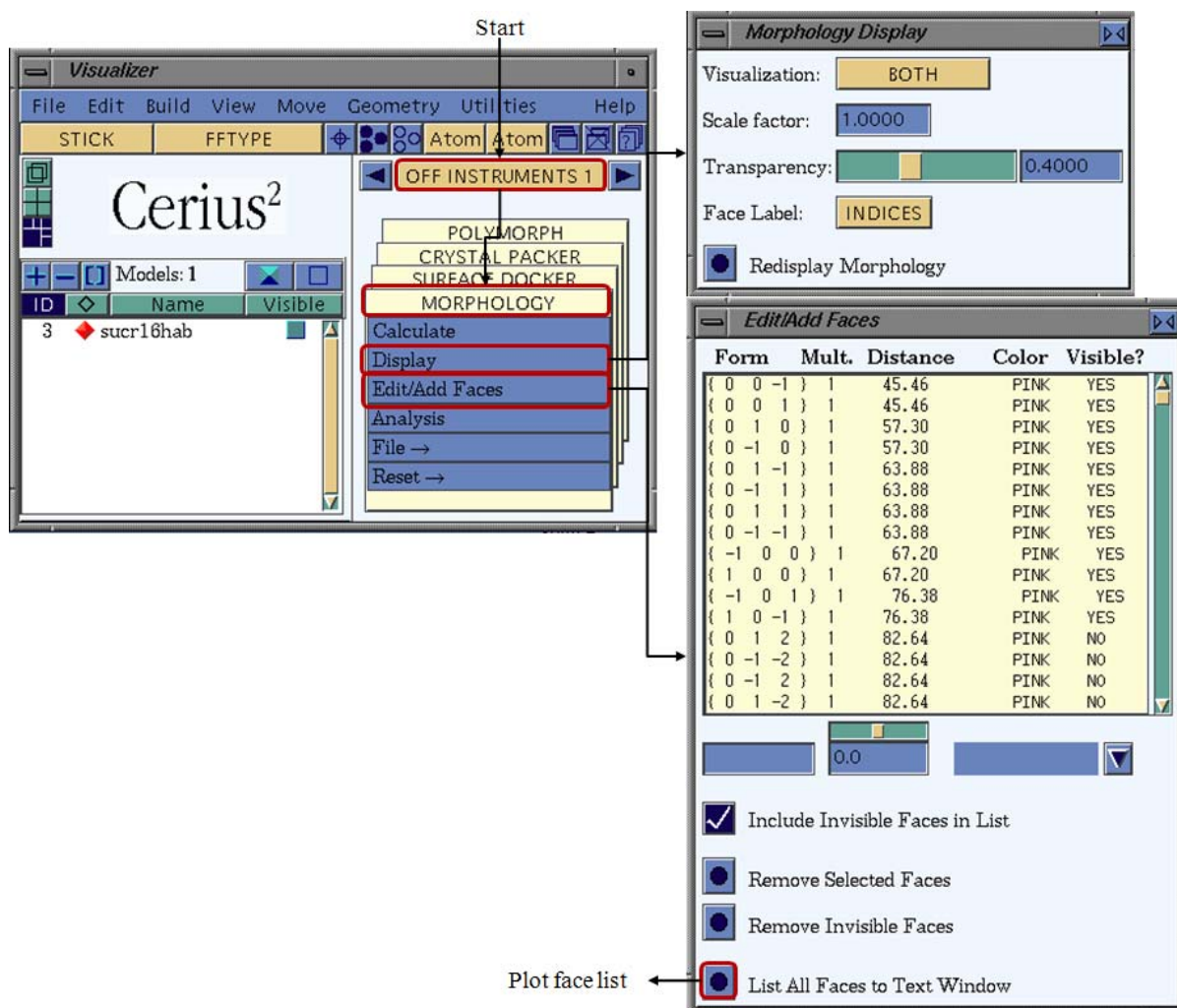


Figure 4-17 The “Edit/ Add Faces” dialogue.

#### 4.2.1.6 Step 6: Preparing Modified Surfaces

The initial task is to cleave the crystal surfaces of the attachment energy morphology. This is obtained via the path OFF Instruments I /MORPHOLOGY/Analysis which is illustrated in Figure 4-18. As the dialogue “Morphology Analysis” is opened enter the miller indices of the face which is to be cleaved next to the “Cleave Selected Face” button, here e.g. {3 2 1} and press the button in order to perform the cleaving.



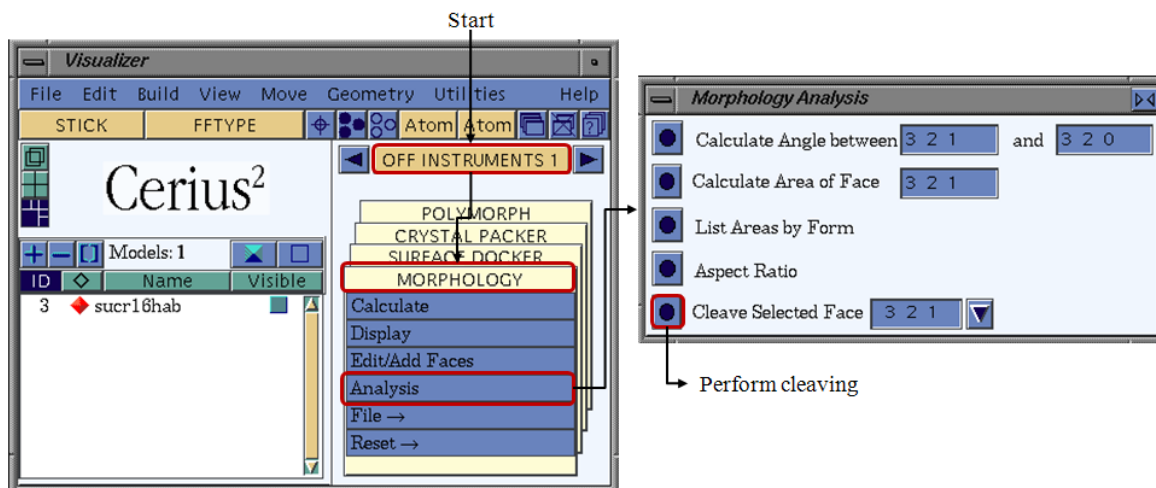


Figure 4-18 The “Morphology Analysis” dialogue.

In order to specify the depth of a cleaved surface follow the path BUILDERS I/SURFACE BUILDER/Cleave Crystal Surface and the dialogue “Cleave Crystal Surface” is displayed (seen in Figure 4-19 middle). From the drop down menu on the top right of the dialogue choose the file containing the morphology from which the face is to be cleaved. Modify the settings in the section “Specify Surface Box” as follows. Enter “Direction (hkl)”, e.g. if face is  $\{-1\ 0\ 0\}$  direction (hkl) is  $(-1\ 0\ 0)$ . In the line below set depth to  $3.0\ \text{\AA}$  and press the “Cleave” button.

The modification of the dimension of the surface box is achieved as follows. In the section “Specify Surface Box” of the dialogue “Cleave Crystal Surface” the boxes “Automatically re-cleave crystal” and “Display surface box” are to be checked (seen in Figure 4-19 middle). By a click on the “More...” button next to the text “Display Surface Box” the dialogue “Surface Box” (seen in Figure 4-19 right) will appear. Enter the “Direction (hkl)” and modify “U (uvw)” and “V (uvw)”. Set the row of U to “0.00 4.00 0.00” and V to “0.00 0.00 6.00” (see Figure 4-19). The visualization should be updated automatically. Save the file which is seen in the model visualization dialogue.

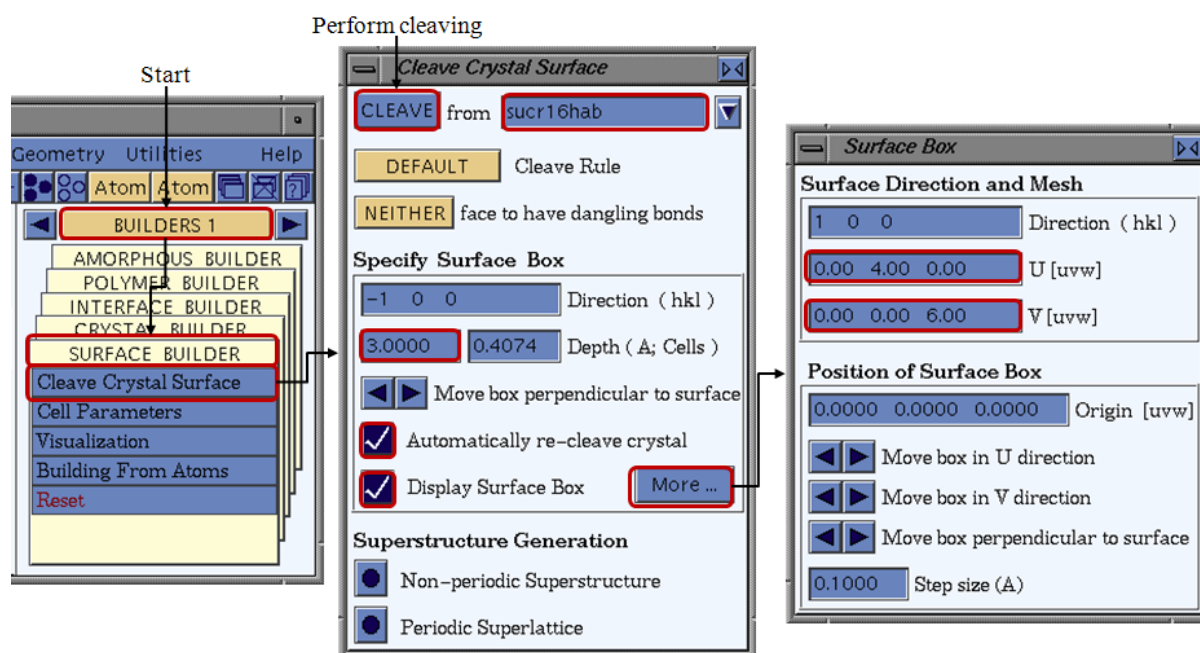


Figure 4-19 The “Cleave Crystal Surface” and “Surface Box” dialogues.

Alternative: Create a surface box via the module path BUILDERS I/SURFACE BUILDER/Visualization. In the displayed “Surface Visualization” dialogue (seen in Figure 4-20) set  $u=4.0$  and  $v=6.0$  and press the “Enter” button.

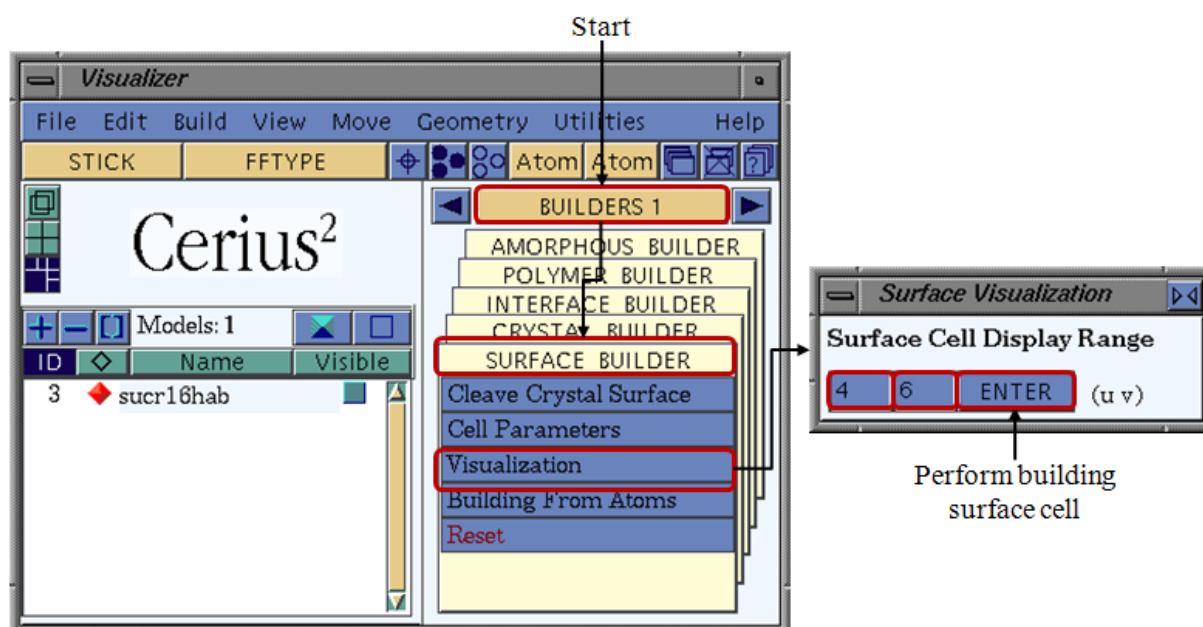
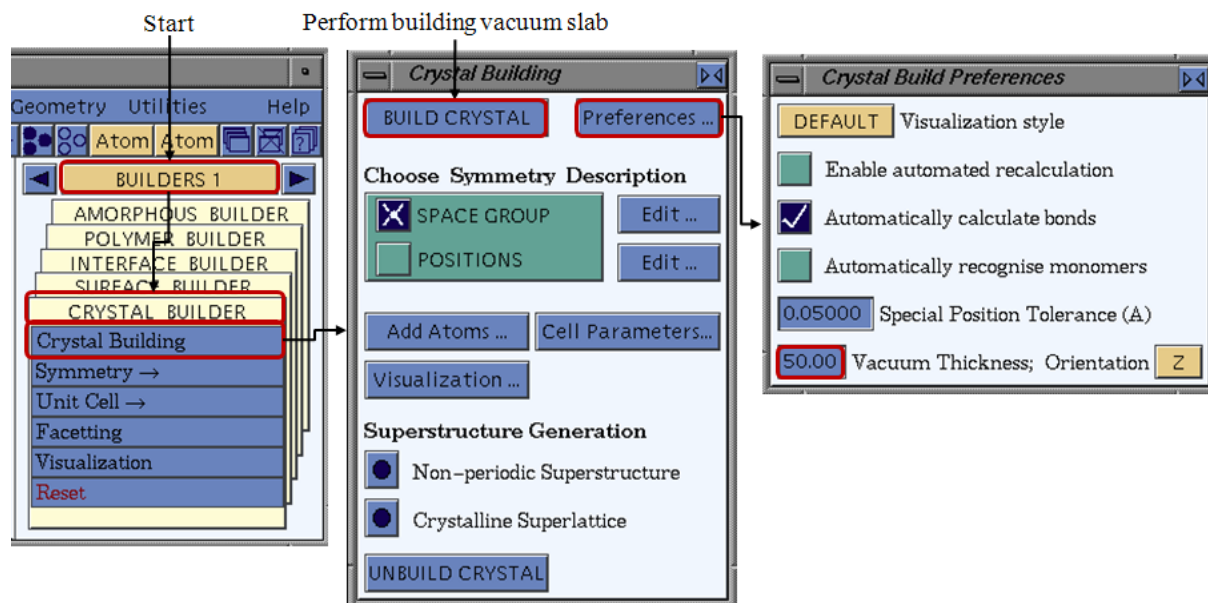


Figure 4-20 The “Surface Visualization” dialogue.

In order to obtain a closed surface box a vacuum slab is created as follows. Via the module path BUILDERS I/CRYSTAL BUILDER/Crystal Building the “Crystal Building” dialogue is accessed (seen in Figure 4-21 middle). Click on “Preferences...” button which is located on the right top of the dialogue. As the “Crystal Build Preferences” dialogue opens the vacuum

thickness should be set to 50.0 Å (see Figure 4-21 right). Repeat this for each of the 8 most important faces and save the files



*Figure 4-21 The “Crystal Building” and “Crystal Build Preferences” dialogues.*

#### 4.2.2 Combined Crystal Surface and Additive

In terms of the surface docking method is required to construct surface boxes for each of the relevant crystal surfaces. Once these boxes are constructed 2 sets of boxes are prepared. The surfaces of the first set are fitted with a molecule of the host crystal and the surfaces of the second set are docked with an additive (or solvent) molecule on the top of each surface.

##### 4.2.2.1 Step 6: Preparing Modified Surfaces

Before calculating the modified crystal morphology from the pure morphology the crystal surfaces are docked with an optimized molecule either of the host crystal or of the additive (or solvent).

Therefore, one native molecule (which is optimized as described in chapters 4.2.1.1 to 4.2.1.3) is docked in the middle of a crystal surface. A second file for each surface is created in which the surface is docked with one additive molecule in the middle of the crystal surface. The final task is to fix the Cartesian position of molecules of the crystal surface by setting constraints. This is achieved via the path OFF METHODS/MINIMIZATION/Constraints/Atoms. Select the atoms of the surface and in the dialogue “Atom Constraints” click on the “Fix Atomic Position” button. To ensure the constraints are applied click on the “Color Atoms by Constraint” button. An illustration is seen in Figure 4-22.

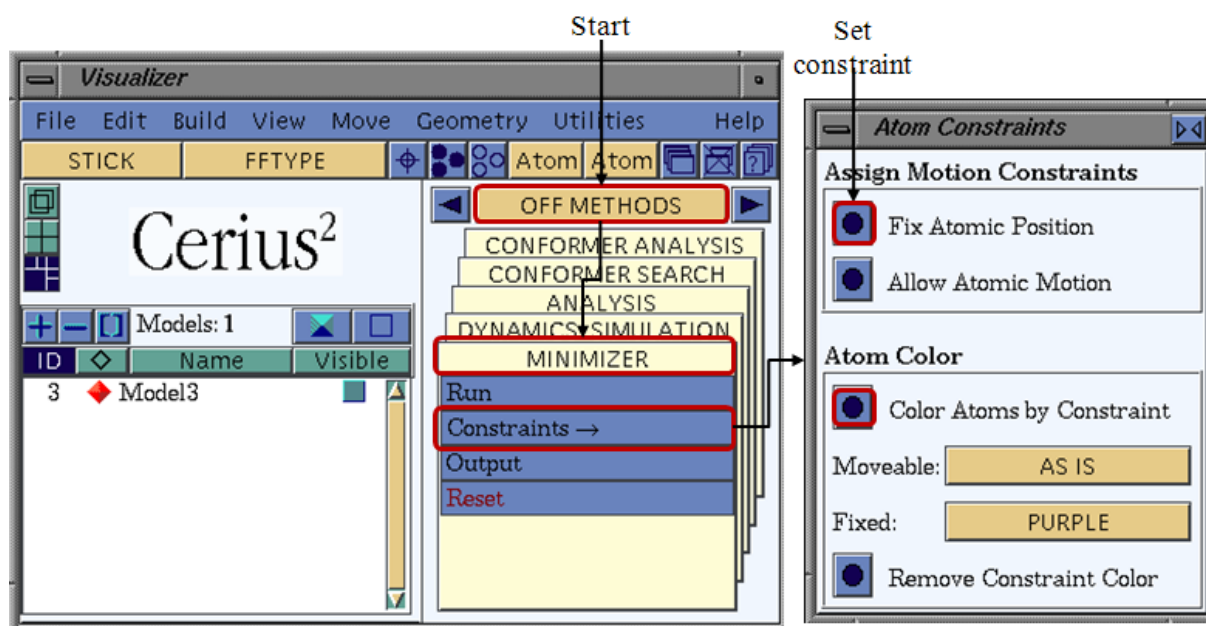


Figure 4-22 The “Atom Constraints” dialogue.

#### 4.2.2.2 Step 7: Molecular Dynamics (NVT)

In order to perform the molecular dynamics on the surface docked with the additive and the host molecule the settings should be applied as seen in Figure 4-23 and described in the present chapter.

Access to the dynamics menu is obtained when following the module path OFF METHODS/DYNAMICS SIMULATION/Run as the dialogue “Dynamics Simulation” is opened the user should select the “Dynamics Method” and check the box “CONSTANT NVT” (seen in Figure 4-23 middle). Via clicking on the button “Preferences...” which is located in the same line the “NVT Dynamics Preferences” dialogue opens (Figure 4-23 top right). In the dialogue the thermostat is selected (recommended is “NOSE” or “T-DAMPING”).

Back in the “Dynamics Simulation” dialogue the “Dynamics Controls” are changed as seen in the illustration (Figure 4-23 middle), the “Required Temperature (K)” is 300 K and the “Number of Steps” is 500. For a later analysis is required to create a dynamics trajectory file. The corresponding settings are done in the dialogue “Dynamics Trajectory Output” which opens by a click on the “TRAJECTORY...” button. Here, check the box “Create Dynamics Trajectory File” and select the “Trajectory Update Frequency (step)”. The “Dynamics Output Preferences” are modified via a click on the Button “Output...” in the “Dynamics Simulation” dialogue. The settings should be a seen in the illustration (Figure 4-23 right middle).

The dialogue “Molecular Dynamics Controls” which is opened from the path OFF METHODS/DYNAMICS SIMULATION/Dynamics Controls should remain default with the

settings as depicted in Figure 4-23 (bottom left). As all the settings are carried the NVT dynamics are started via clicking on the button “RUN” which is located on the top left of the “Dynamics Simulation” dialogue. The simulation is started and may have duration of several hours.

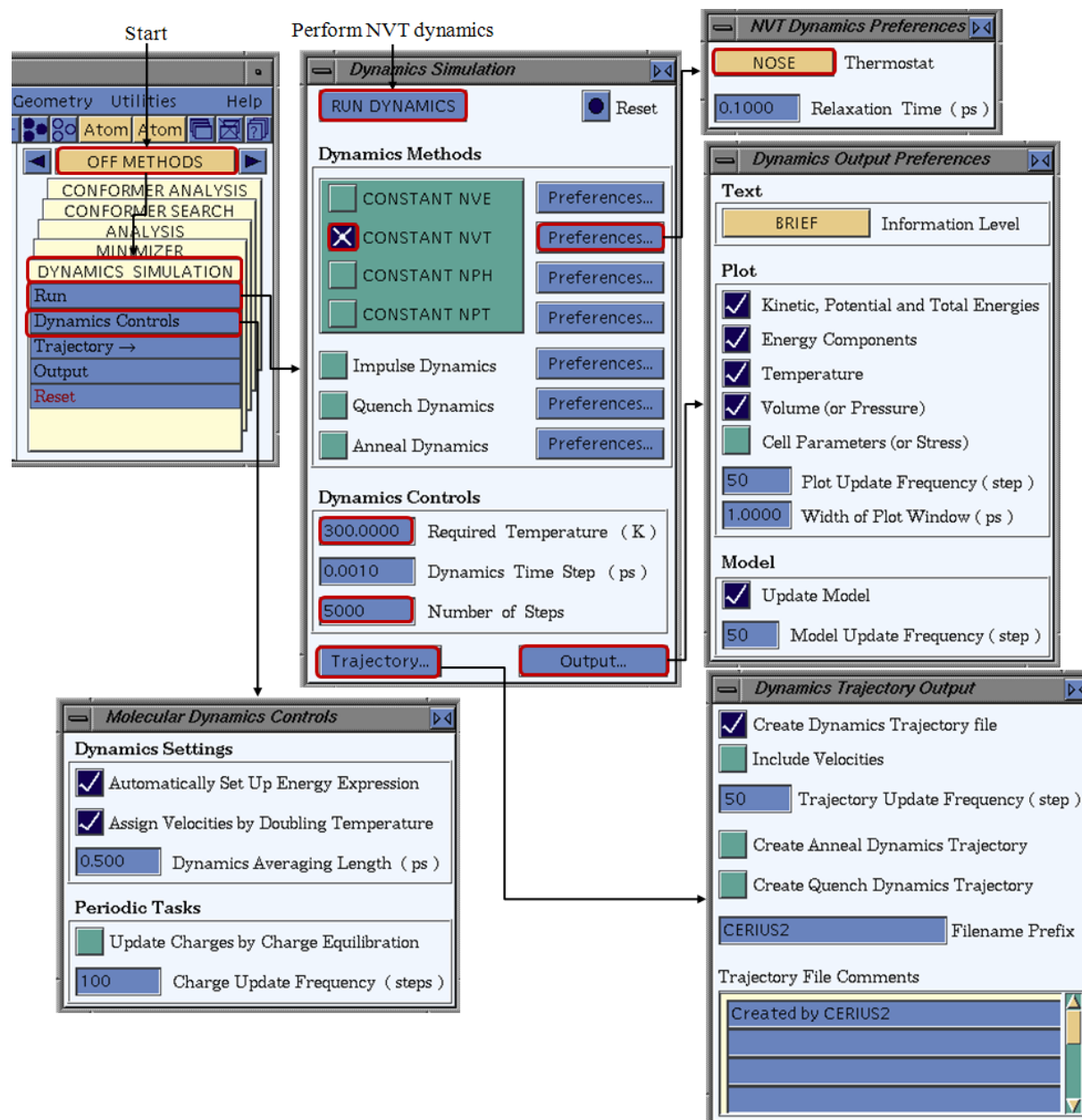


Figure 4-23 The “Dynamics Simulations” dialogue and dynamics settings.

#### 4.2.2.3 Step 8: Trajectory Analysis

The trajectory result file which is obtained from NVT dynamics is analyzed in the present chapter.

In order to conduct the analysis the trajectory is to be selected as input file for the analysis via the path OFF METHODS/ANALYSIS/Input. Here select the trajectory file which was

generated in the previous the dynamics calculation and confirm your choice by pressing the “SELECT” button.

As the document is loaded in order to access the “Analysis Statistics” dialogue follow the module path OFF METHODS/ANALYSIS/Analyze/ Statistics. In the dialogue select from the root structure in “Energy Totals” the property “Total Energy” and at the bottom of the dialogue select “Search for 10 lowest energy frames”. Click on the “OUTPUT...” button and here check the box “Plot” (the output will be given in the scripting window). Back in the “Analysis Statistics” dialogue click on the “Search for 10 lowest energy frames” button. The steps are illustrated in Figure 4-24 at the bottom middle and right. Note the number and the energy of the lowest energy frame.

The model visualization of the lowest energy frame from the trajectory file which has been loaded is obtained via the path OFF METHODS/ANALYSIS/Analyze/ Show Frames. Enter as “Current Frame” the frame number of the lowest energy frame. The model visualization dialogue shows the molecular conformation of the frame of the minimum energy. The path for the step is seen in Figure 4-24 at the bottom left.

The lowest energy frame as seen in the model visualization should be selected and via the copy/paste function transferred to an empty model visualization file. Prior to the minimization the constraints which were applied to the atomic positions of the surface atoms need to be removed. In order to achieve this follow the menu OFF METHODS/MINIMIZER/Constraints/ Atoms. Select the atoms of the surface and in the dialogue “Atom Constraints” click on the “Fix Atomic Position” button. To ensure the constraints are applied click on the “Color Atoms by Constraint” button. An illustration is seen in Figure 4-25. As the document is the input file for the subsequent minimization it should be saved as “Lowest Energy Frame.msi”.



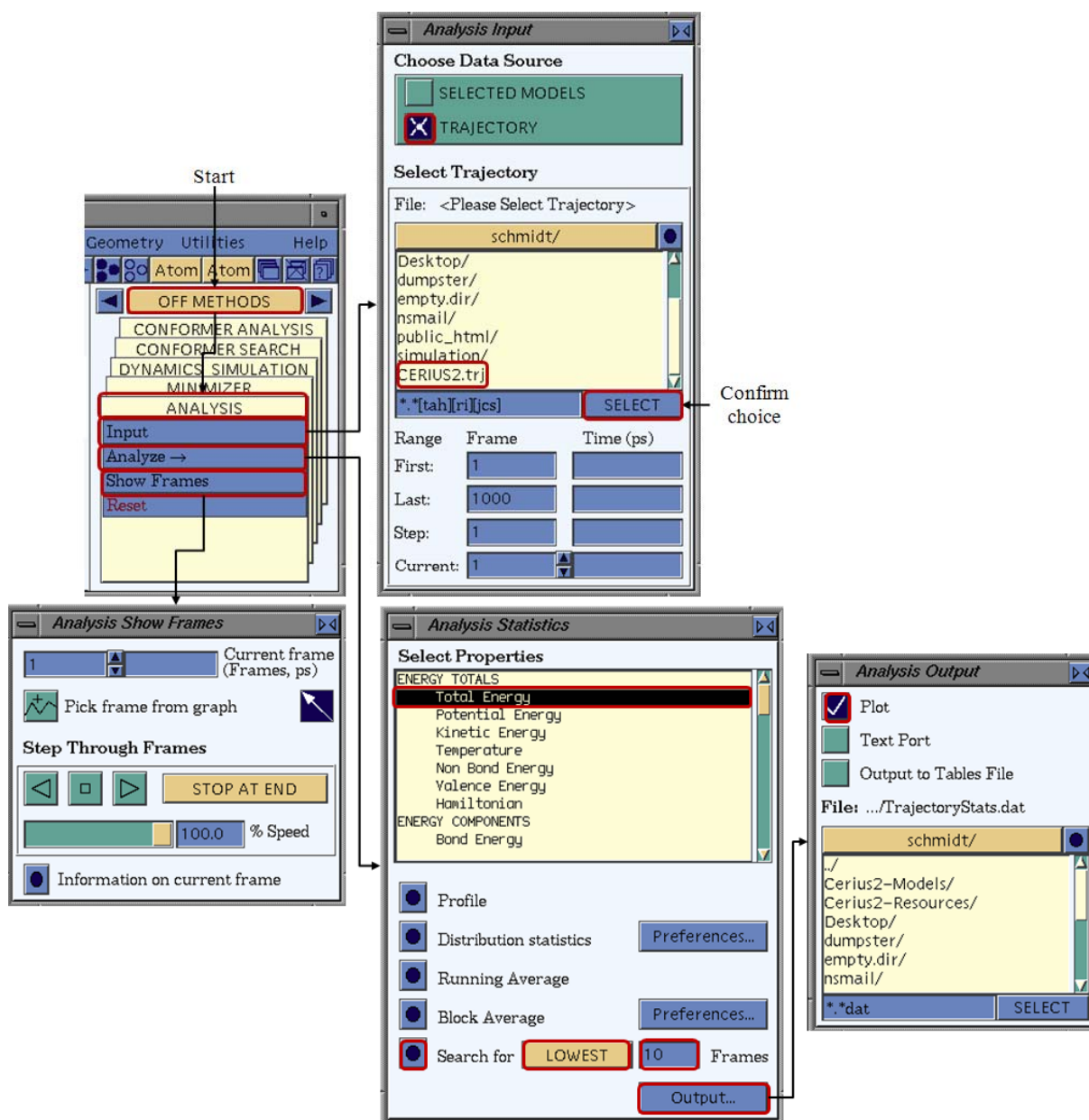


Figure 4-24 Trajectory analysis after the NVT dynamics.

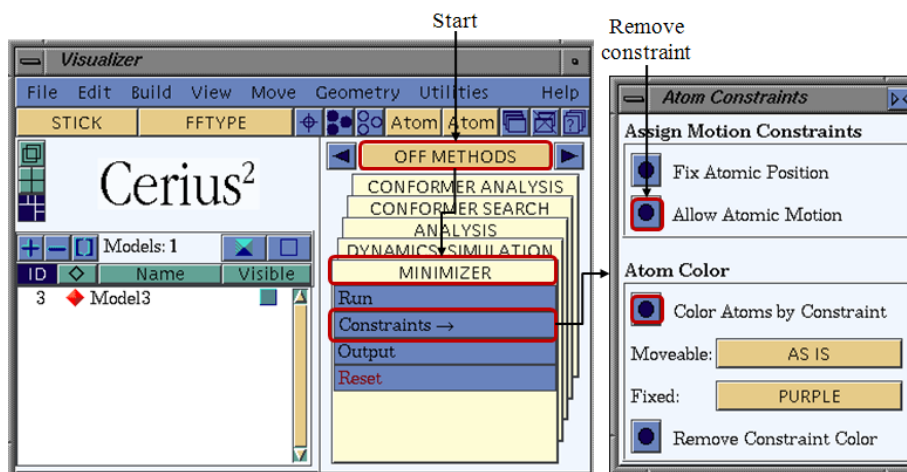


Figure 4-25 The "Atom Constraints" dialog.

#### 4.2.2.4 Step 9: Minimization

The minimization is conducted for the molecular conformation at the lowest energy level. The settings are accessed via the “Energy Minimization” dialogue which is obtained via the module OFF METHODS/MINIMIZER/ with a click on “Run” the “Energy Minimization” dialogue will open. Here the “Maximum Number of Iterations” should be set to “5000”. Furthermore, the menu “Minimizer Output” may require the change of the settings and is accessed via OFF METHODS/ MINIMIZER/Output. If all settings are in accordance with those which are seen in the illustration (Figure 4-15), the “Minimize Energy” button in the “Energy Minimizer” dialogue can be pressed in order to start the minimization. The model visualization which is resulting from minimization and the corresponding total potential energy is employed for further steps of the procedure and should be saved.

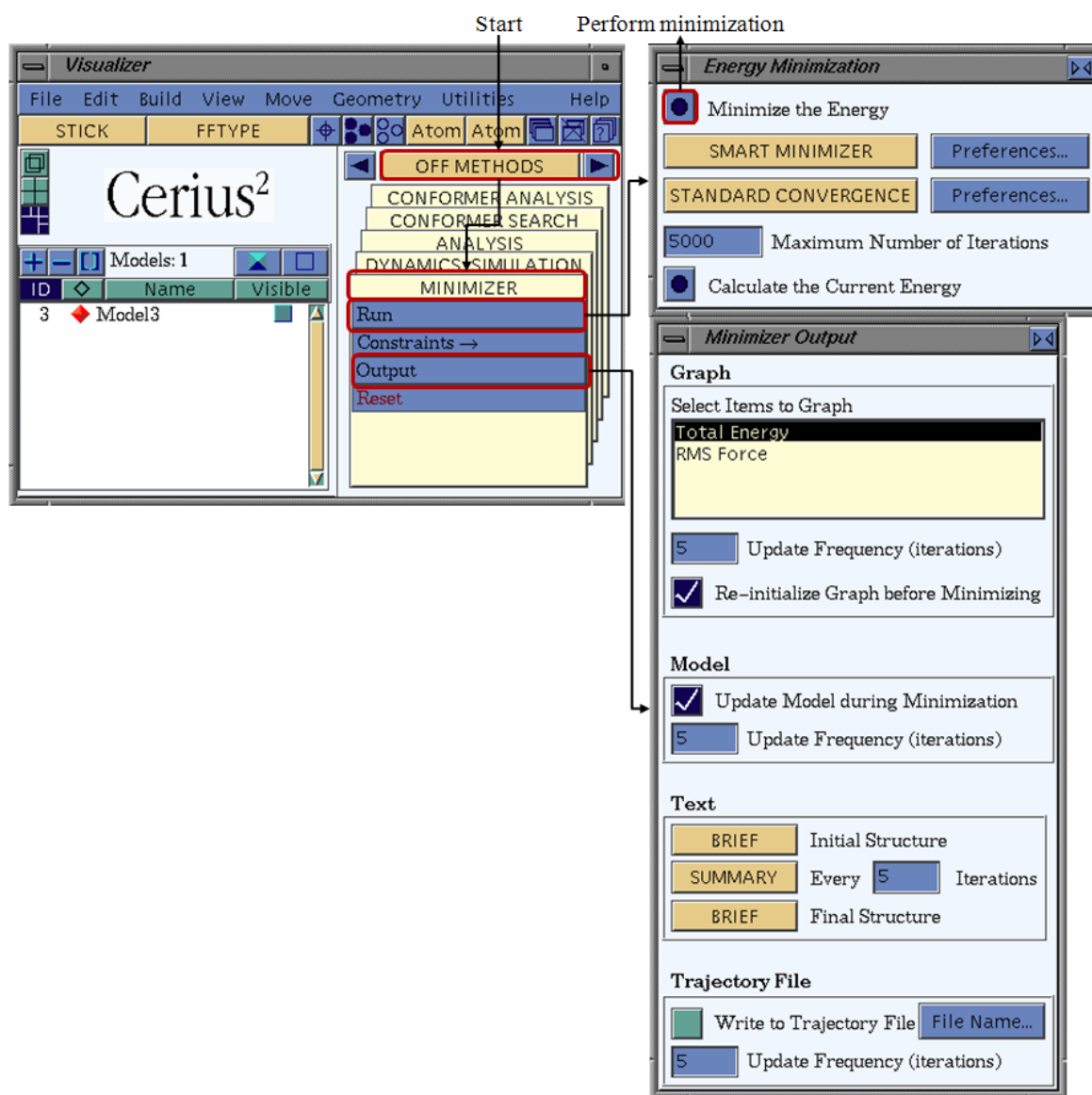


Figure 4-26 The “Energy Minimization” dialogue.



#### 4.2.2.5 Step 10: Calculating the Energy of Surface and Additive

Using the path which is illustrated in Figure 4-27 enables to calculate the current energy of a system. Subsequent steps of the prediction procedure required the calculation of the binding energy. Herefore the total potential energy of only the atoms of the surface and the atoms of the isolated additive/solvent molecule and the isolated host molecule is necessary. In order to calculate these energies the 3D visualization file obtained from the minimization is crucial. As the file is saved the molecule which is docked on the surface should be carefully removed and the new file should be stored as “surface\_only.msi”. The same procedure is conducted for surfaces which are docked with the host crystal molecule. Vice versa all of the surface atoms of the original files are to be removed and the files should be saved as “additive\_only.msi” or “host\_only.msi”. For all of these new files the current energy is to be calculated by following the path OFF METHODS/MINIMIZER/Run. The “Energy Minimization” dialogue opens and the user should click on the button “Calculate the Current Energy”. The obtained total potential energies should be saved.

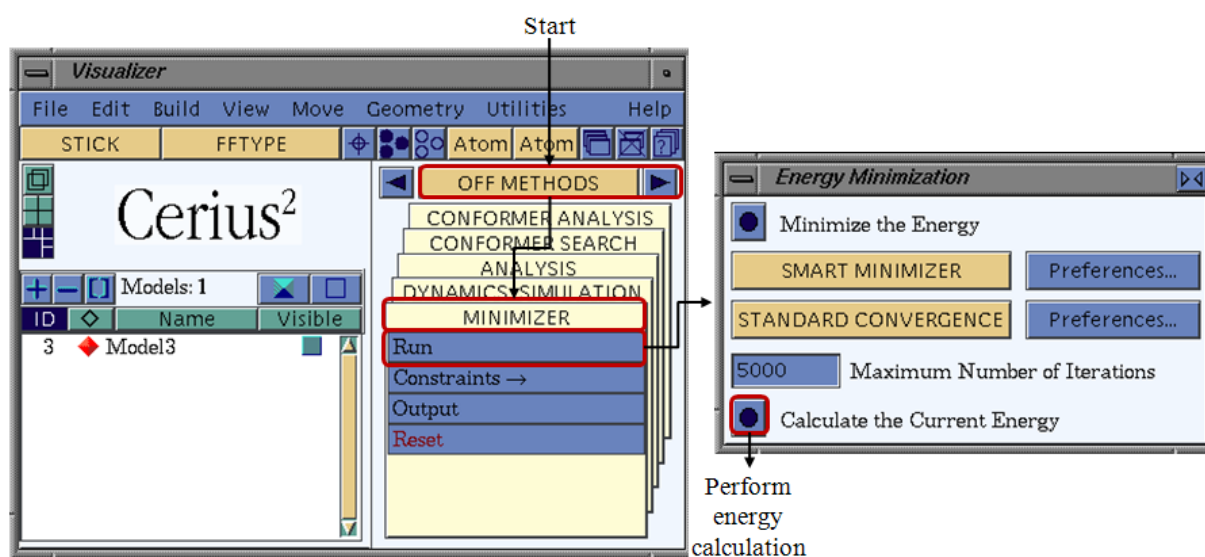


Figure 4-27 Calculation of the current energy.

### 4.2.3 The Modified Morphology

Upon the obtained data the final procedure for the prediction of the modified morphology in the presence of an additive or solvent molecule can be started.

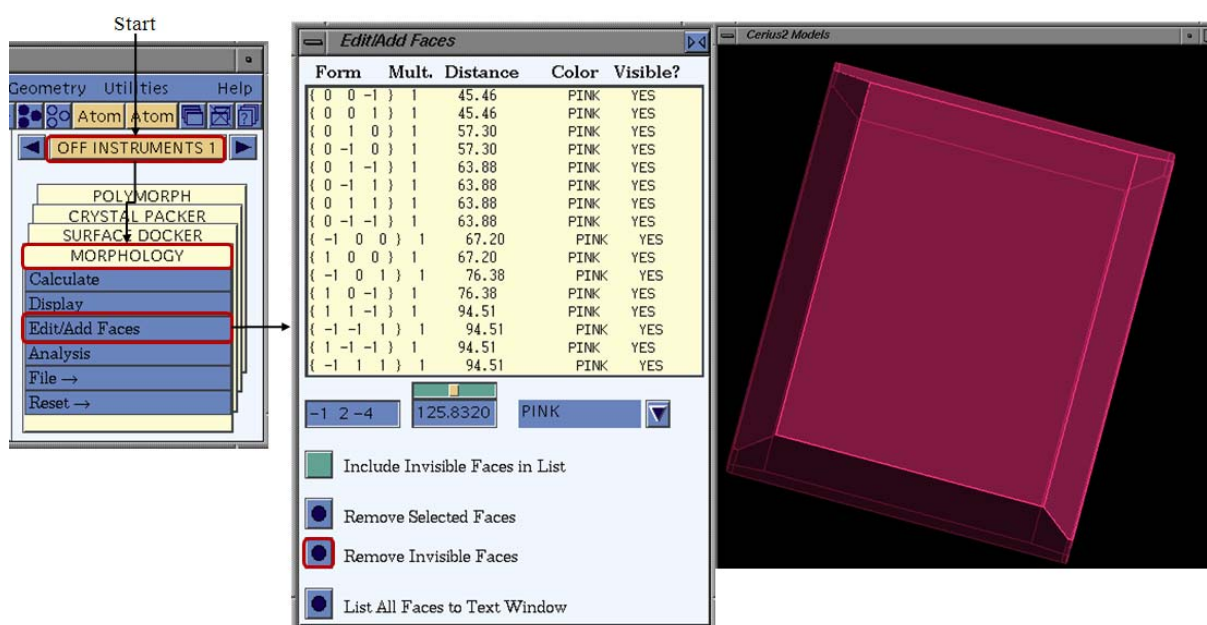
#### 4.2.3.1 Calculating the Modified Attachment Energy

The modified attachment energy is calculated by using the equations which are presented in chapter 3.1.3.1.

### 4.2.3.2 Calculating the Modified Morphology

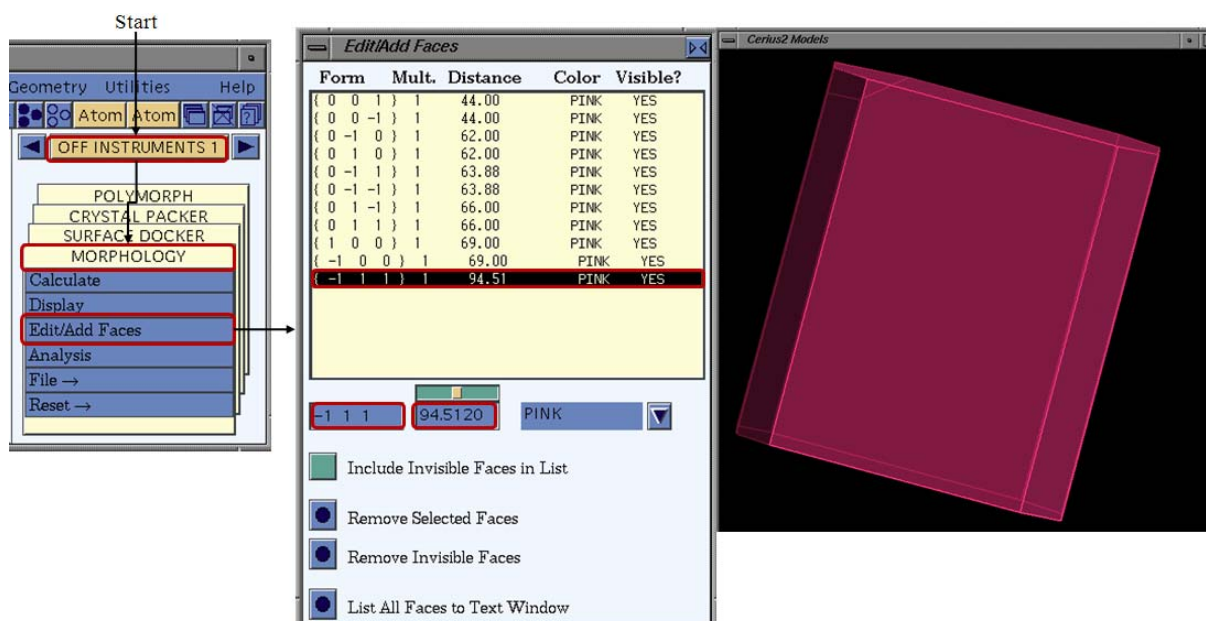
Using the calculated modified attachment energies the modified morphology can be computed using the software overview Cerius<sup>2</sup> 4.5 and 4.7 when following the subsequent steps.

The model visualization dialogue should display the attachment energy morphology of the pure crystal. Follow the module path OFF INSTRUMENTS I/MORPHOLOGY/ and click on Edit/Add Faces. The dialogue “Edit/Add Faces” as seen in the Figure 4-28 opens and gives a listing of all faces of the pure crystal morphology. In order to obtain the modified morphology click on the “Remove Invisible Faces” button (or on the “Remove Selected Faces” button for only removing selected faces).



*Figure 4-28 The face list of the pure morphology seen in the “Edit/Add Faces” dialogue.*

As the list is reduced to the relevant faces click on the line which contains the face for which the value of the modified attachment energy has been calculated (seen in Figure 4-29 middle) and edit the value in the list. The modification of the value in the column “Distance” is achieved as depicted below.



*Figure 4-29 Generating the modified morphology via the “Edit/Add Faces” dialogue.*

### 4.3 The Layer Docking Method

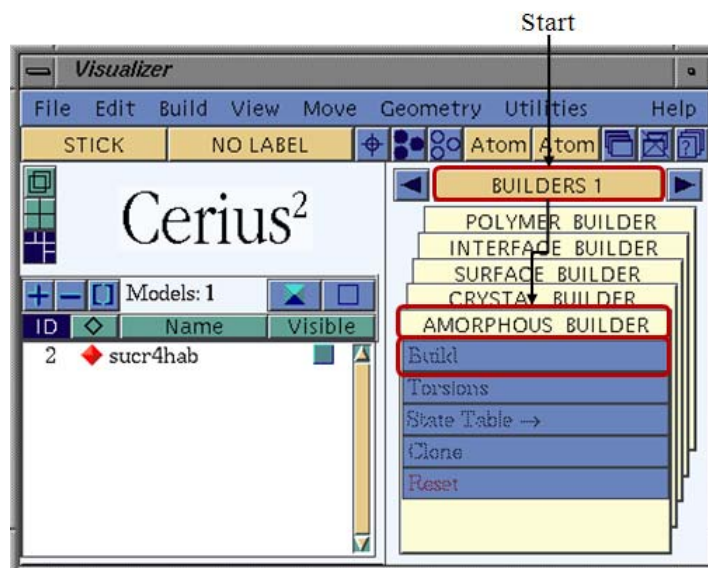
The prediction of crystal morphologies grown from a solution under consideration of the concentration of the solute and the solvent as presented in chapter 3.2 can be employed with Cerius<sup>2</sup>. The therein presented Layer Docking method can achieve the desired results faster when using the software Cerius<sup>2</sup> if using the non graphical simulation run. The present chapter introduces how to adapt the procedure in Cerius<sup>2</sup> in the graphical user interface. The command tracing file can be compiled following chapter 4.1.

#### 4.3.1 The Liquid Side (Solution)

The modeling of the liquid side proceeds in the same steps as in MaterialsStudios. Details for the procedure are presented hereafter.

##### 4.3.1.1 Step 1: Constructing an Amorphous Cell

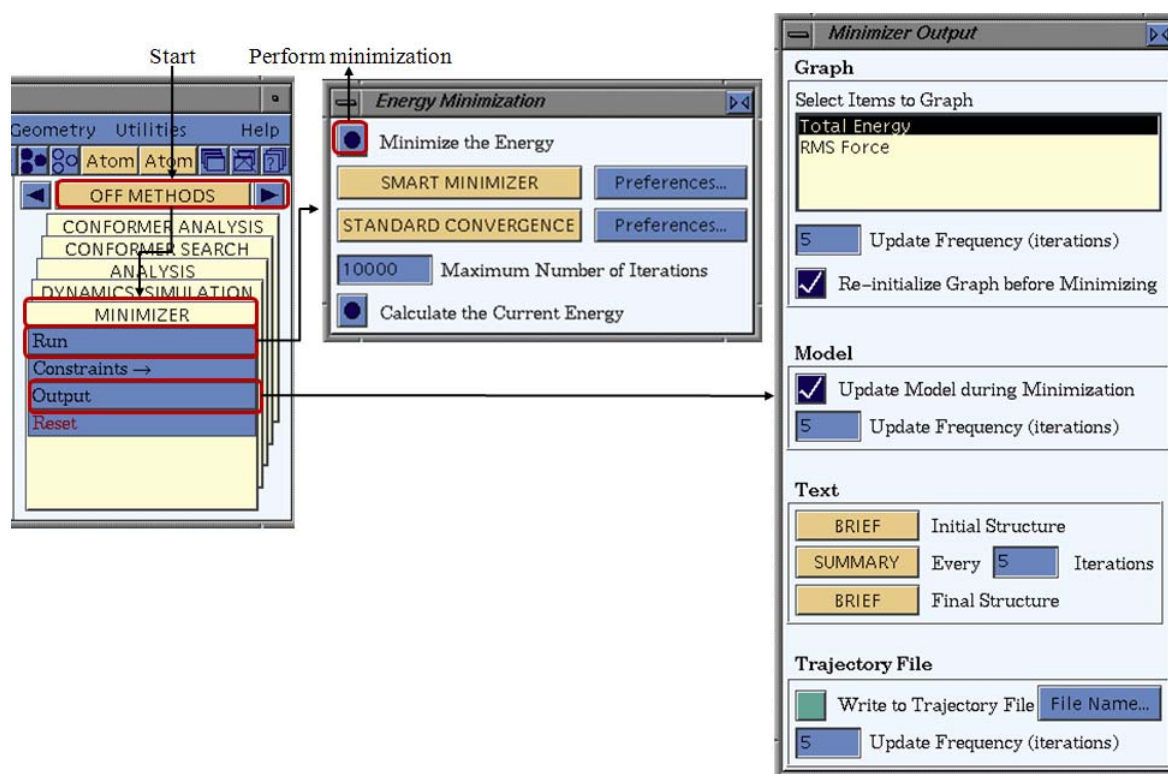
In Cerius<sup>2</sup> the construction of an amorphous cell is achieved in a similar procedure as presented in chapter 3.1.3. In order to get access to the menu from which the settings can be chosen the user should follow the path BUILDERS I/AMORPHOUS BUILDER/Build (Figure 4-30). The further dialogues are not illustrated since the software package which is available at the Martin-Luther-University does not comprise the license for the module “AMORPHOUS BUILDER”. The interested user is therefore referred to the software manual for the corresponding module. The settings which are used in the software MaterialsStudios 4.0 (presented in chapter 3.2.1.1) should be employed in a similar manner in Cerius<sup>2</sup>.



*Figure 4-30 Building an amorphous cell using the “Amorphous Builder”.*

#### 4.3.1.2 Step 2: Minimization

For the minimization of the potential energy of the amorphous cell the “Energy Minimization” dialogue is used. It is accessed via the module OFF METHODS/MINIMIZER/ with a click on “Run” the “Energy Minimization” dialogue will open. Here the “Maximum Number of Iterations” should be set to “10000”. In case the menu “Minimizer Output” may require the change of the settings the dialogue is accessed via OFF METHODS/MINIMIZER/Output. If all settings are in accordance with those which are seen in the illustration (Figure 4-31), the “Minimize Energy” button in the “Energy Minimizer” dialogue can be pressed in order to start the minimization. The model visualization which is resulting from minimization and the corresponding total potential energy are to be saved. The subsequent dynamics steps are conducted on the 3D model which is resulting from the minimization.



*Figure 4-31 The “Energy Minimization” and “Minimizer Output” dialogues.*

#### 4.3.1.3 Step 3: Molecular Dynamics I (NVE)

The molecular dynamics procedure is started with an initial NVE dynamics. The used settings depicted in Figure 4-32. The settings are accessed via the path “OFF METHODS/DYNAMICS”. Select the “Dynamics Methods” should be chosen as “NVE”, at a temperature of “300 K”, the “Dynamics Time Steps” should be “0.0010 ps” for the “Number of Steps” is equal to “100000” (the dynamics time is 100 ps). When pressing the button “Preferences...” the dialogue “NVE Dynamics Preferences” appears but should remain as default (illustrated in Figure 4-32 right). Back in the “Dynamics Simulation” dialogue press the button “Trajectory...” and the dialogue “Dynamics Trajectory Output” will open. Herein, uncheck the box “Create Dynamics Trajectory file”. This setting aims to avoid any frame output as trajectory and to save only the final structure. Any other settings if required should be modified according to the illustrations given in Figure 4-32. Once the settings are adjusted, press the “RUN DYNAMICS” button in order to start the NVE molecular dynamics. The calculation may have duration for several days. The resulting 3D model and the total energies should be saved. The 3D model is the input for the next simulation step.



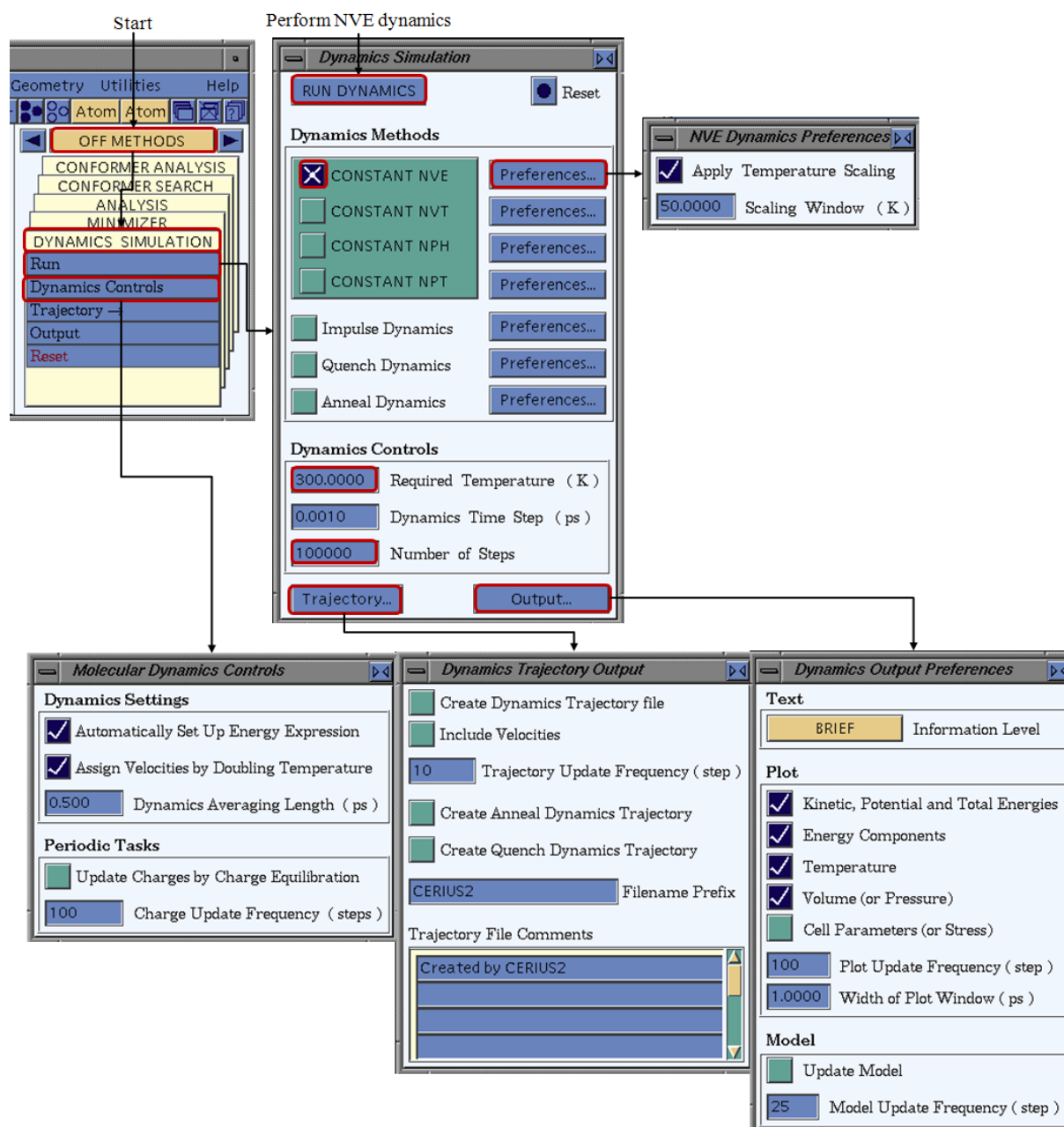


Figure 4-32 The “Dynamics Simulation” dialogue for the NVE dynamics.

#### 4.3.1.4 Step 4: Molecular Dynamics II (NpT)

The NPT molecular dynamics are conducted for the 3D file which is resulting from the previous NVE dynamics. The settings for the NPT are illustrated in Figure 4-33. These molecular dynamics settings are obtained by following the path “OFF METHODS/ DYNAMICS”. Select the “Dynamics Method” “NPT”, the “Temperature” of “300 K”, the “Dynamics Time Steps” are “0.0010 ps” for “10000” as the “Number of Steps” (equal to the dynamics time of 10 ps). After pressing the button “Preferences...” the dialogue “NPT Dynamics Preferences” appears. The “Thermostat” “Nose” should be selected (see Figure 4-33 right). Since no trajectory output is required press the button “Trajectory...” in the

“Dynamics Simulation” dialogue. The dialogue “Dynamics Trajectory Output” will open and here uncheck the box “Create Dynamics Trajectory file”. Any other settings should remain as default (illustrated in Figure 4-33). The NPT dynamics may have duration of several hours. The resulting potential energies and the 3D file are to be saved for further steps.

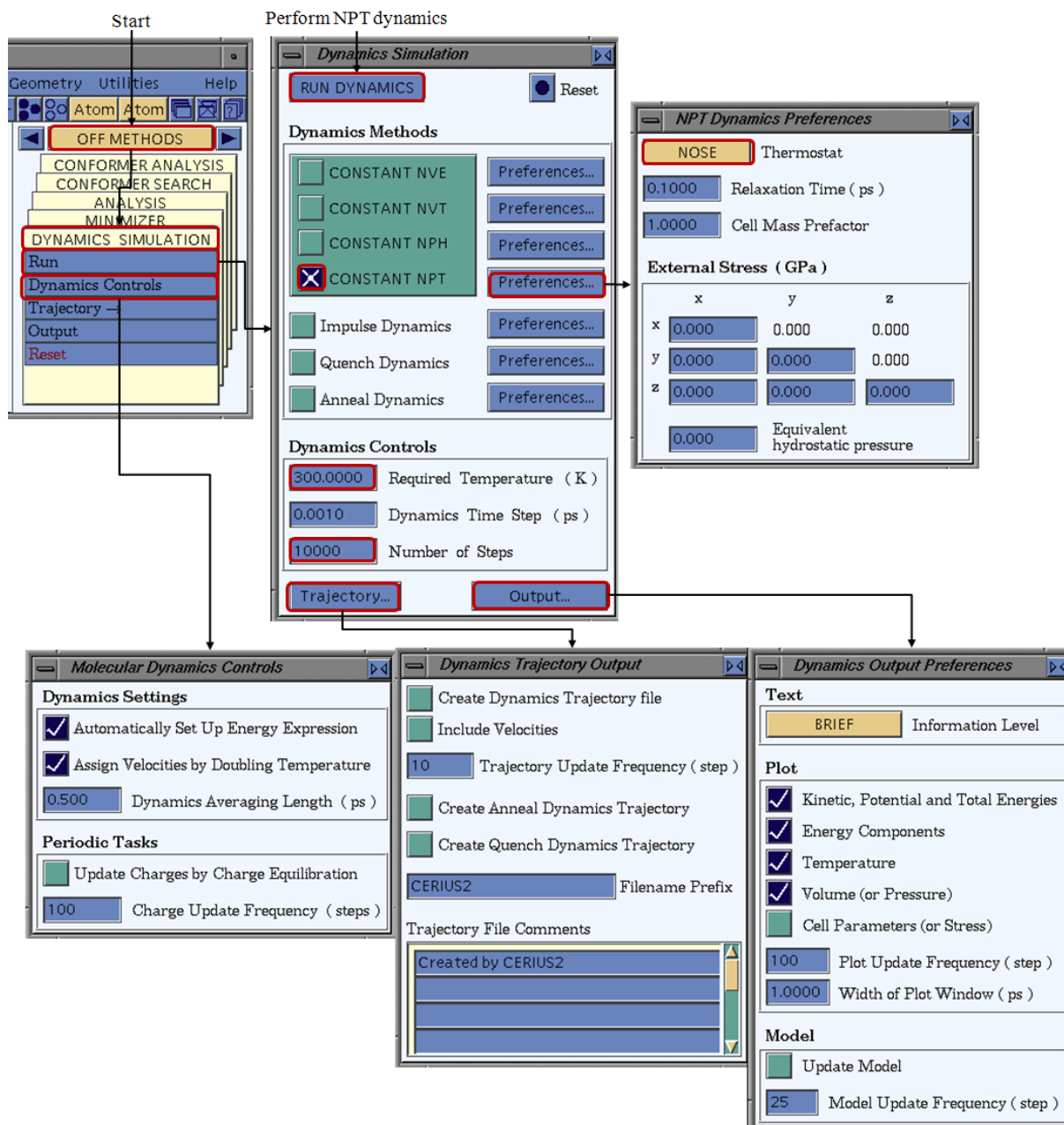


Figure 4-33 The “Dynamics Simulation” dialogue for the NPT dynamics.

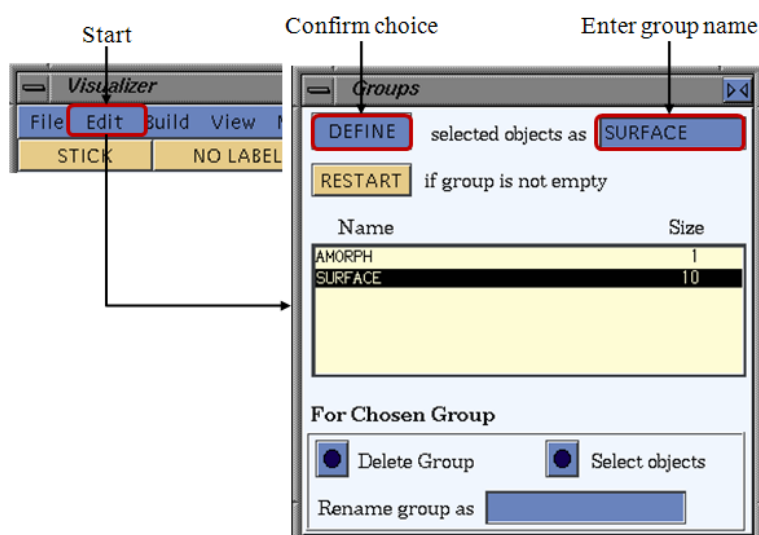
### 4.3.2 Combined Surface and Solution

The simulations on the isolated liquid side are now performed. The combination of the solid and the liquid side is the next task. The present chapter introduces the preliminary steps and the simulations on the combined system.

### 4.3.2.1 Step 1: Constructing Solid/ Liquid System

The initial task is to combine the solid side (crystal surface) and the liquid side (amorphous cell). In Cerius<sup>2</sup> this can be achieved via selecting the molecules in the amorphous cell and drag and drop them into the surface box.

Since further steps of the modeling require a separate analysis of the molecules according to their species the molecules should be edited as groups (Figure 4-34). Via the main menu path Edit/Groups the user gets access to the “Groups” dialogue as it is seen in the illustration. After the molecules of one species (e.g. solvent or solute) are selected the group name can be entered (e.g. “solute”, “solvent” or “surface”) and the button “DEFINE” can be pressed. Now the selected molecules are in the list which gives the name and the size of the group. After the groups are assigned the amorphous layer can be moved closer to the centre of the surface in order to achieve the interaction of the surface and the molecules of the solution.



*Figure 4-34 The “Goups” dialogue.*

The last task is to fix the Cartesian position of molecules of the crystal surface by setting constraints. This is achieved via the path OFF METHODS/MINIMIZATION/Constraints/Atoms. Select the atoms of the surface and in the dialogue “Atom Constraints” click on the “Fix Atomic Position” button. To ensure the constraints are applied click on the “Color Atoms by Constraint” button. An illustration is seen in Figure 4-35.



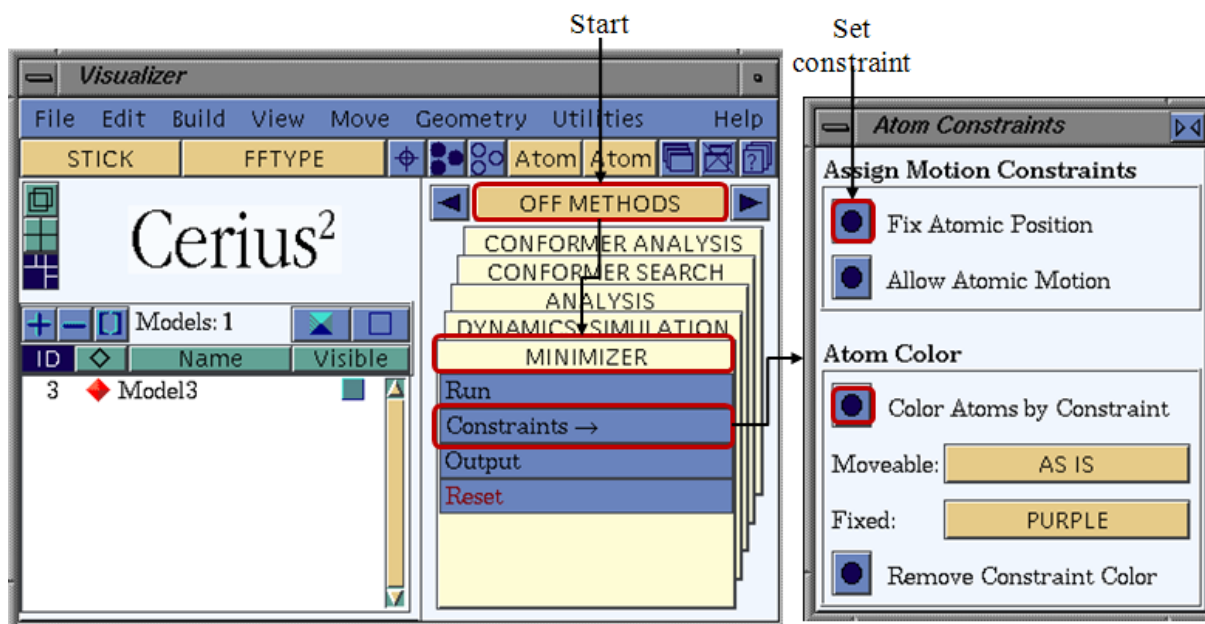


Figure 4-35 The “Atom Constraints” dialogue.

#### 4.3.2.2 Step 2: Molecular Dynamics III (NVT)

In order to perform the molecular dynamics on the surface docked with the additive and the host molecule the settings should be applied as seen in Figure 4-23 and described in the present chapter.

Access to the dynamics menu is obtained when following the module path OFF METHODS/DYNAMICS SIMULATION/Run as the dialogue “Dynamics Simulation” is opened the user should select the “Dynamics Method” and check the box “CONSTANT NVT” (seen in Figure 4-23 middle). Via clicking on the button “Preferences...” which is located in the same line the “NVT Dynamics Preferences” dialogue opens (Figure 4-23 top right). In the dialogue the thermostat is selected (recommended is “NOSE” or “T-DAMPING”).

Back in the “Dynamics Simulation” dialogue the “Dynamics Controls” are changed as seen in the illustration (Figure 4-23 middle), the “Required Temperature (K)” is 300 K and the “Number of Steps” is 500. For a later analysis is required to create a dynamics trajectory file. The corresponding settings are done in the dialogue “Dynamics Trajectory Output” which opens by a click on the “TRAJECTORY...” button. Here, check the box “Create Dynamics Trajectory File” and select the “Trajectory Update Frequency (step)”. The “Dynamics Output Preferences” are modified via a click on the Button “Output...” in the “Dynamics Simulation” dialogue. The settings should be a seen in the illustration (Figure 4-23 right middle).

The dialogue “Molecular Dynamics Controls” which is opened from the path OFF METHODS/DYNAMICS SIMULATION/Dynamics Controls should remain default with the settings as depicted in Figure 4-23 (bottom left). As all the settings are carried the NVT dynamics are started via clicking on the button “RUN” which is located on the top left of the “Dynamics Simulation” dialogue. The simulation is started and may have duration of several hours.

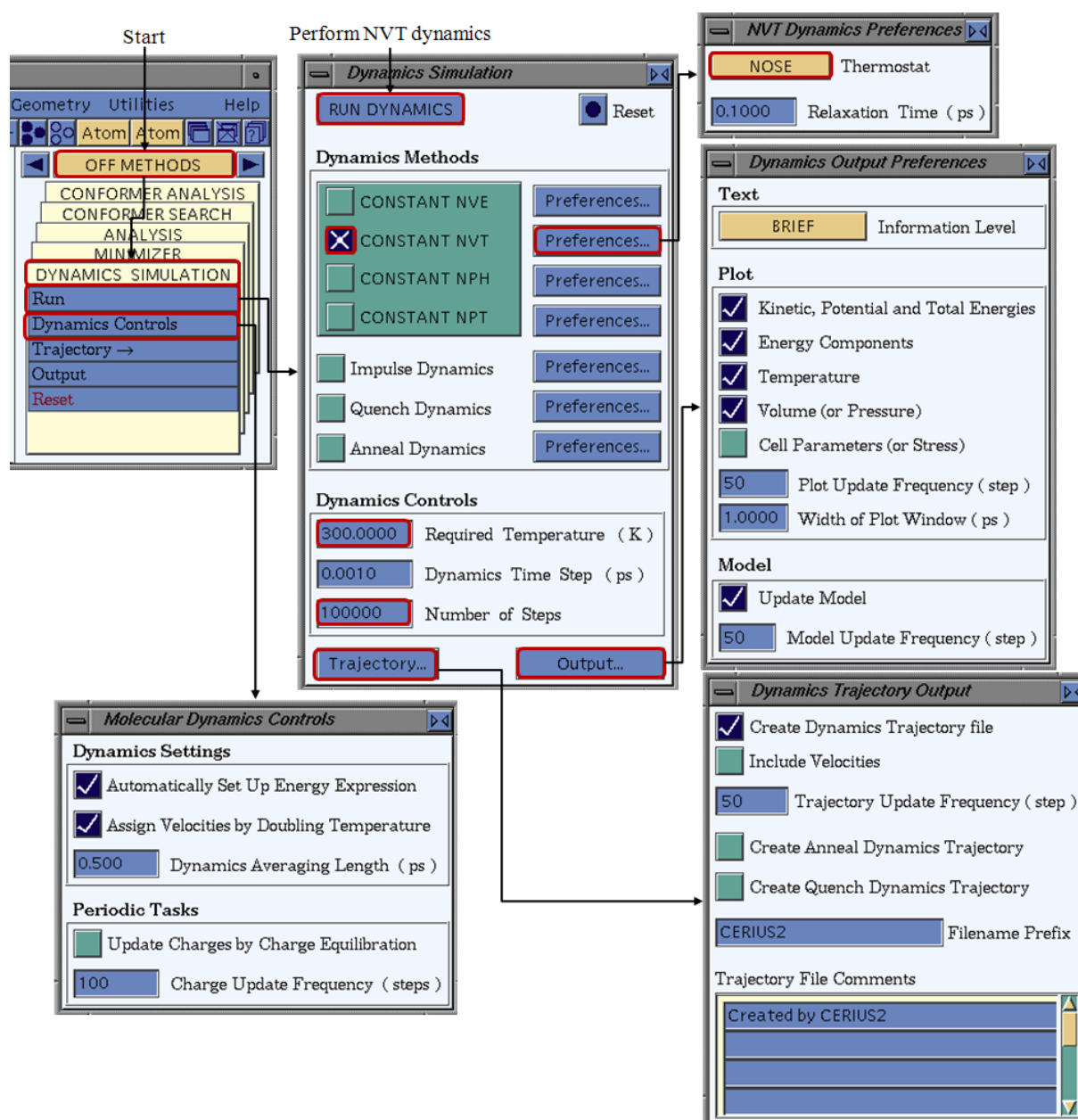


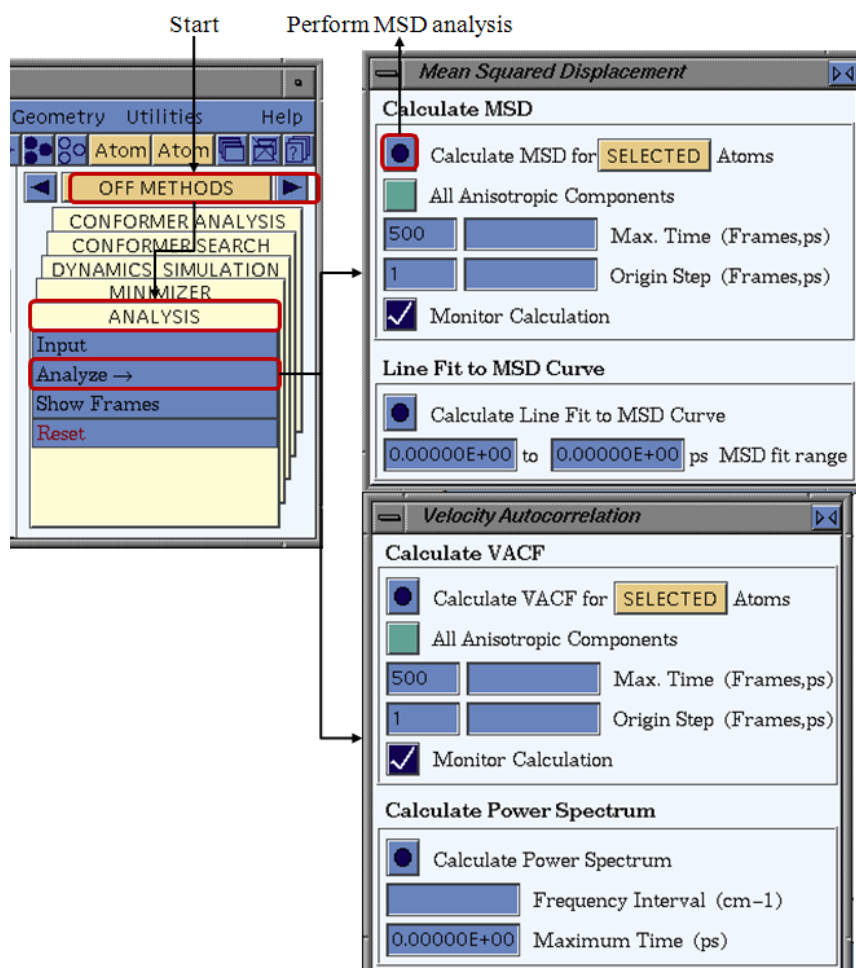
Figure 4-36 The “Dynamics Simulation” dialogue for the NVT dynamics.

### 4.3.2.3 Step 3: Trajectory Analysis

The trajectory result file which is obtained from NVT dynamics is analyzed in terms of the minimum energy frame as presented in chapter 4.2.2.3. Search for the lowest energy frame

and save the molecular conformation of this frame in order to perform the simulations which are described in the subsequent chapter 4.3.2.4.

The second task is to determine the mean squared displacement of the solute molecules on the surface in preparation to the diffusion coefficient calculation. In order to conduct the MSD analysis the input trajectory is selected as presented in chapter 4.2.2.3 and the constraints which are applied to the atoms of the surface should be removed (chapter 3.2.2.3). Follow the path OFF METHODS/ANALYSIS/Analyse/MSD to get access to the Mean Squared Displacement” dialogue which is depicted in Figure 4-37. Select the atoms for which the MSD calculation shall be carried out and start the MSD calculation by clicking on the “Calculate MSD for SELECTED atoms” button. The further step is to save the output data and transfer it to a origin worksheet (see chapter 3.2.2.3). The procedure for obtaining the diffusion coefficient is presented in chapter 3.2.3.1.2.

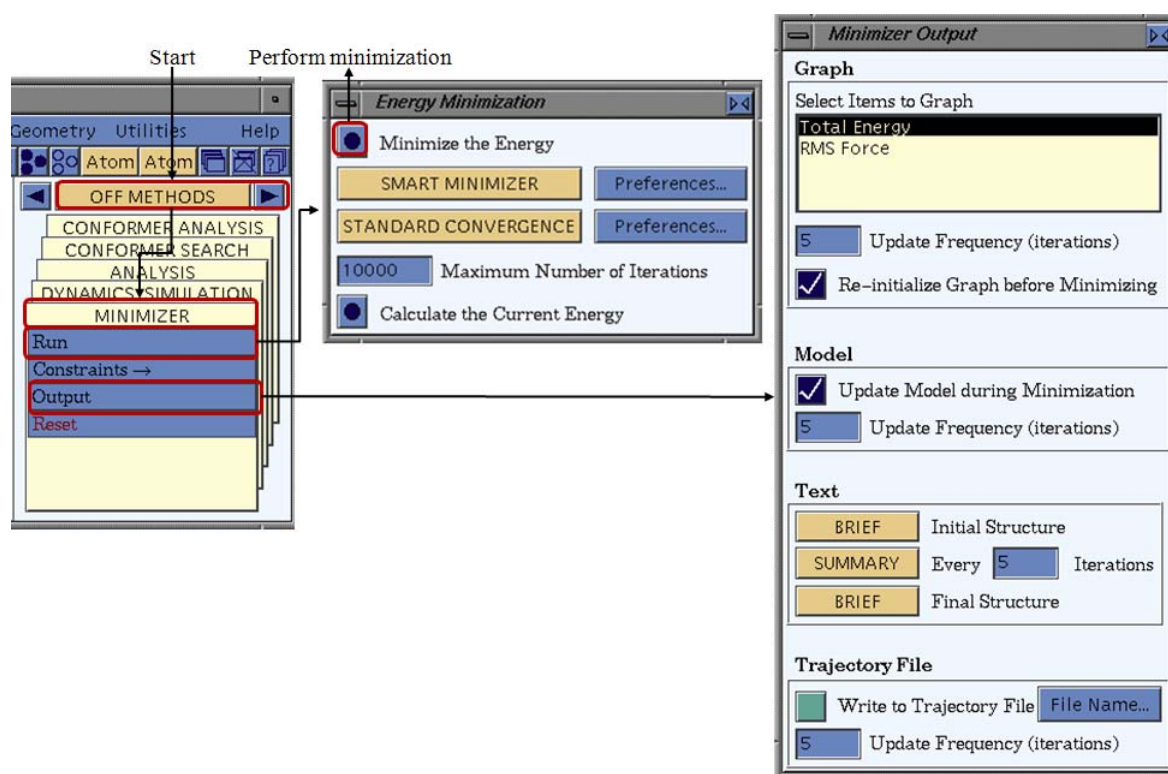


*Figure 4-37 The Mean Squared Displacement” dialogue for the trajectory analysis.*

#### 4.3.2.4 Step 4: Minimization

The minimization is conducted on the 3D file of the lowest energy conformation. The “Energy Minimization” dialogue which enables to start the minimization is accessed via the

module OFF METHODS/MINIMIZER/ by clicking on “Run”. The “Maximum Number of Iterations” is set to “10000”. Any other settings remain as seen in the illustration (Figure 4-38). The “Minimize Energy” button in the “Energy Minimizer” dialogue is pressed in order to start the minimization. The model visualization which is resulting from minimization and the corresponding total potential energy are to be saved. The subsequent steps of the energy calculation are performed on the 3D model which is resulting from the minimization.

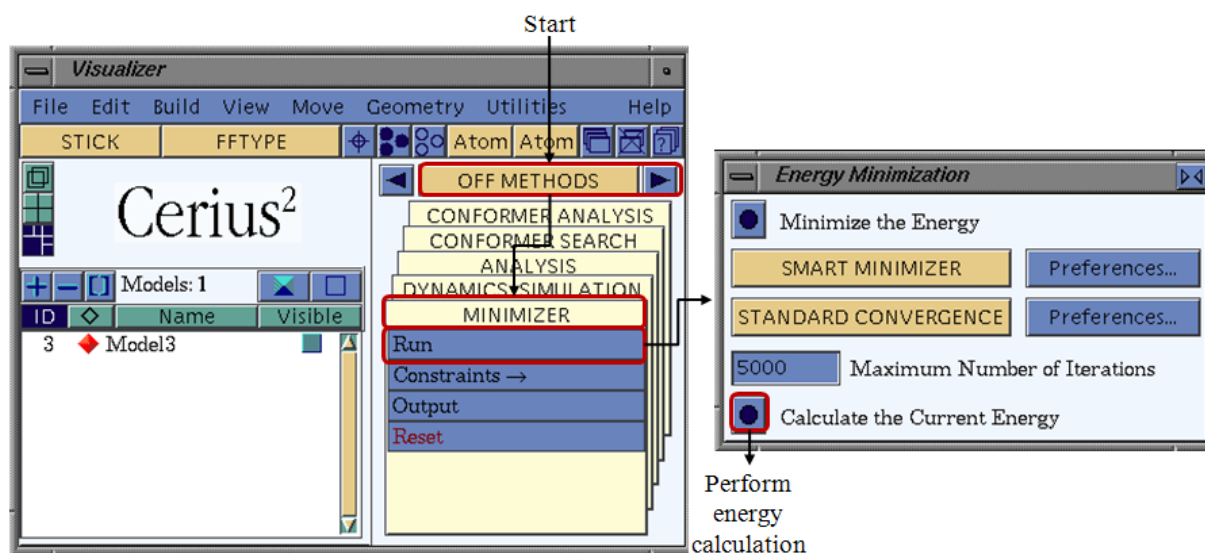


*Figure 4-38 The “Energy Minimization” and “Minimizer Output” dialogues.*

#### 4.3.2.5 Step 5: Calculating the Energy of Surface and Amorphous Layer

The current energy of a system is calculated for the molecules of the surface, the solute molecules and the solvent molecules in the amorphous layer. These molecules are to be separated and saved as isolated files.

In order to perform the current energy calculation for all of these new files follow the path OFF METHODS/MINIMIZER/Run (Figure 4-39). The “Energy Minimization” dialogue opens and the user should click on the button “Calculate the Current Energy”. The obtained total potential energies should be saved.



*Figure 4-39 Calculation of the current energy.*

### 4.3.3 The Modified Morphology

The manner of the morphology calculation is similar to chapter 4.2.3.

#### 4.3.3.1 Step 6: Calculating the Modified Attachment Energy

The methodology is presented in chapter 3.2.3.1.

##### 4.3.3.1.1 Attachment Energy Approach

See chapter 3.2.3.1.1.

##### 4.3.3.1.2 Diffusion Coefficient Approach

See chapter 3.2.3.1.2.

#### 4.3.3.2 Step 7: Calculating the Modified Morphology

The modified morphology is obtained as presented in chapter 4.2.3.2.

## 5. References

- [Acc05] Accelrys Software Inc., MaterialsStudio 4.0, San Diego, USA, 2005.
- [All87] Allen, M.P., Tildesley, D.J., *Computer Simulation of Liquids*, Oxford University Press, London, UK, 1987.
- [Boe92] Boek, E.S., Briels, W.J., van Erden, J., Feil, D., “Molecular-dynamics simulations of interfaces between water and crystalline urea”, *J. Phys. Chem.*, **96** (1992) 7010-7018.
- [Csd09] Cambridge Structural Database Version 5.31, Cambridge Crystallographic Data Centre, Cambridge, UK, 2009.
- [Dow03] Downs, R.T. and Hall-Wallace, M., “The American Mineralogist Crystal Structure Database”, *Am. Mineral.*, **88** (2003) 247-250
- [Lin58] Linke, W.R., Seidell, A., “Solubilities - Inorganic and Metal-organic Compounds Vol. I”, American Chemical Society, Washington D.C., USA 1958.
- [Lin65] Linke, W.R., Seidell, A., “Solubilities - Inorganic and Metal-organic Compounds Vol. II”, American Chemical Society, Washington D.C., USA 1965.
- [Lu04] Lu, J.J., Ulrich, J., “Improved understanding of molecular modelling-the importance of additive incorporation”, *J. Cryst. Growth*, **280** (2004) 203-210.
- [Men11] Private communication with Carsten Menke, Accelrys Software Inc., USA, concerning MaterialsStudio 4.0, Service Reference # 00272272 mean square displacement, in August 2011.
- [Nie95] Niehörster, S., Ulrich, J., „Designing Crystal Morphology by a Simple Approach“, *Cryst. Res. Technol.*, **30** (1995) 389-395.
- [Pdb11] Protein Data Bank, Research Collaboratory for Structural Bioinformatics (RCSB)-Rutgers Department of Chemistry and Chemical Biology, University of New Jersey, USA, 2012.
- [Sch11a] Schmidt, C., Ulrich, J., “Predicting crystal habits grown from aqueous multi-component solutions - Method of Computation involving multiple Solvents”, in Proceedings of 18<sup>th</sup> International Workshop on Industrial Crystallization (BIWIC) 2011, Eds. S.S. Kadam, S.A. Kulkarni, J.H.T. Horst, Delft University of Technology, Delft, Netherlands, 2011, 288-293.
- [Sch11b] Schmidt, C., Ulrich, J., “Crystal Habit Prediction Including the Liquid as well as the Solid Side”, in Proceedings of 18<sup>th</sup> International Symposium on Industrial Crystallization (ISIC) 2011, Ed. M. Mazzotti, AIDIC, Milan, Italy, 2011, 96-97.